pH-responsive Biomaterials for Smart Intravaginal Drug Delivery

by

Seungil Kim

A thesis submitted to the Faculty of Graduate Studies of

The University of Manitoba

In partial fulfillment of the requirements for the degree of

Doctor of Philosophy

Biomedical Engineering

University of Manitoba

Winnipeg, Manitoba, Canada

i

Abstract

For better combating human immunodeficiency virus (HIV), pH-triggered nanocarriers for on-demand intravaginal release of anti-HIV drugs was proposed to reduce side-effects. The pH-triggering was based on the obsevation that the normal human vaginal tract pH is acidic (3.5-4.5) and the pH can be elevated to neutral by the introduction of seminal fluid during heterosexul intercourse. To acheve this goal, new pH-responsive polyurethanes (PUs) were synthesized from polyethylene glycol (PEG), hexamethylene diisocyanate (HDI), methylene di-p-phenyl diisocyanate (MDI), 1,4-bis(2-hydroxyethyl)piperazine (HEP), dimethylolpropionic acid (DMPA), and propylene glycol (PG) for the fabrication of an intravaginal drug delivery device.

Solvent-cast PEG-HEP-HDI-PG and PEG-HEP-MDI-PG membranes were fabricated and showed pH-triggered reversible changes in swelling ratio and surface morphology. The solvent-cast membranes demonstrated pH-responsive switchable on-and-off release of sodium diclofenac (NaDF): triggered release occurred at pH 7.0 (> 10%) but close-to-zero release occurred at pH 4.2.

An electrospun PEG-HEP-MDI-PG membrane was fabricated for the controlled release of nanocarriers since the solvent-cast PU membranes didn't have sufficient interconnected pores to allow storage and release of nanoparticles (NPs). The electrospun membrane demonstrated almost no release of Visiblex^{TM} color dyed polystyrene nanoparticles (PSNs, 200 nm, -COOH) at pH 4.5 (2 ± 1%) but a continuous release at pH 7.0 (60 ± 6%) for 24 h.

These pH-responsive PU membranes were developed as a "window" membrane of reservoir-intravaginal ring (IVR) for the on-demand release of drugs or nanocarriers. The PU membranes did not show noticeable negative impact on viability of VK2/E6E7 human epithelial

cells and Sup-T1 human T-cells or induction of pro-inflammatory cytokines (interleukin-6 (IL-6), interleukin-8 (IL-8), and interleukin-1 beta (IL-1β)) production.

At last, the pH-triggered switchable release of nanocarriers was achieved by fabricated PEG-DMPA-HDI-PG hydrogel (20 wt% in distilled water). The fluorescent dye, orange II, labeled PEGylated poly(aspartic acid)-based NP (251-283 nm) was synthesized for a release study and blended with PU hydrogel to form a supramolecular complex hydrogel. Then the complex hydrogel was filled into the lumen of segmented reservoir-IVRs containing two holes. *In vitro* release study showed close-to-zero release of NPs at pH 4.2, and then 19 ± 5% release of NPs for the next 1 h at pH 7.0, followed by the switchable on-and-off release for 5 h.

Acknowledgements

I always remember that "with knowledge, new opportunities are almost always found."

Table of Contents

List of Schemes and Tables

List of Figures

List of abbreviations

α-CD	α-cyclodextrin
AIDS	acquired immune deficiency syndrome
ATR-FTIR	attenuated total reflectance-Fourier transform infrared
BD	1,4-butanedol
BES	N, N-bis (2-hydroxyethylhydroxyethyl)-2-aminoethane-sulfonic acid
BICINE	N,N-Bis(2-hydroxyethyl)glycine
BSA	bovine serum albumin
C6	coumarin 6
CAP	cellulose acetate phthalate
CDI	carbonyldiimidazole
3DF	three-dimensional fabric
DA	Diels-Alder
DBTDL	dibutyltin dilauarate
DCE	1,2-dichloroethane
DCF	dichlorofluorescein
DCM	dichloromethane
DDS	drug delivery systems

DI   diameter

DiSe   di(1-hydroxyethylene) diselenide

DLS   dynamic light scattering

DMF   N,N-dimethylformamide

DMSO   dimethyl sulfoxide

DMPA   Dimethylolpropionic acid

DNA   deoxyribonucleic acid

DS   degree of substitution

DSC   differential scanning calorimeter

E´   tensile storage modulus

EVA   ethylene-vinyl acetate

FBS   fetal bovine serum

FDA   Food and Drug Administration

Fg   fibrinogen

FPCUs   Fluorocarbon end-capped poly(carbonate urethane)s

FT-IR   Fourier-transform infrared

^{1}H-NMR ^{1}H-nuclear magnetic resonance

HCQ   hydroxychloroquine

HD   hexane diol

HDI	hexamethylene diisocyanate
HEMA	2-hydroxyethyl methacrylate
HEP	1,4-bis(2-hydroxyethyl)piperazine
HIV	human immunodeficiency virus
HMAAm	N-(Hydroxymethyl)acrylamide
HMDI	Bis(4-isocyanatocyclohexyl)methane
HIFP	1,1,1,3,3,3-hexafluoro-2-propanol
HPV	human papillomavirus
HSA	human serum albumin
HSV	herpes simplex virus
IC	inclusion complex
IH	intimal hyperplasia
IL-1β	interleukin-1 beta
IL-6	interleukin-6
IL-8	interleukin-8
INIs	integrase inhibitors
IPDI	isophorone diisocyanate
IVD	artificial intervertebral disc
IVR	intravaginal ring

K-SFM	keratinocyte-serum free medium
LDI	L-lysine ethyl ester diisocyanate
IND	indomethacin
LNG	levonorgestrel
LPS	lipopolysaccharide
MDEA	N-methyldiethanolamine
MDI	Methylene di-p-phenyl diisocyanate
MES	2-(N-morpholino)ethanesulfonic acid
MIO	metal ion oxidative degradation
MRI	magnetic resonance imaging
Mw	molecular weight
MWCO	molecular weight cut off
NaDF	diclofenac sodium
NIPAAm	N-isopropylacrylamide
NNRTI	non-nucleoside reverse transcriptase inhibitor
NP	nanoparticle
NRTI	nucleoside reverse transcriptase inhibitor
NSERC	Natural Sciences and Engineering Research Council of Canada
NtRTI	nucleotide reverse transcriptase inhibitor

OD	outer diameter
PAE	phenylalanine ethylester
PASP	poly(aspartic acid)
PBS	phosphate buffer solution
PCL	polycaprolactone
PDFOL	2,2,3,3,4,4,5,5,6,6,7,7,8,8,8-pentadecafluoro-1-octanol
PDM	poly(N,N-dimethylaminoethyl methacrylate)
PEG	polyethylene glycol
PEO	polyethylene oxide
PEU	poly(ether urethane)
PG	propylene glycol
PGA	poly(γ-glutamic acid)
Ph	phenethylamine
PIB	polyisobutylene
PIs	protease inhibitors
PMAA	poly(methacrylic acid)
POSS-PCU	polyhedral oligomeric silsesquioxane poly(carbonate-urea)urethane
PPG	polypropylene glycol
PPO	polypropylene oxide

PSI	polysuccinimide
PSN	polystyrene nanoparticle
PTMO	poly(tetramethylene oxide)
PU	polyurethane
PVA	poly(vinyl alcohol)
PVDF	poly(vinylidene fluoride)
QAC	quaternary ammonium compounds
RB	rhodamine B
RMS	root mean square
RNA	ribonucleic acid
RP-HPLC	reversed-phase high-performance liquid chromatography
SA	sulfanilamide
SD	standard deviation
SDF	stromal cell-derived factor
SEM	scanning electron microscopy
siRNA	small interfering RNA
STI	sexually transmitted infection
TEA	triethylamine
TFV	Tenofovir

T$_g$ glass transition temperature

THF   tetrahydrofuran

T$_m$ melting temperature

T$_s$ switching temperature

VEGF   vascular endothelial growth factor

VFS   vaginal fluid simulant

WAXD   wide-angle X-ray diffraction

WHO   World Health Organization

XD   cross-sectional diameter

Chapter 1

Introduction

1.1   Overview

Over 30 million people are living with human immunodeficiency virus (HIV).[1] Despite the knowledge of successful HIV prevention strategies (e.g., condoms), HIV continues to spread at an alarming rate especially among women in developing countries. The World Health Organization (WHO) announced that it is essential to support the development of microbicide which can be applied inside the vagina or rectum to protect against sexually transmitted infections (STIs) including HIV.[2] The availability of microbicide would greatly empower women to protect themselves. Unlike male or female condoms, microbicides are a potential preventive option that women can easily control and do not require the cooperation, consent, or even knowledge of the partner. Over the past 20 years, numerous microbicide formulations such as gels, creams, and suppositories have been developed, but all have shown limited efficacy. Recently, a clinical trial involving the CAPRISA gel (1% tenofovir vaginal gel) showed approximately 39% reduction in the acquisition of HIV by women who used the vaginal gel in comparison to the placebo group.[3] Although this result gives hope to the field of microbicides, approval of a preventive product for use by the general population is still a long way off. One of the disadvantages of vaginal gels is the inconvenience since users have to apply the gels immediately before sexual intercourse.[4] Other disadvantages include leakage which may contribute to rapid removal from the application site. As the microbicide field evolves, there is an ever-increasing need for alternative technologies to deliver agents that can treat/prevent HIV infection.

Intravaginal rings (IVRs) are an alternative scaffold, which is approved by the Food and Drug Administration (FDA) for use as contraceptive and hormone replacement therapy and have been developed for topical delivery of anti-HIV drugs recently.[5] As an example, NuvaRing®, a

type of IVR, is designed to deliver etonogestrel and ethinyl estradiol.[6] Clinical trials with magnetic resonance imaging (MRI) have shown that NuvaRing® is well tolerated without causing damage to the vaginal epithelium, has no occurrence of expulsion, and does not cause any adverse reactions.[7] Research conducted using NuvaRing® showed that 96% of the patients were satisfied with the IVR and 97% would recommend it.[8] Overall, these clinical trials may show that IVRs are safe and relatively simple to use. However, the loaded drug could be released consistently from the IVRs after being inserted even when the drug is unnecessary. This undesired exposure to the drug can cause side effects. Therefore, on-demand release of drugs from IVRs only when sexual intercourse occurs is recommended.

Polyurethane (PU) would be recommended for the fabrication of IVRs thanks to its tunable physicochemical characteristics. PUs are found in a variety of biomedical products such as orthopedic braces, catheters, and wound-healing devices.[9,10] In comparison to cross-linked silicone rubbers, many PU elastomers are thermoplastic and can be processed by methods that involve dissolving and melting to allow reshaping of the polymer structure.[11–13] Besides being versatile in its use and easy to reshape, PU is half the price of silicone and ethylene-vinyl acetate, making PU a cost-effective material for use in developing countries.

Nanocarriers such as micelles, vesicles, nanogels, liposomes, solid lipid nanoparticles, dendrimers, and carbon nanotubes have been developed for delivery of drugs and genes.[14,15] Advantages of nanocarriers for drug delivery include: 1) potential increase of delivery efficiency;[16] 2) reduction of off-target effects of drugs; 3) ideal shape and size for cellular uptake; 4) potential enhancement of penetration of mucosal barriers through surface modification;[17] 5) physical protection of the drug from degradation by endogenous acidic or alkali medium; and 6) control of drug release, ranging from days to months through

physicochemical property modification of the polymer, or the inclusion of other polymers in the formulation.[18] Development of drug resistance has always been a concern when treating HIV-infected patients.[19] Targeted delivery of anti-HIV drugs can reduce side effects caused by off-target delivery and drug resistance in HIV-infected patients. Small interfering RNA (siRNA) can be designed to be complementary using known mRNA sequences and targeting specific mRNA. When there are no drugs available to act on a specific target, siRNA can play a big role in degrading mRNA, resulting in gene knockdown.[20] However, nucleic acids, including siRNA, cannot readily cross cell membranes and require a carrier/transfection system for efficient cell uptake[21] and siRNA could be degraded in the normal vaginal tract pH (3.5-4.5, average: 4.2).[22] Therefore, it is necessary to use nanocarriers for delivering anti-HIV drugs and siRNA.

The normal pH range of female genital tract is acidic (pH 3.5-4.5);[23] however, during heterosexual intercourse the introduction of human seminal fluid can elevate the pH to neutral.[24] This change in pH can be used as the triggering signal for responsive intravaginal release of anti-HIV drugs and nanocarriers. In this regard, pH-sensitivity of IVRs could be an important property to reduce unnecessary exposure to anti-HIV drugs and side effects by only releasing the anti-HIV drugs or nanocarriers only when intercourse occurs.

For this thesis, developing novel pH-responsive PU IVRs for the on-demand release of anti-HIV drugs or nanocarriers (with little or no release at acidic pH (< 4.5) and rapid release at neutral pH (> 6.4)) is proposed. To the best of our knowledge, the proposed research is the first to develop pH-responsive IVRs for the switchable on-demand release of anti-HIV drugs or nanocarriers. The pH-responsive IVRs will provide triggered-release of anti-HIV drugs or nanocarriers upon changes in vaginal pH due to human seminal fluid, and potentially reduce side effects.

1.2   Human immunodeficiency virus (HIV)

STIs are bacteria, parasites, and viruses transmitted by sexual intercourse, especially vaginal intercourse. Chlamydia, gonorrhea, and syphilis are major bacterial STIs. Herpes simplex virus (HSV), HIV, and human papillomavirus (HPV) are the main types of viral STIs.[25] Among these, HIV is one of the most significant and worldwide health concerns, since there still is no cure for HIV.[26,27] Moreover, HIV can progress to acquired immune deficiency syndrome (AIDS).[28] Over 30 million people are living with HIV/AIDS infection worldwide.[29] Anti-HIV drugs, which also be called as anti-retroviral drugs, act at a different stage of the infection to block or delay transmission of the virus (**Table 1-1**). Alternative intravaginal drug delivery systems (DDS) are required to increase drug delivery efficiency and decrease side effects.[23]

Table 1-1. Different classes of anti-HIV drugs[30,31]

Class of drug	Description	Name of drugs
Fusion inhibitors	Interfering with the binding, fusion, and entry of HIV into CD4 cells of the immune system.	enfuvirtide
Nucleoside reverse transcriptase inhibitors (NRTIs)	Blocking reverse transcriptase, a viral DNA polymerase, since the enzyme is required for replication of HIV and other retroviruses.	zidovudine, didanosine, zalcitabine, tenofovir disoproxil fumarate, stavudine, lamivudine, abacavir, and emtricitabine
Nucleotide reverse transcriptase inhibitors (NtRTIs)	Blocking reverse transcriptase, a viral DNA polymerase, since the enzyme is required for replication of HIV and other retroviruses.	tenofovir
non-nucleoside reverse transcriptase inhibitors (NNRTIs)	Binding to and later alter HIV reverse transcriptase.	nevirapine, rilpivirine, delavirdine, efavirenz and etravirine
Integrase inhibitors (INIs)	Blocking HIV integrase, a viral enzyme, since the enzyme inserts the viral genome into the DNA of the host immune cell	raltegravir, dolutegravir, and elvitegravir
Protease inhibitors (PIs)	Binding to HIV proteases and blocking cleavage of protein precursors.	saquinavir, ritonavir, indinavir, nelfinavir, amprenavir, lopinavir, atazanavir, fosamprenavir, tipranavir and darunavir

1.3   Intravaginal drug delivery

Topical drug delivery leads to higher drug concentration on the target site than oral administration and reduces off-target side effects.[32] In this regard, intravaginal delivery of anti-HIV drugs or nanocarriers can increase delivery efficiency, decrease side effects, and reduce the chance of drug resistance.

1.3.1 Human vagina

The vagina is an elastic, muscular canal of the female genital tract (**Figure 1-1**). The vaginal epithelium, the tissue lining inside the vagina, is protected by the vaginal mucus. Vaginal mucus, consisting primarily of entangled and crosslinked mucin fibers, is an adhesive and viscoelastic gel which protects the surface of vagina.[17] The normal pH range of the female genital tract is from pH 3.5 to pH 4.5 (average: 4.2, **Table 1-2**),[23] but can be elevated to neutral pH by the introduction of semen during heterosexual intercourse.[24,33]
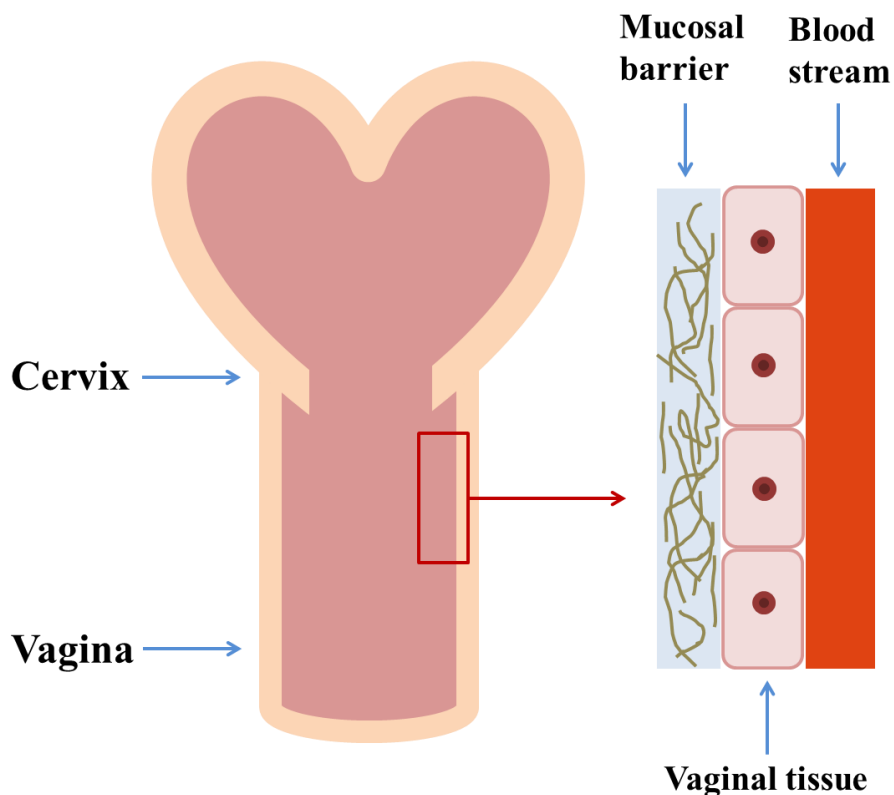
Figure 1-1. Illustration of human vagina[5,34]

Table 1-2. Physiology and characteristics of human vagina

Vaginal physiology	Characteristics	Description
Epithelium	Cyclic changes in thickness by reproductive hormones. Activities of enzymes in the external and basal cell layers of the epithelium.	Thick layers with estrogen play a role as a physical barrier. Vaginal mucus acts as a permeability barrier. Local bacterial flora also serves protection against infection.
Vaginal secretion	Provides moisture and solubilizing dosage formulations.	Composition and volume of vaginal fluid depend on age, infection, and sexual arousal. Hormones influence the composition of the vaginal fluid. Vaginal epithelium has higher absorption of poorly water-soluble drugs when the fluid volume is high.
pH	From 3.5 to 4.5, average 4.2.	Lactic acid produced by Lactobacillus helps in maintaining the acidic condition of the vagina. Varies with age and health condition.

1.3.2 Drug delivery systems for intravaginal administration

Most recently, vaginal drug delivery has been developed as a topical delivery of contraceptive and anti-HIV drugs including peptide and gene therapy.[35] This drug delivery route has many advantages: avoiding first-pass metabolism, high permeability for low molecules due to a dense network of blood vessels, and ease of administration. However, alternative methods have been sought for intravaginal drug delivery because of the physiological barrier of the vagina. So far, vaginal formulations such as creams, gels, IVRs, and intravaginal nanocarriers have been developed.

1.3.2.1 Creams and gels

Creams and gels have been used to deliver contraceptives and anti-bacterial agents, although they have disadvantages such as discomfort, leaking, and messy use.[36] The advantages of vaginal creams and gels rely on their feasibility, acceptability, and non-toxicity against the vaginal tissue. Vaginal creams and gels could become a better option by applying the principle of emulsion or hydrogel-based drug delivery.[35] As an example, a vagina retentive cream suppository (VRCS) of progesterone was developed using oil in water (o/w) emulsion.[37] The most stable formulation of the trials (VRCS 1) was scaled-up for manufacturing and *in vivo* tests. The patient satisfaction studies demonstrated a high satisfaction response to the VRCS 1 from all volunteers. On the other hand, the Center for the AIDS Program of Research in South Africa (CAPRISA) studied the safety and effectiveness of a 1 % of tenofovir (TFV) in the vaginal gel by a pursuit method.[38] The study showed that compared to the placebo gel, the TFV gel reduced HIV acquisition over 39%.

1.3.2.2 Intravaginal rings (IVRs)

IVR is a ring-shaped release device fabricated using elastomeric polymers.[39] IVRs were initially developed as a contraceptive releasing device and approved by the FDA. In general, matrix-IVRs showed sustained release of drugs; otherwise, release of loaded drug in reservoir-IVRs could be controlled by the thickness and physicochemical characteristics of the outer layer of the reservoir. Advantages of IVRs over other dosing formulations are: (1) higher acceptability by end-users;[40] (2) provision of controlled release of drugs for longer periods;[41] (3) more uniform

concentration of released drugs in the vagina; (4) user convenience; and (5) protection of loaded drugs from hydroloysis.[42] Most recently, IVRs have been developed as anti-HIV drug releasing devices. However, the development of IVR still has many gaps and potentials.

1.3.2.3 Intravaginal nanocarrier

Alternative delivery methods for anti-HIV drugs and siRNA are necessary to overcome the barrier of the vaginal mucus, vaginal epithelium, and cellular membrane of target vaginal cells.[43] Intravaginal nanocarriers such as micelles, vesicles, nanogels, solid lipid nanoparticles, liposomes, dendrimers and carbon nanotubes have been developed to increase drug delivery efficiency and decrease drug side effects.[44] In particular, nanocarriers can protect cargo drugs including protein and siRNA against enzymatic degradation and acidic hydrolysis in the human vagina.[45]

1.4 Smart and biostable polyurethanes for long-term implants

Seungil Kim, Song Liu

Revised from the review article published in ACS Biomaterials Science & Engineering. 2018, 4, 1479-1490. Permission for use has been granted by the publisher.

PU was used for this thesis research as a fabrication material for reservoir-IVRs because of its elastomeric, thermoplastic, and tunable physicochemical chracteristics. Section 1.4 is a review of stimuli-responsive and biostable PUs and their application in long-term implants. The review gives key ideas for the preparation of novel PUs developed through the research.

Moreover, the application of PUs in long-term implants focusing on IVRs was discussed in the review to obtain basic ideas for fabrication of smart IVRs that demonstrate pH-triggered on-demand release of drugs or nanocarriers.

1.4.1 Introduction

PU was first synthesized in the 1930s and used in the form of fibers and flexible foams due to its elastomeric and thermoplastic characteristics.[13] PU is synthesized from three components: a long-chain polyol, polyisocyanate, and chain extender. A slight excess of polyisocyanate is typically used to drive the reaction to completion. In the 1960s, PU was found to possess good blood compatibility, and since the 1970s, the biomedical applications of PU have been actively researched. Research throughout the 1990s focused on novel PUs used not only for the formation of a new class of bioresorbable materials but also for the development of biostable biomaterials for *in vivo* long-term applications.[46] Currently, PUs are being developed for both tissue engineering[10,47–50] and smart biomaterials.[9,51–60]

Smart materials are designed to be responsive to external stimuli such as pH, temperature, electric or magnetic fields, biological signals, and pathological abnormalities. In response to environmental stimuli, one or more of their physicochemical, and/or biological characteristics are changed.[61,62] Some examples include: shape-memory materials that can recover their original structure given the right stimulus; pH-responsive materials that can change their solubility, water absorption ratio, and surface charge in response to environmental pH change; and bioactive compounds immobilized materials that can enhance their biological response to the micro-environment.

Suitabile physical properties of PUs can lead to their adoption in biomedical applications. In addition, the physicochemical characteristics of PU can easily be tuned through modifications of the chemical components, thanks to the enormous compatibility of PU synthesis with a wide variety of functional monomers. As a result of these two features, various smart PUs have been developed for biomedical applications that can be thermoresponsive,[51,52,63] have shape-memory,[53–56,64] be pH-responsive,[9,46,53,57–60,65,66] or be self-healing,[49,57] bioresponsive, or self-cleaning.[67,68]

A 1989 review article focusing on biomedical PUs examined the general synthetic chemistry, structure-properties, interaction with tissue, surface properties, application and sterilization of PUs.[12] In contrast, a 1999 review article focused more heavily on the biomedical applications of PU, particularly for PU based artificial organs.[69] More recently, biodegradable PUs in regenerative medicine were reviewed in a 2008 article;[48] and in 2010, an article reviewed thermo-moisture responsive PU shape-memory polymers and composites.[70] These previously published reviews cover a wide range of biomedical applications of PUs. However, none of the reviews discussed the biomedical applications of novel stimuli-responsive and biostable PUs. Since smart PUs have been actively researched since the 2000s, this section reviews PUs with a focus on medical applications entailing long-term stability and stimuli-responsiveness. Although biodegradability is important for regenerative medicine, biostability of PUs is essential for long-term implantable biomaterials. In this section, PU engineered IVRs are reviewed since elastomeric and robust mechanical properties of PUs are well-fitted for such long-term implantable biomaterials.

This section reviews stimuli-responsive and biostable PUs researched after 2008, and discusses potential uses of smart PUs in long-term implantable biomedical applications focusing on IVRs.

1.4.2   Stimuli-responsive polyurethanes

1.4.2.1 Thermoresponsive polyurethanes

PU can be thermoplastic, or thermoset depending on its chemical structure. The thermoplastic PUs have excellent thermal stability for the fabrication of biomaterials by hot melt extrusion. Thermal stability of different types of urethanes is shown in **Table 1-3**.

Thermal-sensitive PUs have distinct characteristics due to their unique block copolymer structure, which consists of a thermally responsive soft segment and a hard segment. Typically, diisocyanate and chain extender become the hard segments after the synthesis reaction of PU. The soft segment has a phase-transition temperature (crystalline melting transition or glass transition temperature) that can act as a switching temperature (T_s).[58] The thermoresponsive characteristics of PU can be controlled by physicochemical properties of the soft segment. For instance, thermoresponsive triblock copolymers such as polyethylene oxide-polypropylene oxide-polyethylene oxide (PEO-PPO-PEO, Pluronic) can be used as a long-chain polyol for controlling the thermoresponsive properties of PU.

Table 1-3. Thermal stability of different types of urethanes.

Type of urethane group	Approximate upper stability temperature (°C)
Alkyl—HN—CO—O—Alkyl	~ 250
Aryl—HN—CO—O—Alkyl	~ 200
Alkyl—HN—CO—O—Aryl	~ 180
Aryl—HN—CO—O—Aryl	~ 120

Thermoresponsive poly(ether carbonate urethane)ureas have been synthesized using a PEO-PPO-PEG triblock copolymer to enhance the thermoresponsive properties of the copolymer.[63] The prepared pentablock poly(ether carbonate urethane)urea demonstrated almost 3 times lower water absorption at 37 °C than at 4 °C because of the gelling transition temperature (around 37 °C) of the PEO-PPO-PEO of the poly(ether carbonate urethane)urea. At 37 °C, the polymer-polymer hydrogen bonding of PEO-PPO-PEO becomes more favorable than the polymer-water hydrogen bonding and the copolymer de-swells.

Stimuli-responsive shape-memory materials recover their original shapes under the appropriate stimulus such as temperature, light, electric field, magnetic field, pH, or enzyme.[71] Generally, thermoresponsive shape-memory polymers consist of chemical or physical crosslinks (a fixed phase for memorization of the original shape) and reversible chains (molecular switch). The reversible chains have a thermal transition at the melting temperature (T_m) or glass transition temperature (T_g) of the chains. Shape-memory materials can be prepared from PU due to its thermoresponsive characteristics. Most recently, studies on poly(ε-caprolactone)-based hyperbranched PUs have been performed to enhance the physical properties of the shape-

memory PUs.[54] Data obtained from wide-angle X-ray diffraction (WAXD) and differential scanning calorimeter (DSC) measurements, confirmed that the highly branched structure of the prepared PU did not affect PU crystallinity. The shape-memory characteristics of the hyperbranched PUs were evaluated and showed a higher tensile storage modulus (E´) ratio (E´glass/E´rubber) and shape-recovery rate than the linear analogues. A highly chemically-crosslinked PU shape-memory foam having an extremely low density was developed using the physical blowing agent, Enovate.[56] The prepared PU shape-memory foam showed a high glass storage modulus of 200–300 kPa and excellent shape recovery of 97–98%. The prepared highly crosslinked shape-memory PU foam was suggested as a promising biomaterial for use in embolic devices based on its unique structure, physical properties, and good *in vitro* biocompatibility test results. Polyaspartimide-urea-based shape-memory polymers were synthesized at tailored high transition temperatures above 120 °C.[55] The prepared shape-memory polymer demonstrated a high degree of toughness and excellent shape recovery within 60 seconds. It was found that the crosslink density, glass transition temperature (T_g) and high-temperature stiffness (EH) were also increased.

Self-healing PU materials have also been developed. Poly(methyl methacrylate)-co-[poly(methyl metharyleate)-graft-(oligo-caprolactone)]urethane networks containing a Diels-Alder (DA) adduct unit (GCPNp-DAs) have been synthesized.[72] The networks demonstrate reversible scratch-healing properties by the crosslinked (at Diels-Alder reaction temperature, 70 °C) and de-crosslinked (at retro-Diels-Alder reaction temperature, 130 °C) structure of the GCPNp-DAs. From the Fourier-transform infrared (FT-IR) spectra, the maleimide double bond peak at 654 cm^{-1} was observed after de-crosslinking at 130 °C and disappeared again after crosslinking at 70 °C. All synthesized networks demonstrated excellent scratch-healing

properties at 130 °C for 10 minutes using a Feltier module and a sphero-conical indenter installed in the scratch test machine.

Thermoresponsive controlled drug release has been developed using thermoresponsive PUs. This was developed using N-isopropylacrylamide (NIPAAm), and N-(Hydroxymethyl)acrylamide (HMAAm) for fabrication of a smart stent consisting of core-shell structured nanofibers.[73] The stent consisted of a thermoresponsive shell and a stretchable core for the smart release of incorporated 5-fluorouracil and/or paclitaxel. The fabricated scaffold demonstrated thermoresponsive on-demand release of drugs for hyperthermia therapy, with a very minimal release rate for normal human body temperatures, and a triggered release at a temperature above 40 °C. A shape-memory PU elastomer has been studied for controlled drug release as well.[74] The prepared shape-memory PU demonstrated shape-memory properties in the temperature range of 15 °C to 30 °C. The hydrophobic drug, dichlorofluorescein (DCF), was used for the drug release test at 22 °C and 37 °C. The results showed almost 4 times faster DCF release at 37 °C than at 22 °C demonstrating that the hydrophobic microdomains of shape-memory PU could be used as reservoirs for the loading and thermoresponsive release of hydrophobic drugs.
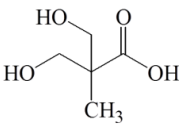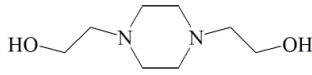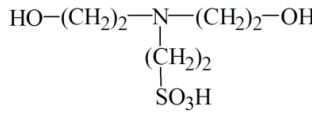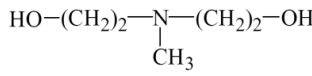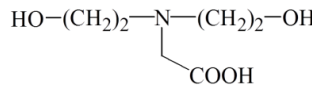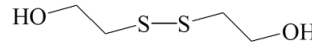
These shape-memory PU accomplishments are encouraging for the fabrication of PU-based biomaterials. However, the most interesting accomplishment is the development of a multi-responsive shape-memory PU, such as electrical-signal-sensitive shape-memory PUs.[75] Bio- and electroactive shape-memory PUs were synthesized using poly(citric acid-co-polycaprolactone), dopamine, and aniline hexamer (an electroactive molecule). This shape-memory PU showed adjustable wet conductivity from 5.0×10^{-6} to 17.1×10^{-4} S/m and elongation from 360 to 550% with excellent shape-memory capacity by changing the aniline

hexamer content. Supplementing the PU with dopamine enhanced cell adhesion, proliferation, and myogenic differentiation of an immortalized mouse myoblast cell line C2C12 cells.

1.4.2.2 pH-responsive polyurethanes

pH-sensitive PU is synthesized using pH-sensitive polyol and/or polyamine.[9,53,58–60,65,66] pH-sensitive molecules can be immobilized on a soft or hard segment of PU to give pH-sensitivity. Popular pH-sensitive polyols used for synthesizing pH-sensitive PUs and their respective pKa values are listed in **Table 1-4**.

Table 1-4. pH-sensitive polyols for pH-responsive polyurethane synthesis.

Chemical name	Structure	pKa
2,2-Bis(hydroxymethyl)propionic acid (DMPA)		4.41
bis-1,4-(hydroxyethyl)piperazine (HEP)		6.40
N,N-bis (2-hydorxyethyl)-2-amino-ethane-sulfonic acid (BES)		7.10
2,2-(methylimino) diethanol (MIDE)		8.52
N,N-Bis(2-hydroxyethyl)glycine (BICINE)		8.30
Bis(2-hydroxyethyl)-disulfide (2-HDS)		6.30

The pH-responsive properties of pH-sensitive PU biomaterials are adjusted by synthesis strategies such as controlling the overall hydrophilic to hydrophobic segment ratio of the pH-sensitive PU, and controlling the position of pH-sensitive molecules on the soft or hard segment of PU. By increasing hydrophobicity or hydrogen bonding of the hard segment of pH-sensitive PUs, the pH-responsive shape-maintain/dissolved behavior can be changed to low-swelling/high-swelling behavior.

pH-responsive polyester-PUs were synthesized using polycaprolactone (PCL) as a long chain polyol.[9] One prepared, polyester-PU possessed pH-responsiveness via the pH-sensitive chain extender N,N-Bis(2-hydroxyethyl)glycine (bicine). The prepared polyester-PU showed a pH-responsive swelling ratio change and a controlled drug release in aqueous conditions. The prepared pH-responsive polyester-PU membrane, which has a pH-sensitive component bicine, showed little or no swelling in an aqueous condition from pH 3 to pH 6. However, the swelling ratio gradually increased as the pH increased from pH 6 to pH 8.3. Above pH 8.3 (pKa of bicine), the prepared pH-responsive PU membrane was able to be dissolved in the buffer solution because of rapid deprotonation of the carboxylic acid group of the bicine. Another pH-sensitive PU was synthesized using PCLdiol (Mn = 530), N, N-bis (2-hydroxyethylhydroxyethyl)-2-aminoethane-sulfonic acid (BES, pKa 7.1), and 4,4′-diphenylmethane diisocyanate (MDI).[10] The inkjet technique was applied for the fabrication of matrix of the PU. The BES incorporated PU matrix demonstrated significantly lower platelet attachment than a non-BES incorporated PU matrix. The PU was stable up to pH 8.7, but started dissolving at higher pH levels.

A stable polyester-PU membrane having both thermo- and pH-responsive characteristics was prepared by controlling the hydrophilic/hydrophobic ratio and using pH-sensitive groups.[58] Dimethylolpropionic acid (DMPA), and N-methyldiethanolamine (MDEA) were used as pH-

sensitive chain extenders for the pH-sensitive polyester-PUs synthesis. Aromatic diisocyanate MDI and the pH-sensitive chain extenders were used in the reaction with prepolymer to increase the molecular weight (Mw) and hydrophobicity of the final polyester-PU products. The polyester-PUs revealed phase-separated structures having similar phase-transition temperatures to a soft segment of the PU. The pH-sensitive component did not have a noticeable effect on the thermal characteristic of the synthesized polyester-PU. In addition, the prepared polyester-PU membranes had thermo- and pH-responsive water permeability due to a free volume hole size change. The prepared PU membranes showed more than 2 times higher water permeability at temperatures higher than the crystalline melting transition temperature of the soft segment. Moreover, the pH-sensitive PU membranes showed more than 2 times higher water permeability when immobilized pH-sensitive molecules DMPA and DMEA were protonated and de-protonated, respectively.

1.4.2.3 Photoresponsive polyurethanes

Photoresponsive PUs are prepared by immobilizing a photosensitive group on PU. For instance, a UV-responsive PU was prepared to increase the mechanical properties and biostability of a fabricated artificial blood vessel.[76] A polytetramethylene glycol-based medical grade PU (Pellethane® 2363-80AE) was reacted with aliphatic and olefinic acyl chlorides to prepare the UV-responsive PU for fabrication of a biostable crosslinked (networked) artificial blood vessel. The prepared ready-to-react PU was crosslinked by UV during and after the electrospinning process. The electrospun crosslinked PU artificial blood vessel showed satisfactory burst pressure (> 550 mmHg), and significant improvement in degradation resistance *in vitro*. The crosslinked graft showed approximately 2 times lower damage scores than the

uncrosslinked graft after *in vitro* degradation test performed in AgNO$_3$ or H$_2$O$_2$ solutions. In addition, a photo-curable PU resin was prepared for fabrication of artificial blood vessels.[77] The PU resin was synthesized for stereolithography using hydroxyl terminated poly(dimethylsiloxane) and poly(tetrahydrofuran) as polyols which reacted with isophorone diisocyanate, 2-hydroxyethyl methacrylate, and 2-methyl-1-propanol. The PU resin was successfully printed as an artificial blood vessel in a wide range of diameters (the smallest diameter was 1 mm). The printed PU artificial blood vessel demonstrated high durability, good mechanical properties, and excellent adhesion and cell proliferation of 3T3 mouse fibroblast cells.

Multi-shape-memory and multi-responsive shape-memory PUs have also been developed to be photoresponsive. A triple-shape-memory PU biomaterial with a pendant cinnamon group was fabricated.[78] A shape-memory polyester-based PU with a cinnamon group was synthesized, and the PU was crosslinked by UV irradiation at 356 nm. The crosslinked PU had a T$_g$-type segment (PCL) and T$_m$-type segment (the crosslinked structure of the PU hard segment). The crosslinked PU memorized three shapes: shape 0 (initial shape), shape I (deformed at 70 °C, cooled at 40 °C), and shape II (deformed at 40 °C, cooled at 0 °C), and recovered its shape as the temperature increased to 40 °C (shape I) and further to 70 °C (shape 0). Moreover, using UV light, the cinnamon group could be reversibly cleaved at $\lambda < 280$ nm and crosslinked at $\lambda = 356$ nm. The triple-shape-memory PU matrix demonstrated good non-cytotoxicity by the Alamar blue analysis. In a similar study, a photo- thermo- staged-responsive shape-memory PU network was developed.[79] The PU network was synthesized with PCL, 4,4-azodibenzoic acid (Azoa, photosensitive group), and HDI, followed by a chemical crosslinking reaction using glycerol, thereby increasing the stability of the PU. The pre-processed PU network with orientated Azoa

demonstrated a curling deformation as a response to UV light (365 nm) and the PU fully recovered its shape at 50 °C.

1.4.2.4 Bioresponsive polyurethanes

Bioresponsive PUs are sensitive to biological triggers such as abnormal pathological features. In addition, bioresponsive PUs have the ability to interact with or be activated by these features. This bioresponsive PU can be synthesized through immobilizing enzyme-cleavable linkages, signal proteins, or anticoagulants, such as vascular endothelial growth factor (VEGF) and heparin. For instance, an enzymatically-switchable antimicrobial PU was synthesized from PCL, isophorone diisocyanate (IPDI), and model biocide sulfanilamide (SA).[80] This enzyme-responsive PU showed substantially high resistance against hydrolysis at 37 °C for 120 hours in the absence of urease. However, bacteria-secreted urease was able to hydrolyze the PU within 24 hours to release SA, which leads to effective inhibition of Staphylococcus aureus, Escherichia coli, Pseudomonas aeruginosa, and Micrococcus luteus. This demonstrated over 10% bacteriostatic efficiency for the first 24 hours. The enzyme-responsive PU-coated surface showed no cytotoxicity to normal human dermal fibroblasts. In addition, a porous PU (ether-free, aliphatic, biostable PU, Medtronic Inc.) scaffold was fabricated and then surface functionalized with heparin.[81] The immobilized heparin binds to enzyme inhibitor, antithrombin III, and then inactivates thrombin to prevent blood coagulation. This heparinized porous PU scaffold demonstrated an increase in the number (66.2 ± 0.8 to 107 ± 1 vessels/mm^2) and the total area (0.9 ± 0.1 to 1.40 ± 0.02%) of capillaries due to anticoagulation resulted from the immobilized heparin, the high porosity of the scaffold, and low inflammatory response. In addition, the PU scaffold showed an increase in arterialization in absolute terms (200% in number).

1.4.3 Biostable polyurethane

Biostability is a key factor for long-term implantable biomaterials since PU can be chemically degraded by oxidative attack. Biologically, reactive oxygen species are released from adherent macrophages, and foreign-body giant cells can activate the biodegradation of PU *in vivo*.[82–84] Therefore, the degree of crystallinity is one of the important aspects in the design of biostable PUs. A higher hard segment content in PU can help increase the hydrolytic resistance because of the higher degree of hydrogen bonding[85] contributing to stable hard segment linkages that can resist enzyme hydrolysis. Possible hydrogen bonding for PUs is seen in **Table 1-5**.

Table 1-5. Potential hydrogen bonding in polyurethanes.
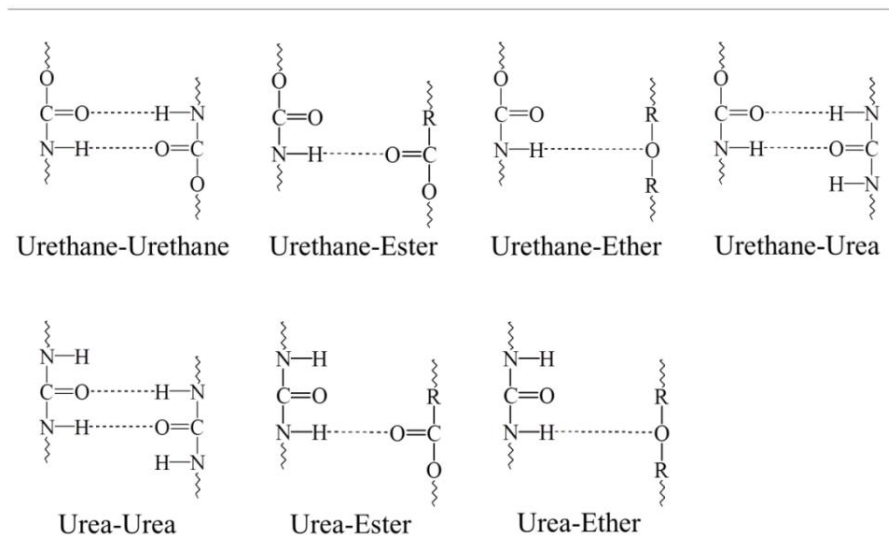
To increase the mechanical strength and physical stability of PUs, a chemically crosslinked PU network can be synthesized. An advantage of a networked PU is that it can be

prepared via reactive molding of two liquid components: a prepolymer of PU and polyol (functionality is > 3). Therefore, the networked PU can be formed into solid resins or porous biomaterials after *in vivo* injection of the components.

Poly(carbonate urethane)s have been studied as biostable elastomers for long-term implantable PU biomaterials. For instance, micro-catheters using poly(carbonate urethane) (Bionate®, the reaction product of hydroxyl terminated polycarbonate, aromatic diisocyanate, and low molecular weight glycol chain extender) and poly(ether urethane) (Pellethane®, the reaction product of polytetramethylene ether and diphenyl methane di-isocyanate/butanediol) were prepared to compare long-term *in vitro* stability.[86] The prepared PU catheters were stretched and exposed to a hydrogen peroxide/cobalt chloride (H_2O_2/$CoCl_2$) solution for up to 10 months. The polycarbonate soft segment was more stable to oxidative degradation than the polyether soft segment. Minimal degradation of the polycarbonate soft segment was detected in the 10-month experimental period.

Fluorinated alcohols are also useful to increase the biostability of PU biomaterials. Fluorocarbon end-capped poly(carbonate urethane)s (FPCUs) were synthesized to increase biostability of PU using a fluorinated alcohol, 2,2,3,3,4,4,5,5,6,6,7,7,8,8,8-pentadecafluoro-1-octanol (PDFOL).[87] The surface of the fabricated material using the fluorocarbon end-capped poly(carbonate urethane)s showed an increased non-polar characteristic due to the orientation of the fluorinated tails on the surface. This has potential to increase the biostability because the fluorocarbons and the hard segments are stable against hydrolysis and oxidation.

Silicon-based PUs have been developed to increase the biostability of the PUs, since silicon is highly stable to temperatures, oxidation, and water. Silicon-based thermoplastic PU nanocomposites were prepared using commercial ElastEonTM E5325, a silicon-based PU.[88] In

vitro biostability of the nanocomposites was tested under physiologically relevant oxidizing conditions. The prepared silicon-based PU nanocomposites showed improved biostability against metal ion-induced oxidation. The nanocomposites showed a marginal toughness change of 9~28 Mpa for 7 weeks compared to an untreated sample of 40 Mpa. The silicon-based PU composite material was suggested for use in long-term implantable biomaterials, such as artificial intervertebral discs (IVDs). In other research, layered silicates, which are more chemically resistant than native PU, were added to the polyether-PU to improve biostability.[89] For the research, commercially available and organically modified montmorillonite, Cloisite® 30B (QACMMT), was used. QACMMT has quaternary ammonium compounds (QAC), methyl tallow bis-2-hydroxyethyl ammonium chloride, as an organic modifier. Following the addition of dispersed QACMMT at loadings lower than 3 wt%, the biostability of the PU was enhanced significantly up to 50 % due to decreased material permeability.

Polyisobutylene-based PUs have been actively researched to increase the biostability of the PUs. A series of polyisobutylene-based polyureas and PUs was synthesized.[90–95] Biostable amine-telechelic polyisobutylene (PIB) oligomers (H2N-PIB-NH2, Mn = 2500 and 6200 g/mol) based polyureas, which had hard segment contents up to 46.5 wt%, were synthesized using various aliphatic diisocyanates and diamine chain extenders.[90] The PIB-based polyureas exhibited unprecedented hydrolytic and oxidative stability because of the presence of a continuous nonpolar PIB matrix. In addition, PIB/poly(tetramethylene oxide) mixed soft segments were used to synthesize biostable polyureas.[94] The prepared mixed soft segment polyurea, which had 12% poly(tetramethylene oxide) (PTMO), showed better oxidative/hydrolytic stabilities than both Bionate® (a medical grade thermoplastic polycarbonate-urethane) and Elast-Eon® (a biostable and biocompatible silicone/urethane

24

elastomer). Bionate® and Elast-Eon® are commercially available oxidation- and hydrolysis-resistant PUs. The PTMO-reinforced PU showed almost no change in tensile strength and elongation at break. However, Bionate® and Elast-Eon® showed about 3 times less tensile strength and elongation at break after exposure to 35% HNO_3 at room temperature for 4 hours. It was explained that the surfaces of the mixed soft segment polyureas were protected by the chemically inert PIB segments which can lead to good biocompatibility. When PIB-based polyureas and Bionate® were implanted in rats for 4 weeks *in vivo,* the PIB-based polyureas showed superior biocompatibility compared to the Bionate® in the rats.[92] The PIB-based polyureas showed 5.0 ± 0.2 while Bionate® showed 7.7 ± 0.1 total mean scores for lymphocyte infiltration, fat infiltration, irregular cells, and irregular tissue evaluations in a peritoneal wall implantation test. PTMO and polyhexamethylene carbonate were used as an additional soft segment to mix with PIB to synthesize PUs.[91] Bis(4-isocyanatocyclohexyl)methane (HMDI), hexane diol (HD), 1,4-butanediol (BD), 1,6-hexamethylene diamine (HDA) were used as a hard segment of the PUs. The PIB-based PU, PIB/PTMO-PU, PIB/polyhexamethylene carbonate-PU, and the commercial PUs Elast-Eon® and Carbothane® (polycarbonate-based thermoplastic PU) were each exposed to H_2O_2/$CoCl_2$ solutions for up to 14 weeks to compare their biostability. The prepared PIB-based PUs showed better results compared with the commercial PUs (Elast-Eon® and Carbothane®). The PIB-based PU showed a noticeable increase in tensile strength (up to 2 times higher) when mixed with the additional soft segments PTMO and polyhexamethylene carbonate.

A polyisobutylene (PIB)-based thermoplastic PU was synthesized using polyisobutylene diol for the soft segment formation, and 4,4´-methylene bis(phenyl isocyanate) (MDI) and BD for hard segment formation.[96] Long-term stability of prepared PIB-based PUs was evaluated

under accelerated conditions in 20% H_2O_2 solution containing 0.1 M $CoCl_2$ at 50 °C to predict resistance to metal ion oxidative degradation (MIO) *in vivo*.[97] Biocompatibility of the prepared PUs was qualified by adsorption of fouling protein fibrinogen (Fg) and passivating protein human serum albumin (HSA).[98] Competitive adsorption experiments were performed by preparing a mixture of Fg and albumin in a physiological ratio followed by the addition of GPIIb-IIIa (a platelet receptor ligand that selectively binds to Fg). The synthesized PIB-based PU showed biostability to oxidative treatment for 12 weeks and similar biocompatibility compared to industrial controls such as PellethaneTM 2363-55D (a polytetramethylene glycol based PU elastomer) and 2363-80A (an aromatic, flexible polyether-based thermoplastic PU). The biostable electrospun membrane, fabricated using the synthesized PIB-based PU, could be a promising biomaterial for use in biostable artificial blood vessels because of its biostability, processability, and the physical properties of the prepared PU.[99]

1.4.4   Polyurethane intravaginal rings

The intravaginal ring (IVR) is a synthetic biomaterial which can be placed on the tract of a vagina, adjacent to the cervix.[5] The IVR has been developed to protect women from unwanted pregnancy, HIV, and other STIs.[100] IVRs are currently gaining popularity because of the success of the NuvaRing®,[101] a contraceptive IVR made of ethylene vinylacetate copolymers approved by FDA. The biomaterial for this flexible soft torus-shaped IVR can contain and release drugs. The concept of sustained drug release from the IVR was first introduced in 1970. Two types of IVR, the matrix type and the reservoir type, are currently fabricated for drug delivery.[5] During fabrication, the matrix type is mixed with drugs which are dispersed throughout the polymeric matrix, so, the release of the drug depends on the drug loading conditions and the device surface

area. The reservoir type is fabricated with drugs loaded into the core or has a hollow structure for drug loading, so the release of the drug can be controlled via thickness, structure, and the physicochemical properties of the outer layer of the IVR. Moreover, the reservoir IVR can have constant daily release rates and linear cumulative release versus time profile characteristics.[6]

PU has been used for the fabrication of drug delivery devices.[102] PU IVRs were developed for the release of relatively hydrophilic drugs. Typically, PU IVRs are fabricated using continuous hot melt extrusion or injection molding methods because of the thermoplastic characteristic of PU. PU has varying degrees of crystallinity and hydrophobicity, which affects the fabricated IVRs and drug release properties. As a result, various types of drugs can be delivered using PU IVRs. Potentially, drug release from IVRs can be controlled by the pH change of vaginal fluid.[103] The normal pH range of the female genital tract is 3.5-4.5.[36,104] However, the pH can be increased to neutral by seminal fluid during heterosexual intercourse[33] and can trigger drug release from IVRs having pH-responsive materials. For instance, cellulose acetate phthalate (CAP) fibers to be used for semen induced anti-HIV drug delivery were fabricated by electrospinning. Because of the pH-dependent solubility of CAP, the incorporated drug in the fiber, Rhodamine 6G, released quickly in pH 7.2 and did not release in the simulated vaginal fluid.[105] pH-responsive PU is a potential biomaterial for pH-responsive IVR fabrication.

PU IVRs have been studied for delivering drugs for birth control and STI, especially HIV. A polyether-PU IVR was fabricated for antiretroviral microbicide UC781 release using Tecoflex® EG-85A (a medical-grade aliphatic polyether-based thermoplastic PU) via a hot melting extrusion process.[106] The prepared polyether-PU IVR presented suitable continued UC781 release characteristics for 30 days. The loaded UC781 in the polyether-PU matrix showed good chemical stability, but crystallization of UC781 on the matrix surface was observed

at high concentrations of loaded UC781 in long-term storage. However, the polyether-PU IVR did not show a significant effect on viability, tissue integrity, or cytokine expression in the tissue irritation model.

Additionally, a hydrophilic polyether-PU IVR was fabricated using custom designed HPEU 20 (a hydrophilic polyether urethane) for sustained delivery of TFV (an HIV-1 nucleotide reverse transcriptase inhibitor).[107] The hot melt extrusion and injection molding method was used for TFV-loaded hydrophilic polyether-PU IVR fabrication. The prepared IVRs showed similar mechanical properties to NuvaRing®. The pseudo-steady-state diffusion model was used to explain the drug release behavior. It was suggested that the prepared hydrophilic polyether-PU IVR system was the first vaginal dosage formulation providing sustained delivery of milligram quantities of TFV for 90 days. TFV disoproxil (TFV D) was formulated in a polyether-PU IVR for prevention of HIV and HSV.[108] The released TFV D from the polyether-PU IVR showed HIV and HSV inhibition properties at a noticeably low concentration in the presence of semen. The prepared TFV D formulated polyether-PU was suggested as a potential drug device for sustained HIV and HSV protection. TFV D formulated PU IVRs were prepared and implanted into the vagina of macaques for evaluation.[109] For the preparation of the PU IVRs, an inner hollow ring shape was fabricated, and sodium chloride (NaCl) was inserted on the inside of the reservoir IVR to establish a drug solubility in the core and to achieve an even drug release. A mediated release is achieved because vaginal fluid hydrates the water-swellable hydrophilic polyether-PU, which then allows water to be driven into the osmotically active drug-NaCl core, resulting in TFV D being dissolved and released from the IVR. The prepared reservoir IVRs showed noticeable anti-HIV properties in a long-term *in vivo* test, performed over 30 days, and were associated with TFV D concentration in the vaginal fluid. The protection was associated

with the TFV D levels found in the vaginal fluid [mean 1.8×10^5 ng/mL (range 1.1×10^4 to 6.6×10^5 ng/mL)]. Anti-retroviral pyrimidinediones, IQP-0528 (PYD1) and IQP-0532 (PYD2), were evaluated for release from polyether-PU IVRs *in vivo* in the pigtail macaques study.[110] The polyether-PU was fabricated using medical grade Tecoflex EG-85A PU using a hot melt extruder. The *in vivo* drug release study showed sustained release of PYD1 and PYD2 over 28 days. The formulated PYD1 and PYD2 in the IVRs were chemically stable for 90 days of storage. The pigtail macaque model of *in vivo* drug release study could be a useful tool for evaluating and screening drug loaded IVRs before pre-clinical and clinical evaluation.

The commercially available hydrophilic aliphatic polyether-PUs: TecophilicTM HP-60D-20, HP-60D-35, and HP-60D-60, were used for IVR fabrication. The reservoir PU IVRs were prepared by filling the interior of the hydrophilic PU IVRs with TFV, glycerol, and a water-based semi-solid paste for sustained drug release.[111] Hydrophilicity of the PU increased the release ratio of TFV. The 35% water swellable PU (HP-60D-35) IVR showed a sustained TFV release for 90 days with no noticeable change in mechanical stiffness the *in vivo* sheep study. The prepared reservoir hydrophilic PU IVRs had no significant toxicity or inflammatory infiltrates in the vaginal epithelia.

Dual-reservoir PU IVRs were developed for the inhibition of HIV infection and pregnancy using a hydrophilic polyether-PU and a non-swellable polyether-PU in the same device to administer two different drugs, TFV and levonorgestrel (LNG); an anti-HIV drug and a contraceptive drug, respectively.[112] The prepared dual-reservoir PU IVR was introduced as the first long-acting multipurpose prevention drug delivery system.

Polyether-PU IVRs have been designed as a device to deliver the potential anti-HIV drug, hydroxychloroquine (HCQ).[113] The prepared IVRs used a surface modified matrix PU IVR and a

reservoir PU IVR. The polyvinylpyrrolidone or poly(vinyl alcohol) (PVA)-coated matrix PU IVR demonstrated significantly reduced burst release compared to uncoated control. Moreover, the reservoir PU IVR showed near zero-order release kinetics with a suitable daily average release rate. The resulting PU IVRs were non-cytotoxic when incubated in the presence of human vaginal and ectocervical epithelial cell lines. The fabricated IVRs were suggested as potential anti-HIV release devices. The fabricated reservoir PU IVRs were used for evaluation of the impact on the growth of Lactobacillus crispatus and Lactobacillus jensenii since the decrease of lactobacillus family leads to inflammation of the female genital tract by the growth of pathogenic bacteria.[114] The drug-free reservoir PU IVRs and the released HCQ had no significant impact on Lactobacillus growth or the viability of vaginal and ectocervical epithelial cells.
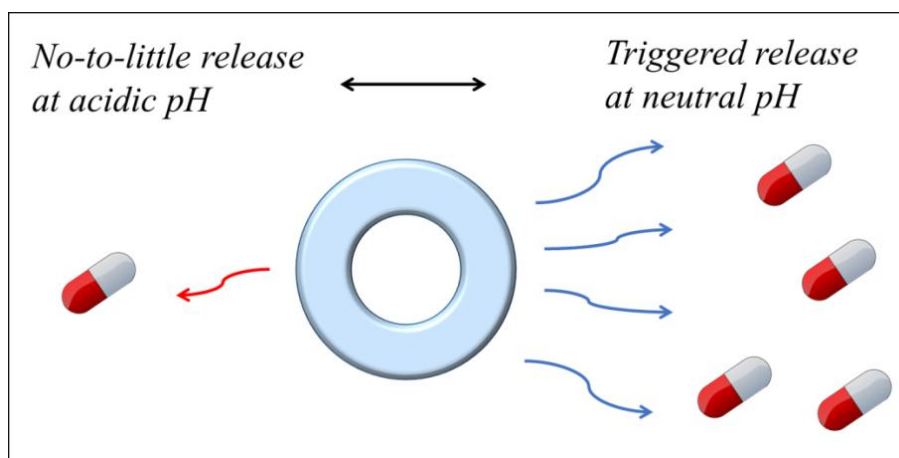
Figure 1-2. Diagram of pH-responsive IVR for the on-demand release of drugs.

Potentially, pH-responsive polyether-PU membranes can be developed as a "window" membrane of reservoir-IVR (**Figure 1-2**). The change of vaginal tract pH when heterosexual intercourse occurs can be a cue for triggered release of anti-HIV drugs or nanocarriers since the

normal pH of human vagial tract is acidic (pH 3.5-4.5) and the pH can be elevated to neutral by introduction of human seminal fluid. Therefore, potentially, pH-change triggered morphology and physicochemical changes of the membranes could control the permeability of anti-HIV drugs or nanocarriers.

1.4.5 Summary of smart biostable polyurethane biomaterials and questions for future outlook

PUs have various applications depending on their chemical structure and fabrication method. PU has been developed as a stimuli-responsive biomaterial because of its tunable physicochemical characteristics. In addition, PU has distinguished thermoresponsive characteristics as a result of its unique soft segment and hard segment block copolymer structure. Shape-memory PUs are prepared by controlling the thermoresponsive characteristic. Also, pH-responsive properties are enabled by placing pH-sensitive polyols or polyamines on the soft or hard segment of the PUs. Moreover, photoresponsive PUs may be synthesized using photosensitive groups as a polyol, chain extender, or end-group of the PU. Additionally, bioresponsive PUs are synthesized by immobilization of enzyme-sensitive molecules and signal proteins.

Biostability is one of the crucial factors to consider for long-term implantable biomaterials, such as for IVRs, artificial blood vessels, or artificial IVDs. The biostability of PUs increases by using polyols, which are stable toward hydrolysis, enhancing the semi-crystalline characteristic of the hard segment, and modifying the ends of PUs. So far, several long-term implantable smart PU biomaterials have been developed as outlined in the foregoing paragraphs.

However, many research questions remain to be answered and several obstacles remain to be overcome for the development of smart and biostable PU biomaterials.

PU IVRs have been designed as a controlled intravaginal drug release device. Most of the developed PU IVRs have been fabricated using the hot injection molding or hot-melt extrusion methods. Stimuli-responsive PU IVRs can be fabricated by these methods. However, macromolecules, such as proteins/peptides drugs, siRNA, and their nanocarriers, have very low diffusion efficiency for crossing the non-porous outer layer of IVR. Nanocarrier is often needed for increasing the delivery efficiency of siRNA and poorly water-soluble drugs through biological barriers, such as vaginal mucus and the cellular membrane. For controlled release of macromolecular nanomedicine from IVRs, novel fabrication methods should be suggested. Can the 3D printing method be used to fabricate interconnected porous IVRs which can tune the release of nanomedicines from the hollow lumen in response to environmental cues? Stimuli-responsive and biostable PUs are potential candidates for the fabrication of novel IVRs. To increase the smart functions of stimuli-responsive PU IVRs, are structural specialties, such as microfluidic channels, necessary? If the microfluidic channels of stimuli-responsive PU IVRs can increase the control of nanocarrier release, how can stability of nanomedicine during penetration be ensured? Antifouling or self-cleaning effects may need to be applied to the surface of IVRs. Potentially, smart PU IVRs can achieve the pH-responsive on-demand release of nanomedicines. Can we use the smart PU IVRs for the early detection of HIV? How can bioresponsive PU detect HIV and respond to the infection?

Although there are many questions for the future development of smart PU biomaterials for long-term implantable application, it is evident that smart PUs can be adopted in a wide range of biomedical applications based on their tunable physicochemical characteristics. It is also

evident that smart long-term implantable biomaterials can be designed and fabricated by controlling the chemical structure of PU and physical structure of fabricated biomaterials.

1.4.6 Acknowledgements

1.4.7   Contribution of Authors

Seungil Kim[†]: initiated and contributed to the scope of the manuscript; wrote the manuscript.

Song Liu[†, ‡, §, *]: initiated and contributed to the scope of the manuscript; contributed writing manuscript; critically reviewed and revised the manuscript.

[†]Biomedical Engineering, Faculty of Engineering, University of Manitoba, Winnipeg, Manitoba, Canada

[‡]Department of Biosystems Engineering, Faculty of Agricultural and Food Sciences, University of Manitoba, Winnipeg, Manitoba, Canada

[§]Department of Medical Microbiology, Rady Faculty of Health Science, University of Manitoba, Winnipeg, Manitoba, Canada.

1.5   Self-assembled poly(aspartic acid) graft copolymers as a nanocarrier.

Poly(amino acid)s have been used to develop biomaterials such as nanocarriers, hydrogels, and scaffolds due to their similarity to naturally occurring proteins.[115,116] Amphiphilic poly(amino acid)s, graft or block copolymers with hydrophobic segments, show similar characteristics to lipid monolayers and can self-assemble into nanocarriers in an aqueous environment through hydrophobic interaction (**Figure 1-3**). These self-assembled nanocarriers have a hydrophobic core and hydrophilic shell allowing hydrophobic drugs to be loaded in the core or hydrophilic drugs in the shell.
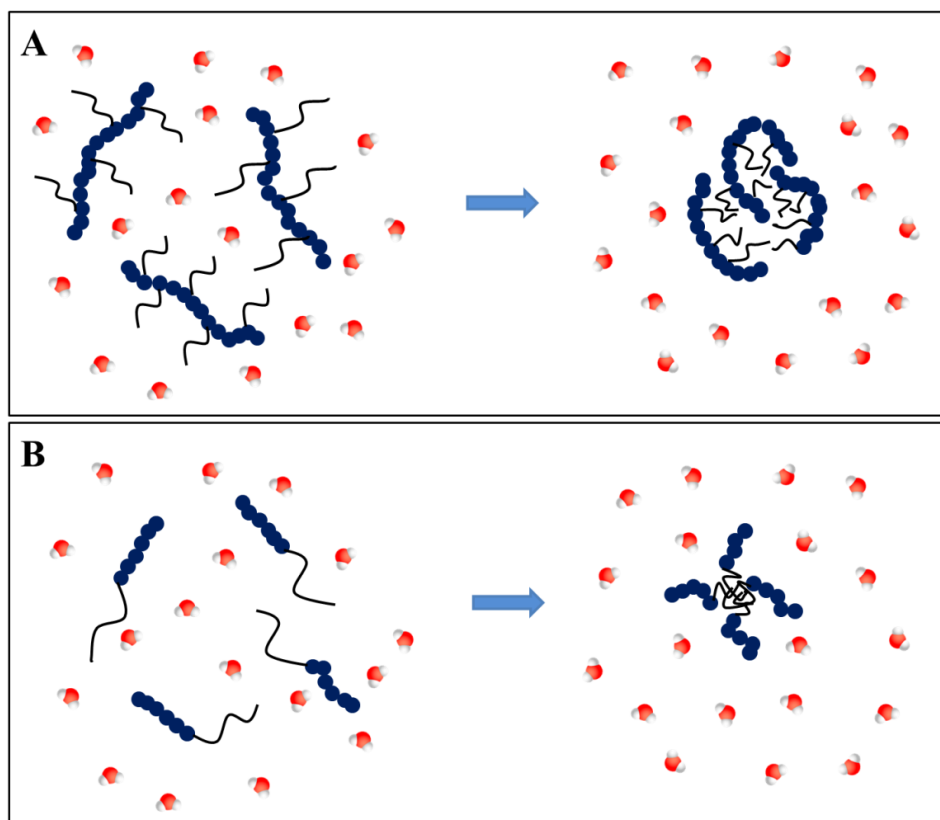
Figure 1-3. Illustration for the self-assembly of amphiphilic poly(amino acid) copolymers (A) graft copolymer and (B) block copolymer driven by hydrophobic associations.

Amphiphilic poly (amino acid) copolymers have different self-assembly structures such as micelles, vesicles, and solid particles resulting from their physiochemical characteristics.[115] As an example, amphiphilic poly(glutamic acid) (PGA, pKa 2.2) copolymers conjugated with phenylalanine (degree of substitution (DS) > 50%) as a hydrophobic segment were synthesized and successfully self-assembled into stable NPs (DI > 100 nm) as a nanocarrier of hydrophobic drugs, proteins, and plasmid DNA.[117–119]

Increasing hydrophobicity

| Micelle | Vesicle | Solid nanoparticle |
| DI < 100 nm | DI > 100 nm | DI > 100 nm |

● **Hydrophilic segment**   ∿ **Hydrophobic segment**
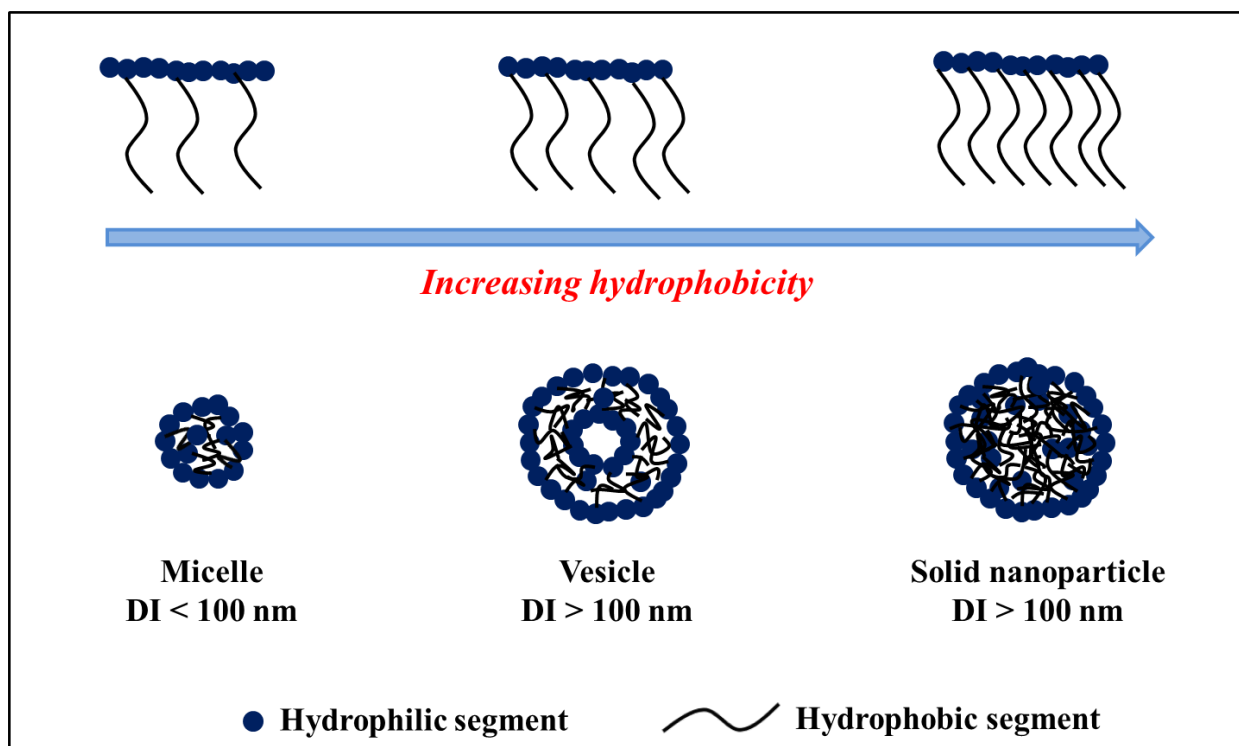
Figure 1-4. The self-assembly of amphiphilic graft poly(amino acid) copolymer into: solid nanoparticles, vesicles, and micelles.

The relative ratio of hydrophilic segments to hydrophobic segments in poly (amino acid) dictates the self-assembly structure. As illustrated in **Figure 1-4**, a higher hydrophilic/hydrophobic ratio gives rise to micelles, an intermediate hydrophilic/hydrophobic ratio leads to vesicles, and a lower hydrophilic/hydrophobic ratio results in the formation of solid nanoparticles. Drugs, targeting moieties, antibodies, and fluorescent tags can be conjugated to the surface of nanocarriers and siRNA can be loaded by electrostatic interaction with the nanocarrier.

Poly(aspartic acid) (PASP, pKa 3.9) is a specific water-soluble and biodegradable poly(amino acid) with nontoxic degradation products[120–122] having carboxylic acid groups which can be used for further chemical derivatization with fluorescent tags or for antibody conjugation. Amphiphilic PASP graft copolymers have been favored because of their relatively facile preparation methods as compared to block copolymers. Direct conjugation of various molecules having nucleophilic primary amine or hydroxyl groups on the backbone of polysuccinimide (PSI) can yield PASP graft copolymers with various funtionalities.[123–127] Amphiphilic PASP graft copolymers can be synthesized from PSI by nucleophilic conjugation of hydrophobic segments such as long chain alkylamine followed by alkaline hydrolysis. The amphiphilic PASP graft copolymers can self-assemble in aqueous solution by hydrophobic interaction and the particle size can be tuned by various structural factors such as length and DS of hydrophobic side chains. The effect of conjugation of alkylamines (DS < 10%) such as dodecylamine (DDA), hexadecylamine (HDA), octadecylamine (ODA) on self-assembly behavior of amphiphilic PASP was studied.[125] The amphiphilic PASP copolymers successfully self-assembled into micelles (DI < 100 nm) by strong hydrophobic interaction. The micelles conjugated with ODA showed the highest surface tension and a minor change of the surface tension by an increase of concentration

because conjugated ODA is in a frozen state below its melting temperature (T_m, 52.9 °C). However, micelles conjugated with DDA or HDA showed a decrease of surface tension with an increase in temperature. The stability of the micelles in aqueous solution was maintained when hydrophobic interaction overcame the stiffness of the PASP backbone. Additionally, an amphiphilic PASP conjugated with 1-hexadecylamine (HDA, DS: 20 %) was synthesized from PSI and then further modified by conjugation of various amino acids such as L-valine, L-serine, L-leucine, and ß-alanine.[121] The HDA conjugated amphiphilic PASP graft copolymer and its derivatives with amino acids self-assembled into micelles (DI: 15-65 nm). The amphiphilic PASP graft copolymers have been successfully used for delivering drugs.[126,128]

Chapter 2

Hypothesis and Objectives

2.1 Rationale and Hypothesis

An intravaginal drug delivery device that would release drugs only at the time of heterosexual intercourse and provide prolonged and continuous protection would improve efficacy and reduce toxicity. Immediately after ejaculation,[24,129,130] during hetero-sexual intercourse, seminal fluid changes the normally acidic vagina from pH less than 4.5 to neutral.[33,104,131] According to TEVI-BE´NISSAN et al,[24] full elimination of semen from the vagina takes 20 h and the vaginal ecological microenvironment only returns to its normal acid pH 48 hours after intercourse. It is inferred that the elevated pH could be maintained around neutral for at least a couple of hours because sperm needs an alkaline or neutral environment to be able to survive and swim to fertilize the egg.[132,133] The overarching hypothesis is that a pH-responsive IVR system can be developed to realize on-demand on-and-off release of drugs or nanoparticles (NPs) in response to vaginal pH change due to sexual intercourse.

2.2   Objectives to be achieved

The objective of this work is to develop and characterize novel, reversibly pH-responsive PU biomaterials that can be incorporated into IVRs for on-demand release of drugs or NPs, i.e. little or no release at $pH < 4.5$ and rapid release at $pH > 6.5$.

Specifically, I have:

1.   Synthesized and characterized new pH-responsive PUs;

2.   Fabricated PU membranes with the pH-responsive PUs to serves as a "window" membrane of two-component IVRs for switchable pH-responsive delivery of drugs which might potentially prevent HIV infection;

3.   Synthesized a new PU gel and incorporated it in "multi-use" reservoir-based IVRs to fulfill pH-responsive on-demand release of NPs;

4.   Established and elucidated the processing-structure-property relationship of successfully synthesized and/or fabricated pH-responsive PU biomaterials.

2.3 New pH-sensitive polyurethanes for smart intravaginal delivery of drugs and nanocarriers

In this thesis, mainly three kinds of new pH-sensitive polyether-PU copolymers (PEG-HEP-HDI-PG, PEG-HEP-MDI-PG, PEG-DMPA-HDI-PG) were synthesized (**Scheme 2-1,2,3**)

1) First step

2) Second step

Scheme 2-1. Synthesis scheme of pH-responsive PU; PEG-HEP-HDI-PG (PHHP)

1) First step

PEG + **HEP** + **MDI**

$$\xrightarrow[60^oC]{3\ h}$$

Prepolymer

2) Second step

Prepolymer + **PG** + **MDI**

$$\xrightarrow[60^oC]{3\ h}$$

Chain-extender
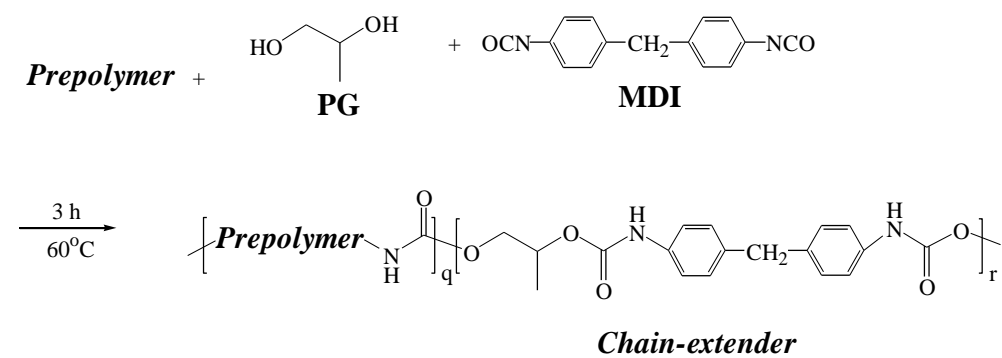
Scheme 2-2. Synthesis scheme of pH-responsive PU; PEG-HEP-MDI-PG (PHMP)

1) First step

PEG   **DMPA**   **HDI**

$$\xrightarrow[60^{\circ}C]{6\ h}$$

Prepolymer

2) Second step

Prepolymer +

PG   **HDI**

$$\xrightarrow[60^{\circ}C]{24\ h}$$

Chain-extender
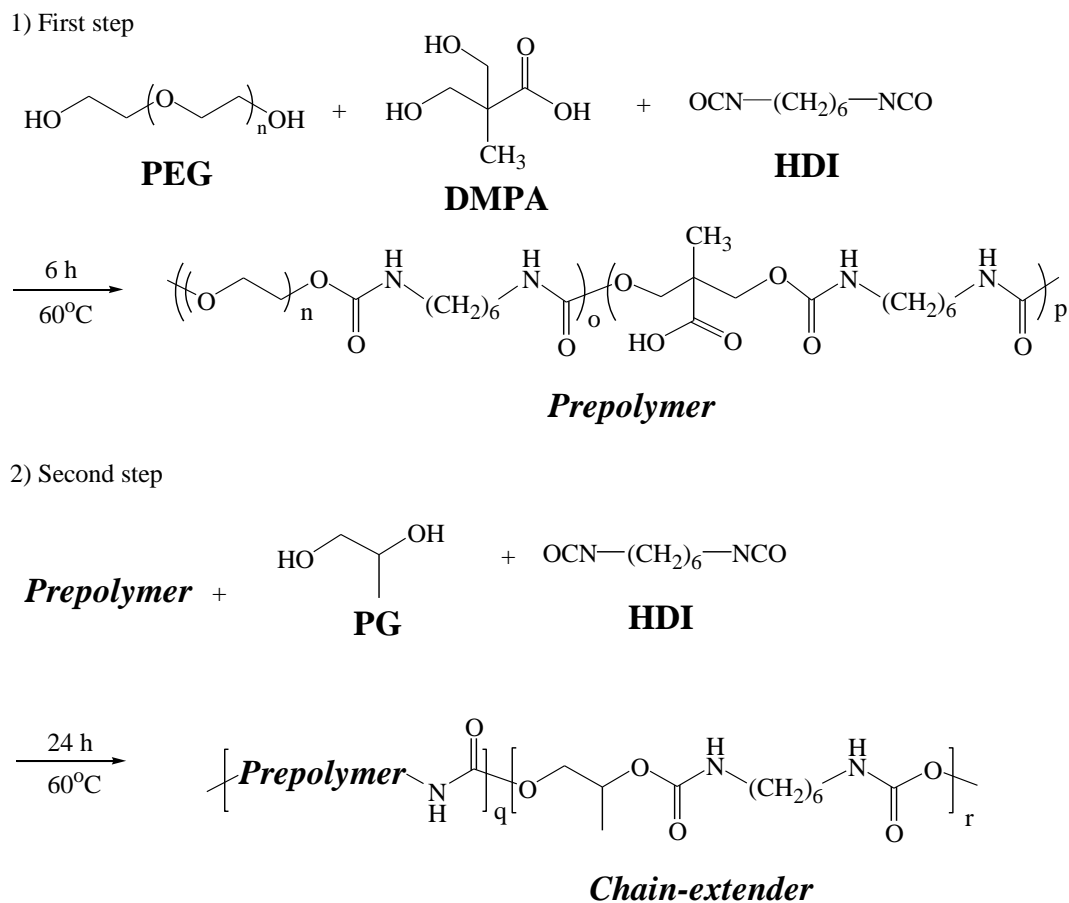
Scheme 2-3. Synthesis scheme of pH-responsive PU; PEG-DMPA-HDI-PG (PDHP)

PEG was used as a hydrophilic soft segment for all PUs. HEP or DMPA was chosen as a pH-sensitive agent since their conjugate acids have a pKa of 6.4 or 4.4, respectively. These pH-sensitive molecules were immobilized in prepolymers to allow rapid and dramatic pH-sensitive response. PG was used as a chain extender with diisocynate to extend the hydrophobic domain of the pH-responsive PU copolymers.

Figure 2-1. Schematic illustration for the pH-responsive behavior of solvent-cast PEG-HEP-HDI-PG and PEG-HEP-MDI-PG membranes (A), electrospun PEG-HEP-MDI-PG membrane (B), and supramolecular PEG-DMPA-HDI-PG hydrogel (C).

The pH-sensitive PUs, PEG-HEP-HDI-PG, PEG-HEP-MDI-PG, PEG-DMPA-HDI-PG, were used fabricate pH-responsive intravaginal biomaterials. Solvent-cast pH-responsive PEG-HEP-HDI-PG and PEG-HEP-MDI-PG membranes showed pH-triggered reversible changes in swelling ratio and morphology (**Figure 2-1, A**). Electrospun pH-responsive PEG-HEP-MDI-PG membranes showed pH-dependent changes of morphology (pore sizes, fiber diameters, and thickness) and surface charge (**Figure 2-1, B**). PEG-DMPA-HDI-PG formed a supramolecular hydrogel at 20 wt% in distilled water and showed pH-responsive change in swelling behavior (**Figure 2-1, C**). Overall, these pH-responsive PU biomaterials successfully demonstrated their potential use in on-demand intravaginal release of drugs or nanocarriers.

Chapter 3

Reversibly pH-responsive polyurethane membranes for

on-demand intravaginal drug delivery

Seungil Kim, Yufei Chen, Emmanuel A. Ho, Song Liu

As a part of this thesis, new pH-responsive PUs, PEG-HEP-HDI-PG and PEG-HEP-MDI-PG, were synthesized and their pH-triggered responsiveness have been confirmed. Overall, solvent-cast pH-responsive PU membranes were prepared and their potential use in intravaginal application for on-demand release of drugs was evaluated. The hypothesis of this research is that the pH-triggered physicochemical responsiveness of the PUs can contribute to switchable on-demand on-and-off release of anionic drugs.

3.1 Abstract

To provide better protection for women against HIV, on-demand intravaginal drug delivery was attempted by synthesizing reversibly pH-responsive polyether-PU copolymers using PEG and HEP. Chemical structure and thermo- characteristics of the synthesized PUs were confirmed by ATR-FTIR, ^{1}H-NMR, and melting point testing. Membranes were cast by the solvent-cast method using the prepared pH-responsive PUs (PEG-HEP-HDI-PG and PEG-HEP-MDI-PG). The impact of varying pH on membrane swelling and surface morphology was evaluated using swelling ratio change and SEM. The prepared solvent-cast pH-responsive PU membranes showed two times higher swelling ratio at pH 4.0 than at pH 7.0 and a pH-triggered reversible surface morphology change. The anionic anti-inflammatory drug diclofenac sodium (NaDF) was used as a model compound for release studies. The solvent-cast pH-responsive PU membranes allowed continuous NaDF release for 24 h at 37 °C and over 20% of total NaDF released at pH 7.0 within 3 h but close-to-zero drug release at pH 4.5. NaDF permeation across the prepared membranes demonstrated a switchable pH-responsiveness. The solvent-cast pH-responsive PU membranes did not show any noticeable negative impact on vaginal epithelial cell viability or induction of pro-inflammatory cytokine production compared to controls. Overall,

the non-cytotoxic pH-responsive PUs, PEG-HEP-HDI-PG and PEG-HEP-MDI-PG, demonstrated their potential to be used in membrane-based implants such as intravaginal rings to achieve on-demand "on-and-off" intravaginal anionic drug delivery.

3.2 Introduction

STIs including HIV are a significant health concern.[134] Over 30 million people in the world are suffering from HIV infection, especially women living in sub-Saharan Africa. Biologically, women are at two times greater risk of heterosexual HIV infection compared to men with male-to-female transmission being eight times more likely to occur than female-to-male transmission due to anatomical differences such as the larger surface area of the anterior female genital tract.[135] For HIV prevention, various strategies such as condoms, vaginal gels, and IVRs have been developed.[35,113] Despite being an effective method of preventing HIV and unplanned pregnancy, condoms require consent of the other partner and may be refused due to socio-cultural reasons.[41,106,136] Vaginal gels are inconvenient and must be applied immediately prior to sexual intercourse.[36] IVRs are torus shaped polymeric devices approved for contraception and are currently being evaluated as an effective dosage form for the anti-HIV drugs delivery.[100,101,114] Benefits of IVRs include the fact that they can provide sustained controlled drug release for prolonged periods of time and can be used discreetly by women without the consent of their partner. There are two main types of IVRs: matrix-type and reservoir-type.[5] Drug release rates from matrix-type IVRs are proportional to both drug loading and device surface area. Although the matrix-type IVRs have certain advantages, they suffer from an initial burst release and following continuously decelerated release, which might be inferior to reservoir-type IVR which can achieve the zero-order release. Zero-order release of

anti-HIV drugs is more desirable in this application.[6] However, it may not be ideal to continuously release drugs when not required as this can result in side effects.[19] We propose to develop a "smart" drug delivery system fabricated from pH-responsive PU which allows permeation of drugs at pH > 6.5 but close-to-zero drug release at pH < 4.5. This is due to the fact that under normal physiological conditions the pH of the human female genital tract is 3.5-4.5 (average 4.2),[35,104] and can be elevated to neutral (> 6.5) in the presence of seminal fluid during heterosexual intercourse.[33] This distinct pH change can be utilized as a stimulus to trigger switchable pH-responsive topical drug release from the "smart" delivery system.

PU is one of the oldest cost-effective synthetic elastomeric polymers for biomaterials.[69] It has been used for IVRs fabrication due to its controllable elastomeric and thermoplastic characteristics.[113,114] Generally, PU elastomers are synthesized from three components: long chain polydiol, polyisocyanate, and chain extender (short chain polyol or short chain polyamine). The elastomeric characteristic of the PU arises from its distinguished chemical structure, which consists of a soft segment and hard segment. Long and flexible polydiol chains typically make up the soft segment, and polyisocyanate and short chain polyols or polyamines constitute the hard segment.[137] The hard segment acts as a physical cross-linking domain because of the arrangement of the hard segment. Upon mechanical deformation, the hard segment prevents irreversible flow of the polymer material.[13] pH-responsive PUs have been synthesized for pH-triggered drug release, however, many of the studies focused on the fabrication of PU nanoparticles for one time pH-responsive drug release, i.e. the pH-triggered drug release was not switchable.[53,138,139] For example, acid hydrolyzable hydrazone linker was embedded in poly(ethylene glycol)-poly(ε-caprolactone)-based PU to yield acid-cleavable self-assembled PU micelles.[138] The PU micelles degraded in acidic media (pH 4-6) to release loaded cargo by the

cleavage of hydrazone linkage in the copolymer backbone. Another study reported a triblock PU in which pH-sensitive HEP served as the hard segment and the core of the self-assembled micelle.[53] At acidic pH, the micelle disintegrated to release the encapsulated drug. Reversibility of the self-assembly and switchable pH-triggered on-and-off drug release were missing and not the focus of these reports.

There are only a few reports of pH-responsive PU membranes.[9,10,58] pH-responsive polyester-PU copolymer membranes were developed using a diol containing carboxylic group as a chain extender for controlled release of cationic compounds.[9] However, the fabricated membranes were shown to be dissolvable at pH ≥ 8 (pKa of the carboxyl acid group is 8.3), disabling switchable pH-responsive release in the end-uses where pH can exceed 8. In another study, pH-responsive polyester-PU membranes which demonstrated pH-responsive water swelling were prepared.[58] However, the pH responsiveness was quite limited (water swelling percentage of 365% at pH 8.5 vs. 325% at pH 10.0), probably due to the fact that the pH-responsive monomers dimethylolpropionic acid, and *N*-methyldiethanolamine were incorporated as the chain extender which serves as a hard segment acting crosslinking point of the PU. As a result, the synthesized PU could not exhibit dramatic change upon pH change.

In this chapter, we designed and synthesized new pH-responsive polyether-PUs that are stable between pH 4-10 and contain pH-sensitive diols in the prepolymer of the PUs to allow rapid and dramatic pH-responsiveness. Specifically, new pH-responsive polyether-PUs were synthesized with PEG and HEP (pKa of the conjugate acid of HEP is 6.4)[52] serving as the hydrophilic soft segment and the pH-sensitive moiety, respectively. The membranes, which were solvent-cast from the new PUs, swell 2 times more at pH 4.5 (the physiological pH of the human vaginal tract) than at pH 7.0 (the pH in the presence of human seminal fluid). Close-to-zero

release of the anionic model drug sodium diclofenac (NaDF) was observed across the solvent-cast pH-responsive PU membrane at pH 4.5, but rapid release of NaDF occurred at pH 7.0. The solvent-cast PU membranes demonstrated the switchable on-and-off release of model drug NaDF. Overall, the solvent-cast pH-responsive PU membranes hold great potential to be used for fabrication of IVRs to achieve on-demand drug release to better protect women who are generally at higher risk and are more vulnerable to HIV.

3.3 Materials and methods

3.3.1 Materials

PEG (Mn = 6,000) was purchased from EMD Chemicals (Mississauga, ON, Canada). Methylene di-p-phenyl diisocyanate (MDI) (98%) was purchased from ACROS (Geel, Belgium), 1,4-Bis(2-hydroxyethyl)piperazine (HEP) (99%), propylene glycol (PG) (> 99.5%), 1,6-hexanediol (HD) (99%), hexamethylene diisocyanate (HDI) (> 99%), dibutyltin dilauarate (DBTDL) (95%), anhydrous N,N-dimethylformamide (DMF) (99.8%), dimethyl sulfoxide (DMSO) (> 99.5%), anhydrous 1,2-dichloroethane (DCE) (99.8%), anhydrous diethyl ether (> 99%) and tetrahydrofuran (THF) were purchased from Sigma Aldrich (St. Louis, MO, USA). Water, methanol, and acetonitrile (all HPLC grade), were purchased from VWR International LLC (Batavia, IL, USA). Sodium diclofenac (NaDF) was purchased from Santa Cruz (> 99%, Dallas, TX, USA). NaDF is a chemical sodium salt of 2-[{2,6-dichlorophenyl} amino] benzene acetic acid with a pKa of 3.8 at 25 °C in aqueous condition.[140]

3.3.2 Synthesis and characterization of pH-responsive PU copolymers (PEG-HEP-HDI-PG and PEG-HEP-MDI-PG)

New pH-responsive PUs were synthesized using HEP and PEG with diisocyanates and PG. Two different diisocyanates, HDI and MDI, were used (**Scheme 2-1 and 2-2**). The synthesized PUs were referred to as PEG-HEP-HDI-PG and PEG-HEP-MDI-PG when HDI and MDI were used, respectively. Briefly, a three-neck flask was set up with nitrogen inlet-outlet purging and mechanical stirring equipment. 5.0 g PEG and 1.3 g HEP (feed mole ratio of PEG: HEP = 0.1: 0. 9) were dissolved in anhydrous DMF and added to the flask. After a catalytic amount of DBTDL was added into the reactor, stoichiometric ratio of diisocyanate (1.4 g HDI, feed mole ratio of OH/NCO = 1) was added into the reactor. The reactor was maintained for 6 h at 60 °C with stirring at 500 rpm under a nitrogen atmosphere. Further synthesis progress was done by adding HDI and PG. PG (feed mole ratio of HEP: PG = 0.9: 1) and a catalytic amount of DBTDL were added to the reaction mixture. After 15 min stirring, stoichiometric ratio of diisocyanate (1.4 g HDI, OH/NCO = 1) was added. The reactor was maintained in a nitrogen atmosphere for 24 h at 60 °C. The reaction mixture was then poured into 8-fold diethyl ether, and the precipitate was washed with excess diethyl ether several times to remove the remaining impurities. The final product (PEG-HEP-HDI-PG, yield: 98.7%) was obtained after being dried in a vacuum oven at room temperature.

In a similar manner, PEG-HEP-MDI-PG was synthesized using aromatic diisocyanate. Briefly, flasks were set up with nitrogen inlet-outlet equipment and condenser at 60 °C. 5.0 g PEG and 1.3 g HEP (feed mole ratio of PEG: HEP = 0.1: 0.9) were dissolved in anhydrous 1,2-dichloroethane (DCE). After the addition of DBTDL into the reactor, a stoichiometric ratio of diisocyanate (2.1 g MDI, feed mole ration of OH/NCO = 1) was added. The reactor was

maintained for 3 h at 60 °C under a nitrogen atmosphere. PG (feed mole ratio of HEP: PG = 0.9: 2) and catalytic amount of DBTDL were added to the reactor. After 15 min, 4.2 g MDI (feed mole ratio of OH/NCO = 1) was added. The reactor maintained nitrogen atmosphere for 3 h at 60 °C. The final product was precipitated in 8-fold diethyl ether and washed with excess diethyl ether several times. The final product (PEG-HEP-MDI-PG: yield: 92.0%) was obtained after being dried in a vacuum oven.

Control non-pH-sensitive PU (PEG-HD-MDI-HD) was also synthesized. Briefly, flasks were set up with nitrogen inlet-outlet equipment at 60 °C. 5.0 g PEG and 0.9 g HD (feed mole ratio of PEG: HD = 0.1: 0.9) were dissolved in anhydrous DCE. After a catalytic amount of DBTDL was introduced, a stoichiometric ratio of diisocyanate (2.1 g MDI, feed mole ration of OH/NCO = 1) was added. The reaction mixture was then continuously stirred for 3 h at 60 °C under nitrogen atmosphere, and HD (feed mole ratio of PEG: HD = 0.1: 1) was added. After 15 min, 2.1 g MDI (feed mole ratio of OH/NCO = 1) was introduced. The reactor maintained nitrogen atmosphere for 3 h at 60 °C. The resulting product was precipitated and washed with excess diethyl ether. The final product (PEG-HD-MDI-HD, yield: 87.0%) was obtained after being dried in a vacuum oven.

The chemical structure of the synthesized PU copolymers was confirmed by ATR-FTIR (Thermo Scientific, Nicolet iS10) and ^{1}H-NMR (Bruker, Karlsruhe, Germany, Avance 300 MHz). T_m of the PU copolymer was characterized using a melting point apparatus (LTS420, PE95/T95, Linkam Scientific Instrument, Surrey, UK). Viscosity average molecular weight of the synthesized PUs was calculated from the Mark-Houwink equation $[\eta] = KM^a$ where $[\eta]$ is the intrinsic viscosity, K and a are experimentally-determined constants which have been reported in the literature,[141] and M is the viscosity average molecular weight which lies between Mn and

Mw. The Mark-Houwink equation for the PU in DMF at 25 °C is $[\eta] = 3.64 \times 10^{-4}M^{0.71}$.[142]

Viscosities were measured using a Cannon-Ubbelohde dilution viscometer at 25.0 ± 0.75 °C to calculate the intrinsic viscosity of the PU solutions. Time taken by the tested liquid to travel between two measurement marks M_1 and M_2 was recorded for pure DMF and the DMF solution of PUs. Each measurement was repeated five times. The concentration of the PUs was diluted from 0.25 g/100 mL to 0.125 g/100 mL.

3.3.3 Fabrication and characterization of solvent-cast pH-responsive PU membranes

The pH-responsive and control non-pH-responsive PU membranes were cast by a solvent-cast method.[143] Supersaturated 2% (g/mL) pH-responsive PU copolymer solution in THF and 2% (g/mL) control PU copolymer solution in DMSO were prepared and poured into a glass dish mold (DI: 90 mm). THF was evaporated at room temperature and membranes were cast for 24 h. For the control PU, DMSO was evaporated at 80 °C under vacuum. The solvent-cast PU membranes were immersed in distilled water for further purification and then detached from the mold. The washed PU membranes were dried at room temperature for 24 h, and then used without further treatment for later evaluations. The dry thickness of solvent-cast PU membranes was 0.20 ± 0.01 mm. Tensile strength and elongation at break of prepared membranes were conducted using an Instron Extension Testing System (Instron, MA, USA) with a crosshead speed of 25 mm/min with a 5 kN load cell.[144] Each sample was cut into lengths approximately 10 × 40 mm. The samples consisted of: dry samples, swollen samples at 37 °C in pH 4.5 and swollen samples at 37 °C in pH 7.0. Each measurement was repeated three times.

For swelling behaviour evaluation of the solvent-cast membranes, various pH buffer solutions from pH 4 ~ pH 10 were prepared from 0.1 M phosphate buffer solution (PBS) by

adjusting pH using 0.05 M HCl and 0.05 M NaOH solution. Prepared membrane (DI: 6 mm, thickness: 0.20 ± 0.01 mm) samples were immersed in different pH buffer solutions at 37 °C until swelling equilibrium was reached. Before weighing the swollen samples at each time point, the surface liquid was gently wiped off. The measurement was repeated three times. Also, cyclic pH-responsive swelling ratio change was evaluated to confirm the tunable pH-responsive behavior of the solvent-cast PU membranes. Three solvent-cast membrane samples (DI: 6 mm) were weighed and immersed in pH 4.5 PBS for 3 h at 37 °C. After the samples were removed and weighed, the samples were immersed into pH 7.0 PBS for another 3 h at 37 °C, then removed and weighed again. This procedure was repeated in pH 4.5 PBS. Surface liquid was gently wiped off before weighing the membranes. The measurement was repeated three times.

pH-responsive morphology change of the solvent-cast PU membranes was evaluated. The membrane (DI: 6 mm, thickness: 0.20 ± 0.01 mm) samples were immersed in different pH buffer solutions (pH 4 ~ 10) at 37 °C for 6 h. The sample was pulled out and frozen at -80 °C. After lyophilisation, the surface morphologies were observed by scanning electron microscopy (SEM, Cambridge Instruments, UK, Cambridge Stereoscan 120) evaluation. Cyclic pH-responsive morphology change of the solvent-cast PU membranes was also evaluated. Three pH-responsive PU membrane samples (PEG-HEP-HDI-PG or PEG-HEP-MDI-PG (DI: 6 mm)) were immersed into pH 4.5 PBS for 3 h at 37 °C. One sample was pulled out and frozen at -80 °C. The other samples were immersed into a pH 7.0 PBS for 3 h at 37 °C, then one sample was removed and frozen at -80 °C. The last sample was immersed into pH 4.5 PBS for 3 h at 37 °C, then pulled out and frozen at -80 °C. After lyophilisation, SEM images were taken.

3.3.4 Drug permeation test

Drug permeation across the solvent-cast pH-responsive PU membranes and control PU membrane was evaluated at 37 °C using a Franz diffusion system.[145] NaDF was used as a model drug of anionic anti-HIV drugs such as betulinic acid and bevirimat which have a molecular weight (Mw) below 1,000 g/mol. Briefly, prepared membranes were cut into square pieces (25 mm × 25 mm), with a thickness of 0.20 ± 0.01 mm at dry conditions. Before evaluation, the samples were immersed in PBS at pH 4.5 or 7.0 over 3 h. Once swollen, the thickness of the membrane samples increased to 0.30 ± 0.05 mm. The swollen membrane was then sandwiched between the donor chamber and the receptor chamber of the Franz cell to cover the orifice. Drug permeability was evaluated using PBS solutions of either pH 4.5 or pH 7.0 in the receptor chamber. 500 µL 50 µg/mL of NaDF was prepared for the donor chamber in PBS with the same pH as the receptor chamber. At intervals of 1, 2, 3, 6, 12, and 24 h, 300 µL of sample solution was withdrawn via the sampling arm, and the equivalent amount of PBS solution at the same pH was replenished through the sampling arm. Sample solutions were stored at -20 °C until reversed-phase high-performance liquid chromatography (RP-HPLC) analysis.

Switchable pH-responsive drug permeability was conducted similarly. Before the evaluation, the samples were immersed in pH 4.5 PBS over 6 h. The prepared sample membranes were then sandwiched between the donor and the receptor chambers to cover the orifice. Switchable drug permeability was evaluated using 50 µg/mL of NaDF prepared in distilled water, and 500 µL was loaded into donor the chamber. Initially, the receptor chamber was filled with PBS (pH 4.5). The entire receptor chamber buffer was replaced with the pH 7.0 and pH 4.5 PBS solutions sequentially at 3 and 6 h, respectively. The solution in the receptor chamber was collected at various time intervals and stored in -20 °C prior to RP-HPLC analysis.

NaDF concentration in the collected samples was quantified using a modified RP-HPLC method.[146] Waters Symmetry® C18 Column (3.5 μm, 4.6 mm × 75.0 mm) along with a Waters® Nova-Pak C18 Guard Column (4.0 μm, 3.9 mm × 20.0 mm) were used under a gradient condition on a Waters® 2690 HPLC system. The mobile phase was comprised of aqueous phase (A) 0.1% trimethylamine in water (v/v, adjusted to pH 5.1 with concentrated phosphoric acid) and organic phase (B) acetonitrile using the following gradient elution: at 0 min: 70% A and 30% B; at 5 min: 50% A and 50% B; 7.01 min: 70% A and 30% B. Each injection was run for 10 min. Flow rate was maintained at 1.0 mL/min with the UV detection set at 284 nm. The column temperature was maintained at 25 °C. The retention time of NaDF was approximately 3.1 min in pH 7.0 PBS samples and 7.0 min in pH 4.5 PBS samples, respectively. A linear calibration curve of NaDF was obtained in the range of 24-1250 ng/mL ($r^2 > 0.999$) using 80 μL injection. The lower limit of quantification for NaDF was 24 ng/mL, with a signal to noise ratio greater than 10.

3.3.5 *In vitro* biocompatibility studies of the solvent-cast PU copolymer membranes

The vaginal mucosa, particularly its major component, the vaginal epithelium, part of the human body's defence system, acts as an effective barrier against many foreign pathogens. However, it is also sensitive to the potential damages induced by topically applied microbicides. The immortalized human vaginal cell lines have been widely used *in vitro* to assess the cytotoxicity of microbicides against vaginal epithelium as well as pro-inflammatory cytokine induction.[147] Elution test methods are usually employed to evaluate the potential toxic PU degradants eluted into the cell media causing cell death.[42,113,114,148] To assess the biocompatibility of the solvent-cast PU membranes, the human vaginal epithelial cell line VK2/E6E7 and T-cell line Sup-T1 (American Type Culture Collection, ATCC, Rockville, MD, USA) were used in the

current study to reflect the vaginal epithelium and intraepithelial lymphocytes, respectively. VK2/E6E7 cells were maintained in a keratinocyte-serum free medium (K-SFM) containing 0.1 µg/mL recombinant human EGF, 50 mg/mL bovine pituitary extract (Life Technologies, Carlsbad, CA, USA), 0.4 mM $CaCl_2$ and 1% penicillin/streptomycin (Sigma-Aldrich, Whitby, Ontario, Canada). Sup-T1 cells were maintained in RPMI-1640 medium containing 10% heat-inactivated fetal bovine serum (FBS, Fisher Canada, Toronto, Ontario, Canada) and 1% penicillin/streptomycin. Both cell lines were cultured in an incubator at 37 °C and 5% CO_2 prior to the treatment.

The impact of fabricated PU membranes on cell viability was evaluated using an elution assay. Briefly, the thoroughly washed (in sterile water) solvent-cast PU membranes were dried and then sterilized by exposure to UV light for 30 min in a sterile biosafety cabinet. The membranes (100 mg) were put into a sterile 15 mL tube containing 5 mL of K-SFM or RPMI-1640 medium using aseptic technique. The membranes were incubated at 37 °C for 1, 7, 15, 30 days in an incubating orbital shaker at a speed of 100 rpm. At the desired intervals, the elution medium was collected using aseptic technique by transferring the elution medium into a sterile 15 mL tube and stored in -80 °C until further analysis.

1 M acrylamide was prepared in K-SFM or RPMI-1640 medium and filtered using a 0.2 µm membrane and used to induce cell death as a positive control for the CellTiter 96® AQueous One Solution Cell Proliferation Assay (MTS assay, Promega Corporation, Madison, WI, USA). Lipopolysaccharide (LPS; from Escherichia coli 0111: B4, Sigma) was suspended in 1 mL sterile PBS to yield a 1 mg/mL stock solution. Diluted LPS (50 µg/mL) prepared in K-SFM or RPMI-1640 medium was used to induce positive controls for IL-6 and IL-8 ELISA (R&D System Inc., Minneapolis, MN, USA). Nonoxynol-9 (N-9, 200 µg/mL; Spectrum Chemical, Corp., New

Brunswick, NJ, USA) in K-SFM or RPMI-1640 medium was used to induce positive controls for IL-1β ELISA (R&D System). Drug-free K-SFM or RPMI-1640 medium was used as negative control for VK2/E6E7 and Sup-T1 cells, respectively. VK2/E6E7 cells were seeded at 2.5×10^4 per 100 µL per well in 96-well plates. After overnight adhesion, the K-SFM medium was replaced with 100 µL of the positive control, negative control, and elution K-SFM medium collected at different time intervals. Similarly for Sup-T1 cells, after seeding the same numbers of cells in each well, the plate was spun down at $500 \times g$ and medium in each well was replaced with 100 µL of positive control, negative control, and elution RPMI-1640 medium.

After 24 h of elution medium treatment, 20 µL MTS assay reagent was added to each well followed by incubation at 37 °C in the dark for 1 h as suggested by the manufacturer. Absorbance of each well at 490 nm was recorded using a Synergy HT Multi-Mode Microplate Reader (Biotek, Winooski, VT, USA). After 24 h of incubation (37 °C, 5% CO_2), supernatants in each well were collected for cytokine ELISA analysis. For Sup-T1 cells, cells were separated from the culture medium by spinning down at $1,000 \times g$ for 5 min. Levels of IL-1β, IL-6, and IL-8 in VK2/E6E7 supernatants or Sup-T1 culture medium were evaluated using ELISA kits obtained from R&D Systems and data analyzed using SigmaPlot 12.2 (Systat Software Inc., San Jose, CA, USA).

3.3.6 Statistical analysis

Data are presented as mean ± standard deviation (SD). The *n*-value refers to the number of replicates performed for each experiment. One-way ANOVA along with Bonferroni's multiple comparisons test was performed on the results with $P < 0.05$ considered to be significant.

3.4 Results and Discussion

3.4.1 Synthesis and characterization of pH-sensitive PUs (PEG-HEP-HDI-PG and PEG-HEP-MDI-PG)

Two kinds of pH-responsive polyether-PU copolymers (PEG-HEP-HDI-PG and PEG-HEP-MDI-PG) were synthesized; PEG was used as a hydrophilic polyether soft segment for both PUs. HEP was chosen as a pH-sensitive agent since its conjugate acid has a pKa of 6.4. The difference between the two pH-responsive PUs lies in the urethane linker: an aliphatic diisocyanate (HDI) for PEG-HEP-HDI-PG and an aromatic diisocyanate (MDI) for PEG-HEP-MDI-PG. PG was used as a chain extender and as part of the hard segment. Anhydrous DMF was selected for PU polymerization when HDI was used. Macromolecular products of the reaction using MDI have more hydrophobic characteristics than that of HDI because of their higher crystallinity, therefore anhydrous DCE was used as a reaction solvent when MDI was used. Overall, the reaction was performed under anhydrous conditions using dried nitrogen gas because diisocyanate can be hydrolysed by water.[12] The reaction temperature was maintained at 60 ± 5 °C.[48]

The viscosity average molecular weight of PEG-HD-MDI-HD, PEG-HEP-HDI-PG and PEG-HEP-MDI-PG were 1.3×10^6, 6.0×10^5 and 4.5×10^5, respectively. The T_m of PEG-HEP-MDI-PG is 160 °C, which is higher than that of PEG-HEP-HDI-PG (140 °C) as shown in **Table 3-1**. This may be explained by the fact that the hard segments of PEG-HEP-MDI-PG have stronger intermolecular interactions than that of PEG-HEP-HDI-PG. The aromatic segment is more rigid than the segment composed of aliphatic isocyanates.[46,149] Differences in the chemical structure of pH-responsive PUs such as soft segment/hard segment ratio and chemical

component can create different tensile strengths of the cast PU membranes at dry and wet conditions and produce different elongation breaks.

Table 3-1. Physical characteristics of solvent-cast pH-sensitive PUs (PEG-HEP-HDI-PG and PEG-HEP-MDI-PG) and control non-pH-responsive PEG-HD-MDI-HD membranes. Data is expressed as mean ± SD; $n = 3$.

Polymer	Melting Temperature (°C)	Tensile strength (kPa)			Elongation at break (dry, %)	Viscosity average molecular weight (Mv)	Yield (%)
		dry	pH 4.5	pH 7			
PEG-HEP-HDI-PG	140 ± 10	165 ± 3	7.3 ± 0.8	10.1 ± 0.3	900 ± 11	6.01×10^5	98.7
PEG-HEP-MDI-PG	160 ± 10	308 ± 7	25.2 ± 0.9	50.9 ± 0.4	570 ± 8	4.54×10^5	92.0
PEG-HD-MDI-HD	195 ± 10	300 ± 10	71 ± 4	68 ± 5	682 ± 21	1.32×10^6	88.7

As presented in **Table 3-1**, PEG-HEP-HDI-PG showed lower tensile strength and higher elongation percentage at break than PEG-HEP-MDI-PG. The cast membranes showed lower tensile strength in wet conditions. Since the membranes were swollen in PBS, polymer density was decreased, and the absorbed water reduced interactions between the polymer chains. The absorbed water reduced Young's moduli causing minor changes in mechanical properties.[150] Despite the decreased tensile strength in wet conditions, all the PU membranes remained intact after the drug permeation test. Since the pH-responsive PU membrane can endure the osmotic pressure of NaDF solution during the permeation test, they can be used as "window" membranes for a reservoir-type IVR as shown in **Figure 3-1**.
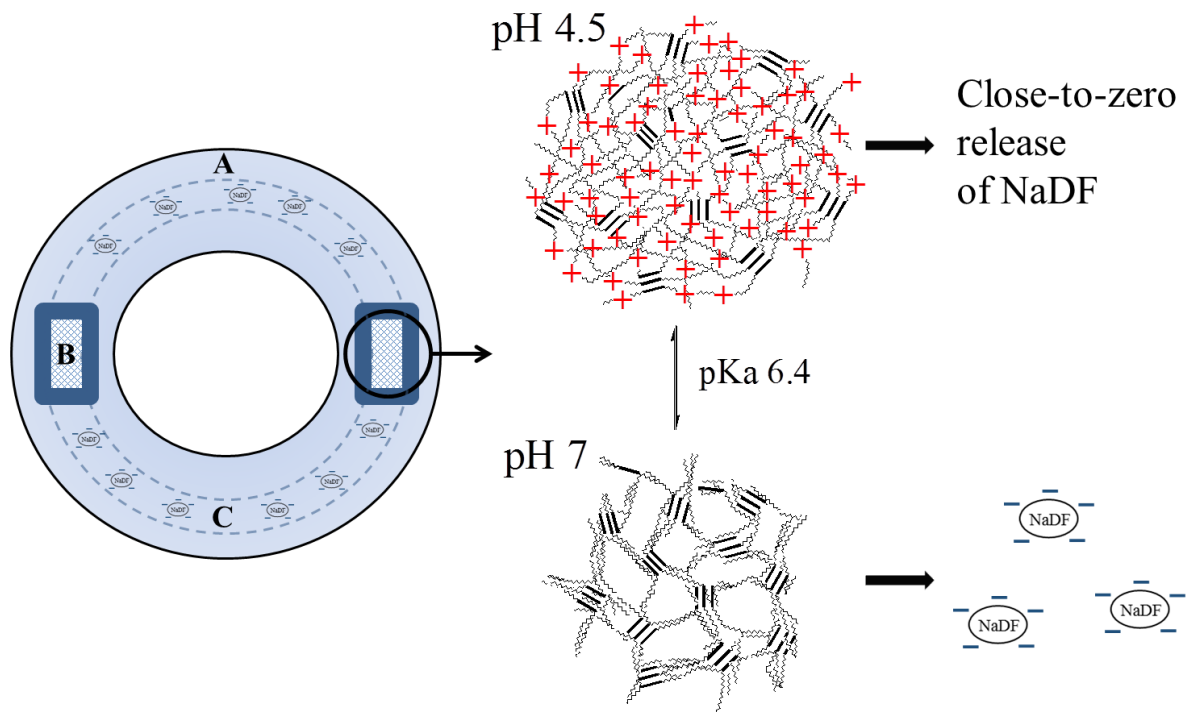
Figure 3-1. Diagram of proposed use of solvent-cast pH-responsive PU membrane as a "window" membrane of reservoir-type IVR for controlled on-demand drug release. (A) reservoir-type IVR made of a non-permeable polymer (B) holes for drug loading which are covered by solvent-cast pH-responsive PU membranes. (C) NaDF loaded in the hollow lumen of the reservoir-type IVR.

Membranes with a wet tensile strength of 7.3 Kpa or more are good for the desired application. When drug concentrations higher than those tested in this study are used (leading to higher osmotic pressure), these pH-responsive PU membranes can be backed up with certain high strength porous meshes for optimal physical stability.

Chemical structures of the synthesized PU copolymers were confirmed by ATR-FTIR and ^{1}H-NMR. In the ATR-FTIR spectrum of PEG-HEP-HDI-PG, the peak at 1706 cm^{-1} could be

assigned to the stretching absorbance of free carbonyl bonds and the 1669 cm^{-1} peak arose from hydrogen bonded carbonyl bonds.[51,52] The N-H bond of urethane and C-O bond in ether were shown at 3328 cm^{-1} and 1106 cm^{-1} respectively. Similarly, three peaks 1722 cm^{-1}, 3315 cm^{-1}, and 1081 cm^{-1} in the ATR-FTIR spectrum of PEG-HEP-MDI-PG were characteristic of carbonyl bond, N-H bond of urethane, and the C-O bond in ether, respectively (**Figure 3-2**).[151]

^{1}H-NMR spectra were collected to identify the chemical structure of the synthesized pH-responsive PUs. **Figure 3-3** shows the chemical structures of the two pH-responsive PU copolymers, PEG-HEP-HDI-PG and PEG-HEP-MDI-PG, and their ^{1}H-NMR spectra. From the PEG-HEP-HDI-PG spectra, the proton peaks e and f were assigned to different methylene protons of HEP as indicated on the structure.[51,52] The bonded PEG was confirmed by the presence of a methylene proton peak at 3.55-3.76 ppm.[51,52] The methyl proton peak i at 1.10-1.30 ppm demonstrated the successful incorporation of PG in the structure.[143,152] The methine proton peak and methylene proton peak of PG were shifted downfield by 4.90-5.10 ppm and 4.00-4.15 ppm, respectively. The methylene protons b, c, and d at 3.02-3.25, 1.40-1.60, and 1.30-1.40 ppm jointly pointed to successfully incorporated HDI.[52,87] The ratio of immobilized PEG and PG was calculated as 0.065: 1 by comparison of the methylene proton peak a and j. Also, the ratio of HEP and PG in PEG-HEP-HDI-PG was 0.28: 1 calculated using methylene proton peak e and j. Similarly, from the PEG-HEP-MDI-PG spectra, incorporated MDI was confirmed by methylene proton peak c at 3.65-3.75 ppm and methine proton peaks b at 7.0-7.4 ppm.[153] The ratio of PEG and PG in the PEG-HEP-MDI-PG was 0.074: 1 calculated using methylene proton peak a, and methine proton peak g; and the ratio of HEP and PG was 0.54: 1 from comparison of methylene proton peak f and methine proton peak g.
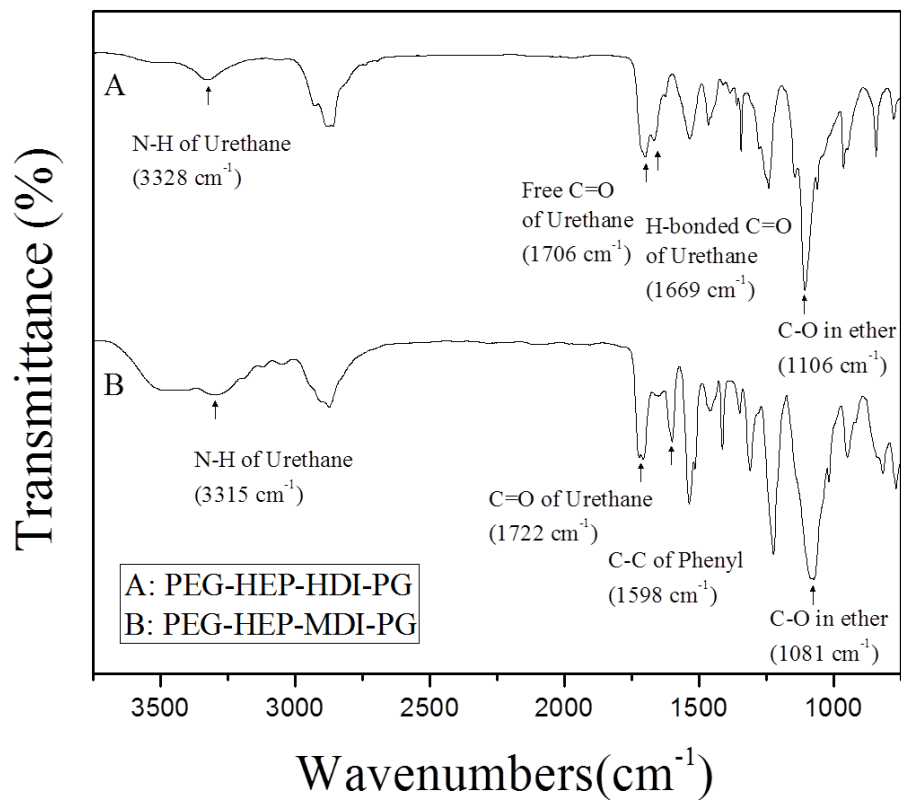
Figure 3-2. Attenuated total reflectance-Fourier transform infrared (ATR-FTIR) spectroscopy of synthesized pH-sensitive polyurethanes. (A) PEG-HEP-HDI-PG, (B) PEG-HEP-MDI-PG.

Figure 3-3. [1]H-Nuclear Magnetic Resonance (^{1}H-NMR) spectra of synthesized pH-sensitive polyurethanes (PEG-HEP-HDI-PG, PEG-HEP-MDI-PG).

3.4.2 Physicochemical characterization of solvent-cast pH-responsive PU membranes

The PU copolymers were designed to exhibit pH-responsive characteristics in aqueous conditions around pH 6.4 due to the tertiary amine of HEP. At pH < 6.4, the tertiary amine groups in the prepolymer of the PU are protonated (the pKa of the conjugate acid of HEP is 6.4, -N(R)- + H$^+$ → -N$^+$H(R)-). When the pH increased above 6.4, the tertiary amine groups are deprotonated (-N$^+$H(R)- → -N(R)- + H$^+$). The cationic group on the PU copolymer can exhibit electrostatic interactions with anionic materials in an aqueous condition until pH 6.4 and can lose the interaction when pH > 6.4.[51,58] The solvent-cast pH-responsive membranes were able to stably maintain their structure in PBS solutions of varying pH (from pH 4 to 10). It is obvious that the prepared pH-responsive PU membranes have strong hydrogen bonding and hydrophobic interaction at pH 4~10 resulting from the chemical structure of the PUs.

Figure 3-4 shows the swelling ratio of the solvent-cast pH-responsive PU copolymer membranes. The swelling ratio (S) was quantified using the following equation

$$S (\%) = (M_s - M_d)/M_d \times 100$$

where M_s and M_d are the mass of swollen and dried samples, respectively.[153] The swelling ratio of PEG-HEP-HDI-PG membrane reached equilibrium after 2 h at pH 4~10. At pH 4.0, the PEG-HEP-HDI-PG membrane showed the highest swelling ratio (668 ± 22%). The swelling ratio at pH 4.0 is more than two times higher than the swelling ratio at pH 7.0. At higher pH, from 7 to 10, there was no significant difference in swelling ratio, because the tertiary amine of the PEG-HEP-HDI-PG was deprotonated from pH 6.4. According to the Henderson–Hasselbalch equation, [R$_1$R$_2$R$_3$N] = [R$_1$R$_2$R$_3$N$^+$H] at pH 6.4. Above pH 7.0, tertiary amines in PEG-HEP-

HDI-PG were deprotonated and became less hydrophilic. The swelling ratio of PEG-HEP-MDI-PG membrane also reached equilibrium after 2 h at pH 4~10. At pH 4.0, the PEG-HEP-MDI-PG membrane also showed the highest swelling ratio.
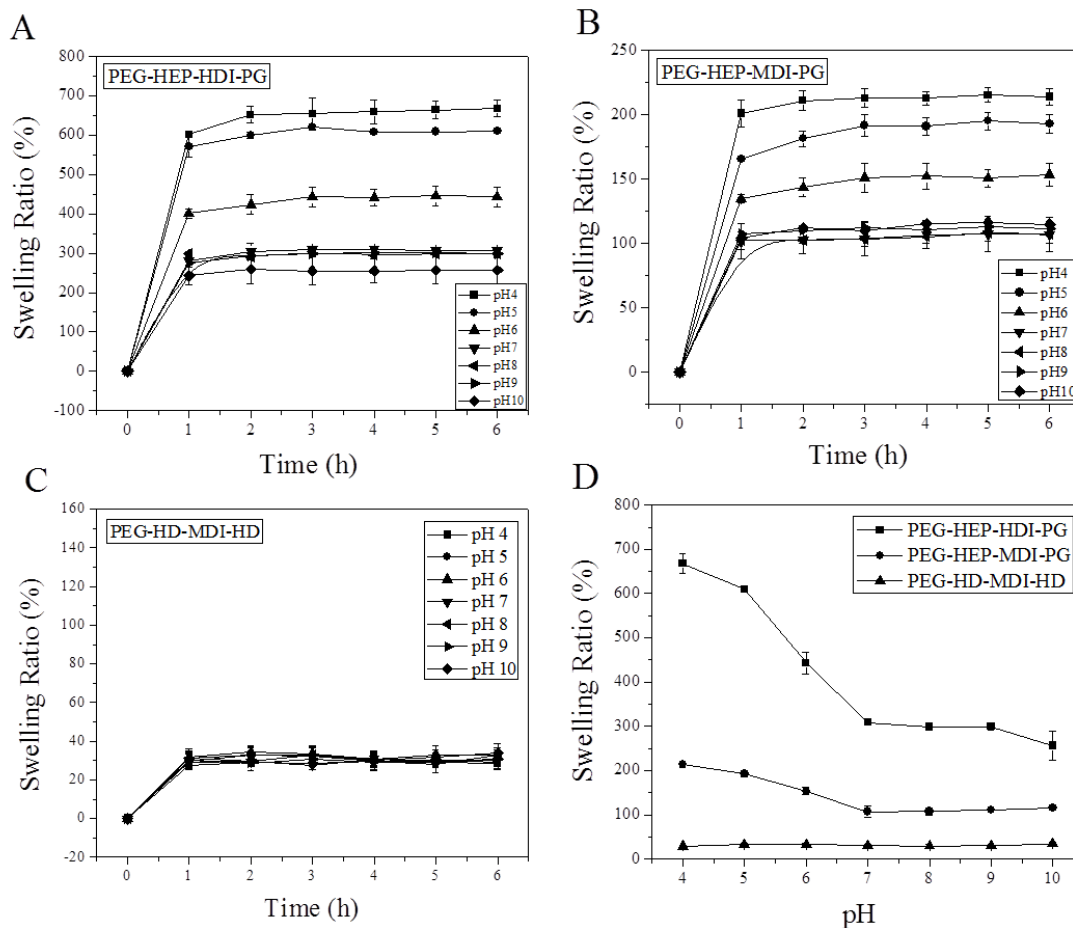
Figure 3-4. Swelling ratio of solvent-cast PU membranes in various pH buffers at 37 °C. (A) PEG-HEP-HDI-PG membrane, (B) PEG-HEP-MDI-PG membrane, (C) non-pH-responsive PEG-HD-MDI-HD control, and (D) Comparison of PEG-HEP-HDI-PG membrane, PEG-HEP-MDI-PG membrane, and non-pH-responsive PEG-HD-MDI-HD control (swelling ratio after immersed for 3 h at different pH). Data is expressed as mean ± SD; $n = 3$.

At higher pH from 7 to 10, there was no significant difference in swelling ratio because the tertiary amine of PEG-HEP-MDI-PG was deprotonated above pH 6.4. PEG-HEP-HDI-PG showed a more sensitive swelling ratio change in comparison to PEG-HEP-MDI-PG following pH change (**Figure 3-4, D**), which may be a result of them having different hydrophilic characteristics. PEG-HEP-HDI-PG and PEG-HEP-MDI-PG were synthesized with aliphatic diisocyanate and aromatic diisocyanate, respectively. Prepolymer of PEG-HEP-HDI-PG may have a better mobility than that of PEG-HEP-MDI-PG in aqueous conditions since the prepolymer of PEG-HEP-HDI-PG has lower crystallinity than PEG-HEP-MDI-PG.

From the SEM images, distinct pH-responsive morphology changes were observed (**Figure 3-5**). At pH 4.5, there were no pores on PEG-HEP-HDI-PG and PEG-HEP-MDI-PG membrane surfaces. However, the membranes showed a remarkable number of cavities on the surface at pH 7.0 because of the pH-sensitive tertiary amine group on HEP. The average cavity size on the surface of PEG-HEP-HDI-PG membranes at pH 7.0 was 16 ± 1 μm, and that of PEG-HEP-MDI-PG was 16 ± 2 μm ($n = 50$). At pH 4.5, tertiary amines of HEP were protonated and expanded in the PBS due to the ionic repulsion between neighbouring polymer chains. As a result, membranes at pH 4.5 buffer solution can uptake more water than at pH 7.0 and expand the prepolymer chains. The size of free volume hole, a free space between the PU copolymer chains, was decreased and the total volume of the pH-responsive PU membranes was increased at pH 4.5 buffer solution. The volume change made no cavities on the surface at pH 4.5.
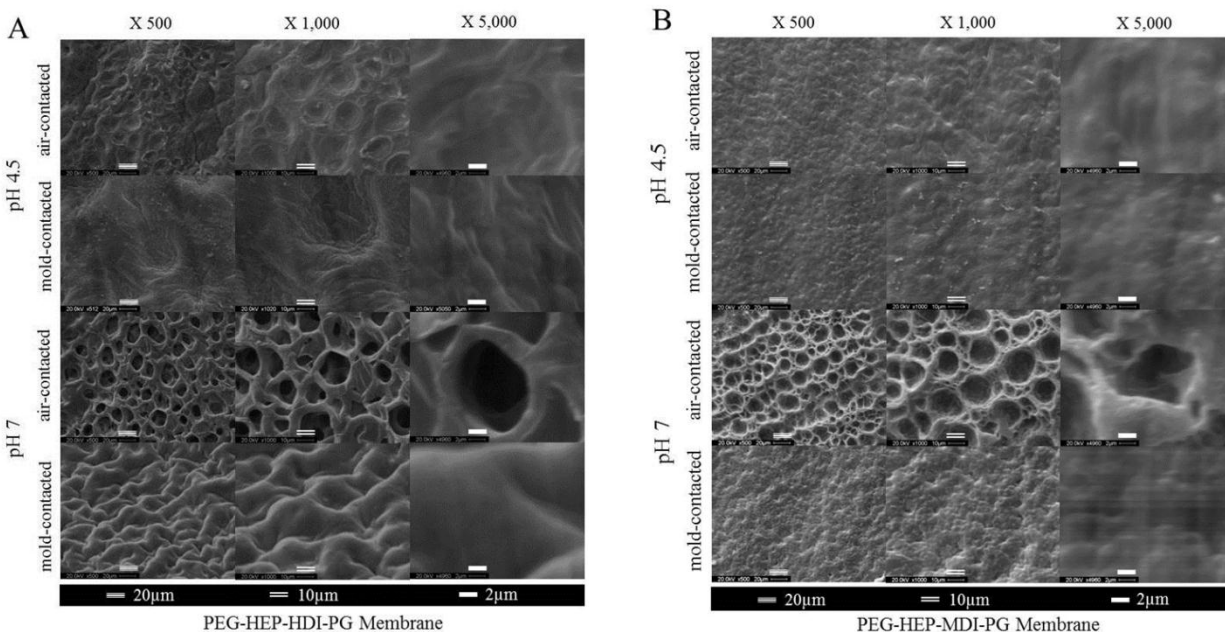
Figure 3-5. Scanning electron microscope (SEM) images of solvent-cast pH-responsive PU membranes (A) PEG-HEP-HDI-PG membrane and (B) PEG-HEP-MDI-PG membrane at pH 4.5 and pH 7.0. Air-contacted surface during casting membrane and mold-contacted surface during casting membrane were characterized.

At pH higher than pKa, the tertiary amine of HEP was de-protonated and started to become less hydrated. The prepolymer chains shrank and/or moved to hydrophobic hard segment at pH ≥ the pKa because the prepolymer chains became less hydrophilic. As a result, free volume hole increased and cavities were formed on the surface at pH higher than the pKa.[58,154] However, the prepared membranes did not display any visible interconnected porous structure. When pH-responsive PU membranes were cast, one side of the pH-responsive PU solution was in contact with air and the other side was in contact with the glass mold surface. It is reasonable to believe that different polymer arrangements may have formed between the air-contacted surface and the

mold-contacted surface. Because the polymer concentration was different on the air-contacted part versus the mold-contacted part during solvent evaporation, the air-contacted part was influenced by solvent evaporation pressure until the finalization of membrane casting.[155]
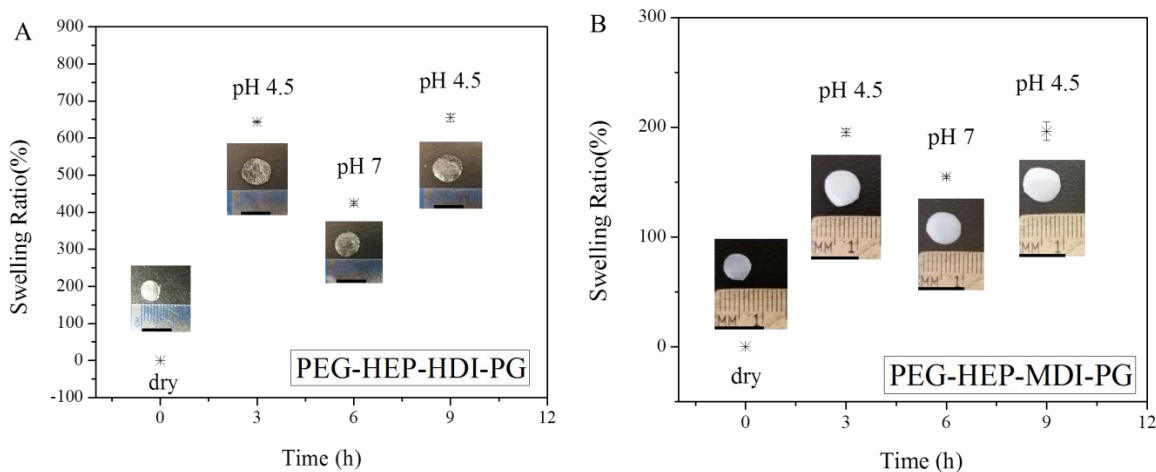
Figure 3-6. Reversible swelling ratio change of solvent-cast pH-responsive PU membranes (A) PEG-HEP-HDI-PG membrane and (B) PEG-HEP-MDI-PG membrane at 37 °C. Data is expressed as mean $\pm$ SD; $n = 3$.

The cyclic pH-responsive behaviors of the solvent-cast PEG-HEP-HDI-PG and PEG-HEP-MDI-PG membranes were characterized via cyclic swelling ratio and morphology changes. As can be seen in **Figure 3-6**, PEG-HEP-HDI-PG membrane showed 644% swelling ratio after being immersed in 0.1 M PBS pH 4.5 at 37 °C for 3 h, consistent with the swelling data presented in **Figure 3-4**. This swelling ratio decreased with deionization of the tertiary amine of HEP to 424% swelling ratio after immersion in 0.1 M PBS pH 7.0 at 37 °C for 3 h. After 3 h immersion in 0.1 M PBS pH 4.5, the swelling ratio of PEG-HEP-HDI-PG membrane showed

70

successful cyclic swelling ratio changes up to 655%. The cyclic pH-responsive swelling ratio of PEG-HEP-MDI-PG membrane was also evaluated. PEG-HEP-MDI-PG membrane showed a cyclic pH-responsive swelling ratio change to around 200% (pH 4.5), 150% (pH 7.0), and 200% (pH 4.5) at 3 h, 6 h, and 9 h respectively. From the results of the pH-responsive swelling ratio tests, it was expected that the swelling ratio of PEG-HEP-HDI-PG membrane and PEG-HEP-MDI-PG membrane decreased to around 300% and 100% at pH 4.5, respectively. However, the swelling ratios of the PEG-HEP-HDI-PG membrane and the PEG-HEP-MDI-PG membrane did not reach these values at the 6 h time point. This hysteresis might be because the PUs had already hydrogen bonded with water and it takes a longer time to dehydrate to reach equilibrium.

The pH-responsive morphology changes of prepared pH-responsive PU membranes are shown in **Figure 3-7**. At pH 4.5, the PEG-HEP-HDI-PG membrane showed almost no pores or traces of cavities (sunken spaces) on its surface. After the membrane was fabricated, it was washed with distilled water (pH 6.5~7) over 12 h. During the washing process, the membrane potentially had cavities on surface. At pH 4.5, images appear to show signs of pre-existing cavities. After being immersed in pH 7.0 PBS, the cavities re-opened and showed a sunken porous topography on the air-contacted side. After being re-immersed in pH 4.5 PBS solution, the cavities appeared to have closed. The PEG-HEP-MDI-PG membranes also showed similar cyclic pH-responsive morphology changes. However, the PEG-HEP-MDI-PG membrane showed less clear morphology changes upon pH change than the PEG-HEP-HDI-PG membrane. From **Figure 3-6** and **3-7**, it is obvious that the aliphatic diisocyanate based pH-responsive membrane demonstrated more rapid pH-responsivity than the aromatic diisocyanate based pH-responsive membrane.
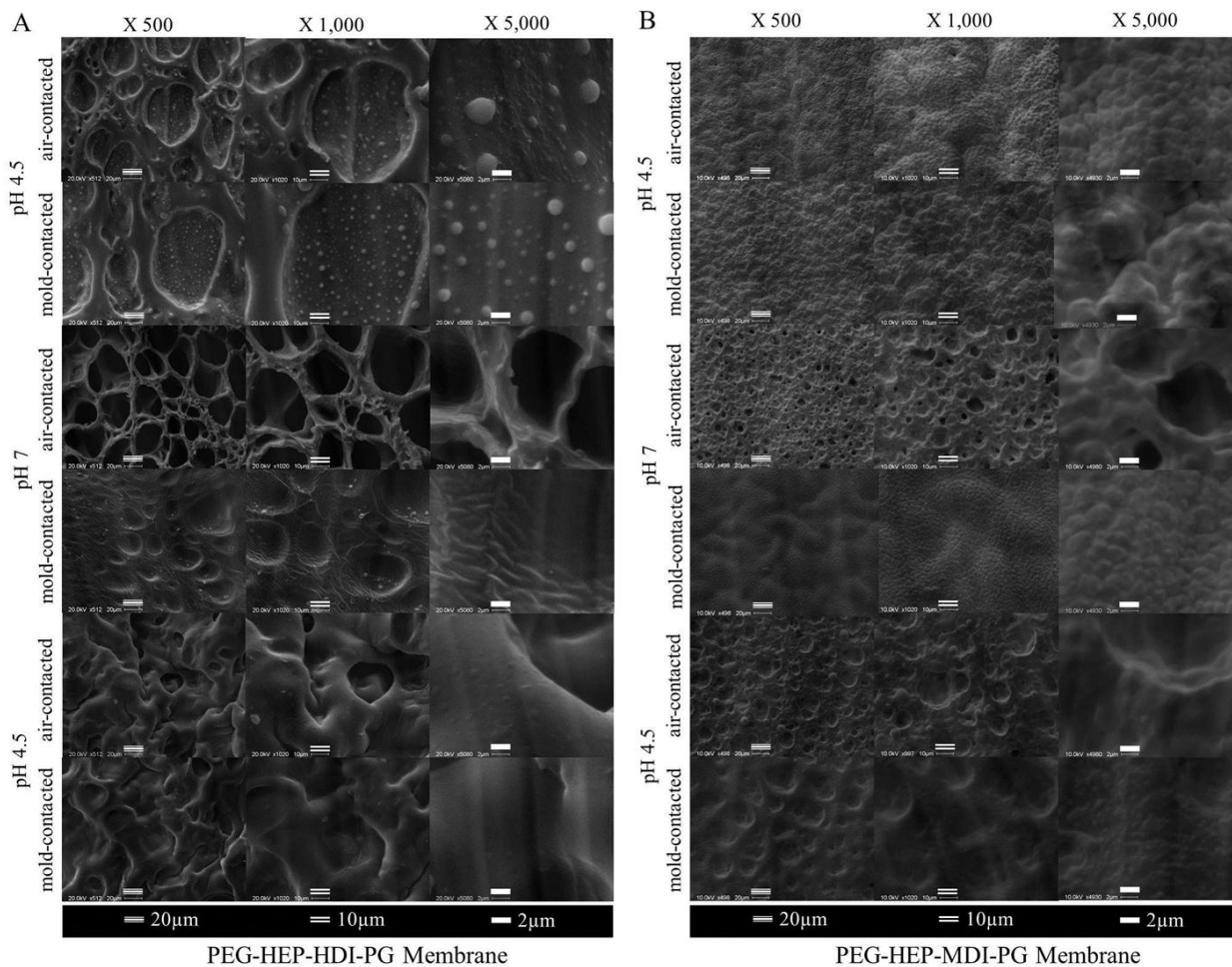
Figure 3-7. Reversible morphology change of solvent-cast pH-responsive PU membranes (A) PEG-HEP-HDI-PG membrane and (B) PEG-HEP-MDI-PG membrane. Air-contacted surface during casting membrane and mold-contacted surface during casting membrane were characterized.

3.4.3 Drug permeation studies

NaDF is a water-soluble anionic nonsteroidal anti-inflammatory drug which has Mw 296.148 g/mol. NaDF was selected as a model drug to represent the anionic category of anti-HIV drugs[156–160] since it shares several common structural features with those anionic anti-HIV drugs

such as betulinic acid and bevirimat. Specifically, betulinic acid, bevirimat, and NaDF all have carboxylic acid groups, a hydrophobic six membered ring structure (fused cyclohexane or benzene ring) and amines or hydroxyl groups which are capable of forming hydrogen bonding. NaDF solubility tests determined that the maximum solubility of NaDF in PBS (pH 4.5) was 417.9 µg/mL, and in PBS (pH 7.0) was 5631.4 µg/mL. Thus, sink conditions were maintained during the permeation studies. Permeation of NaDF across PEG-HEP-HDI-PG and PEG-HEP-MDI-PG membranes showed distinct pH-responsive patterns (**Figure 3-8, A-C**). Almost no release of NaDF was observed during the 24 h permeation test at pH 4.5 ($< 0.2\%$ of total NaDF) for PEG-HEP-HDI-PG and PEG-HEP-MDI-PG membranes, while significant amounts of NaDF were released at pH 7.0 ($41 \pm 7\%$ and $52 \pm 6\%$ cumulative release of NaDF for PEG-HEP-HDI-PG and PEG-HEP-MDI-PG membranes, respectively). The PEG-HD-MDI-HD membrane, fabricated using non-pH-responsive PU, allowed significant release of NaDF at both pH 4.5 ($26.0 \pm 0.6\%$) and pH 7.0 ($63 \pm 1\%$) in comparison to the solvent-cast pH-responsive membranes. The cause for higher drug release at pH 7.0 than that at pH 4.5 through the non-pH-responsive PU membrane may due to the difference in zeta-potential at pH 4.5 (-7.9 mV) and 7.0 (-25.4 mV). At pH 7.0, a higher repulsive interaction between control membrane and anionic model drug had an effect on faster release than at pH 4.2. The non-pH-responsive PU membrane, however, failed to give the most desirable pH-triggered on-and-off drug release. The pH-responsive PU membranes attained better control over the release of NaDF: undetectable release at pH 4.5 and significant release at pH 7.0 ($> 40\%$). The benefits of the pH-responsive PU membranes are further elucidated in the following section.
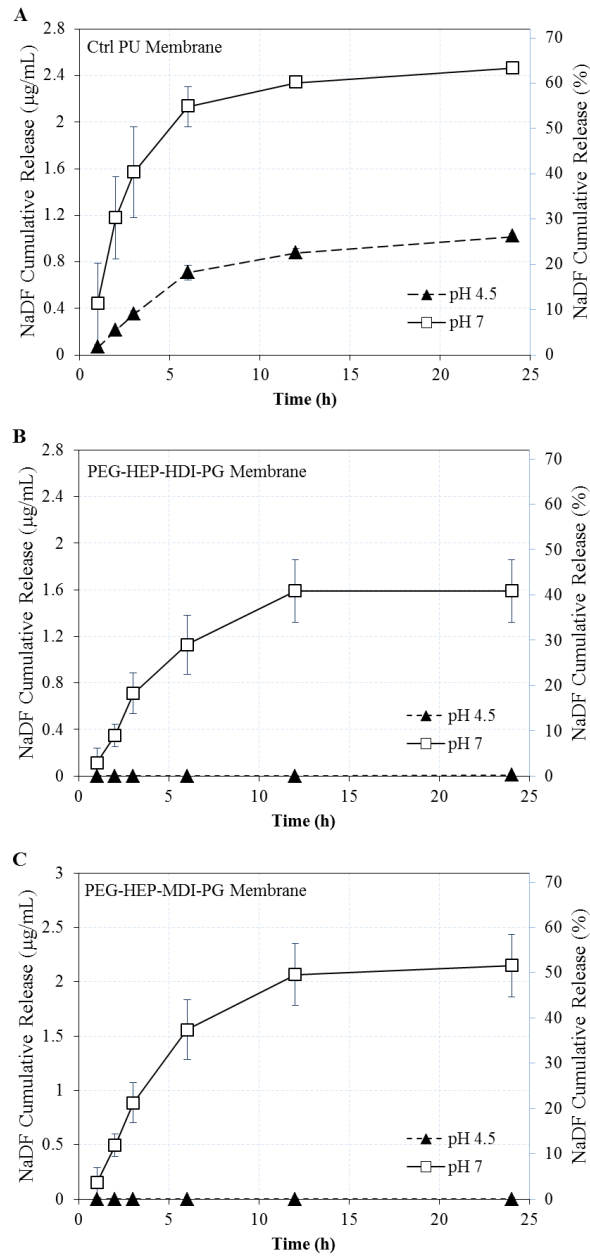
Figure 3-8. *In vitro* drug permeation study of NaDF using (A) non-pH-responsive PEG-HD-MDI-HD control, (B) PEG-HEP-HDI-PG membrane, and (C) PEG-HEP-MDI-PG membrane. Cumulative release of NaDF both in concentration (µg/mL) and percentage (%) over 24 h was evaluated at both pH 4.5 and pH 7. Temperature was maintained at 37 °C. Data is expressed as mean ± SD; $n = 3$. Ctrl, control; PU, polyurethane.
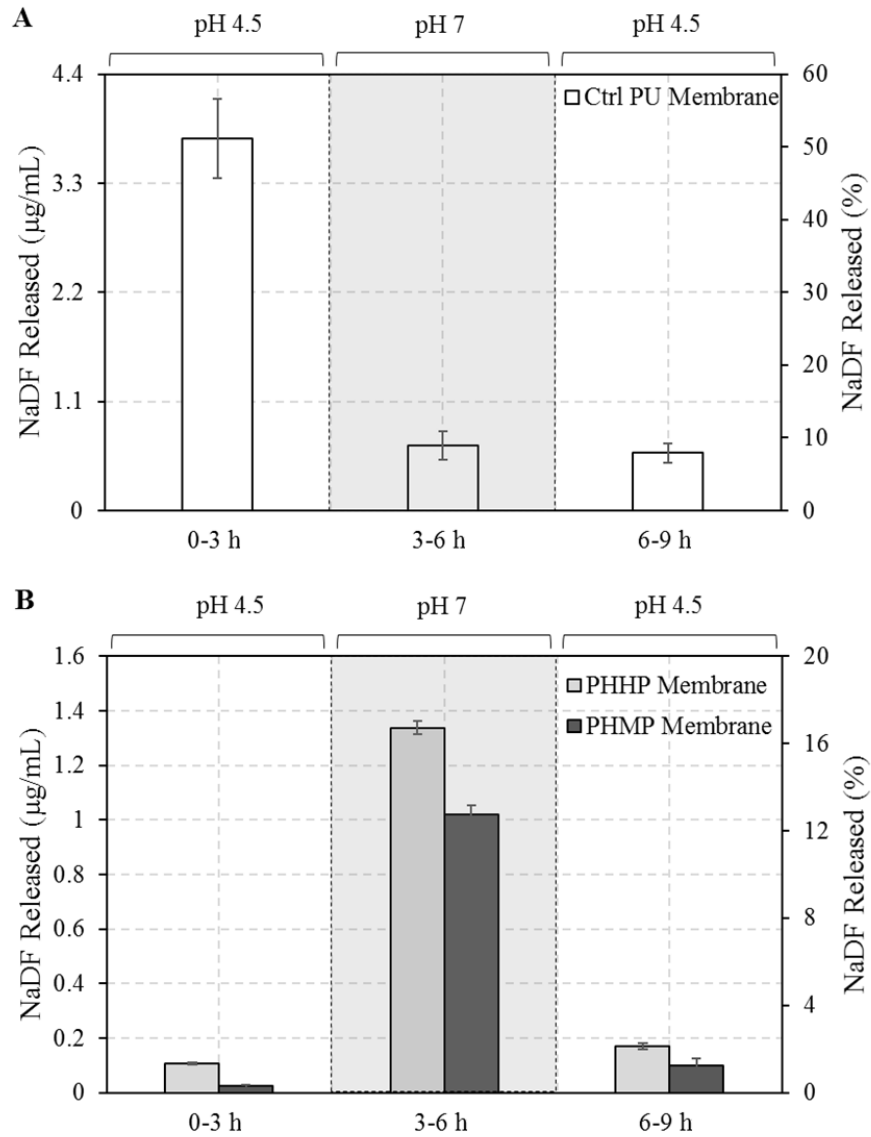
Figure 3-9. *In vitro* switchable drug permeation studies using (A) non-pH-responsive PEG-HD-MDI-HD control and (B) pH-responsive PEG-HEP-HDI-PG membrane and PEG-HEP-MDI-PG membrane. Switchable permeation studies were conducted by shifting the pH of the receptor chamber medium from 4.5 to 7.0 every 3 h. Temperature was maintained at 37 °C. Data is expressed as mean ± SD; $n = 3$.

All the PU membranes were then exposed to alternating pH every 3 hours to examine how the drug release through the membranes responded to pH changes. The prepared pH-responsive membranes demonstrated noticeable switchable pH-responsive drug permeability (**Figure 3-9, B**) in comparison to the control PEG-HD-MDI-HD membrane (**Figure 3-9, A**). The control membrane showed a burst release of NaDF (51 ± 5%) during the first pH 4.5 phase and decreased release of NaDF in the following pH 7.0 phase and the second pH 4.5 phase. However, the PEG-HEP-HDI-PG and PEG-HEP-MDI-PG membranes showed close-to-zero or little release of NaDF at the two pH 4.5 phases but 17 ± 4% and 13.0 ± 0.4% of NaDF released at pH 7.0 phase, respectively. Both pH-responsive membranes showed an immediate reduction in NaDF release during the second pH 4.5 phase (< 2%). The observed pH-responsiveness in PEG-HEP-HDI-PG and PEG-HEP-MDI-PG membranes may be attributed to two factors: electrostatic interaction between tertiary amines of the pH-responsive PUs and carboxylic groups of NaDF at different pHs and morphological changes of the PU membranes at different pHs. The carboxylic group of NaDF was de-protonated and had a negative charge at pH 4.5. (83.4% de-protonated). Consequently, anionic NaDF can form ionic bonds with positively charged tertiary amines in the pH-sensitive PUs, thus resulting in reduced permeation of NaDF through the pH-responsive PU membranes.[9] At pH 7.0, tertiary amine (pKa 6.4) on the synthesized pH-responsive PU was not protonated and exhibited neutral charge. Even though NaDF still carried negative charges at pH 7.0, there was little or no electrostatic interaction between the neutral pH-responsive PU and anionic NaDF at pH 7.0. Therefore, NaDF was released from the donor chamber to the receptor chamber by diffusion at pH 7.0. In addition, at pH 4.5, tertiary amine (pKa 6.4) on the synthesized pH-responsive PU is protonated and led to the expansion of the prepolymer chains as

evidenced by the significantly higher swelling ratios at pH 4.5 than pH 7.0. The expanded prepolymer chains reduced free volume in the PU polymer and hence further decreased drug penetration through the pH-responsive PU membranes.[58,66,161,162] These unique pH-responsive features of the synthesized PEG-HEP-HDI-PG and PEG-HEP-MDI-PG in the current study demonstrate great utility in developing responsive vaginal microbicides against HIV infection. This is due to the evident pH elevation in the human female genital tract due to the presence of seminal fluid during heterosexual intercourse. Since healthy human vaginal fluid is acidic under normal non-menstrual conditions[104] and the normal pH of seminal fluid ranges from pH 7.1 to 8.4,[33] the high buffering capacity of seminal fluid will rapidly neutralize the acidic vaginal fluid.[24] It was observed in the current study that our synthesized pH-responsive membranes allowed immediate release of anionic drug NaDF at pH 7.0 within 1 h ($3 \pm 3\%$ and $4 \pm 4\%$ for PEG-HEP-HDI-PG and PEG-HEP-MDI-PG membranes, respectively) but close-to-zero release at acidic pH (**Figure 8, B** and **C**). The reversible nature of the pH-responsiveness PEG-HEP-HDI-PG and PEG-HEP-MDI-PG PUs membranes (**Figure 9**) will help minimize undesired drug release.

3.4.4 PU copolymer membrane *in vitro* cytotoxicity studies

In vitro cytotoxicity studies of PEG-HEP-HDI-PG and PEG-HEP-MDI-PG membranes were evaluated using the vaginal epithelial cell line VK2/E6E7 and T-cell line Sup-T1. Based on the results, no significant change in cell viability was observed using the collected elution medium (up to 30 days) to treat both cell lines in comparison to negative controls (**Figure 3-10**). Since IL-1β, IL-6, and IL-8 were reported to be the most important pro-inflammatory markers for evaluating microbicide toxicity,[163] we quantitated their production levels in the supernatant of

the elution medium treated cells (**Figure 3-11**). No statistically significant induction of these pro-inflammatory cytokines was observed in comparison to controls. Overall, our pH-responsive PUs were non-cytotoxic to human vaginal epithelial cells and T lymphocytes.
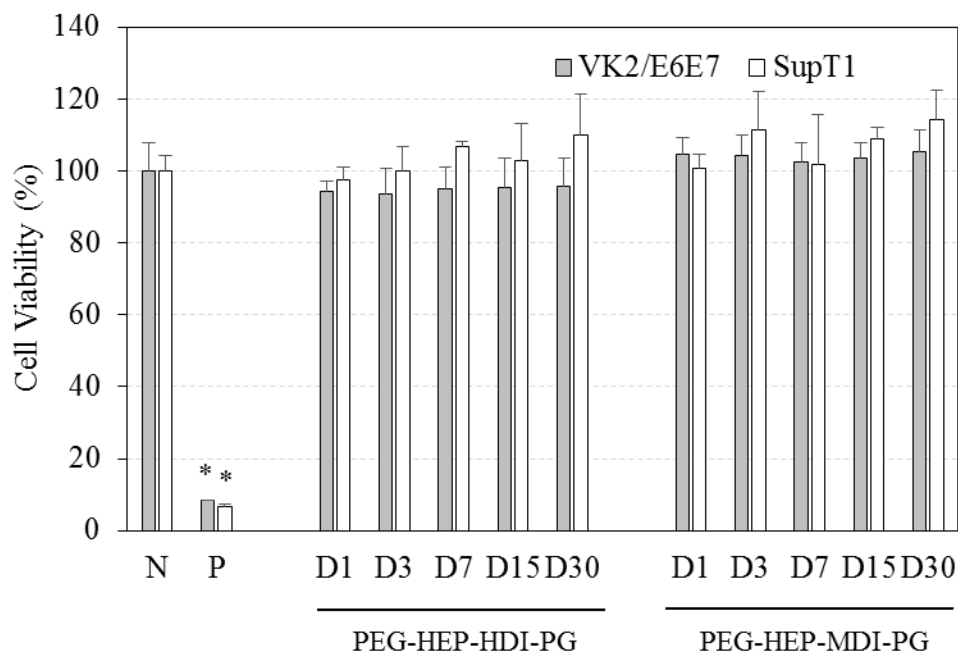
Figure 3-10. *In vitro* biocompatibility evaluations of the solvent-cast pH-responsive membranes using VK2/E6E7 and Sup-T1 cells. MTS assay was performed to determine the cell viability. MTS, a tetrazolium compound, can be bioreduced by live cells into a colored formazan product measurable at 490 nm. Data is normalized to the negative control and expressed as mean $\pm$ SD; n = 4. Cells cultured in plain medium were used as negative control. 1 M acrylamide dissolved in regular cell culture medium was used to induce cell death in positive control groups. N, negative control; P, positive control. * $P < 0.05$ versus negative control.
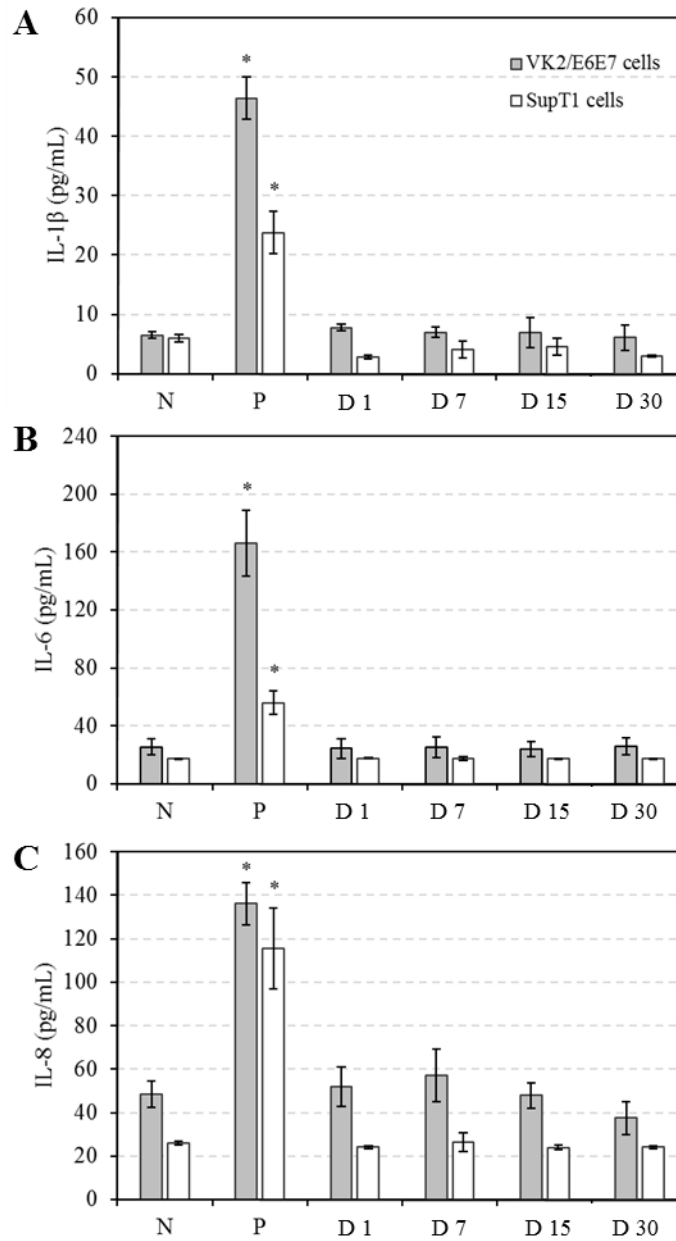
Figure 3-11. Impact of solvent-cast pH-responsive PU membranes on proinflammatory cytokine production (A) Interleukin (IL)-1β, (B) IL-6, and (C) IL-8 production. Plain medium was used as a negative control, and 200 μg/mL of nonoxynol-9 or 50 μg/mL of lipopolysaccharide-treated cells were used as positive controls for IL-1β and IL-6/IL-8, respectively. Data is expressed as mean ± SD; $n = 4$. * $p < 0.05$ versus negative control.

3.5 Conclusions

pH-responsive polyether-PUs containing HEP were successfully synthesized and used for the preparation of solvent-cast membranes. The prepared membranes demonstrated pH-triggered reversible changes in swelling ratio and morphology. The pH-responsive release of NaDF was sensitive and rapid at pH 7.0 but demonstrated close-to-zero release of NaDF at pH 4.5. The pH-responsive PU membranes were non-cytotoxic toward the human vaginal epithelial cell line VK2/E6E7 and T-cell line Sup-T1. In summary, the newly synthesized pH-responsive PUs demonstrate potential utility as a novel biomaterial for the development of "smart" intravaginal drug delivery devices.

3.6 Acknowledgements

3.7 Contribution of Authors

Seungil Kim[a,‡]: initiated and contributed to the scope of the manuscript; performed synthesis and characterization of PU copolymers; performed fabrication and characterization of solvent-cast PU membranes; performed drug permeation test; wrote the manuscript.

Yufei Chen[b,‡]: performed HPLC measurement; performed *in vitro* biocompatibility studies; wrote the manuscript.

Emmanuel A Ho[a,b,*]: initiated and contributed to the scope of the manuscript; contributed writing manuscript; critically reviewed the manuscript.

Song Liu[a,c,d,*]: initiated and contributed to the scope of the manuscript; contributed writing manuscript; critically reviewed and revised the manuscript.

[a] Biomedical Engineering, Faculty of Engineering, University of Manitoba, Winnipeg, Manitoba, Canada

[b] Laboratory for Drug Delivery and Biomaterials, College of Pharmacy, Faculty of Health Sciences, University of Manitoba, Winnipeg, Manitoba, Canada

[c] Department of Biosystems Engineering, Faculty of Agricultural and Food Sciences, University of Manitoba, Winnipeg, Manitoba, Canada

[d] Department of Chemistry, Faculty of Science, University of Manitoba, Winnipeg, Manitoba, Canada

‡ = Equal contributions; * = Corresponding authors

Chapter 4

Design and development of pH-responsive polyurethane membranes for intravaginal release of nanomedicines

As a part of this thesis, electrospun pH-responsive porous PU, PEG-HEP-MDI-PG, membranes were developed to achieve on-demand release of nanocarriers since the solvent-cast pH-responsive PU membranes did not allow permeation of nanocarriers due to their insufficient interconnected space for penetration of nanocarriers. The hypothesis of this research is that pH-responsive change in surface charge, cavity size, and thickness of the electrospun PU membrane can contribute to the permeability change of nanocarriers.

4.1   Abstract

The objective of this study was to develop and characterize a novel intravaginal film platform for pH-triggered on-demand release of NPs which is essential for efficient intravaginal delivery of certain effective but acid labile anti-STIs therapeutic agents such as siRNA. A pH-responsive PU (PEG-HEP-MDI-PG) was electrospun into a porous nanofibrous mat. The diameter of the fibers as well as the thickness and pore sizes of the membrane at dry and wet (pH 4.5 and 7.0) were determined from SEM micrographs. pH-dependent zeta-potential (ζ) of the membrane was evaluated using a SurPASS electrokinetic analyzer. VisiblexTM color dyed polystyrene NPs (PSNs, 200 nm, -COOH) were used for *in vitro* NP release studies in a vaginal fluid simulant (VFS) at pH 4.5 (normal physiological vaginal pH) and 7.0 (vaginal pH neutralization by semen). There was close-to-zero release of PSNs at pH 4.5 ($2 \pm 1\%$) but a continuous release at pH 7.0 ($60 \pm 6\%$) for 24 h. The pH-responsive release of NPs hinged on the electrostatic interaction between the pH-responsive membranes and the anionic NPs, and the pH-responsive morphology change of the membrane. *In vitro* biocompatibility studies of the membranes showed no significant cytotoxicity to VK2/E6E7 human epithelial cells and Sup-T1 human T-cells and no significant changes in the expression of pro-inflammatory cytokines (IL-6,

IL-8 and IL-1β). Overall, these porous pH-responsive PU membranes demonstrated their potential in serving as "window" membranes of reservoir-IVRs for pH-responsive intravaginal release of nanocarriers.

4.2   Introduction

Over 30 million people globally live with HIV that can potentially progress to AIDS.[28,164] HIV is a life-threatening disease, and no cure has been found yet. Prevention and early treatment are important in decreasing the prevalence and incidence of HIV.

Intravaginal drug delivery is beneficial for HIV prevention since unprotected heterosexual intercourse is the typical route of the HIV transmission. Moreover, the advantages of intravaginal drug delivery include increased drug delivery efficiency to the target site, drug bioavailability, pharmacological response, and drug compliance of patients.[32,165] Intravaginal formulations such as ointments, creams, gels, films, vaginal tablets and IVRs have been developed for the release of drugs.[23] Among intravaginal formulations, IVRs have advantages over other vaginal formulations because they can provide sustained, controlled drug release for a prolonged period.[110] The availability of the intravaginal formulations could greatly empower women to protect themselves from infection since the application of formulations does not require the consent of their partner.[166]

Anti-HIV drugs and siRNAs act on T-cells at different stages of the HIV life cycle including receptor interaction, virus-cell fusion, reverse transcription, integration, and proteolytic processing to block the transmission progress.[30,167] Hydrophilic anti-HIV drugs have advantages due to their solubility in an aqueous environment in comparison to the poorly water-soluble anti-

HIV drugs. However, it is cumbersome to achieve a high delivery efficiency of hydrophilic anti-HIV drugs to the T-cells because the drugs cannot effectively penetrate through the vaginal mucus barrier and cross the lipid bilayer of the cell membrane.[35,168] On the other hand, poorly water-soluble anti-HIV drugs have a limitation in their application because of their relatively low solubility and bioavailability in an aqueous environment.[169] Similarly, siRNAs have a high potential to prevent HIV transmission by simultaneously targeting host genes and viral genes,[21] but they have low stability in the acidic vaginal pH.

In this regard, an alternative method is needed to deliver anti-HIV drugs and siRNAs to increase the delivery efficiency and reduce side effects.[170] DDS using nanocarriers, such as micelles, vesicles, nanogels, solid lipid nanoparticles, and liposomes have been developed for the delivery of drugs and genes.[14,15] A nanocarrier can improve dispersion of poorly water-soluble anti-HIV drugs, protect cargos from the acidic conditions, and increase delivery efficiency.[171,172] DDS using nanocarriers can also reduce systemic toxicity and off-target effects of HIV treatment.[16]

While nanocarriers are beneficial for the intravaginal delivery of anti-HIV drugs and siRNA, a continual release of drugs and siRNAs is not desirable. For prevention of HIV, it is desirable that anti-HIV drug- or siRNA- loaded nanocarrier be released only during heterosexual intercourse to avoid unnecessary exposure to drugs and reduce the side effects. Therefore, it is necessary to release nanocarriers from IVRs upon pH change from 4.5 to 7.0 since vaginal pH can be increased to neutral pH from normal acidic vaginal pH (3.5-4.5) by the introduction of seminal fluid during heterosexual intercourse.[21,24,33,35,104]

Our research group fabricated solvent-cast pH-responsive PU membranes as "window" membranes of reservoir-IVR.[103] The solvent-cast membranes showed the continuous release of

hydrophilic model drug NaDF at pH 7.0 but close-to-zero release of NaDF at pH 4.5. Although the solvent-cast pH-responsive PU membranes demonstrated on-demand drug release, the membranes failed to achieve the pH-responsive NPs permeation due to the insufficient interconnected space for NPs. In this study, our research group proposed electrospun pH-responsive interconnected porous PU membranes as "window" membranes of reservoir-IVR for on-demand release of NP.

Stimuli-responsive membranes have been developed for various types of applications including drug delivery devices and separation processes.[66] As an example, a blends of poly(vinylidene fluoride) (PVDF) and poly(vinylidene fluoride)-g-poly(methacrylic acid) (PVDF-g-PMAA) have been used to fabricate pH-responsive membrane.[173] Such pH-responsive membrane could be prepared by immersion precipitation process and its switchable pH-responsive water flux at pH 2.0 and 8.0 has been demonstrated. The pH-dependent increase of pure water flux at pH 2.0 can be explained by pH-responsive conformational changes of surface-localized PMAA. A thermo- and pH-responsive polymeric composite membrane made of poly(N-isopropylacrylamide-co-methacrylic acid) has been investigated for permeability change triggered by environmental stimuli.[174] The permeability of vitamin B_{12} is increased with increasing temperature or decreasing pH. The pH-responsive permeation change of vitamin B_{12} is supported by pore size change of the membrane due to swelling and shrinking of the polymer chains. Similarly, pH-responsive electrospun membrane has been fabricated using a mixture of PVA and poly(acrylic acid).[175] The membrane has demonstrated a pH-responsive change of swelling ratio and thickness increase with increasing pH. Likewise, a pH-responsive gating membrane system with a pumping effect consisting of a porous membrane and cross-linked hydrogel has also been studied.[176] The porous membrane is fabricated using PVDF and

conjugated with PMAA chains on its surface. Moreover, the hydrogel is prepared by plasma-graft pore-filling polymerization of poly(N,N-dimethylaminoethyl methacrylate) (PDM) for the inside of the reservoir as a pumping material. When pH is lower than the pKa of PMAA (4.65-5.35) and protonated PDM (4.5-5.5), the release is accelerated by the shrinking of PMAA chains and the swelling of the PDM hydrogel. Also, a pH-responsive switchable membrane has been fabricated by self-assembly of polystyrene-b-poly(4-vinyl pyridine) in the presence of metal ions [copper(II), cobalt(II), nickel(II), and iron(II)] and nonsolvent-induced phase separation.[177] Such a membrane has demonstrated pH-responsive pore size change (larger pore at pH 10.0 than at pH 2.0), water flux change, and permeation of polyethylene glycol (Mw 1,500~10,000) (higher permeation at pH 7.0 than pH 2.0). However, to the best of our knowledge, no study has reported the pH-responsive release of NPs from a reservoir-IVR.

In the present study, a pH-responsive interconnected porous PU membrane was developed for smart intravaginal release of NPs. The pH-responsive PU membrane was fabricated using electrospinning to facilitate the fabrication of thin interconnected porous membranes. The permeability of the NPs through the electrospun porous membrane was controlled by pH-responsive change of morphology of the membrane and electrostatic interaction between the membrane and NPs. Therefore, this is the first study that has developed a pH-responsive membrane for pH-dependant intravaginal release of NPs. The pH-responsive interconnected porous PU membrane has potential utility for pH-dependent release of NPs from medical devices including IVRs.

4.3 Materials and methods

4.3.1 Materials

1,1,1,3,3,3-hexafluoro-2-propanol (HFIP, 99.99%), 1,4-Bis(2-hydroxyethyl)piperazine (HEP, 99%), 1,6-hexanediol (HD, 99%), 4,4′-Methylenebis(phenyl isocyanate) (MDI, 98%), anhydrous 1,2-dichloroethane (DCE, 99.8%), anhydrous diethyl ether (> 99%), anhydrous N,N-dimethylformamide (DMF, 99.8%), dibutyltin dilaurate (DBTDL, 95%), dimethyl sulfoxide (DMSO, ≥ 99.5%), propylene glycol (PG, > 99.5%), and tetrahydrofuran (THF) were purchased from Sigma Aldrich (St. Louis, MO, USA). Polyethylene glycol (PEG, Mn= 6,000) was purchased from EMD Chemicals (Mississauga, ON, Canada). Visiblex[TM] color dyed polystyrene nanoparticles (PSNs, 200 nm, COOH on its surface, media: 0.1% Tween 20 in DI water) were purchased from Phosphorex Inc. (Hopkinton, MA, USA). VFS was prepared by dissolving 1.0 g acetic acid, 0.018 g bovine serum albumin, 0.222 g $Ca(OH)_2$, 0.6 g glycerol, 5.0 g glucose, 1.4 g KOH, 2.0 g lactic acid, 3.51 g NaCl, and 0.4 g urea in 1 L of distilled water. The pH of VFS was adjusted by adding 0.1 N HCl and 0.1 N NaOH solution [104].

4.3.2 Synthesis of pH-responsive polyurethane copolymer (PEG-HEP-MDI-PG)

pH-responsive and non-pH-responsive PU copolymers were synthesized and purified according to a procedure reported by our research group previously.[103] Briefly, a three-neck round-bottom flask was set up with nitrogen inlet-outlet purging to synthesize pH-responsive PU (PEG-HEP-MDI-PG). PEG and HEP (feed mole ratio of PEG:HEP = 0.1:0.9) were dissolved in anhydrous DCE and added to the reactor. A catalytic amount of DBTDL and a stoichiometric ratio of diisocyanate (MDI, feed mole ratio of OH/NCO = 1) were added to the reactor. The

reactor was maintained at 60 °C for 3 h with stirring under a nitrogen atmosphere. After the reaction, PG (feed mole ratio of HEP:PG = 0.9:1) and a stoichiometric ratio of diisocyanate (MDI, OH/NCO = 1) were added. The reactor was maintained at 60 °C for 3 h under a nitrogen atmosphere. The product was then precipitated in 8-fold diethyl ether and washed with excess diethyl ether. The product was re-dissolved in DMSO, re-precipitated in 8-fold distilled water, and washed with excess distilled water several times to remove remaining impurities. HD was used to synthesize control non-pH-responsive PU (PEG-HD-MDI-HD) instead of HEP and PG. The overall feed mole ratio of raw chemicals for PEG-HDI-MDI-HD was PEG: HD: MDI = 0.1: 2.9: 3.0. The viscosity average molecular weight (Mv) of synthesized PEG-HEP-MDI-PG and PEG-HD-MDI-HD copolymer was calculated from the Mark-Houwink equation ($[\eta] = 3.64 \times 10^{-4}M^{0.71}$) for the polyether-PU in DMF at 25 °C.[142] A Cannon-Ubbelohde dilution viscometer was used to measure viscosities with a constant temperature bath set at 25.0 ± 0.5 °C. Pure DMF and 25 mg of PU in 10 mL DMF were prepared for measurement. PU solution was diluted from 2.50 mg/mL to 1.25 mg/mL. Travel times of pure DMF and polymer solutions between two measurement marks were recorded. Mv values of PEG-HEP-MDI-PG and PEG-HD-MDI-HD were 1.23×10^6 and 2.36×10^6, respectively.

4.3.3   Electrospinning of pH-responsive polyurethane copolymer

pH-responsive PU (PEG-HEP-MDI-PG) was electrospun to fabricate fibrous, interconnected, and porous PU membranes using an electrospinning apparatus (Ne300, Innovenso, Istanbul, Turkey). Different mixing ratios of DMF and THF were applied to determine the most suitable electrospinning conditions for fabricating fibrous pH-responsive PU membrane (**Table 4-1**). The viscosity of pH-responsive PU solution was evaluated using an

Advanced Rheometer (AR 2000, TA Instruments) and was calculated from the relationship between shear stress and shear rate at 0.1-100 rad/s using 20 mL of 20 wt% PU solutions. The concentration of PU in mixed-solvents (20 wt%), voltage applied on the nozzle (30 kV), feeding speed of pH-responsive PU solution (0.7 mL/h), nozzle to collector distance (15 cm), and dispensed volume of PU solution (1 mL) were optimized by trial-and-error, before the electrospinning process. These electrospun pH-responsive PU membranes were washed with excess distilled water to remove remaining impurities then dried at room temperature.

Table 4-1. Electrospinning of pH-responsive PU (PEG-HEP-MDI-PG) using different mixed solvent ratios.

NO.	Polymer	Concentration (wt %)	Solvent (DMF: THF, Vol.)	Voltage (kV)	Feeding Speed (mL/h)	Nozzle to collector distance (cm)	Dispensed Volume (mL)
A	PEG-HEP-MDI-PG	20	10: 0	30	0.7	15	1
B	PEG-HEP-MDI-PG	20	7: 3	30	0.7	15	1
C	PEG-HEP-MDI-PG	20	5: 5	30	0.7	15	1
D	PEG-HEP-MDI-PG	20	3: 7	30	0.7	15	1

Control PU membranes were fabricated using a custom-designed electrospinning setup with the following conditions: 9% w/v solution in HFIP, needle-collector distance of 18 cm, flow rate of 1 mL/h, voltage of 15 kV, and a 21-gauge needle. The needle was clamped to the positive electrode of a high-voltage power supply (ESP200D, NanoNC, Seoul, South Korea) while the negative electrode was connected to a rotating aluminum drum collector (250 rpm). The solution was delivered using a syringe pump (ESP200D). Electrospun nanofibers were dried in a vacuum oven at ambient temperature for three days, and stored in a desiccator for subsequent use.

Scanning electron microscope (SEM, FEI Quanta E-SEM) images of these fabricated PU membranes were captured to evaluate diameters (DIs) of fibers, pore size, and thickness of these membranes. Membrane samples were coated with 10 nm Au-Pd before capturing images. The diameter, pore size, and thickness were manually measured using ImageJ, a free picture editing software, from SEM images using their size bar as reference.[73,178–181] The threshold of pores was set to the blackest area versus the gray area using SEM images at $1,000 \times$ magnification.

4.3.4 Physicochemical characteristics of electrospun porous pH-responsive PU membranes

pH-responsive morphology (pore size, thickness, and diameter) changes of electrospun PU membranes were evaluated from SEM images. For evaluation, electrospun porous pH-responsive (DMF: THF = 3: 7) and control PU membranes were cut into 2×2 cm squares and immersed in VFS at pH 7.0 or pH 4.5 at 37 °C for 3 h with gentle shaking. Swollen samples were extracted from VFS and kept at -80 °C followed by lyophilization. Fracture surfaces of these electrospun PU membranes for cross-section imaging were prepared by cracking membranes under liquid nitrogen.

The streaming current was measured for the electrospun PU membranes using SurPASS electrokinetic analyzer (Anton Paar) at pH ranging from 3.5 to 8.5.[182–184] Briefly, rectangular membrane samples (20 mm $\times$ 10 mm) were prepared and attached to sample holders using double-sided adhesive tape. The measurement was conducted with an adjustable-gap cell, and the flow channel gap was set at 100 µm. As a background electrolyte, 1 mM KCl solution was used and the pH was adjusted using 0.05M HCl or 0.05M NaOH solution. Zeta-potential (ζ) of

the membranes was automatically calculated using the following Helmholtz-Smoluchowski equation.

$$\zeta = \frac{dI}{dP} * \frac{\mu}{\varepsilon\varepsilon_0} * \frac{L}{A}$$

where dI/dP is the slope of the streaming current versus pressure, μ is the solution dynamic viscosity, ε is the dielectric constant of the solution, ε_0 is the vacuum permittivity, L is the streaming channel length, and A is the cross-section of the streaming channel.

4.3.5   Permeation of nanoparticles from the electrospun pH-responsive PU membranes

Commercially available blue-dyed polystyrene nanoparticles (PSNs, -COOH) were used for pH-responsive NPs release tests. Before release studies, the average particle size of PSNs was evaluated by dynamic light scattering (DLS) using ZetaPALS potential analyzer (Brookhaven Instrument, Holtsville, NY, USA). 0.1 µg/mL of PSNs in VFS at pH 4.5 and 7.0 were prepared by vortex shaking for 3 min at 3,000 rpm. The pH of PSNs suspension in VFS was adjusted by adding 0.1 N HCl or 0.1 N NaOH solution. A scattering angle of 90° and laser light at 659 nm were applied for DLS measurement.

The ZetaPALS potential analyzer was used to evaluate the zeta-potential of PSNs. Two suspensions of PSNs (0.1 µg/mL) in distilled water (one at pH 4.5 and one at pH 7.0) were prepared. The pH of the suspension was adjusted using 0.1 N HCl or 0.1 N NaOH solutions. A Smoluchowski model was used to evaluate surface charge.

pH-responsive NP release studies were performed using Franz cells. Briefly, electrospun porous pH-responsive (DMF: THF = 3: 7) and control PU membranes were cut to 2×2 cm

squares and sandwiched between the upper and bottom chambers of Franz cells. Two suspensions of PSNs at 1 mg/mL (at pH 4.5, pH 5.5, and pH 7.0) in VFS were prepared for the upper chamber of the Franz Cells. The bottom chamber was filled with VFS of the same pH as that in the upper chamber. The bottom chamber was kept at 37 °C. The VFS in the bottom chamber was gently stirred with a magnetic bar. After adding 800 µL of the prepared PSNs suspension to the upper chamber of Franz cells, 300 µL sample solution was collected to evaluate released amounts of PSNs at 1 h, 2 h, 3 h, 6 h, 12 h, and 24 h from each arm of Franz cells. The amount of PSNs released was quantified by reading absorbance at 300 nm using a plate reader.

Associated amounts of PSNs with electrospun porous PU membranes (DMF: THF = 3: 7) in VFS at pH 4.5, 5.5, and 7.0 were evaluated. Round cut pH-responsive and control PU membranes (DI: 0.8 cm) corresponding to an area of 0.5024 cm^2 between upper and bottom chambers of Franz cells were prepared. Prepared electrospun PU membrane samples (DI: 0.8 cm) were immersed in 6.4 mL of 0.125 mg/ml PSNs suspension at 37 °C with gentle horizontal shaking (100 rpm) since 0.8 mL of 1 mg/mL PSNs was used for the upper chamber, while 5.6 mL of release medium (VFS at pH 4.5, 5.5, or 7.0) was used for the bottom chamber of the Franz cells to evaluate the pH-responsive NP release. At each time point (1, 2, 3, 6, 12, and 24 h), 300 µL of sample solution was taken to evaluate the amount of PSNs associated with electrospun PU membranes (DI: 0.8 cm). Fresh VFS was replenished for the suspension. The concentration of free PSNs was quantified by measuring absorbance at 300 nm using a plate reader. The associated percentage of PSNs was back-calculated using the concentration of free PSNs.

4.3.6 *In vitro* biocompatibility studies of electrospun porous pH-responsive PU membrane

The electrospun porous pH-responsive PU membrane (DMF: THF = 3: 7) was evaluated on the vaginal epithelial cells VK2/E6E7 and immune cells Sup-T1 for its cell toxicity and also for the production of the pro-inflammatory cytokines. To assess the cytotoxicity, we used the elution assay method follow by the cell proliferation assay MTS (CellTiter 96® Aqueous One Solution Cell Proliferation Assay, Promega Corporation, Madison, WI, USA) since the elution test methods are widely applied for *in vitro* cytotoxicity testing of biocompatible materials including PU.[42,148,185] Briefly, 50 mg of electrospun membrane sterilized in 70% isopropanol for 10 seconds, dried, and exposed to the UV light for 1 h was incubated in 2.5 mL of either VK2/E6E7 cell medium consisting of keratinocyte-serum free medium (K-SFM) containing 0.1 µg/mL recombinant human epidermal growth factor, 50 mg/mL bovine pituitary extract, 0.4 mM of calcium and 1% of penicillin/streptomycin, or in Sup-T1 cells medium consisting of RPMI-1640 containing 10% heat-inactivated FBS and 1% penicillin/ streptomycin. The polymer was incubated for 1, 7, 15 and 30 days at 37 °C in an orbital shaker set at 100 rpm. At different time points, all of the media were collected aseptically and used to treat 2.5×10^5 VK2/E6E7 cells or Sup-T1 seeded in a 96-well plate and maintained at 37 °C under 5% CO_2 for a period of 24 h. Blank K-SFM or RPMI-1640 medium was used as negative control and 1 M acrylamide prepared in K-SFM or RPMI-1640 was used as positive control.

In addition, 50 µg/mL of lipopolysaccharide (LPS, Thermo Fisher Scientific MA, USA) and 200 µg/mL of nonoxyl-9 (N-9, Spectrum Chemical, Corp., New Brunswick, NJ, USA) were prepared of K-SFM or RPMI-1640 and used to treat VK2/E6E7 cells or Sup-T1 cells as positive control for the pro-inflammatory markers IL-6, IL-8 (induce by LPS) and IL-1β (induce by N-9). After 24 h of treatment, the supernatant in each well was collected for a downstream ELISA

assay for the pro-inflammatory markers and replenished with fresh medium. 20 µl of MTS reagent was added in each well and incubated as specified in the MTS assay protocol and the cell viability was analyzed by reading the absorbance at 450 nm using a Synergy HT Multiplate Reader (Biotek, Winooski, VT, USA). ELISA kits obtained from R&D Systems (Minneapolis, MN, USA) were used to evaluate IL-6, IL-8 and IL-1β production. The Absorbance of each ELISA plate was ready at 450 nm using a micro-plate reader.

4.3.7   Statistical analysis

Data are presented as mean ± standard deviation (SD). The number of replicates is indicated as the *n*-value. One-way analysis of variance was performed on all results with $P < 0.05$ considered to be significant.

4.4   Results and discussion

4.4.1   Preparation of electrospun porous pH-responsive PU (PEG-HEP-MDI-PG) membrane

Interconnected porous PU membranes were fabricated using electrospinning. Various mixing ratios of DMF and THF (10: 0, 7: 3, 5: 5, and 3: 7) were applied to optimize the electrospinning conditions of pH-responsive PU membranes. Electrospinning parameters, such as concentration of PUs, voltage applied on the nozzle, feeding speed of PUs solution, nozzle to collector distance, and dispensed volume of the pH-responsive PU solution were fixed (**Table 4-1**).
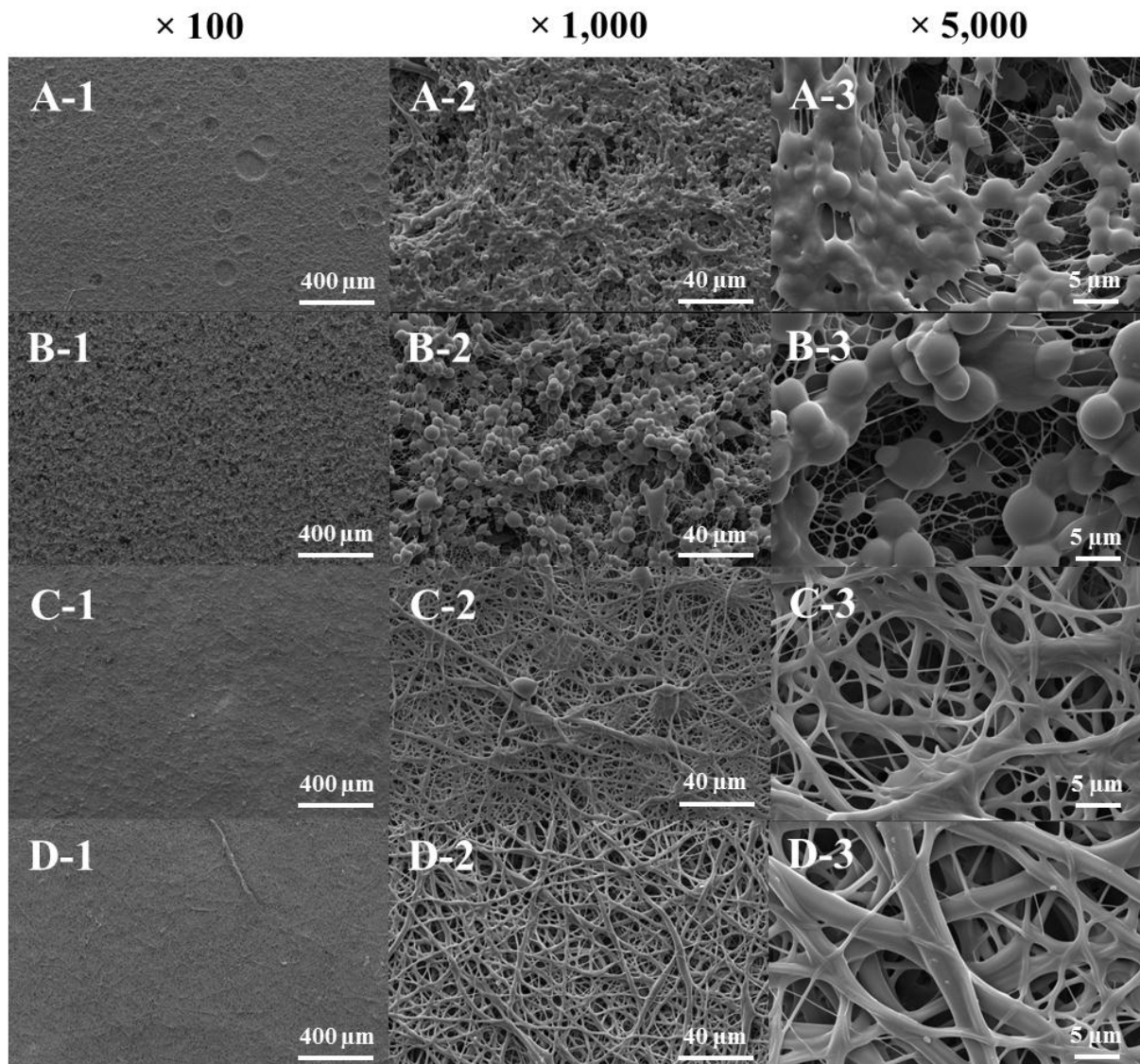
Figure 4-1. SEM images of electrospun pH-responsive PU (PEG-HEP-MDI-PG) membranes at the voltage of 30 kV, concentration of PU 20 wt%. The volume ratios of DMF: THF were (A) 10: 0, (B) 7: 3, (C) 5: 5, and (D) 3: 7. Scale bars have been shown on the images.

The electrospun fibrous structure was fabricated with fine diameters when the DMF ratio was decreased in mixed solvent (**Figure 4-1**). Membranes fabricated by using the higher

concentration of DMF (DMF: THF = 10: 0 and 7: 3) exhibited beaded fibrous structures (**Figure 4-1, A-B**); however, a uniform fibrous structure was observed for the membranes with an increase in the THF content (DMF: THF = 5: 5 and 3: 7) (**Figure 4-1, C-D**). The quality and diameter of electrospun fibers depended upon the boiling point of the solvent. Since THF has a lower boiling point, it can evaporate more rapidly than the DMF, thus resulting in an increased amount of fine fibers with an increase in the THF ratio in the mixed solvent.[186,187]

Pore size and diameter of fibers (*n* = 100) were evaluated using ImageJ (**Figure 4-2**). Average pore sizes of the membranes fabricated using different solvent ratios (DMF: THF = 10: 0, 7: 3, and 5: 5) were 2 ± 1 μm, 1.7 ± 0.6 μm, and 1.8 ± 0.6 μm, respectively. The average fiber diameter of the membranes fabricated using DMF: THF = 5: 5 was 5 ± 2 μm. On the other hand, the membrane fabricated using a higher ratio of the THF in the mixed solvent (DMF: THF = 3: 7) showed the greatest average pore size (2.1 ± 0.7 μm), the smallest average fiber diameter (1.1 ± 0.5 μm), and the narrowest distribution of the diameter. Since the membranes fabricated with the higher content of THF in the mixed solvent (DMF: THF = 3: 7) showed the most uniform fibrous porous structure, they were used for further pH-responsive morphology changes, NP release, and *in vitro* cytotoxicity studies. The viscosity of 20 wt% PEG-HEP-MDI-PG in a mixed solvent (DMF: THF = 3: 7) was 0.306 ± 0.003 Pa.s. Viscosity is one of the important factors for electrospinnability. Polymers need to reach a certain threshold molecular weight as reflected by the viscosity of their solutions to get enough entanglement for fiber formation. The PU solution had sufficiently high viscosity (0.306 ± 0.003 Pa.s.) allowing it to be stretched into continuous fibers. It is important to note that a higher molecular weight polymer or higher solution concentration will lead to an increase in viscosity and greater fiber diameter.
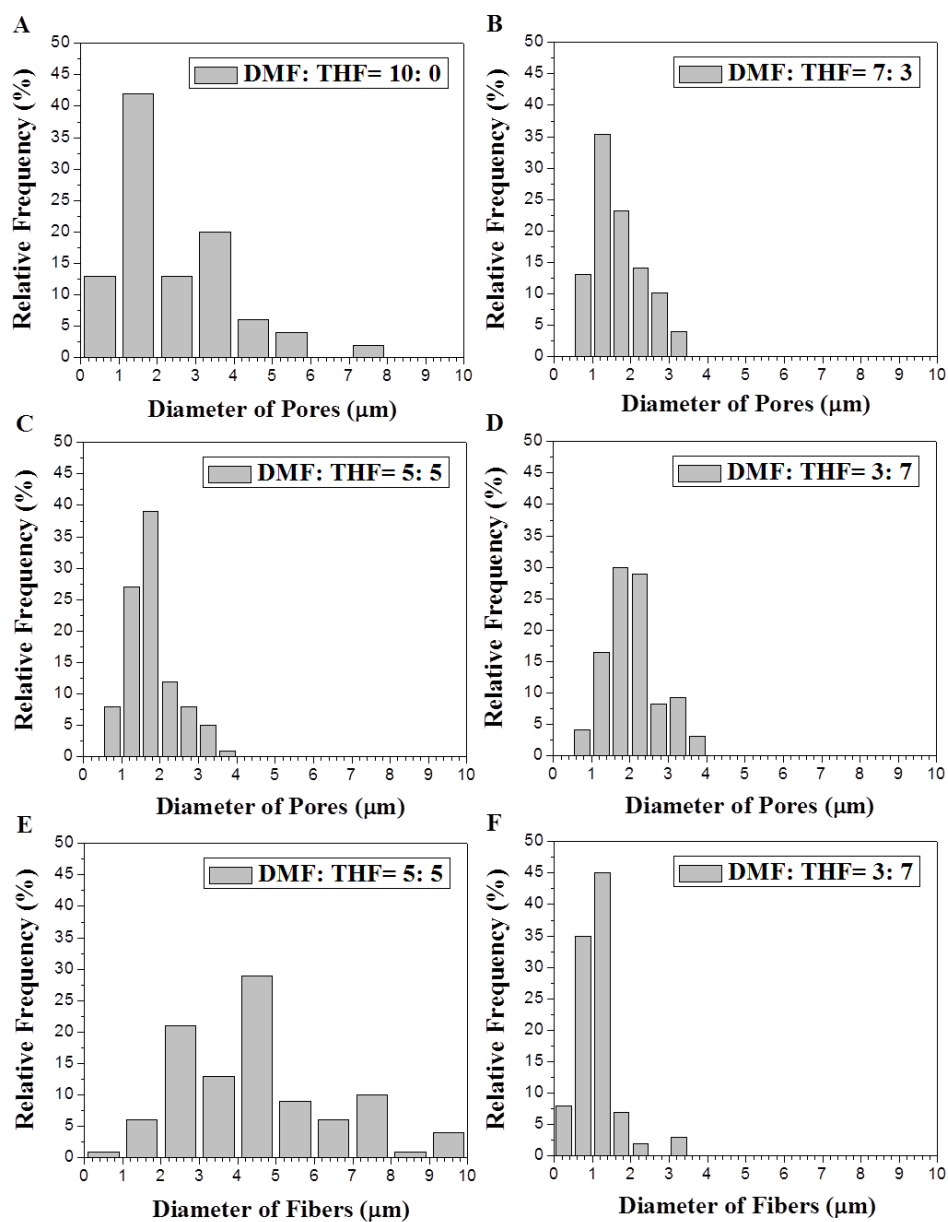
Figure 4-2. Pore sizes distribution and fibers diameter of electrospun pH-responsive PU (PEG-HEP-MDI-PG) membranes using various mixed solvent ratio ($n = 100$). The diameters and pore sizes were manually measured using ImageJ from SEM images.
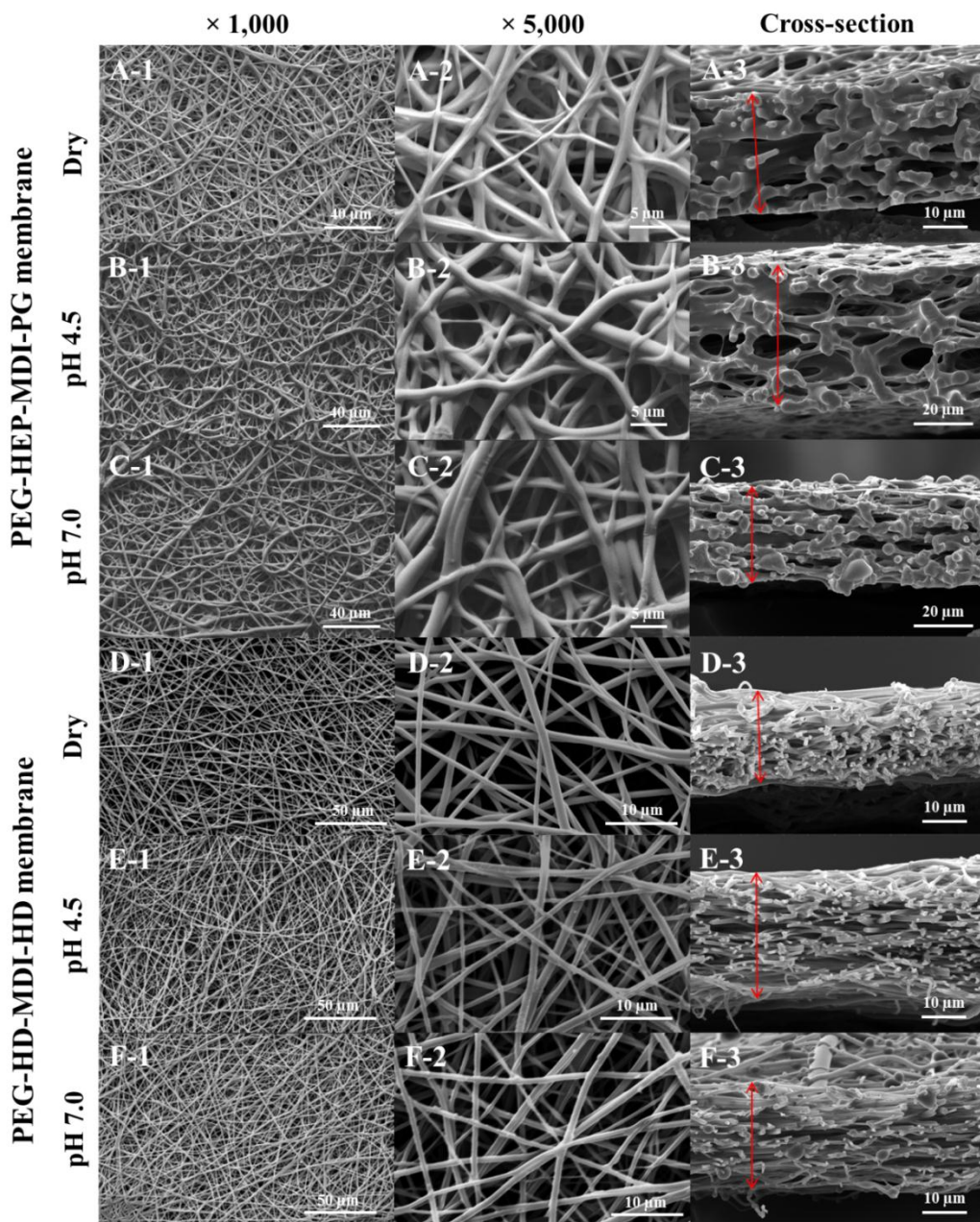
Figure 4-3. Morphology of electrospun porous pH-responsive PU (PEG-HEP-MDI-PG) membrane (DMF: THF = 3: 7): dry (A), pH 4.5 (B), pH 7.0 (C), and control PU (PEG-HD-MDI-HD) membrane: dry (D), pH 4.5 (E), pH 7.0 (F). Scale bars are shown on the images.

The morphology changes of electrospun porous pH-responsive (DMF: THF = 3: 7) and control PU membranes in dry and wet conditions (pH 4.5 and 7.0) were evaluated based on the changes of the average pore size, average diameter of fibers, and the thickness of the membranes (**Figure 4-3**, **Table 4-2**). Pore size, fiber diameter, and thickness of membranes were evaluated by SEM micrographs (magnification: ×1,000) using ImageJ. Pore sizes evaluated from the surface of the electrospun membranes might be different to those of the real situation for NPs penetration because the actual membrane would have more layers than those shown in the SEM images. Average pore sizes of porous pH-responsive PU membrane at dry, pH 4.5, and pH 7.0 were 2.3 ± 0.7 μm, 1.8 ± 0.6 μm, and 2.2 ± 0.6 μm, respectively (**Figure 4-4, Table 4-2**).

Table 4-2. Average pore size and diameter of electrospun porous pH-responsive (PEG-HEP-MDI-PG) and control (PEG-HD-MDI-HD) PU membrane at dry and wet conditions in VFS at pH 4.5 and 7.0.

		dry	pH 4.5	pH 7.0
pH-responsive (PEG-HEP-MDI-PG)	Average pore size (μm)	2.3 ± 0.7	1.8 ± 0.6	2.2 ± 0.6
	Average diameter of fibers (μm)	0.9 ± 0.4	1.4 ± 0.5	1.2 ± 0.5
	Average thickness (μm)	28.6 ± 0.7	50 ± 2	34 ± 1
Control (PEG-HD-MDI-PG)	Average pore size (μm)	2.0 ± 0.6	1.5 ± 0.4	1.7 ± 0.4
	Average diameter of fibers (μm)	0.7 ± 0.2	0.9 ± 0.3	0.8 ± 0.2
	Average thickness (μm)	22.9 ± 0.8	29 ± 2	25.0 ± 0.9
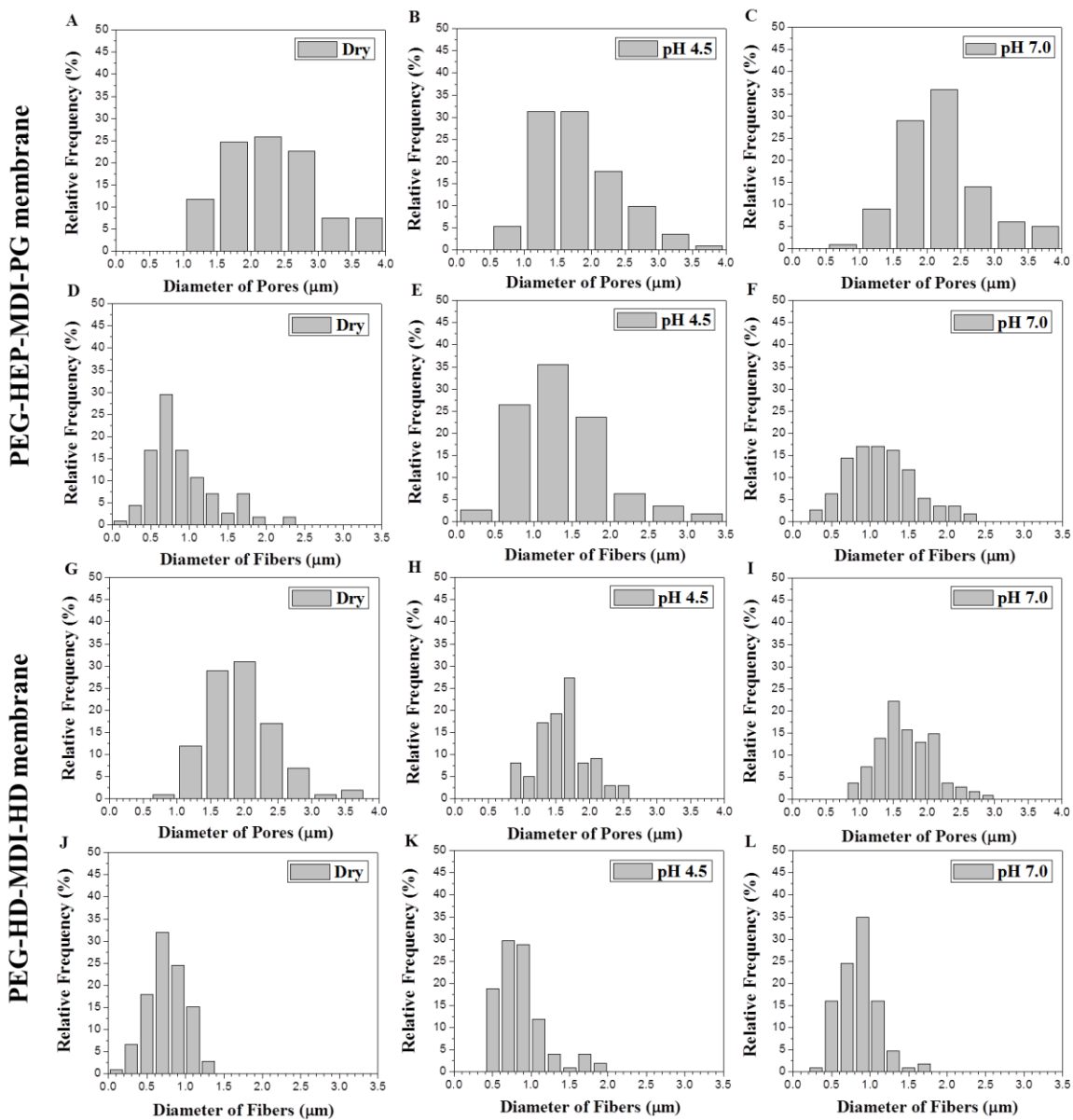
Figure 4-4. Pore sizes and fiber diameters of electrospun porous pH-responsive PU (PEG-HEP-MDI-PG) membranes (DMF: THF = 3: 7) (A-F) and control PU (PEG-HD-MDI-HD) membranes (G-L) ($n = 100$).

Average diameters of fibers of porous pH-responsive membranes at dry, pH 4.5, and pH 7.0 were 0.9 ± 0.4 μm, 1.4 ± 0.5 μm, and 1.2 ± 0.5 μm, respectively. The difference in the pore sizes of porous pH-responsive PU membranes at pH 4.5 and 7.0 was 0.4 μm, representing a 22.2% change in the pore size at pH 4.5; however, the control PU membrane showed a difference of 0.2 μm (13.3% change compared to the pore size at pH 4.5) between pH 4.5 and 7.0. The porous pH-responsive PU membrane at pH 4.5 had a smaller pore size than that at pH 7.0 due to pH-responsive swelling of electrospun fibers. The fiber diameter of pH-responsive membrane was 0.2 μm bigger at pH 4.5 than at pH 7.0. The swollen fiber might occupy space between fibers and reduce pore sizes. The pH-responsive swelling of the fibers contributes not only to change in pore sizes but also to increased membrane thickness. The thickness of porous pH-responsive membrane showed noticeable differences at pH 4.5 (50 ± 2 μm) and pH 7.0 (35 ± 1 μm). At pH 4.5, the thickness of the porous pH-responsive membrane was 1.47 times greater than the thickness at pH 7.0 due to ionization of pH-sensitive groups.[175] Such pH-responsive morphology changes contributed to pH-responsive PSNs permeability as described in the following sections.

Zeta-potentials of control PU (PEG-HD-MDI-HD) and porous pH-responsive PU (PEG-HEP-MDI-PG) membrane (DMF: THF = 3: 7) were calculated from the streaming current at pH values ranging from 3.5 to 8.5 (**Figure 4-5**). Control PU membrane showed an isoelectric point at pH 3.9. It showed a desirable zeta-potential profile as a control membrane, with negative values in pH range from 3.9 to 8.5 compared to the porous pH-responsive membrane. The zeta-potential of the control PU was -7.9 mV at pH 4.5, and -25.4 mV at pH 7.0. The negatively charged surface has no attractive electric force for negatively-charged molecules, but it has repulsive electric force. However, the porous pH-responsive PU membrane may have strong

attractive forces with anionic NPs at pH 4.5 due to the positively charged surface at pH 4.5 (14.2 mV). The isoelectric point of the porous pH-responsive membrane was pH 7.2, and the membrane showed zeta-potential close-to-zero (2.2 mV) at pH 7.0. The porous pH-responsive PU membrane can have a strong electric attractive force at normal human vaginal tract pH (pH 3.5-4.5) and almost no electrostatic force at neutral pH (elevated vaginal tract pH by the introduction of seminal fluid during heterosexual intercourse).
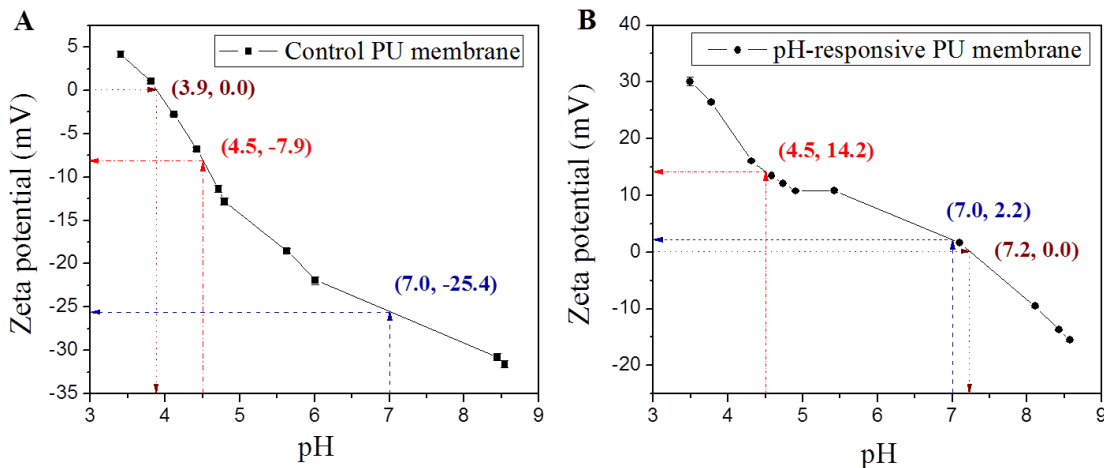
Figure 4-5. Influence of streaming pH on the zeta potential of the electrospun PU membranes at pH ranging from 3.5 to 8.5. (A) control PU (PEG-HD-MDI-HD) membrane and (B) porous pH-responsive PU (PEG-HEP-MDI-PG) membrane. Data is expressed a mean ± SD; $n = 3$. The zeta-potential calculated related to the Smoluchowski equation.
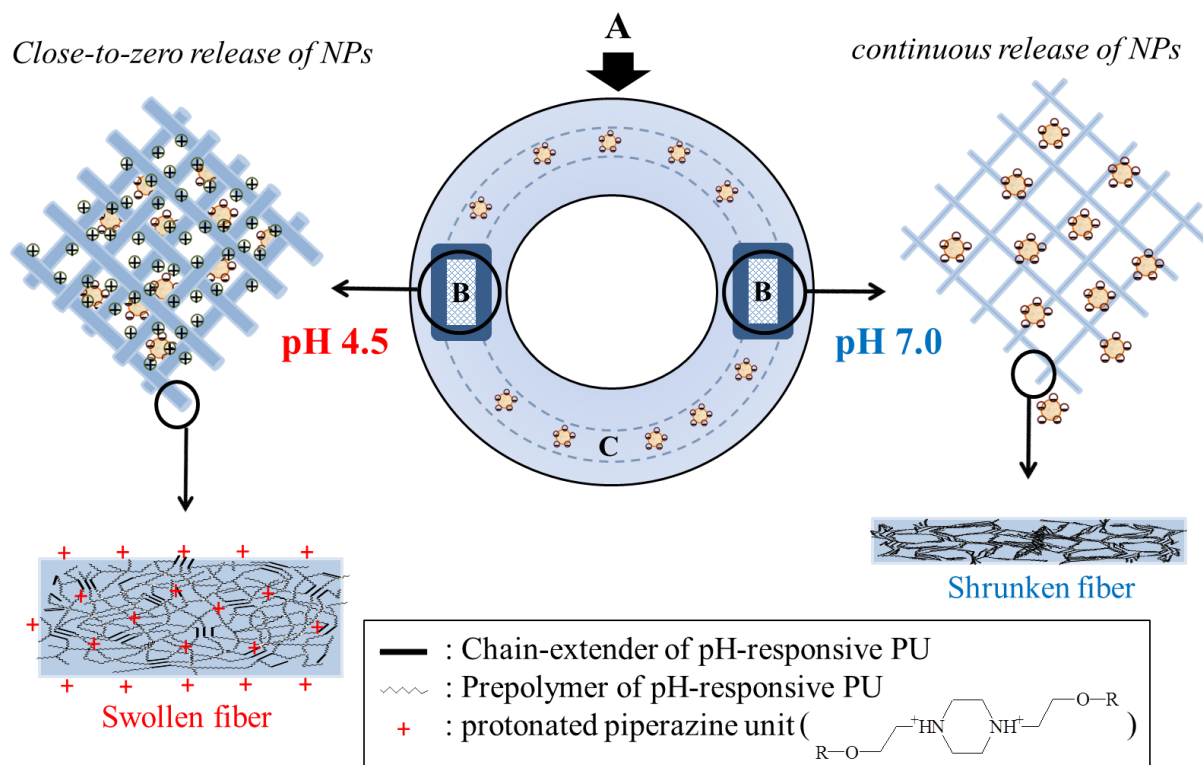
Figure 4-6. Diagram of the proposed use of the electrospun porous pH-responsive PU membrane as a "window" membrane in a reservoir-IVR for controlled on-demand anionic nanoparticle release: (A) IVR; (B) window membrane; (C) reservoir. The pH-responsive change of electrostatic interaction between the pH-responsive membranes and the anionic NPs and morphology of the membrane contribute to the on-demand release of nanoparticles.

The electrospun porous PU membrane can be used potentially as a semi-permeable membrane in reservoir-IVRs for pH-responsive release of NPs as illustrated in **Figure 4-6**. Briefly, a reservoir-IVR can be made of water swellable non-pH-responsive polyurethane, and the reservoir can be filled with a nanoparticle suspension. The suspension of nanoparticles would be recommended to avoid air bubbles in the reservoir and achieve fast out-diffusion of nanoparticles due to pH change, i.e. fast pH-responsiveness. The electrospun pH-responsive PU

(PEG-HEP-MDI-PG) membrane showed a positively charged surface and bigger DI of electrospun fibers, thicker cross-section, and smaller pore size at pH 4.5 than at pH 7.0. This is because the pH-sensitive molecule HEP (pKa 6.4) on the prepolymer chain of the PU was protonated at pH 4.5 and de-protonated at pH 7.0.[103] Protonated HEP causes the electrospun fibers to swell more at pH 4.5. The higher swelling ratio leads to the larger diameter of fibers, therefore, the thicker cross-section and the smaller inter-fiber pore size. Overall, the "window" membrane (electrospun porous pH-responsive PU membrane) can control the release of the NPs from the reservoir by the pH-responsive change of the electrostatic interaction between loaded NPs and morphologies (pore size and thickness of the membrane).

4.4.2 pH-responsive nanoparticles release studies

Anti-HIV drugs and siRNAs can be loaded onto the nanocarriers by hydrophobic or electrostatic interactions. Commercially available blue-dyed polystyrene nanoparticles (PSNs), the surfaces of which were modified to bear the carboxylic group (COOH), were used for the NPs release studies as a model nanocarrier. The PSNs could be a model NP of siRNA loaded nanocarriers which have a negatively charged surface such as NPs fabricated using PLGA-PEG-COOH and PVA by a double-emulsion solvent evaporation method [22,171,188,189]. Moreover, polystyrene nanoparticles have been used as a model nanocarrier for *in vitro* mucus penetration [190] and cellular uptake [191–194] studies. The PSNs showed narrow polydispersity in VFS (0.23 ± 0.02 and 0.04 ± 0.01 at pH 4.5 and 7.0, respectively) and could be observed with the naked eye. The average particle size and zeta-potential of PSNs were measured at pH 4.5 and 7.0 (**Table 4-3**). These PSNs showed a minor difference in average zeta-potential and hydrodynamic particle

size, at pH 4.5 (-16 ± 3 mV, 174 ± 1 nm) and at pH 7.0 (-20 ± 4 mV, 215 ± 2 nm), due to the deprotonation of the carboxylic groups at pH 7.0.[195]

Table 4-3 Physicochemical characteristics of blue dyed polystyrene nanoparticles (PSNs) (data are expressed as mean ± SD; n = 3).

	pH 4.5	pH 7.0
Particle size (DI, nm, 0.1 μg/mL)	174 ± 1	215 ± 2
Zeta potential (mV, 0.1 μg/mL)	-16 ± 3	-20 ± 4

In vitro NP release studies were performed using porous pH-responsive (PEG-HEP-MDI-PG) (DMF: THF = 3: 7) and control (PEG-HD-MDI-HD) PU membranes (**Figure 4-7**). The pH-responsive NP permeability of the porous pH-responsive PU membrane is distinguished from the NP release profile of the control PU membrane (**Figure 4-7, A-B**). These porous pH-responsive membranes revealed close-to-zero release of PSNs at pH 4.5, however, they showed sustained release of PSNs at pH 7.0 (**Figure 4-7, B-C**). At pH 7.0, 60 ± 6% of the feed amount of NPs (0.8 mL of 1mg/mL PSNs) were released after 24 h. There was a rapid release of NPs at pH 7.0 for 3 h (51 ± 5%) driven by the relatively larger difference in concentration between the upper chamber and bottom chamber of Franz cells.
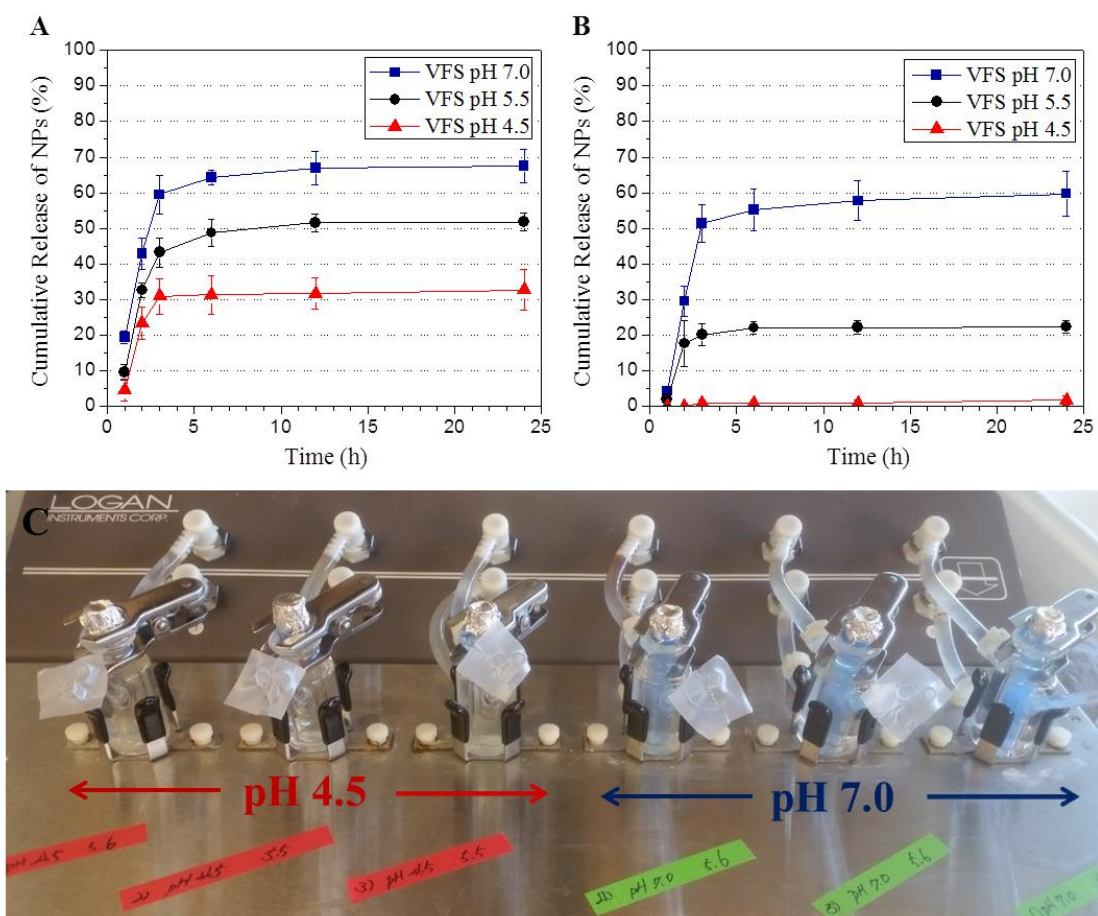
Figure 4-7. *In vitro* nanoparticle permeation studies (A) control PU (PEG-HD-MDI-HD) membrane, (B) porous pH-responsive PU (PEG-HEP-MDI-PG) membrane, and (C) photo of the study using porous pH-responsive PU (PEG-HEP-MDI-PG) membrane by Franz cells. Cumulative release of the nanoparticle in percentage (%) over 24 h was evaluated at both pH 4.5, 5.5, and pH 7.0. Anionic blue dyed nanoparticles (200 nm) were used. Temperature was maintained at 37 °C. Data is expressed as mean ± SD; $n = 3$.

Such pH-responsive release of anionic NPs has two principal mechanisms. First, changes of the electrostatic interaction between the NPs and the electrospun porous pH-responsive

membranes at pH 4.5 and pH 7.0 could lead to the pH-responsive NP release. The zeta-potential of porous pH-responsive membrane was positive (14.2 mV) at pH 4.5 and close to zero at pH 7.0 (2.2 mV) because the conjugate acid of the pH-sensitive moiety piperazine has a pKa of 6.4. The porous pH-responsive membrane had an electrostatic interaction with anionic PSNs at acidic pH (pH 4.5) but almost no electrostatic interaction at the neutral pH. Second, morphology changes of the membrane at pH 4.5 and pH 7.0 might contribute to the pH-responsive release of NPs. The porous pH-responsive PU membrane was thicker at pH 4.5 (50 ± 2 μm) than that at pH 7.0 (34 ± 1 μm) with smaller pore size at pH 4.5 (1.8 ± 0.6 μm) than that at pH 7.0 (2.2 ± 0.6 μm) due to the swelling of the electrospun pH-responsive PU fibers.

The intravaginal pH change by seminal fluid happens immediately after ejaculation of semen.[24,129,130] According to TEVI-BE´NISSAN et al, full vaginal elimination of semen takes 20 h and the vaginal ecological microenvironment returns to its normal acid pH 48 hours after intercourse.[24] It is inferred that the elevated pH could be maintained around neutral for at least a couple of hours because sperm needs an alkaline or neutral environment to be able to survive and swim to fertilize the egg.[132,133] The pH-responsive PU membranes allowed rapid release of PSNs at pH 7.0 for 2 h (30 ± 4%). This result reveals the pH-responsive PU membranes have a potential use serving "window" membrane of IVRs for the on-demand release of nanocarriers. In addition, the PSNs release study was performed at pH 5.5 as an intermediate pH of 4.5 and 7.0 for further assessment of the pH-responsive release. The results of PSNs release studies at pH 5.5 showed around middle point between pH 4.5 and 7.0 in the case of control PU (52 ± 2% for 24 h). For the pH-responsive PU membrane, increasing pH from 4.5 to 5.5 allowed NPs to start to pass through the membrane. But the 24 h release percentage was 22 ± 2% which was only one third of the release at pH 7.0 (60 ± 6%). This result correlates well with the zeta-potential of the

membrane. At pH 5.5, the pH-responsive PU membrane is still positively charged as reflected by its zeta-potential of 10.5 mV at pH 5.5 (closer to 14.2 mV at pH 4.5 than 2.2 mV at pH 7.0), and exerts an attractive electric force on PSNs, restricting their release across the membranes. On the other hands, the cumulative amount of the released PSNs from the control membranes was found to be $32 \pm 6\%$ at pH 4.5, $52 \pm 2\%$ at pH 5.5, and $67 \pm 5\%$ at pH 7.0 for 24 h. According to these results, the control membrane did not show the desired pH-responsive on-demand release of PSNs.

To better explain the pH-responsive release of NPs, the association between the electrospun PU (porous pH-responsive and control) membranes and the PSNs was evaluated (**Figure 4-8**). Round membrane samples (DI: 0.8 cm) were prepared and immersed in 6.4 mL of 0.125 mg/ml PSNs suspension at 37 °C with gentle horizontal shaking (100 rpm). These PSNs showed a relatively constant difference ($12 \pm 3\%$) in the number associated with porous pH-responsive membrane between pH 4.5 and pH 7.0 for 24 h. Such difference resulted from changes in the electrostatic interaction between porous pH-responsive membrane and PSNs, as well as morphology changes of the membrane. Although the average pore size at pH 4.5 (1.8 ± 0.6 µm) was smaller than that at pH 7.0 (2.2 ± 0.6 µm), the strong electric attractive force at pH 4.5 might have caused higher amounts of PSNs associated with porous pH-responsive membrane than that at pH 7.0. The control membrane showed the lowest amount of associated PSNs at pH 7.0 because of the strong repulsion force between the negatively charged control membrane surface (-25.4 mV) and PSNs (-20 ± 4 mV).
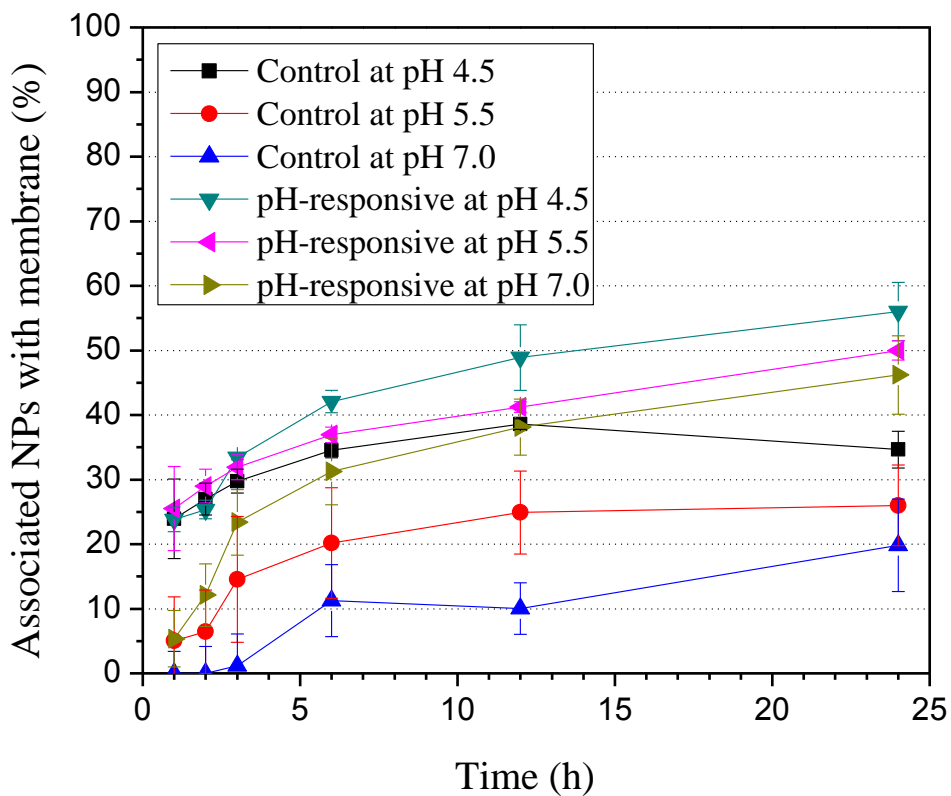
Figure 4-8. Association of anionic NPs to be stored on electrospun control and porous pH-responsive PU membranes at pH 4.5, pH 5.5 and pH 7.0. Data is expressed as mean ± SD; $n = 3$.

To further explore the pH-responsive release of NPs, release profiles of PSNs were re-calculated by following equation:

$$a\,(\%) = \frac{b}{c - d} \times 100$$

Where a is % of released PSNs at each time point, b is released amount of PSNs (μg) in bottom chamber, c is feed amount of PSNs to upper chamber (μg), and d is associated amount of PSNs

with the membrane (µg). The determination of percent release by deducting adsorbed particles gives a clearer idea of the mechanism and role of the pH-responsive membrane by presenting a release ratio of pharmacologically relevant particles (released amount from free nanoparticles). Most free PSNs were released at pH 7.0 (100 ± 11%). However, there was almost no release at pH 4.5 (4 ± 4%) through the porous pH-responsive PU (PEG-HEP-MDI-PG) membrane (**Figure 4-9**).
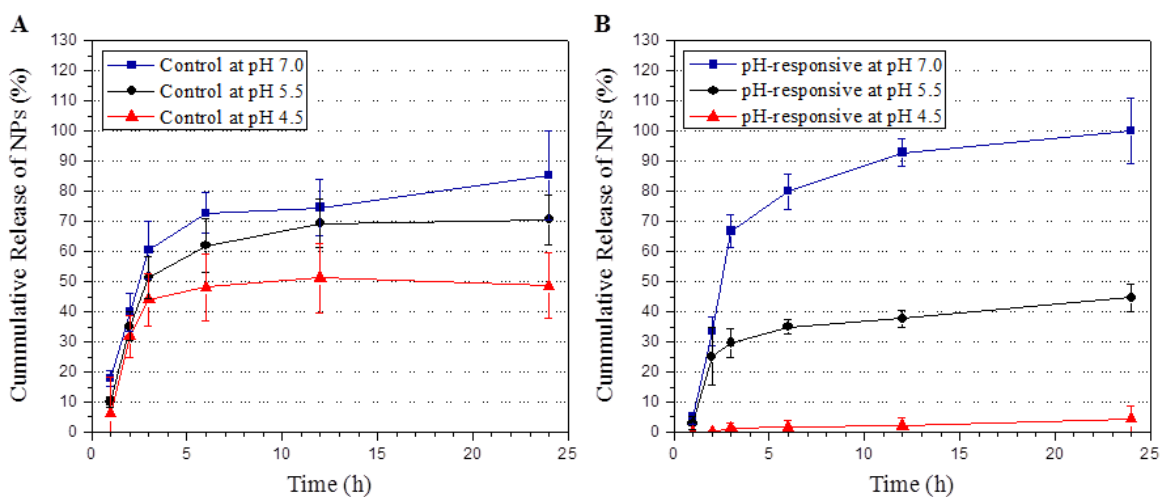
Figure 4-9. *In vitro* nanoparticle release profiles after deduction of the associated NPs with membrane (A) control PU (PEG-HD-MDI-HD) membrane, (B) porous pH-responsive PU (PEG-HEP-MDI-PG) membrane. Cumulative release of the nanoparticles in percentage (%) over 24 h evaluated at pH 4.5, pH 5.5, and pH 7.0. Data is expressed as mean ± SD; $n = 3$.

The control PU membrane showed a minor difference in the cumulative release of PSNs (36.7% at 24 h) compared to porous pH-responsive PU membrane. The difference in the release

of PSNs between pH 4.5 and pH 7.0 through the control PU membrane could be due to the difference in surface charge of the control PU at pH 4.5 and 7.0. Control PU has a much more negative zeta-potential at pH 7.0 (-25.4 mV) than at pH 4.5 (-7.9 mV) as per Figure 3. A much stronger coulomb repulsion exists between PSNs and the control PU membrane at pH 7.0 than pH 4.5 and contributes to accelerated nanoparticle penetration through the membrane.

4.4.3 *In vitro* cytotoxicity studies of electrospun pH-responsive PU (PEG-HEP-MDI-PG) membrane

Human vaginal epithelial cell line VK2/E6E7 and human T-cell line Sup-T1 were used for an *in vitro* cytotoxicity assay of electrospun porous pH-responsive PU membranes considering their potential application as "window" membranes in reservoir-IVRs for the pH-responsive release of NPs which may serve as nanocarriers for anti-HIV drugs and siRNAs. Electrospun porous pH-responsive PU (PEG-HEP-MDI-PG) membrane elution medium used to treat the cells did not present a cytotoxicity effect compared to the positive control (**Figure 4-10**). We also evaluated the production of pro-inflammatory cytokines (IL-6, IL-8 and IL-1β) after treating the cells with the elution medium and the obtained results are shown in **Figure 4-11**. Compared to the positive controls induced by the LPS and N-9, the PU membrane eluent did not generate significant changes in the expression of the pro-inflammatory markers, suggesting that the membranes did not induce an inflammatory microenvironment.
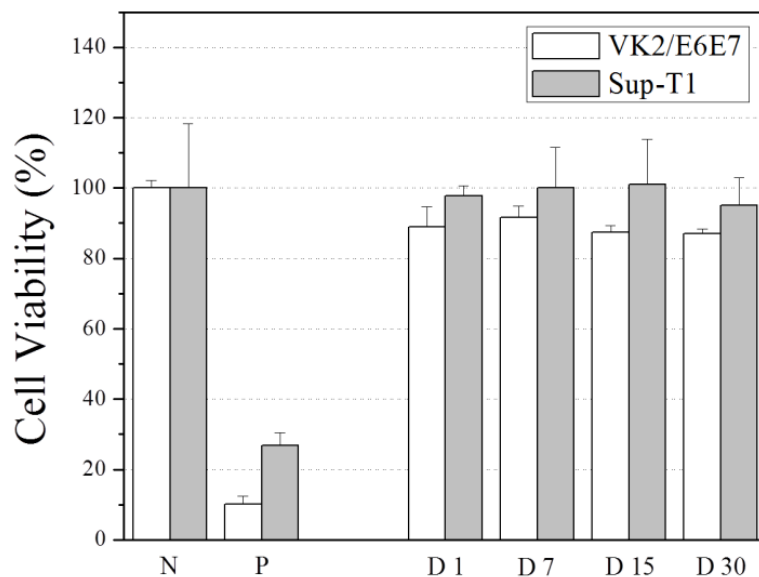
Figure 4-10. *In vitro* biocompatibility of porous pH-responsive PU (PEG-HEP-MDI-PG) membranes versus VK2/E6E7 and Sup-T1 cells. MTS assay was applied for the cell viability test. Data is normalized to the negative control and expressed as mean $\pm$ SD; $n = 3$. One-way analysis of variance was performed with all results with $P < 0.05$ considered to be significant. Negative control includes the cells cultured in the medium only. To induce cell death in positive control, 1 M acrylamide dissolved in regular cell culture medium was used. N: negative control, P: positive control.
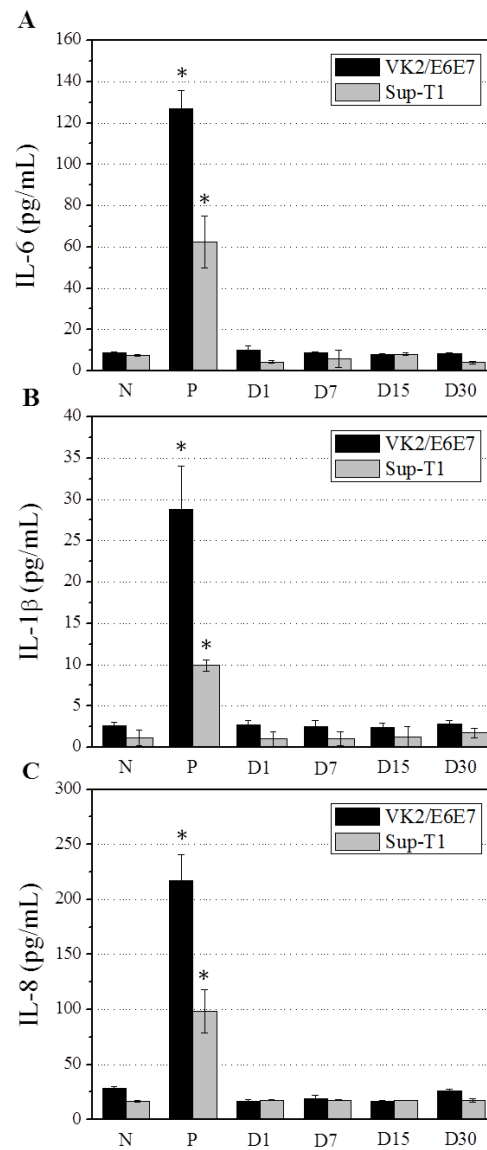
Figure 4-11. Impact of porous pH-responsive PU (PEG-HEP-MDI-PG) membranes on proinflammatory cytokine production (A) Interleukin IL-1β, (B) IL-6, and (C) IL-8 production. Negative control was a plain medium and positive control was 200 μg/mL of nonoxynol-9 or 50 μg/mL of lipopolysaccharide-treated cells for IL-1β and IL-6/IL-8, respectively. Data is expressed as mean ± SD; $n = 3$. One-way analysis of variance was performed with all results with * $P < 0.05$ considered to be significant.

4.5 Conclusions

The pH-responsive interconnected porous PU membrane was fabricated on an electrospinning apparatus using pH-responsive PU (PEG-HEP-MDI-PG) copolymer. The porous pH-responsive membranes showed pH-dependent changes in morphology (pore sizes, fiber diameters, and thickness) and surface charge. Such porous pH-responsive PU membranes demonstrated pH-dependent release of color-dyed polystyrene nanoparticles (PSNs, -COOH). There was close-to-zero release of PSNs in VFS at pH 4.5 (normal human female genital tract pH); however, a demonstrated continuous release of PSNs in VFS at neutral pH (elevated human female genital tract pH). These electrospun porous pH-responsive PU membranes showed no noticeable toxicity to human vaginal epithelial cell line (VK2/E6E7) and human T-cell line (Sup-T1). Besides, the elution medium collected from the membranes did not induce an inflammatory microenvironment. Overall, the newly electrospun porous pH-responsive PU membrane demonstrated potential use as a novel biomaterial for "smart" intravaginal NPs release.

4.6 Acknowledgements

4.7   Contribution of Authors

Seungil Kim[a]: initiated and contributed to the scope of the manuscript; performed synthesis and characterization of PU copolymers; performed fabrication of electrospun pH-responsive PU membranes; performed characterization of electrospun PU membranes; performed evaluation of *in vitro* nanoparticles release; wrote the manuscript.

Yannick Leandre Traore[b,c]: performed *in vitro* biocompatibility studies; contributed writing manuscript.

Emmanuel A Ho[b,c]: contributed writing manuscript; critically reviewed the manuscript.

Muhammad Shafiq[d]: performed fabrication of electrospun control PU membranes; contributed writing manuscript.

Soo-Hyun Kim[d]: contributed writing manuscript.

Song Liu[a,e,*]: initiated and contributed to the scope of the manuscript; contributed writing manuscript; critically reviewed and revised the manuscript.

[a] Biomedical Engineering, Faculty of Engineering, University of Manitoba, Winnipeg, Manitoba, Canada

[b] Laboratory for Drug Delivery and Biomaterials, School of Pharmacy, University of Waterloo, Kitchener, Ontario, Canada

[c] Waterloo Institute for Nanotechnology, Waterloo, Ontario, Canada

[d] Centre for Biomaterials, Biomedical Research Institute, Korea Institute of Science and Technology (KIST), Seoul, South Korea

[e] Department of Biosystems Engineering, Faculty of Agricultural and Food Sciences, University of Manitoba, Winnipeg, Manitoba, Canada

Chapter 5

Switchable on-demand release of intravaginal nanocarrier via segmented reservoir-IVR filled with a pH-responsive supramolecular polyurethane hydrogel

As a part of this thesis, new pH-responsive PUs, PEG-DMPA-HDI and PEG-DMPA-HDI-PG, were synthesized, and their supramolecular hydrogels were prepared to achieve the pH-triggered switchable on-demand release of nanocarriers from reservoir-IVRs. The hypothesis of this research is that the pH-change triggered physicochemical responses of the supramolecular PU hydrogel can result in a switchable on-demand release of nanocarrier.

5.1 Abstract

To achieve pH-responsive switchable on-demand release of NPs from IVR, a new pH-sensitive PU copolymer bearing DMPA (PEG-DMPA-HDI-PG) was synthesized to encapsulate NPs within a segmented reservoir IVR. A new PEGylated PASP-based amphiphilic copolymer conjugated with fluorescent dye orange II (PASP-PEG-Ph-Orange) was synthesized to self-assemble in aqueous solution into 251-283 nm diameter NPs for the release study. Chemical structures of the synthesized copolymers PEG-DMPA-HDI-PG and PASP-PEG-Ph-Orange were confirmed by ATR-FTIR and ^{1}H-NMR spectroscopy. The orange II dye conjugated NPs PASP-PEG-Ph-Orange showed the highest fluorescent emission at 570 nm for tracking, and the pH-responsive PUs PEG-DMPA-HDI-PG became a pH-responsive supramolecular hydrogel in distilled water at 20 wt%. Acid-base titration and evaluation of turbidity change were performed for PEG-DMPA-HDI-PG to confirm its pH-responsive characteristics. PASP-PEG-Ph-Orange NPs were blended with the pH-responsive supramolecular PU hydrogel PEG-DMPA-HDI-PG to form an inclusion complex and then filled into segmented reservoir-type PU IVRs containing two holes. The segmented IVR filled with the NP-encapsulated hydrogel demonstrated continuous release of the NPs at pH 7.0 but close-to-zero release at pH 4.2 for 12 h. Moreover, the *in vitro* release studies demonstrated pH-responsive switchable on-demand NPs release.

PASP-PEG-Ph-Orange and PEG-DMPA-HDI-PG showed no and low cytotoxicity toward human vaginal epithelial cell line VK2/E6E7, respectively. Overall, the segmented IVR filled with pH-responsive supramolecular PU hydrogel demonstrated its potential use for switchable on-demand intravaginal release of nanocarriers and hence more effective intravaginal drug delivery.

5.2   Introduction

HIV is a global pandemic that can potentially develop into AIDS.[45] More than 30 million people, especially women living in developing countries such as sub-Saharan Africa, suffer from HIV.[164] Protection against HIV transfection at the beginning of the infection is extremely important since invaded HIV can spread to major human organs within a few weeks. Various topical drug delivery strategies including IVR have been developed to provide better protection against vaginal HIV infection.[23] Moreover, compared to condoms, intravaginal releasing formulations such as gels or IVRs could greatly empower women to use these convenient dosage forms to protect themselves from HIV without the consent of the partner.[103] Therefore, intravaginal delivery of anti-HIV agents could potentially prevent HIV in the early stages of the infection since the major route of the HIV transmission is unprotected heterosexual intercourse.[43]

Anti-HIV drugs and siRNA prevent HIV transmission by blocking the transmission progress[30] and knocking down certain genes involved in the HIV infection, respectively.[196] siRNA has been shown to interfere with HIV infections at the genetic level, targeting not only host genes but also viral genes;[21] however, there are several challenges in increasing the delivery efficiency of therapeutic siRNA to T-cells (the major HIV targeted cells) crossing the vaginal mucus barrier,[45] such as rapid degradation of siRNA nuclease,[22] potential immunogenicity

response caused by siRNA,[197] and the low cellular uptake in the absence of appropriate transfection reagents.[198]

Nanocarriers such as micelles, vesicles, nanogels, liposomes, and solid lipid nanoparticles have been developed for the delivery of anti-HIV drugs and siRNA.[170,199,200] Drug delivery using nanocarriers could improve dispersion of poorly water-soluble drugs, increase delivery efficiency and cellular uptake, and protect cargos from acidic degradation in the female genital tract. Moreover, PEGylation of nanocarriers enhances the penetration efficiency through the mucus barrier.[17,21]

Previously, our research group developed PEGylated poly(amino acid)-based NPs[43] since poly(amino acid) derivatives have been successfully used for delivering drugs and siRNA,[115,116,201] and PEGylated amphiphilic polyaspartamide was demonstrated to possess excellent mucus penetrating properties.[202] The PEGylated PASP conjugated with phenethylamine (PASP-PEG-Ph) self-assembled into a spherically shaped NP with a diameter of approximately 200 nm.[43] This nanocarrier demonstrated encapsulation efficiency of $92 \pm 6\%$ and a zero-order release profile of a model drug (coumarin 6). Moreover, strong cellular uptake by the human immune cell line Sup-T1 was achieved without significant cytotoxicity observed against the Sup-T1 and human vaginal epithelial cell line VK2/E6E7 up to 1 mg/mL. In the current study, fluorescent dye orange II was conjugated to PASP-PEG-Ph to allow easy tracking of the NPs in the release study.

On-demand release of anti-HIV drugs at therapeutic concentrations through nanocarriers when heterosexual intercourse occurs may decrease side effects. Since the average pH of the human vaginal tract is 4.2,[23] and can be elevated to neutral pH in the presence of seminal

121

fluid,[24,33] the pH change of the human vagina during heterosexual intercourse could be used to trigger the release of a nanocarrier from intravaginal formulations such as gels and rings.

Our research group has developed pH-responsive solvent-cast[103] and electrospun PU membranes for the on-demand intravaginal release of anionic drugs and nanocarriers, respectively. The solvent-cast membranes fabricated using pH-responsive PUs, PEG-HEP-HDI-PG and PEG-HEP-MDI-PG, showed the continuous and switchable release of model drug NaDF at pH 7.0 and close-to-zero release at pH 4.5. Even though on-demand delivery of small molecules has been achieved, it was very challenging to attain the same for nanocarriers since the fabricated membrane did not contain pores large enough to allow the traverse of NPs across the membrane. In this regard, interconnected porous pH-responsive PU, PEG-HEP-MDI-PG, membranes were fabricated using an electrospinning apparatus. The electrospun pH-responsive PU membrane successfully showed pH-dependent release of PSNs: almost no release at pH 4.5 and continuous release at pH 7.0. Overall, the pH-responsive solvent-cast and electrospun PU membranes demonstrated their potential use in membrane-controlled DDS such as IVRs for on-demand intravaginal drug delivery. However, the electrospun membranes fabricated from pH-responsive PU, synthesized using pH-sensitive HEP, demonstrated on-demand release of only anionic NPs. Also, pH-triggered switchable on-and-off release of NPs could not be demonstrated by the electrospun PU membrane. It would be recommended to develop a new pH-responsive PU for switchable on-demand release of nanocarriers having a close to zero surface zeta-potential since PEGylated NPs with close to zero absolute value of zeta-potential showed high mucus penetration efficiency.[190,202]

PUs have been used for fabrication of IVRs due to their appealing elastomeric and thermoplastic characteristics which benefit from a unique block copolymer structure consisting

of a soft segment and a hard segment.[6,106] Moreover, stimuli-responsive PU has been developed for the delivery of low molecular drugs. For instance, temperature-responsive PU NPs have been synthesized from PEG and diisocyanate (HDI or L-lysine ethyl ester diisocyanate (LDI)).[203] The synthesized PU NPs showed reversible dispersion-aggregation changes at the temperature that is close to human body temperature. 1 mg/mL of the PU NPs formed a colloid dispersion at 25 °C while at 55 °C they became a turbid solution by hydrophobic interactions of hard segments. The formation of H-bonding with water is an exothermic process and higher temperature disfavours H-bonding, causing interactions between the hydrophobic parts of the copolymers to become stronger leading to the aggregation of hard segments at higher-than-the-transition temperature. These PU NPs were used for the delivery of adriamycin.[204] At higher-than-body temperature, the physicochemical interaction between the adriamycin and the copolymer weakens causing a dramatic increase in the release ratio of adriamycin (higher than 70% for 10 h) compared to the lower release rate (lower than 20% for 10 h) at room temperature (25 °C).

Additionally, pH- and temperature dual sensitive injectable PU hydrogels have been synthesized using HEP as a pH-sensitive molecule.[51,52] The PU copolymers showed pH- and temperature dependent sol-gel transitions. At a pH higher than 6.8, 20 wt% of the copolymer solution demonstrated a sol-gel transition with increased temperature up to body temperature (37 °C). The PU hydrogel synthesized from PEG, HEP, and HDI and PEG, HEP, HDI and PCL showed continuous *in vitro* release of chlorambucil for two weeks and paclitaxel for one month, respectively at pH 7.4 and 37 °C. More recently, an injectable, pH and oxidation-responsive supramolecular hydrogel has been developed for controlled dual drug delivery of the hydrophobic drug indomethacin (IND) and hydrophilic model drug rhodamine B (RB).[205] The dual sensitive poly(ether urethane) (PEU) was synthesized using PEG, di(1-hydroxyethylene)

diselenide (DiSe), DMPA and 3-isocyanatomethyl-3,5,5-trimethylcyclohexyl isocyanate (IPDI). The PEU copolymer could self-assemble into NPs and encapsulate IND, and then a supramolecular inclusion complex (IC) hydrogel was fabricated by adding α-cyclodextrin (α-CD) and RB. The supramolecular hydrogel showed a faster release of the drugs at pH 9.2 than that at pH 7.4, and demonstrated oxidation-responsive release by adding H_2O_2. However, so far, there have been no pH-responsive hydrogels reported capable of releasing NPs in a switchable manner for the intravaginal application.

Our research group proposes a pH-responsive supramolecular PU hydrogel which could be filled in the lumen of reservoir-IVRs for the on-demand release of nanocarriers. The new pH-responsive supramolecular PU hydrogel demonstrated switchable pH-responsive release of NPs when incorporated into a segmented reservoir-IVR, and showed low cytotoxicity towards vaginal epithelial cell VK2/E6E7 only at the concentration higher than 0.8 mg/mL. Overall, the pH-responsive supramolecular PU hydrogel demonstrated its potential use in biomaterials such as the on-demand intravaginal release of NPs.

5.3   Materials and methods

5.3.1   Materials

Orange II dye (pure, certified) and PEG (Mn 6,000) were purchased from ACROS (Geel, Belgium). Methoxy polyethylene glycol amine (Me-PEG-NH$_2$, Mw 5,000) was purchased from Alfa Aesar (Ward Hill, MA, USA). Dialysis membrane tubing (MWCO 12-14 kD) was purchased from Fisher Scientific (Nepean, ON, Canada). Dibutyltin dilaurate (DBTDL, 95%), anhydrous diethyl ether (> 99%), L-aspartic acid (> 98%), phenethylamine (Ph, ≥ 99%),

propylene glycol (PG, > 99.5%), hexamethylene diisocyanate (HDI, > 99%), o-phosphoric acid (98%), triethylamine (TEA, ≥ 99%), anhydrous N,N-dimethylformamide (DMF, 99.8%), 1,1′-Carbonyldiimidazole (CDI, ≥ 90%), 1,2-dichloroethane (DCE, 99.8%), and 2,2-dimethylolpropionic acid (DMPA, 98%) were purchased from Sigma Aldrich (St. Louis, MO, USA) and used without further purification. Hydrophilic aliphatic PU Tecophilic™ HP-60D-35 (PU-60D) was purchased from Lubrizol Advanced Materials (Cleveland, OH, USA). Smooth-Cast® 300 was purchased from Smooth-On Inc. (Macungie, PA, USA).

5.3.2 Synthesis and characterization of fluorescent PEGylated poly(aspartic acid) nanoparticles

PSI (Mw 1.5×10^5) was synthesized from the L-aspartic acid by polycondensation.[206,207] PEGylated PASP copolymer (PASP-PEG-Ph) was prepared from PSI by conjugation of Me-PEG-NH$_2$ (3% feed mole to PSI) and phenethylamine (55% feed mole to PSI) followed by a ring opening reaction.[43] Fluorescent PEGylated PASP copolymer (PASP-PEG-Ph-Orange) was prepared by conjugation of orange II to the PEGylated PASP copolymer as described in **Scheme 5-1**.

Briefly, PASP-PEG-Ph (0.3 g, 0.2×10^{-5} mol) and CDI (0.02 g, 1.2×10^{-4} mol) were dissolved in anhydrous DMF (15 mL) stirring with a magnetic bar at 40 °C in a three-neck round-bottom flask under nitrogen atmosphere. After activation of carboxylic acids of PASP-PEG-Ph by CDI for 3h, a mixture of orange II (0.03 g, 8.5×10^{-5} mol) and TEA (0.06 mL, 4.3×10^{-4} mol) in DMF (5 mL) was added to the reactor. The reactor was left for 48 h at 40 °C under nitrogen atmosphere. After the reaction, the final product was precipitated in 8-fold cold diethyl ether and kept at 4 °C overnight. The precipitate was separated from the solution by centrifuge at

3,000 rpm for 15 min, then was re-suspended in diethyl ether and separated three times to remove the remaining impurities. The final product (PASP-PEG-Ph-Orange, 0.187 g, yield: 57%) was obtained, after being dried under vacuum. The dried product was resuspended in distilled water, then dialyzed against distilled water using membrane tubing (MWCO 12-14 kD) and frozen, then lyophilized. The chemical structure of PASP-PEG-Ph-Orange was confirmed by ATR-FTIR and ^{1}H-NMR.[120,206–209]

ATR-FTIR of PASP-PEG-Ph-Orange: 961, 1101, 1466, 1537, 1651, 1722, and 3300 cm^{-1}. ^{1}H-NMR (300 MHz, D$_2$O) of PASP-PEG-Ph-Orange: δ 2.6-2.8 (2H$_{PASP}$, *CH$_2$*-CH-CO-NH-CH$_2$), 3.3-3.4 (2H$_{Ph}$, NH$_2$-*CH$_2$*-CH$_2$), 3.5-3.7 (4H$_{PEG}$, *CH$_2$-CH$_2$*-O), 3.8-3.9 (2H$_{Ph}$, NH$_2$-CH$_2$-*CH$_2$*), 4.3-4.7 (1H$_{PASP}$, *CH*-CH$_2$-CO-NH), 7.1-7.3 (5H$_{Ph}$, *CH-CH-CH-CH-CH*-C), 6.5-8.4 (10H$_{OrangeII}$, *C$_{16}$H$_{10}$*N$_2$NaO$_4$S)
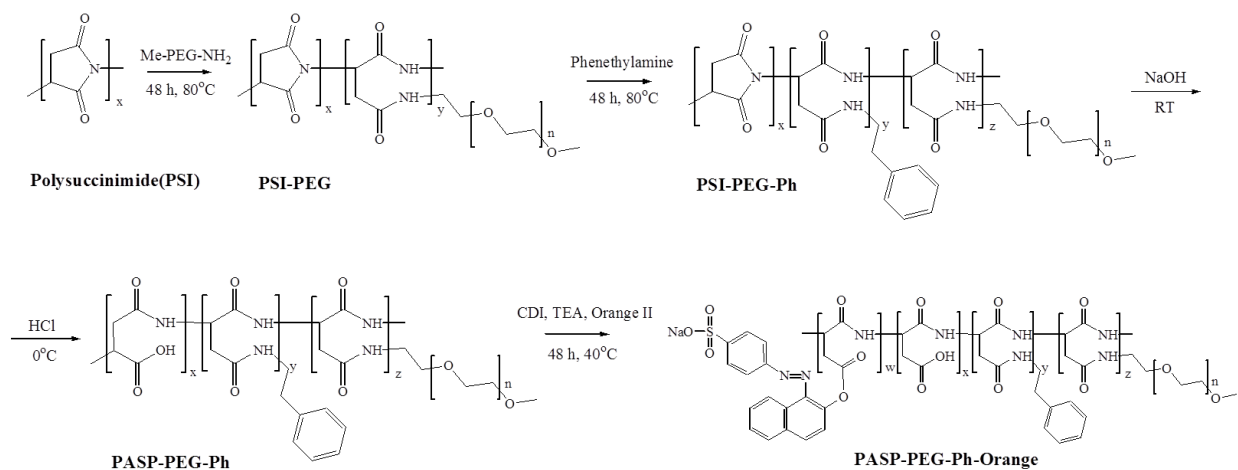
Scheme 5-1. Synthesis of Orange II conjugated amphiphilic copolymer based on PEGylated poly(aspartic acid) (PASP-PEG-Ph-Orange).

Average particle size and zeta-potential of the PASP-PEG-Ph-Orange was characterized using ZetaPALS (Brookhaven Instrument, Holtsville, NY, USA). 0.1 mg/mL of PASP-PEG-Ph-Orange NPs suspension was prepared in 0.1 M phosphate buffer solution (PBS) solution at pH 3.5, 4.5, and 7.0 using a probe sonicator (Sonifier 150, Branson, MO, U.S.A.) for 30 s at 40 kHz and 5 root mean square (RMS). The average particle size of the NPs was evaluated by DLS with a scattering angle of 90° and laser light at 659 nm. To measure zeta-potential of the NPs, PASP-PEG-Ph-Orange was re-suspended in distilled water as 0.1 mg/mL. pH of the suspension was adjusted by adding 0.1 N NaOH or 0.1 N HCl solution. The Smoluchowski model ($\mu = \varepsilon\zeta/\eta$) was automatically applied for calculation of the surface charge, where μ, ε, ζ, and η are electrophoretic mobility, electric permittivity of the liquid, zeta-potential, and viscosity, respectively.[210]

The UV-visible spectra of PASP-PEG-Ph-Orange and Orange II at pH 3.5, 4.5, and 7.0 were recorded by a microplate reader (Synergy H4, BioTek, Winooski, Vermont, USA) using a 96 well plate. The wavelength ranged from 400 to 700 nm. 100 µL of 0.1 mg/mL PASP-PEG-Ph-Orange and orange II in 0.1 M PBS at pH 3.5, 4.5, and 7.0 were used for the measurement. The molar extinction coefficient (ε) of PASP-PEG-Ph-Orange and orange II was characterized using the Beer-Lambert Equation $A = \varepsilon c L$, where A, ε, c, and L are the absorbance, molar extinction coefficient, concentration, and path length, respectively. PASP-PEG-Ph-Orange and orange II in 0.1 M PBS at pH 7.0 was prepared in concentrations from 10^{-5} to 10^{0} mg/mL. Absorbance at a maximum wavelength of 100 µL of PASP-PEG-Ph-Orange (490 nm) and orange II (480 nm) at different concentrations were recorded using a microplate reader. The ε was calculated from the curve by plotting absorbance versus concentration,[211] where the L was 0.29 cm since 100 µL of sample was used in a 96 well plate for reading absorbance.[212]

The fluorescence spectra of PASP-PEG-Ph-Orange and free orange II at pH 3.5, 4.5, and 7.0 were evaluated by a microplate reader. All emission spectra were carried out in a 96 well plate using λ_{exc}= 480. 100 µL of 0.1 mg/mL PASP-PEG-Ph-Orange and orange II in 0.1 M PBS at pH 3.5, 4.5, and 7.0 were used, and the emissions were measured from 510 to 700 nm, increments of 10 nm.

5.3.3 Synthesis and characterization of pH-responsive PU copolymers (PEG-DMPA-HDI and PEG-DMPA-HDI-PG)

pH-responsive PUs were synthesized by reacting DMPA and PEG with HDI. To enhance the hydrophobic hard segment of pH-responsive PU, PG was used. The synthesized pH-responsive PUs were referred to as PEG-DMPA-HDI and PEG-DMPA-HDI-PG (**Scheme 5-2**).

Briefly, PEG (3 g, 0.5 mmol) and DMPA (0.684 g, 5.0 mmol) were dissolved in anhydrous DMF (30 mL), stirring with a magnetic bar at 80 °C in a three-neck round-bottom flask under nitrogen atmosphere. 15 min after the catalytic amount DBTDL (50 µL) was dropped into the reactor, a stoichiometric amount of diisocyanate, HDI (0.91 mL, 5.5 mmol), was added to the reactor. The reactor was left for 6 h with stirring under nitrogen atmosphere. The final product (PEG-DMPA-HDI: 4.14 g, yield: 90%) was obtained by precipitating in 8-fold diethyl ether and washed with excess diethyl ether to remove remaining impurities.
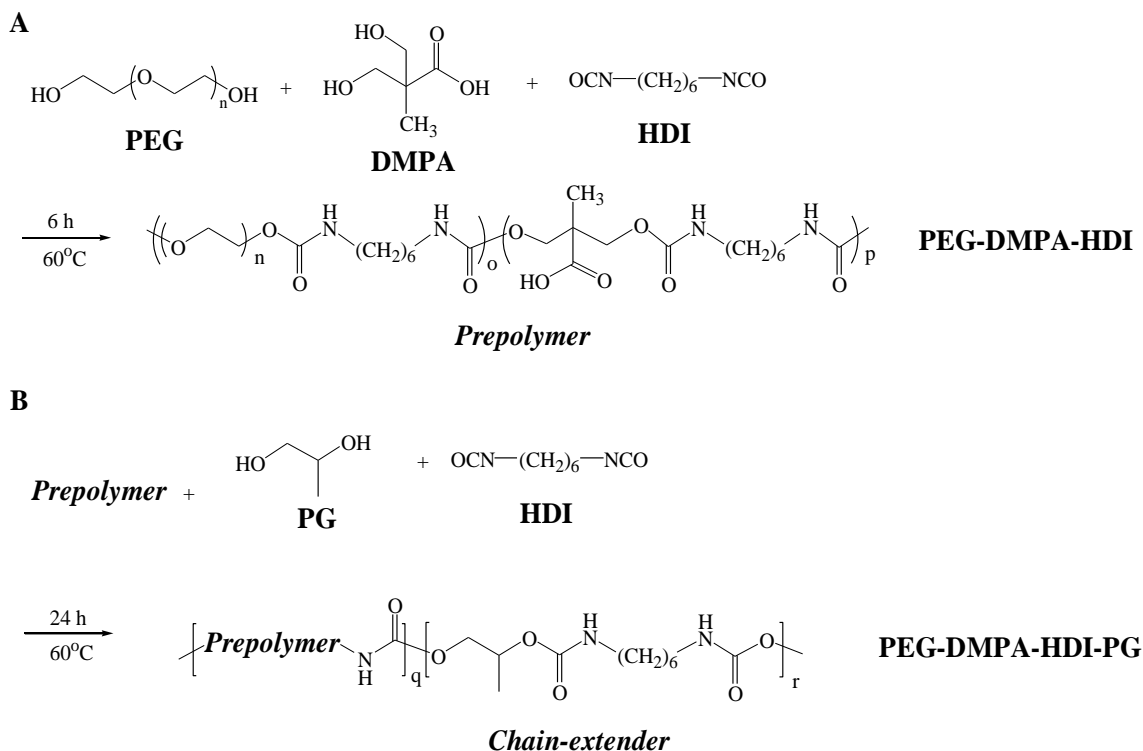
Scheme 5-2. Synthesis of pH-sensitive PU copolymers A: PEG-DMPA-HDI and B: PEG-DMPA-HDI-PG.

For synthesis of PEG-DMPA-HDI-PG, PG (0.369 mL, 5.0 mmol) and HDI (0.82 mL, 5.0 mmol) were added to the reactor of PEG-DMPA-HDI after 6 h of the reaction. The reactor was maintained at 80 °C for 24 h under dry nitrogen atmosphere. The resulting product was precipitated and washed with excess diethyl ether. The fine powder (PEG-DMPA-HDI-PG: 5.43 g, yield: 94%) was obtained after drying under vacuum. The chemical structure of PEG-DMPA-HDI and PEG-DMPA-HDI-PG was confirmed by ATR-FTIR and ^{1}H-NMR.[9,51,52,58,65]

ATR-FTIR of PEG-DMPA-HDI and PEG-DMPA-HDI-PG: 1106, 1238, 1667 and 1706 cm^{-1}. ^{1}H-NMR (300 MHz, CDCl3) of PEG-DMPA-HDI; δ 1.20-1.30 (3H_{DMPA}, O-CH2-C-*CH3*), 1.30-1.40 (4H_{HDI}, NH-CH2-CH2-*CH2-CH2*-CH2-CH2-NH), 1.40-1.60 (4H_{HDI}, NH-CH2-*CH2*-CH2-CH2-

CH_2-CH$_2$-NH), 3.05-3.25 (4H$_{HDI}$, NH-CH_2-CH$_2$-CH$_2$-CH$_2$-CH$_2$-CH_2-NH), 3.60-3.75 (4H$_{PEG}$, CH_2-CH_2-O)n, 4.15-4.35 (4H$_{DMPA}$, O-CH_2-C-CH_2-O), and PEG-DMPA-HDI-PG; δ 1.10-1.30 (6H$_{DMPA+PG}$, O-CH$_2$-C-CH_3 + O-CH-CH_3), 1.30-1.40 (4H$_{HDI}$, NH-CH$_2$-CH$_2$-CH_2-CH_2-CH$_2$-CH$_2$-NH), 1.40-1.60 (4H$_{HDI}$, NH-CH$_2$-CH_2-CH$_2$-CH$_2$-CH_2-CH$_2$-NH), 3.02-3.27 (4H$_{HDI}$, NH-CH_2-CH$_2$-CH$_2$-CH$_2$-CH$_2$-CH_2-NH), 3.55-3.76 (4H$_{PEG}$, CH_2-CH_2-O)n, 4.03-4.15 (2H$_{PG}$, CH-CH_2-O), 4.17-4.32 (4H$_{DMPA}$, O-CH_2-C-CH_2-O), 4.90-5.10 (1H$_{PG}$, O-CH-CH$_3$).

The viscosity average molecular weight of PASP-DMPA-HDI and PASP-DMPA-HDI-PG was calculated using the Mark-Houwink equation for PUs [η]= $3.64 \times 10^{-4} M^{0.71}$, where [η] and M are the intrinsic viscosity and viscosity average molecular weight, respectively.[142] The intrinsic viscosity was calculated from measures using a Cannon-Ubbelohde dilution viscometer at 25 °C. The concentration of the pH-sensitive PUs was diluted from 2.5 mg/mL to 1.25 mg/mL. The travel time of pure DMF and the PU in DMF from measurement mark M_1 to M_2 was recorded. Five repetitions were done for the calculation.

Average particle size of PEG-DMPA-HDI and PEG-DMPA-HDI-PG was evaluated by DLS using a ZetaPALS (Brookhaven Instrument, Holtsville, NY, USA). 0.1 mg/mL of NPs suspension was prepared in 0.1 M PBS at pH 4.2 and 7.0 using a probe sonicator (Sonifier 150, Branson, MO, U.S.A.) for 30 s at 40 kHz and 5 RMS. The average particle size of the NPs was characterized with a scattering angle of 90 ° and laser light at 659 nm. pH of the suspension was adjusted by adding 0.1 N NaOH or 0.1 HCl.

Turbidity measurement was performed using a UV-visible spectrometer (Ultrospec 4300 pro, Amersham Biosciences, Little Chalfont, UK) at different pH from 8.0 to 3.0 and 360 nm. 10 mg/mL of PEG-DMPA-HDI and PEG-DMPA-HDI-PG in 0.1 M PBS was prepared for the

measurement. The pH of the solution was adjusted by adding 0.1 N HCl or 0.1 N NaOH. The turbidity was calculated from transmittance (T, %) as (100-T)/100.[213]

Acid-base titration was carried out on PEG-DMPA-HDI and PEG-DMPA-HDI-PG. 30 mL of 1 mg/mL PEG-DMPA-HDI and PEG-DMPA-HDI-PG in distilled water were prepared. The pH of the solution was adjusted to 3.0 using 0.1 N HCl. The pH was increased by adding 200 µL of 0.1 N NaOH, after each addition, the pH was recorded using a pH meter.[53]

5.3.4   Fabrication of segmented IVR filled with the inclusion complex of pH-responsive supramolecular PU hydrogels and PASP-PEG-Ph-Orange NPs

Segmented IVR was fabricated from commercially available PU HP-60D-35 at 160 °C by hot-melt injection molding (Medium Machinery, LLC, Woodbridge, VA, USA).[113] The HP-60D-35 pellets were loaded into the feeder, and then the melted PU was manually injected into a custom-fabricated aluminum mold with cavities for dimensions of 5.5 mm outer diameter (OD) and 0.6 mm cross-sectional diameter (XD). The OD and XD of the fabricated segment of IVR were measured with a caliper.

pH-responsive supramolecular PU hydrogels including PASP-PEG-Ph-Orange NPs by inclusion complex were prepared and loaded into the segmented IVR. Briefly, 3 mL of 1 mg/mL PASP-PEG-Ph-Orange NPs in distilled water was prepared. 300 µL of the 1 mg/mL PASP-PEG-Ph-Orange NPs was kept as a standard (for drawing a standard curve). pH-responsive PU (PEG-DMPA-HDI or PEG-DMPA-HDI-PG) was added to 2.7 mL of the PASP-PEG-Ph-Orange NPs solution as 20 wt% and stirring at 40 °C for 1 h to form a viscous hydrogel. 100 µL of the prepared viscous complex hydrogel of pH-responsive PU and PASP-PEG-Ph-Orange NPs was

loaded into the reservoir of the segmented IVR. The ends of each segmented IVR were capped with custom-fabricated plastic lids and sealed with a commercially available polymer resin (Smooth-Cast® 300, Smooth-On Inc., Macungie, PA, USA). Two holes (DI: 1/32") were made on the segmented IVR using a drill (Dremel 100, Racine, WI, USA).

5.3.5 *In vitro* nanoparticle release studies

The pH-responsive release of PASP-PEG-Ph-Orange NPs from segmented IVRs was studied at pH 4.2 and 7.0. Segmented IVRs filled with pH-responsive supramolecular hydrogel bearing the PASP-PEG-Ph-Orange NPs were prepared as described above in section 5.3.4. The segmented IVRs filled with the complex hydrogel were immersed in 3 mL of 0.1 M PBS (pH 4.2 and pH 7.0) at 37 °C with gentle shaking (100 rpm). 200 µL of release medium 0.1 M PBS was taken for calculation of released PASP-PEG-Ph-Orange NPs at 1 h, 2 h, 3 h, 6 h, 12 h, and 24 h. After taking each sample, the medium was replenished with 200 µL of fresh 0.1 M PBS. The amount of PASP-PEG-Ph-Orange NPs released was evaluated using a microplate reader (E_x, E_m= 490 nm, 570 nm).

The switchable pH-responsive release of PASP-PEG-Ph-Orange NPs was evaluated. The segmented IVRs filled with the complex hydrogel were prepared, and then the IVRs were immersed in 3 mL of 0.1 M PBS at pH 4.2 and 37 °C with gentle shaking (100 rpm). Every 1 h, the segmented IVRs were pulled out and immersed in different pH (pH 4.2 → pH 7.0 → pH 4.2 → pH 7.0 → pH 4.2) over a 5 h period. The amount of PASP-PEG-Ph-Orange NPs released was evaluated using a plated reader (E_x, E_m= 490 nm, 570 nm).

5.3.6 *In vitro* cytotoxicity tests

In vitro cell cytotoxicity of PASP-PEG-Ph-Orange and PEG-DMPA-HDI-PG were evaluated using human vaginal epithelial cell line VK2/E6E7. VK2/E6E7 was maintained in keratinocyte-serum free (K-SFM) supplemented with 0.1 ng/mL of recombinant human epidermal growth factor, 50 ng/mL bovine pituitary extract, 0.4 mM $CaCl_2$ and 1% penicillin/streptomycin. In a 96-well plate, 2.5×10^4 VK2/E6E7 was seeded in each well and incubated overnight to allow the cells to be attached. PEG-DMPA-HDI-PG and PASP-PEG-Ph-Orange re-suspended in VK2/E6E7 cell culture medium at the concentration of 1mg/mL were used to treat the VK2/E6E7 cell using blank medium as negative control and 1M acrylamide (in K-SFM medium) as positive control and incubating at 37 °C under 5% CO_2 for 24 h. After 24 h of incubation, the media of each cell-line were discarded and replenished with fresh medium and 20 µl of MTS assay reagent were added. The plates were incubated again for 1 h and protected from light. Absorbance of each plate was read at 490 nm using a Spectramax M5 microplate reader.

5.3.7 Statistical analysis

Data are presented as mean ± standard deviation (SD). The number of replicates is indicated as the *n*-value. One-way analysis of variance was performed with all results with $P < 0.05$ considered to be significant.

5.4 Results and discussion

5.4.1 Synthesis and characterization of fluorescent dye (Orange II) conjugated nanoparticle based on PEGylated poly(aspartic acid) copolymer (PASP-PEG-Ph-Orange)

PEGylated amphiphilic polyaspartamide NPs have been shown to be useful for the delivery of siRNA and can traverse across mucus. Amphiphilic PEGylated PASP NPs (PASP-PEG-Ph NPs) with an average particle size of 186 ± 3 nm had been synthesized in our lab. They showed high drug encapsulated efficiency (93 ± 6%) of C6, low cell cytotoxicity towards VK2/E6E7 human epithelial cells and Sup-T1 human T-cells, and cellular uptake by Sup-T1 cells.[43] So we decided to use PASP-PEG-Ph NPs for the NP release study. To better track their release, a fluorescent dye orange II was conjugated onto PASP-PEG-Ph to yield PASP-PEG-Ph-Orange.

The chemical structure of PASP-PEG-Ph-Orange was confirmed by ATR-FTIR and ^{1}H-NMR spectra. Absorption peaks at 1651 cm^{-1} and 1537 cm^{-1} assigned to amide I and amide II bands of PASP, respectevely (**Figure 5-1**).[120–122] Also, the conjugated methoxy PEG (mPEG) and phenethylamine were confirmed from C-O-C stretch absorption at 1101 cm^{-1},[214] aromatic C=C stretch (1466 cm^{-1}), and Aryl C-H bend absorption (961 cm^{-1}).[215] As a result of conversion of PASP-PEG-Ph to PASP-PEG-Ph-Orange, the OH bond in carboxylic acid at 3300 cm^{-1} noticeably disappeared, and the peak of C=O stretching in ester at 1722 cm^{-1} increased in the ATR-FTIR spectra.[121]
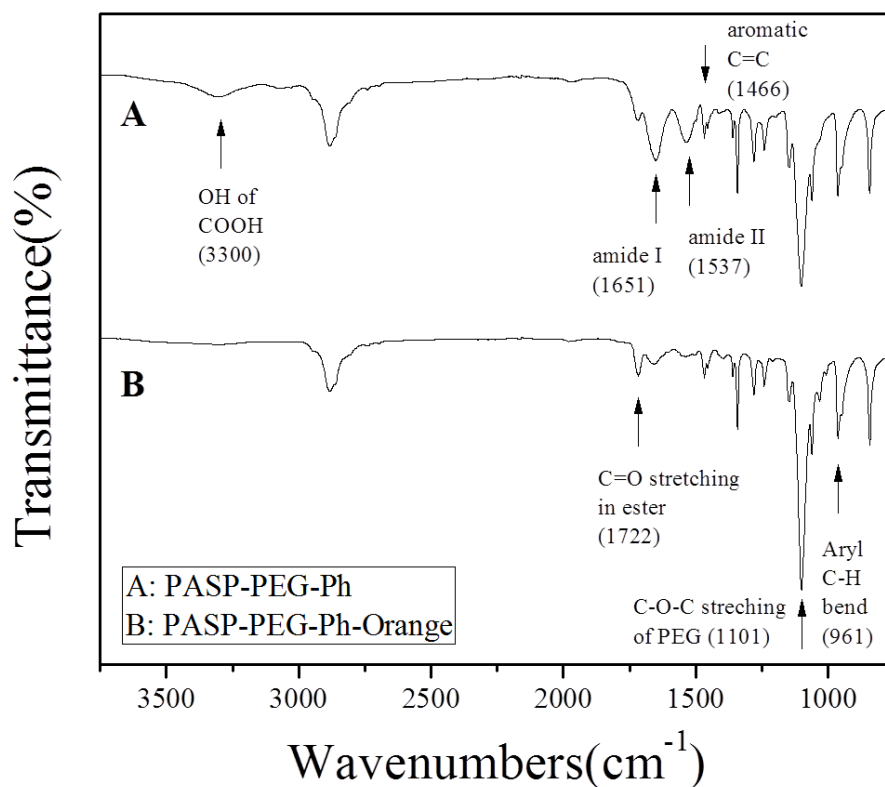
Figure 5-1. Attenuated total reflectance-Fourier transform infrared (ATR-FTIR) spectra of PASP-PEG-Ph-Orange.

^{1}H-NMR spectra of PASP-PEG-Ph-Orange showed the intrinsic proton peaks of orange II from 6.5-8.4 ppm (**Figure 5-2**).[216] The proton peaks of a and b were assigned to the methine and methylene protons of the copolymer backbone.[120,121] The conjugated mPEG was confirmed by peak f as the methylene protons.[209,214] The conjugated phenethylamine was confirmed by peak e as methine protons.[217] The degrees of substitution of orange II, phenethylamine, and Me-PEG-

NH$_2$ were 40.3%, 54.2%, and 2.0% calculated by comparing the peak area of g assigned to a proton of conjugated orange II, the methylene proton peaks c and f to that of peak b.
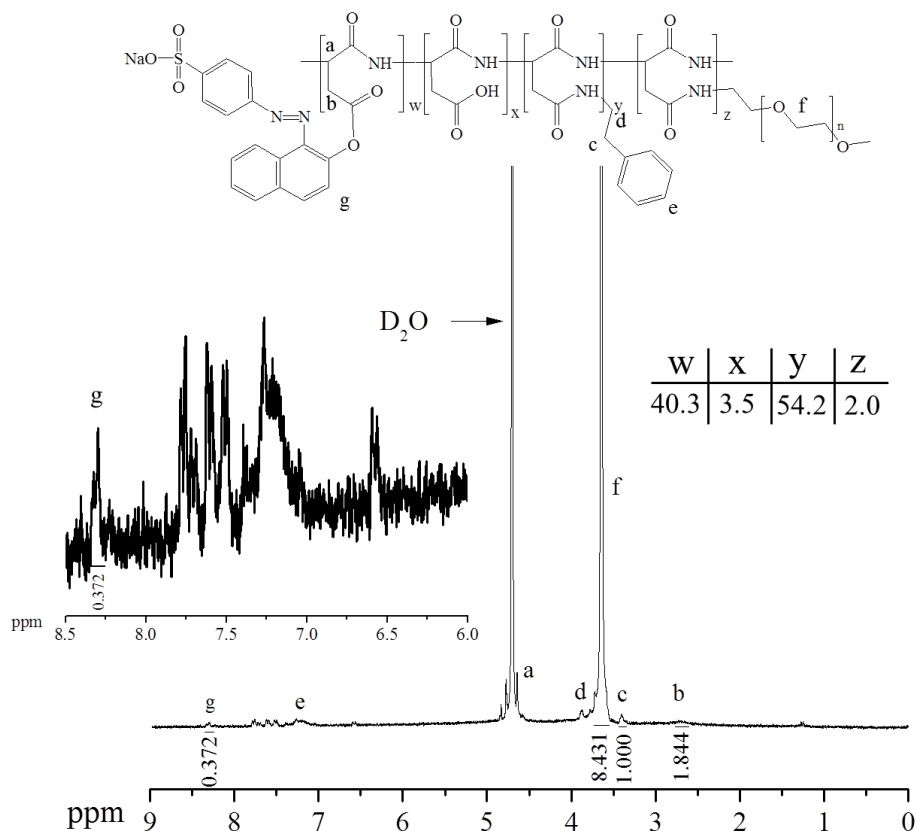
Figure 5-2. [1]H-Nuclear Magnetic Resonance (^{1}H-NMR) spectra of PASP-PEG-Ph-Orange.

The average particle size of PASP-PEG-Ph-Orange NPs was evaluated in 0.1 M PBS at pH 3.5, 4.5, and 7.0 (**Table 5-1**). The average particle size of the NPs showed no noticeable difference in size at pH 3.5, 4.5 or 7.0 since most of the carboxylic acid groups of PASP-PEG-Ph were converted to an ester bond by conjugation with orange II. The zeta-potentials of PASP-PEG-Ph-Orange NPs at pH 3.5, 4.5, and 7.0 were -6 ± 1, -2.1 ± 0.1, and -1 ± 2 mV, respectively.

136

These close to zero surface zeta-potential of the NPs also supports conversion of the carboxylic acid groups to the ester bond, and it would be beneficial for mucus penetration of the NP_S since it was reported that the PEGylated NP with close to zero absolute value of zeta-potential demonstrated high mucus penetration efficiency.[190,202]

Table 5-1. Average particle size (0.1 mg/mL in 0.1 M PBS pH 3.5, 4.5 and 7.0) and Zeta-potential (0.1 mg/mL in distilled water pH 3.5 4.5 and 7.0) of PASP-PEG-Ph-Orange nanoparticles. Data is expressed as mean ± SD; $n = 3$.

	pH 3.5	pH 4.5	pH 7.0
Average particle size (nm)	283 ± 2	262 ± 7	251 ± 4
Zeta-potential (mV)	-6 ± 1	- 2.1 ± 0.1	-1 ± 2

UV-visible absorbance spectra and fluorescence emission spectra of PASP-PEG-Ph-Orange were recorded and compared with those of orange II (**Figure 5-3**). The PASP-PEG-Ph-Orange showed no pH-dependence to the emission. However, free orange II showed relatively higher emission at neutral pH than acidic pH (pH 3.5 and 4.5). Also, it is well known that conjugation of fluorescent molecules to polymers can cause not only the shift of maximum absorbance wavelength or maximum emission wavelength but also the reduction of molar extinction coefficient (ε).[218,219] The shift of maximum absorbance wavelength from 480 nm to 490 nm was observed after conjugation of orange II to PASP-PEG-Ph.
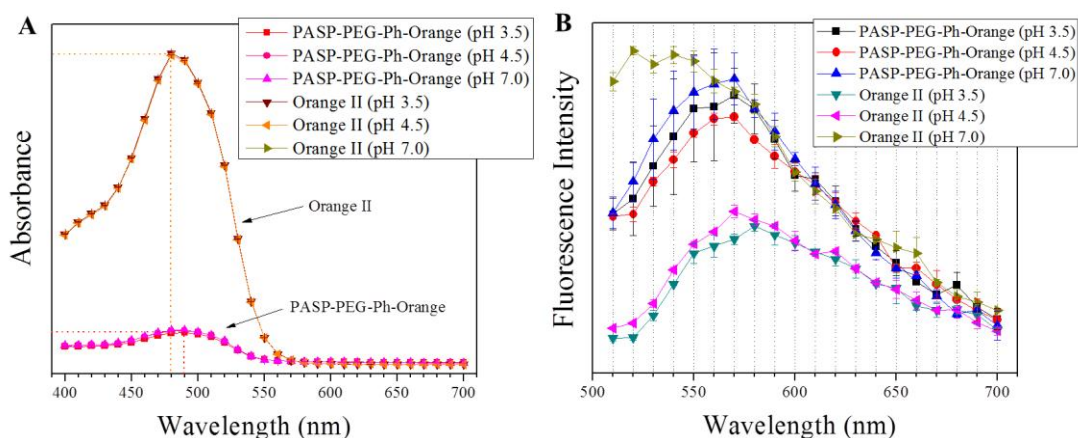
Figure 5-3. (A) UV−visible absorbance spectra of Orange II conjugated NPs (PASP-PEG-Ph-Orange) (0.1 mg/mL, in PBS, at pH 3.5, 4.5, 7.0 and 37 °C), (B) Fluorescence emission spectra of PASP-PEG-Ph-Orange with excitation at 480 nm (0.1 mg/mL, in PBS, at pH 3.5, 4.5, 7.0 and 37 °C). Data is expressed as mean ± SD; $n = 3$.

Moreover, the maximum emission wavelength also shifted from 520 nm to 570 nm when scanning fluorescence spectra using λ_{exc}= 480 at pH 7.0. The molar extinction coefficient (ε) of PASP-PEG-Ph-Orange and orange II was also calculated using the Beer-Lambert Equation A= εcL. The curve obtained by plotting absorbance versus concentration of PASP-PEG-Ph-Orange at 490 nm was y= 2.251χ + 0.0028 (R^2= 1); while for orange II, the curve at 580 nm was y = 20.12χ + 0.0068 (R^2 = 0.9999). From the curves, the ε of PASP-PEG-Ph-Orange was calculated as 7.76 $(mg/mL)^{-1}cm^{-1}$, and the ε of orange II was 69.38 $(mg/mL)^{-1}cm^{-1}$ since the path length was 0.29 cm when 100 μL of sample was used in 96 well plate for reading absorbance.[212] The ε for orange II at 480 nm and pH 8.0 was reported as 23,352 M^{-1} cm^{-1} and this is close to the calculated ε of orange II at 480 nm and pH 7.0 (24,305 M^{-1} cm^{-1}).[220] The ε of PASP-PEG-Ph-

Orange is still high enough to confer fluorescence properties of PASP-PEG-Ph-Orange, although the value of ε dropped after conjugation.

5.4.2 Synthesis and characterization of pH-responsive PUs (PEG-DMPA-HDI and PEG-DMPA-HDI-PG)

New pH-responsive PUs were synthesized using the pH-sensitive diol DMPA (pKa= 4.41). The reaction progressed in an anhydrous environment, and under dried nitrogen conditions, since H_2O could consume diisocyanate by hydrolysis. The viscosity average molecular weight of PEG-DMPA-HDI and PEG-DMPA-HDI-PG were 7.8×10^5 and 9.4×10^5, respectively (**Table 5-2**).

Table 5-2. Chemical component and viscosity average molecular weight (Mv) of the pH-sensitive PU copolymers (PEG-DMPA-HDI, PEG-DMPA-HDI-PG). Data is expressed as mean $\pm$ SD; $n = 3$.

Polymer	Feed mole ratio	Composition molar ratio	Mv
PEG-DMPA-HDI	PEG: DMPA: HDI = 1: 10: 11	PEG: DMPA: HDI = 0.22: 0.78: 1.00	7.8×10^5
PEG-DMPA-HDI-PG	PEG: DMPA: HDI: PG = 1: 10: 21: 10	PEG: DMPA: HDI: PG = 0.09: 0.32: 1.00: 0.46	9.4×10^5

The chemical structures of PEG-DMPA-HDI and PEG-DMPA-HDI-PG were confirmed by ATR-FTIR and ^{1}H-NMR. In the ATR-FTIR spectrum (**Figure 5-4**), the absorbance of the free carbonyl bond and hydrogen-bonded carbonyl bond stretching are shown at 1704 cm^{-1} and 1667 cm^{-1}, respectively.[52] Also, the N-H stretching band of urethane was observed at 3264 cm^{-1}. The

absorbance at 1106 cm^{-1} corresponds to the stretching vibration of C-O-C in PEG,[151] and the absorbance at 1238 cm^{-1} was attributed to the stretching vibration C-O of carboxylic acid.[58] The absence of absorbance at 2267 cm^{-1} reveals that the product does not contain unreacted isocyanate groups.[52] The ^{1}H-NMR spectra showed the coexistence of PEG and DMPA in PEG-DMPA-HDI and PEG-DMPA-HDI-PG (**Figure 5-5**). The successfully bonded PEG was confirmed by the presence of a methylene proton peak a at 3.55-3.76 ppm,[51,52] and incorporation of DMPA into the polymers was confirmed by methylene protons peak e at 4.15-4.35 ppm and a methyl proton peak at 1.10-1.30 ppm.[221–223] Similarly, the methylene proton peak g at 4.03-4.15 ppm, the methine proton peak h at 4.90-5.10 ppm and the methyl proton peak i at 1.10-1.30 ppm jointly pointed to the successful incorporation of PG in the structure.[143,152] The methylene protons of incorporated HDI b, c, and d were observed at 3.02-3.27, 1.40-1.60, and 1.30-1.40 ppm, respectively.[52,87] The methane peak b was shifted downfield by deshielding effects. Based on the integration of methylene proton peaks a, e, b, and g, the composition molar ratio of PEG-DMPA-HDI and PEG-DMPA-HDI-PG was calculated as PEG: DMPA: HDI= 0.22: 0.78: 1 and PEG: DMPA: HDI: PG= 0.09: 0.32: 1.00: 0.46, respectively.
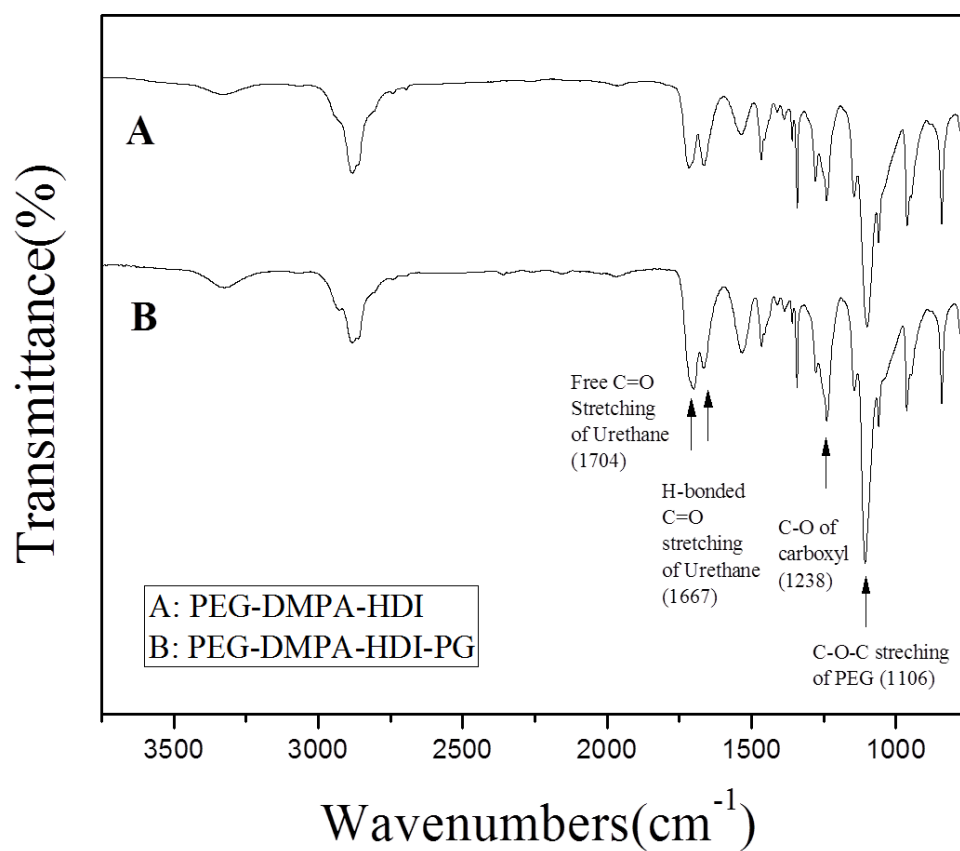
Figure 5-4. Attenuated total reflectance-Fourier transform infrared (ATR-FTIR) spectra of pH-sensitive PUs (A) PEG-DMPA-HDI, (B) PEG-DMPA-HDI-PG.
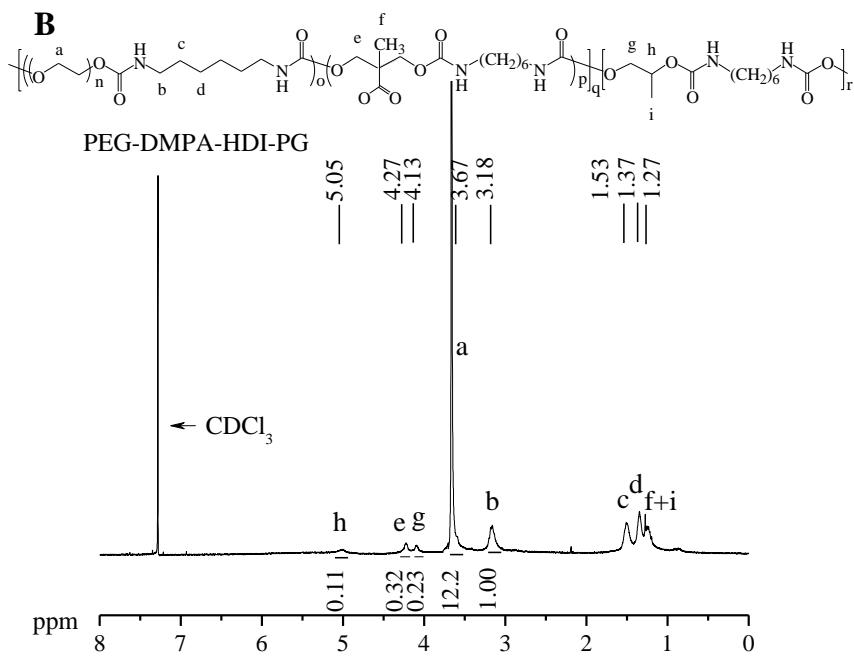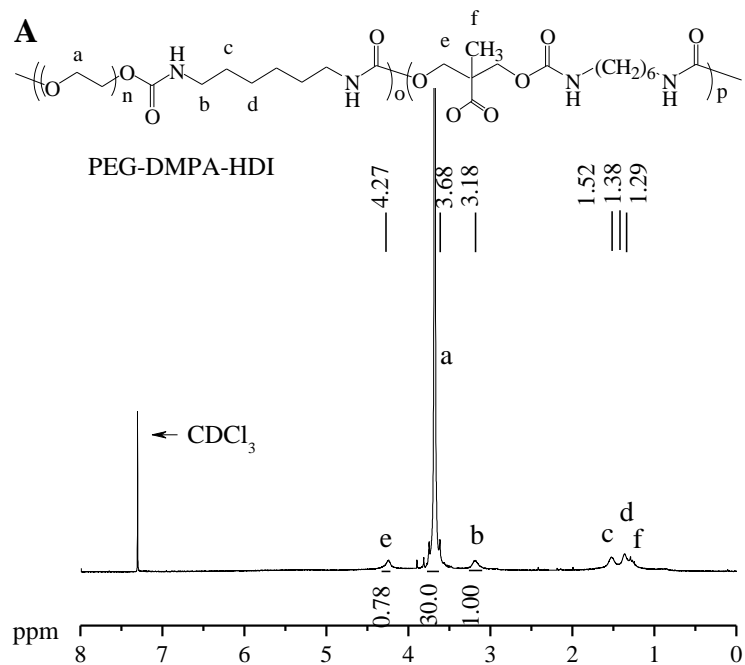
Figure 5-5. ^{1}H-NMR spectra of pH-sensitive PUs (A) PEG-DMPA-HDI, (B) PEG-DMPA-HDI-PG.

The average particle size of 0.1 mg/mL of PEG-DMPA-HDI and PEG-DMPA-HDI-PG NPs in 0.1 M PBS at pH 4.2 and 7.2 were evaluated (**Table 5-3**). PEG-DMPA-HDI NPs showed smaller particle size at pH 4.2 (164 ± 14 nm) than that at pH 7.0 (298 ± 10 nm). However, PEG-DMPA-HDI-PG NPs has a larger particle size at pH 4.2 (386 ± 11 nm) than that at pH 7.0 (267 ± 11 nm). This difference in particle size due to the change in pH could be explained by the different chemical structure in the hard segment. PEG-DMPA-HDI-PG has an additional hydrophobic hard segment by adding PG, resulting in higher hydrophobic interactions between hard segments (PG-HDI and DMPA-HDI) of the polymer backbone than that of PEG-DMPA-HDI (DMPA-HDI). As a result, PEG-DMPA-HDI-PG NPs rearranged and aggregated with more polymer chains at pH 4.2; while PEG-DMPA-HDI NPs shrink by protonation of the carboxylic acid of DMPA at pH 4.2 because of lower charge repulsion.

Table 5-3. Particle size of pH-responsive PUs, PEG-DMPA-HDI and PEG-DMPA-HDI-PG, at different pHs (0.1 mg/mL). Data is expressed as mean ± SD; $n = 3$.

Polymer	0.1 M PBS at pH 4.2	0.1 M PBS at pH 7.0	Distilled water
PEG-DMPA-HDI	164 ±14	298 ±10	190 ± 26
PEG-DMPA-HDI-PG	386 ±11	267 ±11	277 ± 5

pH-dependant turbidity change and acid-base titration profile of pH-responsive PUs were studied to evaluate pH-responsive properties of PEG-DMPA-HDI and PEG-DMPA-HDI-PG (**Figure 5-6**). The turbidity of 10 mg/mL of PEG-DMPA-HDI and PEG-DMPA-HDI-PG increased from 0.071 at pH 5.5 to 0.164 at pH 4.0, and from 0.527 at pH 6.5 to 0.813 at pH 4.0, respectively (**Figure 5-6, A**). As pH decreased, turbidity increased near the pKa of the

carboxylic acid of DMPA (4.41) due to protonation of the carboxylic acid of DMPA in the copolymer and therefore aggregation of the copolymer. The turbidity change of PEG-DMPA-HDI-PG was higher and began at a higher pH (0.286, pH 6.5) than that of PEG-DMPA-HDI (0.093, pH 5.5) since PEG-DMPA-HDI-PG has a higher content of hydrophobic segments contributed by PG. PEG-DMPA-HDI-PG may have stronger intramolecular hydrophobic interactions and therefore more serve an aggregation following a decrease in pH than PEG-DMPA-HDI.
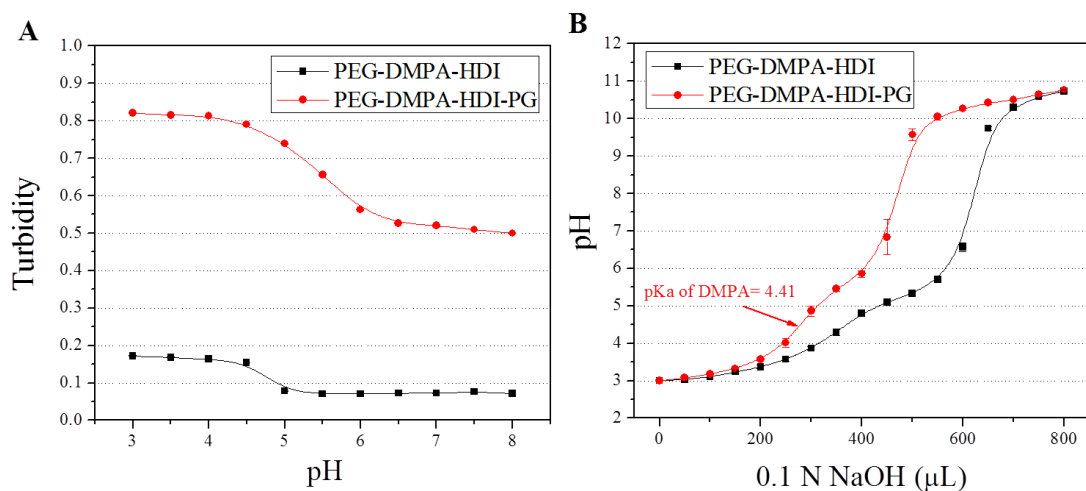
Figure 5-6. Turbidity change at 10 mg/mL (A) and acid-base titration profile at 1 mg/mL (B) of PEG-DMPA-HDI and PEG-DMPA-HDI-PG. Data is expressed as mean ± SD; $n = 3$.

Acid-base titration curves of PEG-DMPA-HDI and PEG-DMPA-HDI-PG revealed that PEG-DMPA-HDI consumes more ions (hydroxide) for deprotonation of DMPA than PEG-DMPA-HDI-PG at the same mass concentration (**Figure 5-6, B**). From the results of turbidity

change and titration curves, at the same mass concentration of PU, a more dramatic physicochemical change could be expected from PEG-DMPA-HDI-PG than PEG-DMPA-HDI in response to environmental pH change from pH 4.2 to 7.0, or from pH 7.0 to 4.2.

5.4.3 Segmented IVR filled with the inclusion complex of pH-responsive supramolecular PU hydrogels and PASP-PEG-Ph-Orange NPs

1 mg/mL of fluorescent NPs (PASP-PEG-Ph-Orange) was included in 20 wt% of pH-responsive supramolecular PU hydrogels (**Figure 5-7**), and the complex hydrogel was filled in segments of IVRs. Through hot injection molding of PU-60D, reservoir-IVR segments (cross-sectional diameter of 5 mm and a wall thickness of 0.75 mm) were fabricated so that there were no interconnected pores big enough for NP diffusion. To enable the diffusion of NPs, two holes (DI: 1/32") were drilled on the middle of the segmented IVR.
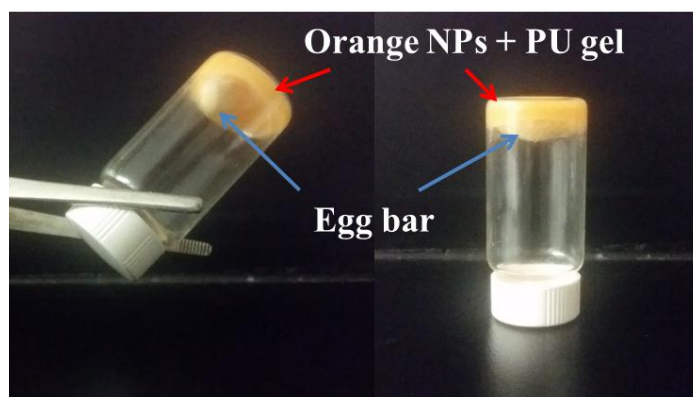
Figure 5-7. Pictures of complex hydrogel (1 mg/ml of PASP-PEG-Ph-Orange NPs in 20 wt% aqueous solution of pH-responsive PU, PEG-DMPA-HDI-PG).
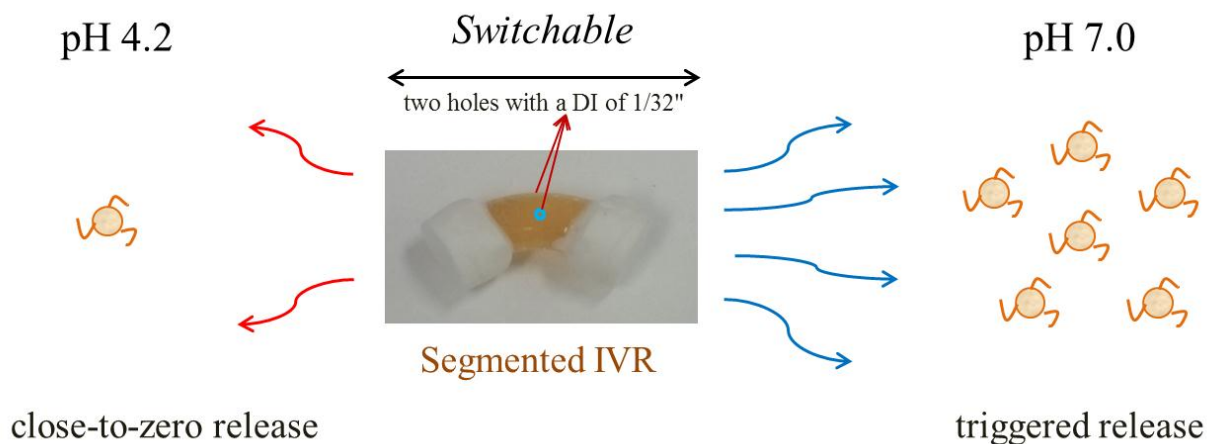
Figure 5-8. Diagram of the proposed use of pH-responsive supramolecular PU hydrogels in reservoir-IVR for the switchable on-demand release of nanoparticles.

The proposed use of the segmented reservoir-IVR filled with pH-responsive complex hydrogels is illustrated in **Figure 5-8.** The segment could be a part of the full-sized reservoir-IVRs and the lumen of the reservoir-IVR could be filled with complex hydrogel. The complex hydrogels have a higher release ratio of PASP-PEG-PH-Orange NPs through the holes of the segmented reservoir-IVR at pH 7.0 than at acidic pH 4.2 because the supramolecular PU hydrogel has an immobilized pH-sensitive molecule DMPA (pKa 4.41). The IVR segments are expected to show close-to-zero release of the nanocarrier at the normal pH of a woman's genital tract (average pH is 4.2) while a triggered release of the nanocarrier is induced by the elevated pH (neutral) of the genital tract. Ideally, this on-demand release is expected to be triggered on and off repeatedly in response to pH change. DI of the holes, acting as a release window on the IVR, can be adjusted to control the release amount of included nanocarriers.

5.4.4 *In vitro* nanoparticle release studies

The *in vitro* release of PASP-PEG-Ph-Orange NPs from complex hydrogels filled in segmented IVRs was studied and showed a pH-responsive release of PASP-PEG-Ph-Orange NPs. PEG-DMPA-HDI-PG supramolecular hydrogel demonstrated close-to-zero release of PASP-PEG-Ph-Orange NPs at pH 4.2 for 12 h, then $14.0 \pm 0.5\%$ of PASP-PEG-PH-Orange NPs was released from 12 h to 24 h. At pH 7.0, a continuous release of PASP-PEG-Ph-Orange NPs, up to $42 \pm 7\%$ for 24 h, was observed (**Figure 5-9**).
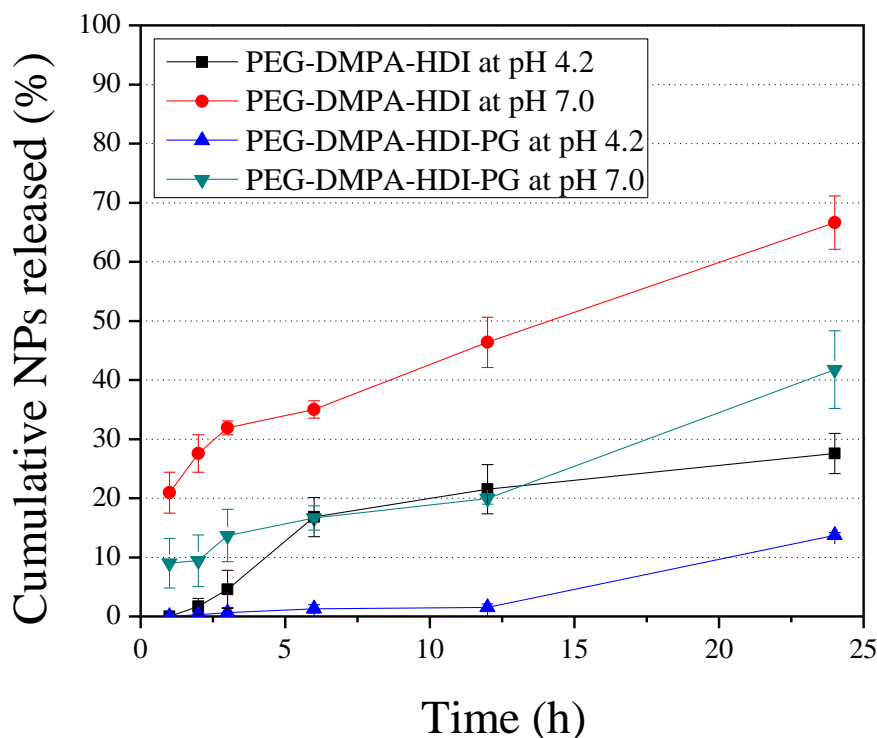
Figure 5-9. *In vitro* release profile of PASP-PEG-Ph-Orange NPs at pH 4.2 and 7.0. Data is expressed as mean $\pm$ SD; $n = 3$.

PEG-DMPA-HDI supramolecular hydrogel showed a continuous release of PASP-PEG-Ph-Orange NPs, up to $28 \pm 3\%$ at pH 4.2, and $67 \pm 5\%$ at pH 7.0 for 24 h. The release of PASP-PEG-Ph-Orange NPs, which are included in pH-responsive supramolecular PU hydrogels, was controlled by pH-responsive change in physicochemical interaction of PU copolymer chains. The pH-responsive supramolecular PU hydrogels have a weaker hydrophobic interaction between the copolymer chains and an increased space between particles at pH 7.0 than those at pH 4.2, thus releasing PASP-PEG-Ph-Orange NPs at a higher rate at pH 7.0. Moreover, strong hydrophobic interaction of condensed PEG-DMPA-HDI-PG NPs allowed close-to-zero release at pH 4.2 for 12 h. The observed release of PASP-PEG-Ph-Orange NPs at pH 4.2 after the 12 h time point may be due to leakage of PEG-DMPA-HDI-PG supramolecular hydrogel through the holes of the segmented IVRs.

The switchable, on-demand release of nanocarriers was desired for reducing unwanted systemic toxicity of anti-HIV agents. Using PEG-DMPA-HDI-PG supramolecular hydrogel, the pH-responsive switchable release of NPs for 5 h was accomplished. PASP-PEG-Ph-Orange NPs were released at pH 7.0, but released less than 2.5% at pH 4.2 (**Figure 5-10**). Only $1.5 \pm 0.9\%$ of PASP-PEG-Ph-Orange NPs were released for the first 1 h at pH 4.2; then $19 \pm 5\%$ of PASP-PEG-Ph-Orange NPs were released for the next 1 h at pH 7.0, followed by the switchable off/on/off release of PASP-PEG-Ph-Orange NPs for another 3 h. However, PEG-DMPA-HDI supramolecular hydrogel released $37 \pm 4\%$ of PASP-PEG-Ph-Orange NPs during the second 1 h at pH 7.0, after $7 \pm 5\%$ of release during the first 1 h at pH 4.2, followed by no switchable release. The relatively weak hydrophobic interaction of PEG-DMPA-HDI NPs caused a rapid release of PASP-PEG-Ph-Orange NPs at pH 7.0, and PEG-DMPA-HDI might leak too much through the holes of segmented IVRs at the first raising of pH to 7.0. From these PASP-PEG-Ph-

Orange NPs release studies, it is obvious that the pH-responsive supramolecular PEG-DMPA-HDI-PG hydrogel is a potential candidate of biomaterials for the proposed use in reservoir-IVR for switchable on-demand release of nanocarriers.
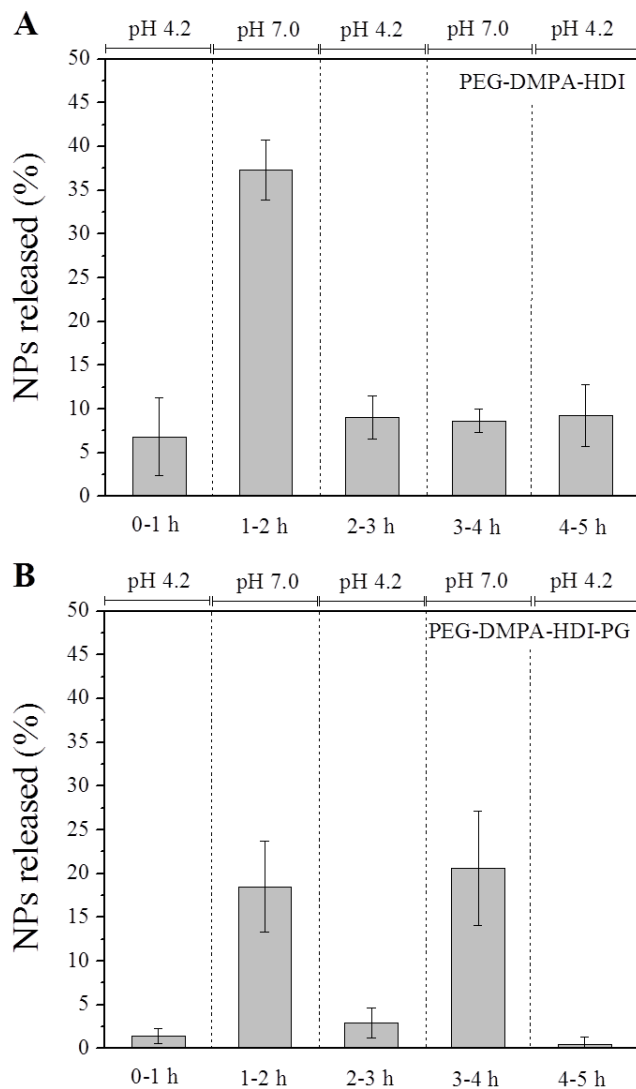
Figure 5-10. *In vitro* switchable on-demand release of PASP-PEG-Ph-Orange NPs using pH-responsive supramolecular PU hydrogels; (A) PEG-DMPA-HDI, (B) PEG-DMPA-HDI-PG. Data is expressed as mean ± SD; $n = 3$.
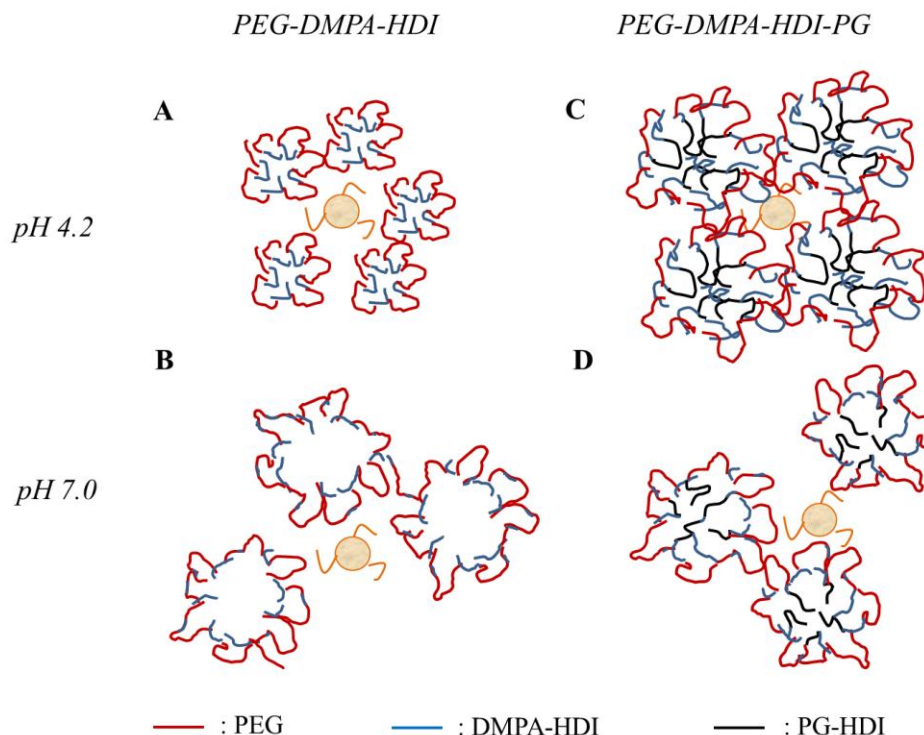
Figure 5-11. Schematic illustration for the pH-responsive release of PASP-PEG-Ph-Orange NPs from supramolecular PU hydrogels (PEG-DMPA-HDI and PEG-DMPA-HDI-PG).

A potential explanation of the pH-responsive behavior of PEG-DMPA-HDI and PEG-DMPA-HDI-PG supramolecular hydrogels is illustrated in **Figure 5-11**. At pH 4.2, PEG-DMPA-HDI and PEG-DMPA-HDI-PG shrink and trap PASP-PEG-Ph-Orange NPs (**Figure 5-11, A** and **C**). At pH 7.0, with the ionization of carboxylic acid of DMPA on the copolymers, hydrophobic interaction between copolymer chains is weakened resulting in increase of space for releasing entrapped PASP-PEG-Ph-Orange NPs (**Figure 5-11, B** and **D**). PEG-DMPA-HDI-PG could

demonstrate pH-responsive switchable release since the hydrophobic hard segment PG-HDI maintained a sturdy hydrophobic domain at both pH 4.2 and 7.0.

5.4.5 *In vitro* cytotoxicity studies

In vitro cell cytotoxicity of PASP-PEG-Ph-Orange and PEG-DMPA-HDI-PG were evaluated versus VK2/E6E7 cell lines by the MTS assay. The VK2/E6E7 was treated with concentrations ranging from 0.2 mg/mL to 1mg/mL and the viability of the cells was evaluated after 24 h (**Figure 5-12**).
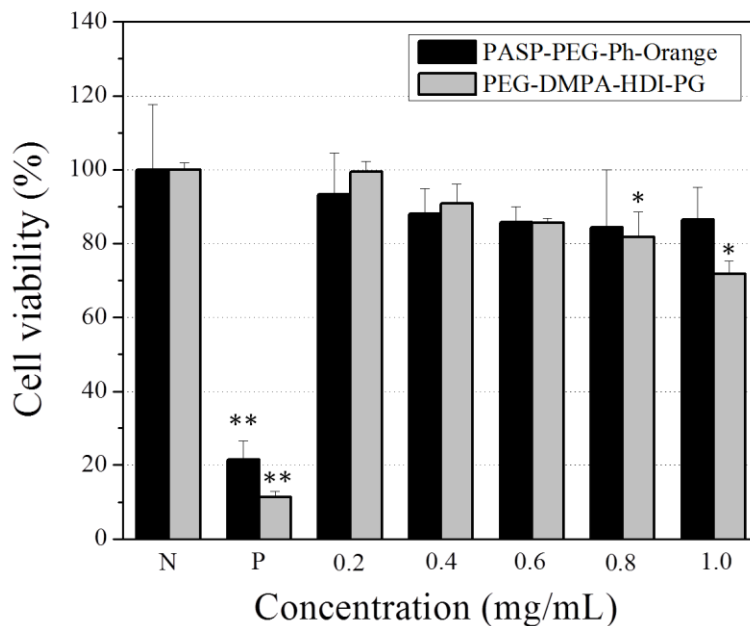
Figure 5-12. *In vitro* cytotoxicity of PASP-PEG-Ph-Orange and PEG-DMPA-HDI-PG towards VK2/E6E7 cells. Data is expressed as mean ± SD; $n = 3$; * $P < 0.05$, ** $P < 0.01$ versus the negative control.

At all concentrations studied, the PASP-PEG-Ph-Orange showed no significant cytotoxicity and the PEG-DMPA-HDI-PG showed, a significant cytotoxicity toward the VK2/E6E7 cell line compared to positive control only when the concentration is higher than 0.8 mg/mL. According to the results, it was demonstrated that the copolymers were suitable for the proposed use as an intravaginal drug delivery within the female genital track.

5.5 Conclusions

Fluorescent PASP-PEG-Ph-Orange NPs (DI: 262 ± 7 nm at pH 4.2) and pH-responsive PUs (PEG-DMPA-HDI, PEG-DMPA-HDI-PG) were synthesized, and their chemical structures were confirmed by ATR-FTIR and ^{1}H-NMR spectra. Excitation (490 nm) and maximum emission (570 nm) of PASP-PEG-Ph-Orange NPs were evaluated and used for tracking the release amount of NPs in *in vitro* release studies. pH-responsive supramolecular PU hydrogels were prepared in distilled water using 20 wt% PEG-DMPA-HDI or PEG-DMPA-HDI-PG. 1 mg/mL PASP-PEG-Ph-Orange NPs in distilled water was blended with the pH-responsive PUs to form complex hydrogels, and then filled in segmented IVR having two holes (DI: 1/32"). *In vitro* tests showed the pH-responsive release of PASP-PEG-Ph-Orange NPs from both supramolecular PU gels. Moreover, PEG-DMPA-HDI-PG supramolecular hydrogel demonstrated pH-responsive switchable on-demand on-and-off release of PASP-PEG-Ph-Orange NPs triggered by pH changes from pH 4.2 to 7.0 and from pH 7.0 to 4.2. The PASP-PEG-Ph-Orange and PEG-DMPA-HDI-PG showed no and low cytotoxicity, respectively, toward VK2/E6E7. Overall, this new pH-responsive PEG-DMPA-HDI-PG supramolecular hydrogel

successfully demonstrated its potential utility as a novel biomaterial for the development of an intravaginal drug delivery device for pH-responsive switchable on-demand release of NPs.

5.6   Acknowledgements

5.7   Contribution of Authors

Seungil Kim[a]: initiated and contributed to the scope of the manuscript; performed synthesis and characterization of fluorescent PEGylated poly(aspartic acid) nanoparticles; performed synthesis and characterization of pH-sensitive PU copolymers; performed fabrication of segmented IVR filled with the inclusion complex of pH-responsive supramolecular PU hydrogels and PASP-PEG-Ph-Orange NPs; performed evaluation of *in vitro* nanoparticle release; wrote the manuscript.

Yannick Leandre Traore[b]: performed *in vitro* cytotoxicity tests; contributed writing manuscript.

Yufei Chen[b]: performed fabrication of IVR segments; contributed writing manuscript.

Emmanuel A Ho[b]: contributed writing manuscript; critically reviewed the manuscript.

Song Liu[a,c,d,*]: initiated and contributed to the scope of the manuscript; contributed writing manuscript; critically reviewed and revised the manuscript.

[a] Biomedical Engineering, Faculty of Engineering, University of Manitoba, Winnipeg, Manitoba, Canada

[b] Laboratory for Drug Delivery and Biomaterials, School of Pharmacy, University of Waterloo, Kitchener, Ontario, Canada

[c] Department of Biosystems Engineering, Faculty of Agricultural and Food Sciences, University of Manitoba, Winnipeg, Manitoba, Canada

[d] Department of Chemistry, Faculty of Science, University of Manitoba, Winnipeg, Manitoba, Canada

Chapter 6

Summary and Conclusions

STIs caused by bacteria and viruses transmitted by sexual intercourse are one of the most significant public health concerns. Prevention and early treatment of STIs are important in decreasing their prevalence and incidence. In particular, HIV has been proclaimed as a pandemic and no cure has been found yet. Globally, over 30 million people are living with HIV which can potentially progress to AIDS.

Topical drug delivery has been developed for treating local infections. The advantages of topical drug delivery include increased drug delivery efficiency to the target site, drug bioavailability, pharmacological response, and drug compliance of patients. As one of the topical DDS, IVRs have been developed for intravaginal delivery of drugs. The availability of IVRs could greatly empower women to protect themselves and their partners from HIV since the application of formulations does not require the consent of their partner. However, the loaded drug is released consistently from the IVR ring after being inserted even when the drug is unnecessary. Such undesired drug exposure can cause side effects. In this regard, it is desirable that the anti-HIV drug and siRNA be released only when heterosexual intercourse occurs to reduce side effects.

Moreover, nanocarrier is necessary to overcome barriers of mucus vaginal epithelial and T-cells to increase drug delivery efficiency and reduce side effects of drugs. While siRNA has a high potential to interfere with HIV at the genetic level,[21] it has a low stability in acidic vaginal pH. Therefore, it is necessary to release anti-HIV drug, siRNA, or their nanocarrier upon pH change from acidic to neutral since human vaginal pH can be elevated to neutral pH (> 6.5) from normal acidic vaginal pH (3.5-4.5, average: 4.2) by the introduction of human seminal fluid during heterosexual intercourse.

In this thesis research, new pH-sensitive PU copolymers were synthesized using HEP (pKa 6.4) for PEG-HEP-HDI-PG and PEG-HEP-MDI-PG, or DMPA (pKa 4.41) for PEG-DMPA-HDI and PEG-DMPA-HDI-PG as pH-sensitive diols. The pH-sensitive diols were immobilized in the soft segment to give dramatic pH-triggered responses and the physical property of the PUs was enhanced by adding PG on the hard segment. In addition, new PEGylated nanocarrier, PASP-PEG-Ph, and fluorescent dye conjugated nanocarrier, PASP-PEG-Ph-Orange, were synthesized from PSI.

To achieve on-demand intravaginal release of anionic drugs, solvent-cast pH-responsive PU, PEG-HEP-HDI-PG and PEG-HEP-MDI-PG membranes were fabricated. The solvent-cast PEG-HEP-HDI-PG and PEG-HEP-MDI-PEG membranes demonstrated pH-triggered reversible changes in swelling ratio and morphology. The pH-responsive release of NaDF was sensitive and rapid at pH 7.0 (over 20% of total NaDF released within 3 h), but demonstrated close-to-zero drug release at pH 4.5. Moreover the solvent-cast pH-responsive membranes demonstrated switchable on-demand release of NaDF.

In addition, electrospun PEG-HEP-MDI-PG semi-permeable membranes were fabricated for the controlled intravaginal release of nanocarriers since the solvent-cast PU membranes failed to achieve the pH-responsive NPs permeation due to the insufficient interconnected space for traverse of NPs. The electrospun PEG-HEP-MDI-PG membranes showed pH-dependent changes in morphology (pore sizes, fiber diameters, and thickness) and surface charge. Such porous electrospun PEG-HEP-MDI-PG membranes demonstrated pH-dependent release of color-dyed polystyrene nanoparticles (PSNs, -COOH). They had almost no release of PSNs in VFS at pH 4.5: however, they demonstrated a continuous release of PSNs at pH 7.0.

These pH-responsive PU membranes were developed as a "window" membrane of reservoir-IVR for the intravaginal on-demand release of anti-HIV drugs or nanocarriers. The pH-responsive PU membranes showed no cytotoxicity to VK2/E6E7 and Sup-T1. Moreover, the elution medium collected from the membranes did not induce an inflammatory microenvironment.

Finally, the switchable on-demand release of nanocarriers from reservoir-IVR was achieved by pH-responsive supramolecular PU hydrogel which was prepared using PEG-DMPA-HDI-PG. The fluorescent dye Orange II was conjugated onto PASP-PEG-Ph NPs to get PASP-PEG-Ph-Orange, allowing easy quantification of released NPs *in vitro* release studies. Excitation (490 nm) and maximum emission (570 nm) of PASP-PEG-Ph-Orange NPs were confirmed. 1 mg/mL PASP-PEG-Ph-Orange NPs in distilled water was blended with the pH-responsive PUs, PEG-DMPA-HDI or PEG-DMPA-HDI-PG, to form complex hydrogels, and then filled in a segmented IVR with two tiny holes (DI: 1/32"). *In vitro* tests showed the pH-responsive release of PASP-PEG-Ph-Orange NPs from both PEG-DMPA-HDI and PEG-DMPA-HDI-PG gels. Moreover, PEG-DMPA-HDI-PG supramolecular hydrogel demonstrated pH-responsive switchable on-demand on-and-off release of PASP-PEG-Ph-Orange NPs triggered by pH changes: almost no release for the first 1 h at pH 4.2; then pH-triggered release ($19 \pm 5\%$) for the next 1 h at pH 7.0, followed by off/on/off switchable release for another 3 h.

Overall, the present results suggest that these new pH-responsive PU biomaterials and PEGylated nanocarriers are potential candidates to prepare smart reservoir-IVRs for combating HIV. The pH-responsive PU biomaterials could be applied with most anionic anti-HIV drugs, poorly water-soluble anti-HIV drugs, siRNA, and their nanocarriers. Although the response time of the pH-responsive PU hydrogel seems fast enough since HIV needs several hours to overcome

the human mucus barrier to reach human immune cells, the hydrogel potentially can be further optimized by controlling the soft segment and hard segment ratio to obtain a faster response for better protection against HIV transmission.

Further studies to optimize the developed nanocarriers for intravaginal delivery of siRNA are warranted. The desired characteristics of the nanocarrier are: (1) high density of low MW PEG on the surface; (2) close to zero absolute value of zeta-potential with loaded siRNA; (3) particle size around 200 nm after loading siRNA; (4) high stability against repeated dramatic pH changes; (5) high buffering capacity to avoid leaking cargo siRNA. Also, it would be necessary to establish an animal model for *in vivo* pH-responsive switchable intravaginal release study. In order to conduct an *in vivo* study, we will need to: (1) increase the number of cycles of switchable release of drug or nanocarrier; (2) use an appropriate fabrication technique to incorporate the developed pH-responsive PU membranes into reservoir-type IVRs as window membranes.

In future, the pH-responsive PU, PEG-DMPA-HDI-PG, hydrogel potentially can contribute to pH-triggered release of drugs, siRNA, or their nanocarriers not only for intravaginal administration but also for oral and transdermal administration. The pH-responsive PU synthesized using HEP is also useful for oral delivery of drugs or nutrients targeting the intestine. Little release at acidic gastric pH and pH-triggered release at the small intestine can be attained. On the other hand, the PEGylated nanocarrier can be applied not only for anti-HIV therapy but also for other diseases such as cancer and cystic fibrosis, especially, where crossing the mucus barrier is necessary.

Chapter 7

Appendix: Self-assembled nanoparticles made from a new PEGylated poly(aspartic acid) graft copolymer for intravaginal delivery of poorly water-soluble drugs

Seungil Kim, Song Liu

As a side project of this thesis (also for Ph.D. candidate examination of Biomedical Engineering Program at University of Manitoba), PEGylated PASP-based NP was developed as an intravaginal nanocarrier. The hypothesis of this research is the PEGylated PASP-based copolymer can stably self-assemble to NPs at pHs from 3.5 to 7.5 for intravaginal delivery of poorly water-soluble anti-HIV drugs.

7.1   Abstract

New amphiphilic PEGylated PASP graft copolymer (PASP-PEG-Ph) was synthesized as a nanocarrier for intravaginal drug delivery of poorly water-soluble drugs. PASP-PEG-Ph self-assembled into negatively charged spherically shaped NPs in the presence of pH 4.5 and pH 7.0 VFS with a diameter of approximately 200 nm as evidenced by Zeta-potentiometer, SEM, and DLS analysis. A significant number of stable NPs could be maintained at pH 4.5, 37 °C for 13 days. The PASP-PEG-Ph NP showed no significant cytotoxicity toward the T-cell line Sup-T1 and human vaginal epithelial cell line VK2/E6E7 up to 1 mg/mL. The highest encapsulation efficiency of the model drug C6 by PASP-PEG-Ph was $93 \pm 6\%$. The sustained release profile of the encapsulated C6 was demonstrated by an *in vitro* release study. An *in vitro* cellular uptake study revealed strong cellular uptake of the C6 loaded NP by Sup-T1 cells within 2 h.

7.2   Introduction

HIV/AIDS is a global pandemic and the leading infectious disease. HIV infection causes significant mortality: 1.1 million in 2015 according to WHO.[2] Unfortunately, there is currently no cure for HIV. Most anti-HIV drugs merely slow down the course of the infection by

interfering with the proliferation of HIV in human T-cells,[30] so prevention of HIV transmission is critical in the battle against AIDS. HIV is typically transmitted (> 70%) via heterosexual intercourse.[224] Intravaginal delivery of anti-HIV drugs would be desirable because it can potentially prevent transmission of HIV in the early stage of infection. Non-nucleoside reverse transcriptase inhibitor (NNRTI) efavirenz is an FDA approved anti-HIV drug used by more than 70% of AIDS patients in developing countries. However, efavirenz and other NNRTIs such as etravirine are poorly water-soluble anti-HIV drugs (solubility 2.81 and 0.36 μg/mL at 25 °C predicted using the US Environmental Protection Agency's EPISuiteTM, respectively). Since poor water-solubility limits effective intravaginal delivery of anti-HIV drugs such as efavirenz and etravirine, it is necessary to develop nanocarriers for efficient intravaginal drug delivery, thus preventing HIV transmission at the inception of the infection and reducing side effects of the drugs.

Nanocarriers such as micelles, vesicles, nanogels, liposomes, solid lipid nanoparticles, dendrimers, and carbon nanotubes have been developed for DDS.[225–228] These organic and inorganic nanocarriers increase the delivery efficiency and stability of the drugs encapsulated within them. Moreover, the nanocarriers have been designed for anti-HIV drug delivery.[31,200,229] It was reported PEGylation of the surface of the NPs increases penetration efficiency crossing vaginal mucus and particles of 200-500 nm in size have a higher penetration efficiency through mucus than 100 nm size NPs.[190] NPs with a diameter of 150-500 nm were reported to be suitable for cellular uptake.[230]

The desired characteristics of NPs for intravaginal delivery of poorly water-soluble anti-HIV drugs are: 1) high stability in the pH range from 3.5 to 8.0; 2) high loading efficiency of hydrophobic anti-HIV drugs; 3) low cytotoxicity toward human T-cell line; 4) availability of

functional groups on the surface to allow further surface modifications such as conjugation of anti-human CD4 antibody or fluorescent tag.

Amphiphilic poly(amino acid) copolymers have been developed as a drug delivery nanocarrier because of their similarity to naturally occurring proteins.[115] Most currently, amphiphilic poly(amino acid) copolymers have been developed for anti-cancer drug delivery, so the nanocarriers of the copolymers were designed to specifically dissociate at acidic pH in cancer cells (below pH 7.0)[231,232] or late endosomal pH (pH 4.5-5.5)[233] for effective release. However, this acid-triggered disassembling property is not desirable for intravaginal anti-HIV drug delivery because of the acidic pH (pH 3.5-4.5) of the normal human vaginal tract[35,104] and an elevated female genital tract pH near neutral during heterosexual intercourse when anti-HIV drugs are needed.[24,33] Amphiphilic Poly(γ-glutamic acid) (PGA, pKa 2.2) derivatives, which were conjugated with amino acids such as L-phenylalanine and L-leucine, were studied as nanocarriers.[234,235] Among the amphiphilic PGA derivatives, the L-phenylalanine ethylester (L-PAE) conjugated copolymer demonstrated a suitable NP size (200 nm) for drug delivery and enzymatic degradation. It also demonstrated its potential use as a nanocarrier for proteins, peptides, plasmid DNA and hydrophobic drugs.[117–119] Most recently, PEGylated poly(aspartamide) based NP was reported to possess a higher penetrating efficiency across cystic fibrosis artificial mucus than the non PEGylated poly(aspartamide) based NP.[202] In this research, new amphiphilic PASP, with conjugated hydrophobic phenethylamine and hydrophilic PEG branches, was prepared as a potential intravaginal nanocarrier for poorly water-soluble anti-HIV drugs. PASP is a promising water-soluble and biodegradable poly(amino acid) with non-toxic degradation products. Furthermore, PASP has carboxylic acid groups for further chemical derivation such as conjugation with an antibody or a fluorescent tag. PEG is a non-toxic and non-

immunogenic water-soluble polymer. PEGylation of the amphiphilic PASP derivatives may increase the stability of the self-assembled nanostructure in acidic pH. Moreover, PEGlyation reduces the association of particles with vaginal mucus.[17] Phenethylamine is a natural monoamine alkaloid and biosynthesized from the amino acid phenylalanine by enzymatic decarboxylation. Coumarin 6 (C6) is a poorly water-soluble (0.25 µg/mL) dye which has been used as a model hydrophobic drug in drug delivery studies involving release and tracking of localized delivery.[236–239] In this project, C6 was used as a model drug for poorly water-soluble anti-HIV drugs such as efavirenz (2.81 µg/mL) and etravirine (0.36 µg/mL) because of their similarities in solubility and chemical structure.

To our knowledge, the new amphiphilic PASP nanocarrier is the first developed PEGylated amphiphilic PASP copolymer which can self-assemble in water into NPs that are bigger than 200 nm and bear a derivatizable functional group on their surface. Moreover, the nanocarrier has a stable structure at pH >4.5 due to its low pKa: 3.9. At pH higher than 4.5, the nanocarrier showed the average diameter of 200 nm when drug-free, and 330 nm when loaded with C6. The hydrophobic model drug C6 was successfully encapsulated in the core of the nanocarrier with an encapsulation efficiency as high as 92.8%. The nanocarrier demonstrated a noticeable sustained release profile of the loaded hydrophobic model drug and cellular uptake by T-cell line Sup-T1 in *in vitro* tests. Moreover, carboxylic acid groups are available on the surface of the nanocarrier, enabling further desirable chemical derivatization such as conjugation of an anti-human CD4 antibody.

7.3 Materials and methods

7.3.1 Materials

L-aspartic acid ($\geq$ 98%), o-phosphoric acid (98%), phenethylamine ($\geq$ 99%, Ph), coumarin 6 (98%, C6), N,N-dimethylformamide (99.8% anhydrous, DMF), methanol ($\geq$ 99.8%), and ethanol ($\geq$ 99.8%) were purchased from Sigma-Aldrich (St. Louis, MO, USA). Methoxypolyethylene glycol amine (Me-PEG-NH$_2$, M.W. 5,000) was purchased from Alfa Aesar (Haverhill, MA, USA), dichloromethane (99.5%) was purchased from Acros Organics (Geel, Belgium), phosphate-buffered saline (PBS, 1X, without calcium & magnesium) was purchased from Mediatech, Inc (Manassas, VA, USA). 1 N hydrochloric acid solution (HCl) was purchased from Fisher Chemical (Waltham, MA, USA), 1 N sodium hydroxide (NaOH) was purchased from EMD Chemicals (Mississauga, ON, Canada), Kolliphor$^®$ HS 15 was donated from BASF (Ludwigshafen, Germany). Dialysis membrane (Spectra/pore with MWCO 12-14 kD and 500-1000 D) was purchased from Spectrum Laboratories, Inc (Rancho Dominguez, CA, USA). VFS consisted of 3.51 g NaCl, 1.40 g KOH, 0.222 g Ca(OH)2, 0.018 g BSA, 2.0 g lactic acid, 1.0 g acetic acid, 0.6 g glycerol, 0.4 g urea, and 5.0 g glucose in 1 L of distilled water. The pH of the VFS was adjusted with 1 N HCl and 1N NaOH.[104]

7.3.2 Synthesis of new amphiphilic PEGylated poly(aspartic acid) copolymer (PASP-PEG-Ph)

PSI was synthesized by polycondensation of L-aspartic acid with the following procedure:[206,207] Briefly, 20 g of L-aspartic acid and 20 g of o-phosphoric acid (50: 50) were mixed at 4 °C. The mixture was then placed in a round bottom flask and stirred under reduced

pressure at 200 °C for 5 h. 200 mL of DMF was added to dissolve the reaction product completely after it cooled down. The solution was filtered through a fritted funnel filter (porosity: 10-15 μ) and then precipitated into excess MeOH. The precipitate was washed with excess distilled water until the pH of the used distilled water was increased to around 6.0. The product was finally dried at 80 °C in vacuum. The synthesized PSI had a reduced viscosity of 0.49 dL/g in DMF. The evaluated molecular weight was 152 kDa and was calculated from an empirical equation relating the solution viscosity to the molecular weight.[208]

The preparation of the amphiphilic PEGylated PASP copolymer, Me-PEG-NH$_2$ and phenethylamine were conjugated to the prepared PSI by aminolysis reaction, followed by a ring opening reaction of the remaining imide rings (**Scheme 7-1**). Briefly, 0.5 g PSI was dissolved in 15 mL anhydrous DMF under nitrogen inlet and outlet conditions. 0.773 g Me-PEG-NH$_2$ (3% feed mole to PSI) dissolved in 5 mL anhydrous DMF was added to the reactor. After the reactor had been maintained for 48 h at 80 °C, 0.357 mL of phenethylamine (55% feed mole to PSI) was added to the reactor. After 48 h reaction for conjugation of the phenethylamine, 160 mL cold distilled water was added to the reactor. 5 mL of 0.5 N NaOH (0.1 g NaOH) solution was added in the reactor for the hydrolysis of the remaining imide rings, thus keeping the solution pH below 10.8 at room temperature. 12.23 mL 0.5 N HCl (0.223 g of 37% HCl) solution was added in the reactor until the pH of the solution remained at 4.0 in an ice bath for the acidification.[120] The reaction solution was dialyzed using a membrane tubing (MWCO 12-14 kD) to remove low molecular weight impurities. After three days dialysis with 10-times change of distilled water (2 L of distilled water were used for each time), the purified product was frozen followed by freeze-dried (Yield: 85%). ATR-FTIR: 1651, 1537, 1466, 1101, and 961 cm^{-1}. ^{1}H-NMR (300 MHz,

DMSO): 2.5-2.7 (2H, *CH₂–CH–CO–NH–CH₂*), 3.4-3.5 (4H, *CH₂–CH₂-O*), 4.3-4.7 (1H, *CH–CH₂–CO–NH*), 7.0-7.3 (5H, *CH–CH–CH–CH–CH–C*).
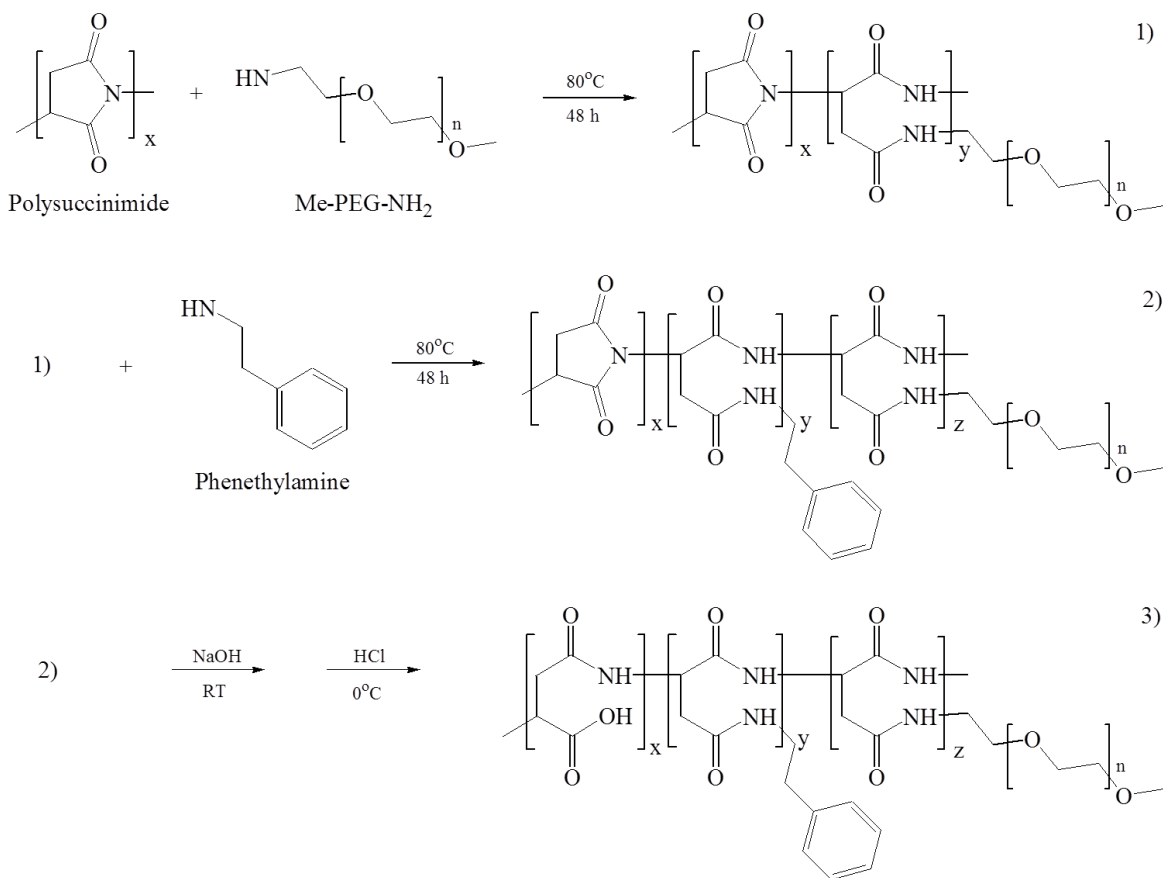
Scheme 7-1. Synthesis of the amphiphilic PEGylated poly(aspartic acid) copolymer (PASP-PEG-Ph).

7.3.3 Physicochemical characterization of the amphiphilic PEGylated poly(aspartic acid) copolymer nanoparticle (PASP-PEG-Ph NP)

The average particle size of the PASP-PEG-Ph NP was characterized in distilled water (pH 7.0), VFS (pH 4.5 and 7.0), PBS (pH 7.4), and MES (pH 6.0), respectively. 1 mg of the

PASP-PEG-Ph NP was re-suspended in 10 mL of each solution by vortexing for 2 min at 3,000 rpm. The particle size of the PASP-PEG-Ph NP was evaluated by DLS using ZetaPALS (Brookhaven Instrument, Holtsville, NY, USA) with a scattering angle of 90 ° and laser light at 659 nm.

Images of the NPs were taken using a SEM (FEI Nova-Nano SEM 450). For the imaging, 1 mg/mL of the NP in distilled water was prepared by re-suspension of the amphiphilic copolymer using a vortex mixer for 2 min at 3,000 rpm. The prepared solution was dropped on Cu-grids (200 mesh copper, with a carbon film). After the deposited PASP-PEG-Ph NP solution was dried at room temperature, the NPs sample was coated with 10 nm Au-Pd. The images of the prepared sample were taken using the SEM at secondary electron mode with a through-lens detector.

The average particle size of the PASP-PEG-Ph NP at different pH from 3.0 to 8.0 were characterized by the following methods: The PASP-PEG-Ph NP was re-suspended in 10 mL VFS at 100 μg/mL by vortexing for 2 min at 3,000 rpm. The pH of the prepared PASP-PEG-Ph NP solution was adjusted using a 1 N HCl or 1 N NaOH solution. The particle size of the PASP-PEG-Ph NP was evaluated by DLS using the ZetaPALS with a scattering angle of 90 ° and laser light at 659 nm.

The zeta-potential of the PASP-PEG-Ph NP was characterized by the following method: The PASP-PEG-Ph was re-suspended in 10 mL distilled water at 100 μg/mL by vortexing for 2 min at 3,000 rpm. The pH of the prepared solution was adjusted from 3.0 to 8.0 by adding 1 N HCl or 1 N NaOH solution. The ZetaPALS was used for the Zeta-potential evaluation. The Smoluchowski model was applied for evaluating the surface charge of the NP in distilled water.

The physical stability of the PASP-PEG-Ph NPs in VFS (pH 4.5, 7.0) at 37 °C was evaluated using the following method: 30 mL of 100 µg/mL PASP-PEG-Ph NP was prepared by re-suspension (2 min of vortexing at 3,000 rpm was applied) of the PASP-PEG-Ph in VFS at pH 4.5 and 7.0 respectively. The NP solution was kept at 37 °C in a shaking bath (100 rpm) for 504 h. The particle size of the NP was characterized until the NP showed a bigger size than 1,000 nm.

7.3.4 Preparation of Coumarin 6-loaded NP (C6-NP)

PASP-PEG-Ph NP with encapsulated C6 was prepared using the solvent casting method. Briefly, four 1 mg/mL PASP-PEG-Ph in 5 mL DCM solutions were made ready followed by vortexing for 2 min and sonication for 3 min using a sonication bath (Ultrasonic LC 60H, Elma Hans Schmidbauer GmbH & Co. KG, Kolpingstr, Singen, Germany). 1 mL of 4 mg/mL C6 in DCM was prepared as a stock solution. The C6 was added to the prepared PASP-PEG-Ph solution as different feed ratios ranging from 0.05: 1 to 0.3: 1 (C6: PASP-PEG-Ph= 0.05: 1, 0.1: 1, 0.2: 1, 0.3: 1) respectively. After the solvent had been evaporated using a rotary evaporator at 37 °C under 35-65 mbar, a thin film of C6 and copolymer mixture was dispersed by adding 5 mL of distilled water. Vortex shaking for 2 min at 3,000 rpm was applied to the dispersion, followed by sonication for 6.5 min (3 min using the sonication bath followed by 30 sec using a probe sonicator (Sonifier 150, Branson, MO, USA) at 40 kHz, 5 root mean square (RMS) followed by 3 min using the sonication bath). The C6-NP was filtered through a filter paper with 11 µm pores to remove free C6, after vortex shaking 2 min at 3,000 rpm. The C6-NP was washed with excess distilled water three times to remove loosely attached C6. C6 loading efficiency, particle size, and Zeta-potential were evaluated using the prepared C6-NP. For the C6 loading efficiency, the

C6-NP was dissolved by adding ethanol (1: 1 vol ratio to distilled water) for quantification. The loaded C6 was quantified using a fluorescent spectrometer at 485 nm (λ_{ex}) and 528 nm (λ_{em}). When C6 is dissolved in 50 % EtOH, the excitation and emission maxima for C6 are 472 (λ_{ex}) and 506 (λ_{em}).[240] The C6 loading efficiency (%) and C6 loading content (wt%) were calculated by the following equations:

C6 loading efficiency (%)

= (Weight of loaded C6/Weight of C6 in feed) × 100

C6 loading content (wt%)

= (Weight of loaded C6/Weight of the copolymer) × 100

7.3.5 *In vitro* **model drug release study**

C6 release from the NP was evaluated by the dialysis membrane method: Briefly, the *in vitro* release profiles of the C6 were investigated as a function of time. The release medium was prepared from phosphate-buffered saline (PBS) containing 2 wt% Kolliphor® HS 15. Polyglycol mono- and di-esters of 12-hydroxystearic acid (lipophilic part) and about 30% of free PEG (hydrophilic part) are the main components of the Kolliphor® HS 15. For the release study at pH 4.5, pH was adjusted by adding 0.1 N HCl solution. For the release study, 1 mL of the C6-loaded NP was prepared as described in the earlier paragraph 7.3.2. The C6 was added to the PASP-PEG-Ph solution as feed ratio of 0.1: 1.0 (C6-NP 10, Feeding ratio of C6 versus NP is 0.1: 1.0) because this ratio showed the most balanced loading content (6.4%) and loading efficiency (63.7%). 1 mL of prepared C6-NP 10 was added to membrane tubes (MWCO 12,000-14,000, Mw of the C6 is 350.43). The dialysis tubing was immersed in a vial containing 19 mL of the

release medium. The vial was incubated in a shaking bath at 37 °C at 100 rpm. At regular intervals of time (1, 3, 6, 12, 24, 48 and 72 h), 1 mL of the medium was removed and replenished with 1 mL of fresh medium. The cumulative amount of released C6 was determined by fluorescence.

7.3.6 *In vitro* cytotoxicity studies

Cell cytotoxicity of the PASP-PEG-Ph NP was evaluated via an MTS assay. VK2/E6E7 human vaginal epithelial cells and human T-cell line Sup-T1 cells (American Type Culture Collection, ATCC, Rockville, MD, USA) were plated at 2.5×10^4 cells/well in 96-well plates. The medium was keratinocyte-serum free medium (K-SFM) supplemented with recombinant human epidermal growth factor, bovine pituitary extract, calcium and penicillin/streptomycin for the VK2/E6E7 cells and Roswell Park Memorial Institute (RPMI) medium supplemented with FBS and antibiotics for Sup-T1. The pH of the medium was neutral. Varying concentrations of drug-free NPs (200–1,000 µg/mL) were prepared for the evaluation. The prepared drug-free NPs were sterilized by exposure to UV light for 30 min in a sterile biosafety cabinet. The negative control was blank cell media, and the positive control was 1 M acrylamide in cell media. 1 M acrylamide was prepared in the K-SFM medium and RPMI medium filtered through a 0.2 µm membrane filter. The 1 M acrylamide in the medium was used as a positive control to induce cell death for the CellTiter 96® Aqueous One Solution Cell Proliferation Assay (MTS Assay, Promega Corporation, Madison, WI, USA). After seeding 2.5×10^4 cells/well in 96-well, the VK2/E6E7 cells were incubated for 24 h for the cells to attach. 2.5×10^4 of Sup-T1 cells were seeded as well and spun down to discard the supernatant. The cells were treated with 100 µL of the negative control, positive control, and the prepared drug-free NP solutions. After 24 h of the treatment,

the medium was replaced with fresh medium containing 20 µL of MTS solution. The MTS treated cells were incubated in the dark for 2 h under 5% CO_2 at 37 °C. The plate was analyzed using a Synergy HT multi-mode microplate reader (Biotek, Winooski, VT, USA) at 490 nm.

7.3.7 Cellular uptake test

1 mL fresh C6 loaded NP (C6-NP 10) was prepared at a feeding ratio of C6 and the NP is 0.1: 1. Sup-T1 cells were plated at 2.5×10^4 cells/well in 96-well tissue culture treated plates in 100 µL of cell culture medium. The medium was RPMI medium supplemented with FBS and antibiotics. The pH of the medium was neutral. Varying concentrations of C6-NP 10 (0.4, 0.8, 1.0 mg/mL) were prepared for the evaluation. The control was 0 mg/mL C6-NP 10. After 2 h and 4 h of treating 100 µL of different concentration C6-NP, fluorescent intensity of C6-NP 10 was evaluated by a flow cytometry (FACSCanto) and images were taken using a fluorescent microscope (Nikon TE 2000) for evaluation. Before the flow cytometry analysis, the cells were washed thoroughly to remove free C6.

7.4 Results and discussion

7.4.1 Synthesis and characterization of the amphiphilic PEGylated poly(aspartic acid) copolymer (PASP-PEG-Ph)

The PASP-based graft copolymer was designed as an intravaginal delivery nanocarrier using non-toxic raw molecules and relatively simple reactions for achieving low cytotoxicity and ease of industrial scale-up of the nanocarrier. The precursor PSI was synthesized by polycondensation of L-aspartic acid. For the synthesis of high molecular weight PSI, the vacuum

was increasingly applied up to full vacuum. The high vacuum condition was also essential for the removal of by-product H_2O from the reactor. The *o*-phosphoric acid was used not only as a reaction catalyst, but also as a solvent for the L-aspartic acid. After the reaction, the reaction product was carefully washed with MeOH and distilled water to remove by-products. The amphiphilic PASP copolymer conjugated with PEG and phenethylamine (PASP-PEG-Ph) was synthesized from PSI. Since PEGylation was reported to increase mucus penetration by NPs,[17] Me-PEG-NH$_2$ was introduced to PSI to form PEGylated PASP. Phenethylamine was conjugated to serve as a hydrophobic segment for the PASP-PEG-Ph NP. Phenethylamine was chosen because of its chemical structure and origin. The phenethylamine was conjugated at a relatively high ratio versus the hydrophilic segment resulting in PASP-PEG-Ph forming a self-assembled solid NP in aqueous medium. For the Me-PEG-NH$_2$ and phenethylamine conjugation, aminolysis reaction was applied. Resulting from conjugation of the molecules, the imide of PSI was converted to an amide bond.[209] A 48 h reaction time was given for each Me-PEG-NH$_2$ and phenethylamine conjugation to maximize the conversion ratio. After the aminolysis reaction, a mild hydrolysis reaction was performed using 0.5 N NaOH at room temperature to convert the remaining imides to a sodium polyaspartate structure. 0.5 N NaOH was slowly added to the reaction mixture to keep the pH under 10.8, avoiding unnecessary hydrolysis of the polymer backbone. After the hydrolysis, 0.5 N HCl was slowly added to the reactor at 4 °C to convert sodium carboxylates to free carboxylic acids.[120] A dialysis tubing was used for removing low molecular weight impurities. During the dialysis process, the reaction solvent DMF was diffused out from the dialysis membrane resulting in the synthesized amphiphilic copolymer forming a self-assembled nanostructure inside of the dialysis tubing. The self-assembled NPs were frozen at -80 °C and then freeze-dried to be obtained as a fine powder.
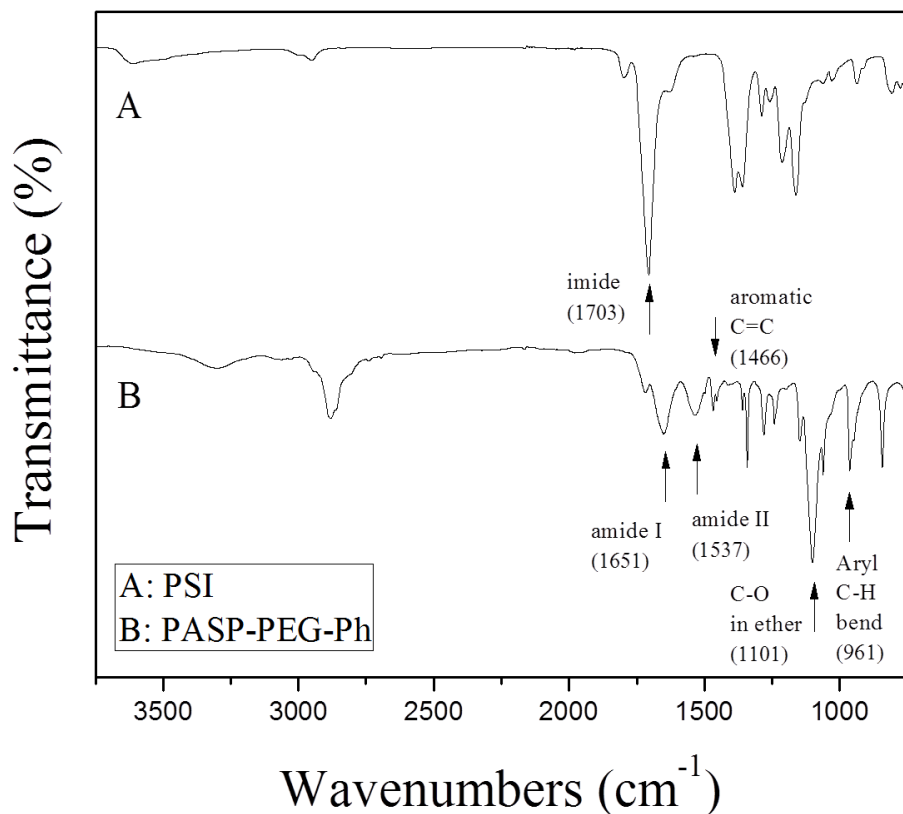
Figure 7-1. Attenuated total reflectance-Fourier transform infrared (ATR-FTIR) spectrum of (A) polysuccinimide (PSI) and (B) synthesized amphiphilic PEGylated poly(aspartic acid) copolymer (PASP-PEG-Ph).

The ATR-FTIR spectrum of PSI (**Figure 7-1**, **A**) showed stretching vibrations absorption of imide at 1703 cm^{-1}. The conversion of PSI to PASP was confirmed by the presence of amide I (1651 cm^{-1}) and amide II (1537 cm^{-1}) bands in the ATR-FTIR spectrum (**Figure 7-1, B**).[121,122] The conjugated mPEG and phenethylamine were confirmed from ether C-O stretch absorption at 1101 cm^{-1},[214] aromatic C=C stretch (1466 cm^{-1}), and Aryl C-H bend absorption (961 cm^{-1}).[215]
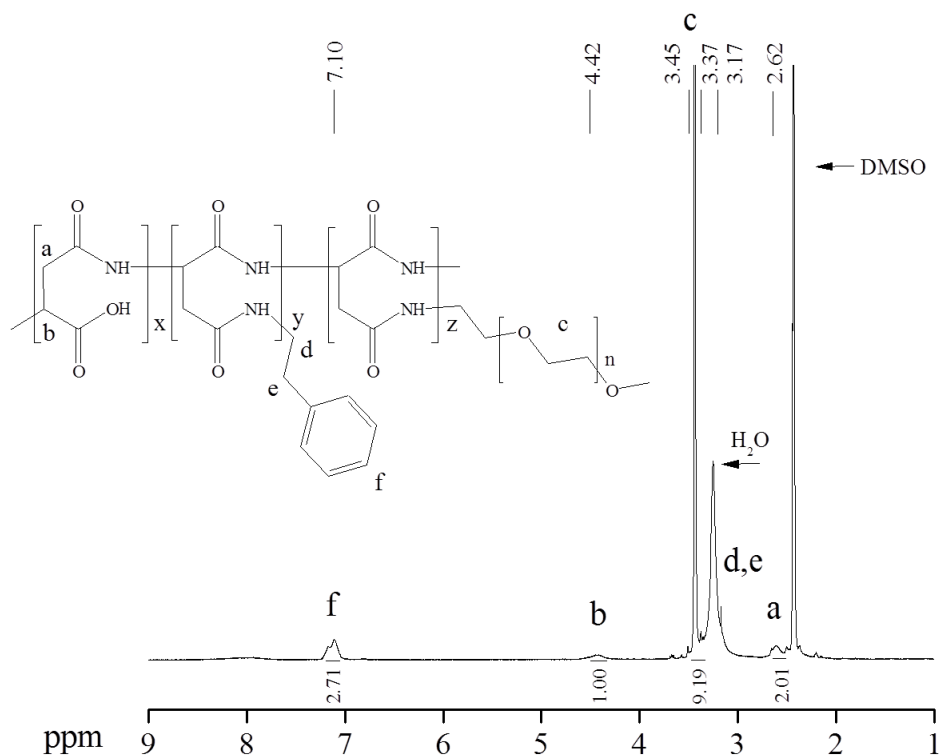
Figure 7-2. [1]H-Nuclear Magnetic Resonance (^{1}H-NMR) spectra of the PEGylated amphiphilic poly(aspartic acid) copolymer (PASP-PEG-Ph) (DMSO-d6 was used as a solvent).

A ^{1}H-NMR spectrum of PASP-PEG-Ph was collected for identifying the chemical structure. In **Figure 7-2**, the proton peaks of b and a were assigned to the methine and methylene protons of the copolymer backbone.[121,122] The conjugated mPEG and phenethylamine were confirmed by peak c as the methylene protons of mPEG[209,214] and peak f as methine protons of the phenethylamine.[217] The methylene peaks of the phenethylamine d and e were overlapped with the ^{1}H-NMR solvent DMSO-d$_6$. The degree of substitution of phenylene amine was

calculated as 54.2% by comparing the peak area of the methine protons peaks b and f. The degree of substitution of mPEG amine was calculated as 2.0%, using the peak area of methylene protons peak c in comparison to the methine protons peak b. The chemical structure of synthesized PASP-PEG-Ph was confirmed by ATR-FTIR and ^{1}H-NMR.

7.4.2 Physico-chemical characteristics of the nanoparticle (NP)

The average particle size of the NP was evaluated in distilled water and with various buffer solutions at the concentration of 100 μg/mL (**Table 7-1**). The pH of VFS was adjusted using a 1 N NaOH solution. The PASP-PEG-Ph NP was re-suspended in 10 mL distilled water or the buffer solutions at 100 μg/mL by vortexing for 2 min at 3,000 rpm. The particle size was evaluated by DLS using the ZetaPALS with a scattering angle of 90 ° and laser light at 659 nm. The NP showed suitable particle size (150-200 nm) for a drug delivery carrier in different buffer conditions, and the particle size showed only a minor difference ($\pm$ 25 nm) in the various environments tested.

Table 7-1. Average particle size of the PASP-PEG-Ph NP in distilled water and various buffer solutions ($n = 3$) based on DLS.

Suspension (100 μg/mL)	Distilled water (pH 7.0)	VFS (pH 4.5)	VFS (pH 7.0)	PBS (pH 7.4)	MES (pH 6.0)
Particle size (nm)	186 ± 3	201 ± 3	201 ± 2	152 ± 3	146 ± 3
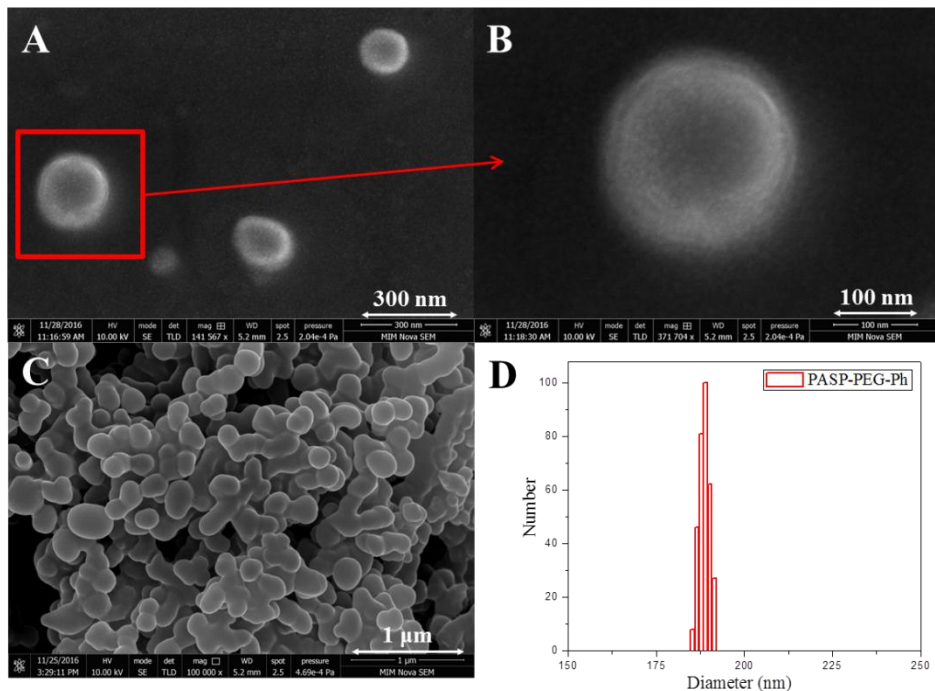
Figure 7-3. Image of the PASP-PEG-Ph nanoparticles with a concentration of 1 mg/mL in distilled water: individual nanoparticles (A), magnified image of the individual nanoparticle (B), regular size of nanoparticles 207 ± 8 nm was manually measured using ImageJ (*n*=200) (C), and DLS histogram of the nanoparticles with a concentration of 100 μg/mL in distilled water. Average size is 186 ± 3 nm) with a narrow polydispersity (0.097) (D).

SEM images were taken for confirmation of the structure and size of the NPs. From **Figure 7-3, A** and **B**, it is evident that the synthesized copolymer PASP-PEG-Ph formed self-assembled spherical NPs in an aqueous environment. The particle size was also confirmed by the SEM image (**Figure 7-3, C**) and DLS measurements (**Figure 7-3, D**). In image C, agglomeration was observed possibly resulting from the evaporation of distilled water during the preparation of the SEM sample. However, it was still possible to evaluate the average particle size of the NPs, and it was 207 ± 8 nm (calculated based on 200 NPs), in close agreement with the DLS

measurements. Also from the **Figure 7-3, D**, it can be concluded that self-assembled NPs (186 ± 3 nm) were formed with a narrow polydispersity (0.097) in distilled water at 100 µg/mL.

Figure 7-4 shows the average particle size of the NP at different pH from 3.0 to 8.0. The particle size was evaluated by DLS using 3 mL of the 100 µg/mL NP in VFS. The PEGylated PASP copolymer demonstrated its self-assembled nanostructure in VFS pH from 3.5 to 8.0, although the NP showed a larger particle size than 200 nm at a pH lower than 4.5 (406 nm at pH 4.0, 712 nm at pH 3.5) because of the pKa of the carboxylic acid (3.9) of the NP. According to the Henderson-Hasselbalch equation, 47.6% of the carboxylic acid is deprotonated at pH 3.5 and 11.3% of the carboxylic acid is deprotonated at pH 3.0. The particle size was increased near pH < pKa because the hydrophilic part of the PASP-PEG-Ph NP was becoming less hydrophilic by protonation of the carboxylic acid. Especially, charge repulsion prevents particle aggregation at pH above 4.5, but as the particles are neutralized, they are free to associate by H-bonding and van der Waal's interaction. The protonation of the carboxylic acid led to minor aggregation of the NPs, resulting in bigger particles at pH lower than the pKa. Although the carboxylic acid of the PASP-PEG-Ph was protonated at pH 3.9 to 3.0, the PASP-PEG-Ph maintained the self-assembled structure without precipitation because of the conjugated PEG. The nanocarrier is developed as an intravaginal nanocarrier which can be applied with intravaginal formulations such as intravaginal rings or vaginal gels. Size increase of the PASP-PEG-Ph NPs at pH lower than 4.5 could present synergistic effect when the NP is applied with nanoporous reservoir-IVRs. On-demand vaginal drug release is beneficial in terms of reducing side effects of drugs and minimizing off-target waste of drugs.[103]
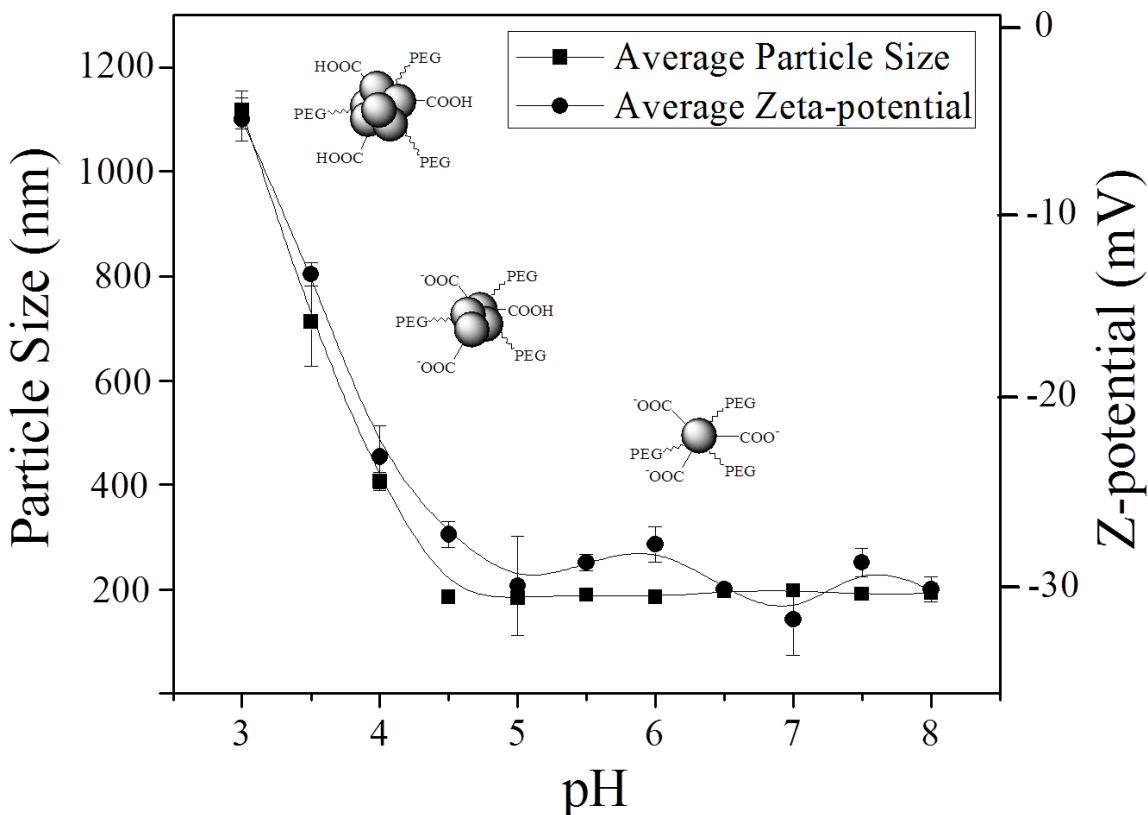
Figure 7-4. Average particle size (VFS, 100 µg/mL, n=3) and Zeta-potential (distilled water, 100 µg/mL, $n = 3$) of the PASP-PEG-Ph in various pH from 3.0 to 8.0.

Vaginal release of anti-HIV drug is needed most when heterosexual intercourse occurs. pH of the female genital tract can be elevated from its normal physiological pH around 4.2 to neutral during heterosexual intercourse due to the presence of seminal fluid. As a result, we can design a nanoporous reservoir-IVR with a cut-off pore size of 300 nm into which PASP-PEG-Ph NPs can be loaded. At normal conditions (pH 4.2), PASP-PEG-Ph NPs aggregate to give a size of > 300 nm (**Figure 7-4**; for the sake of convenience, size of PASP-PEG-Ph NPs without payload are used for discussion) and therefore cannot pass through the IVR, remaining in the

ring. As can be seen from the discussion below, payload release from NPs at acidic pH is much less than that at neutral pH. When pH rises to neutral because of heterosexual intercourse, PASP-PEG-Ph NPs disperse at a size of < 200 nm and therefore can be released from the IVR, leading to effective release of encapsulated payload to prevent infection.

Zeta-potential profile of the NP at different pH was evaluated (**Figure 7-4**). The NP showed negative zeta-potential values over the entire pH range from 3.0 to 8.0. The Zeta-potential changes dramatically with pH near the pKa of carboxylic acid (3.9). The average Z-potential of the PASP-PEG-Ph NP was -27.0 ± 0.7 at pH 4.5 and -32 ± 2 at pH 7.0. The zeta-potential of the NP well supports the above explanation of particle size change of the NP at different pH.

Physical stability of NPs in VFS at pH 4.5 and 7.0 at 37 °C was evaluated for 312 h (**Figure 7-5**). For the initial 72 h, the NPs appeared to be stable and had a diameter of around 200 nm at both pHs. However, at pH 7.0 the particle size was dramatically increased to 1 μm after 100 h. This size change of NPs at neutral pH may arise from the interaction of de-protonated carboxylic acid and contents of the VFS at pH 7.0. Also, BSA in VFS has low solubility at neutral pH. The BSA could affect the physicochemical stability of the NPs at neutral pH. Overall, the NP demonstrated its physical stability in size at pH 4.5 and pH 7.0 for 315 h and 72 h respectively. Good physical stability of PASP-PEG-Ph NP at pH 4.5 confirmed the suitability of the NP for intravaginal drug delivery since the normal pH range of human vaginal tract is 3.5-4.5.
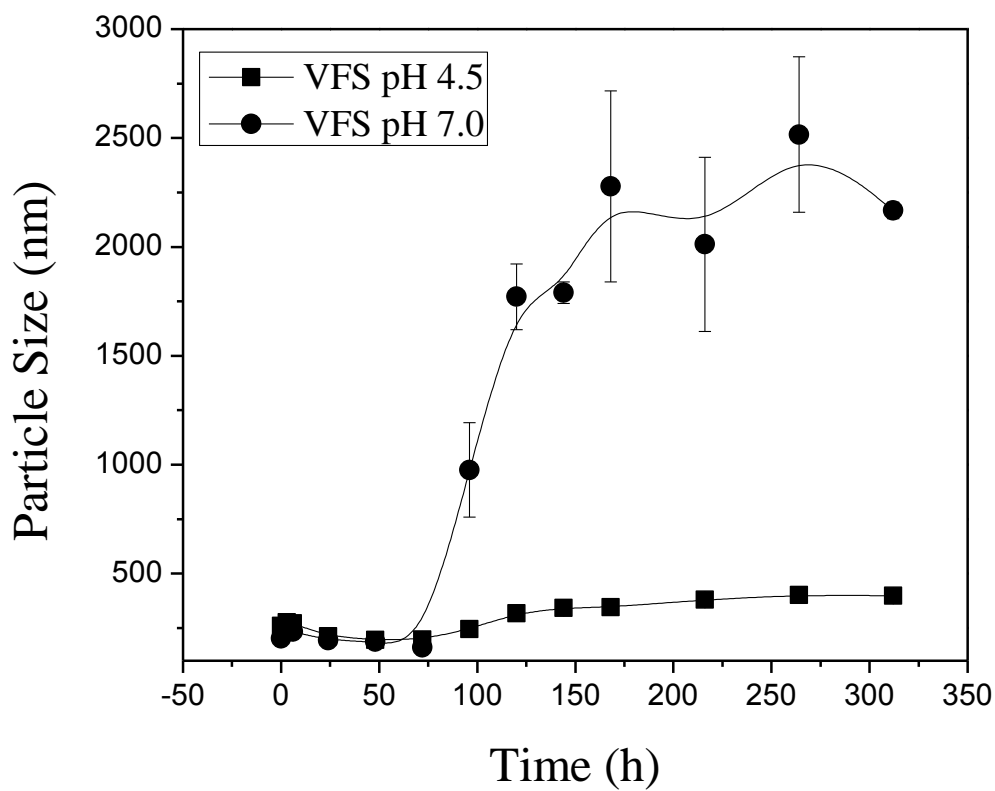
Figure 7-5. Physical stability of the PASP-PEG-Ph nanoparticles in VFS (pH 4.5, 7.0) at 37 °C ($n = 3$).

7.4.3 Model drug encapsulation and release studies

C6 is an excellent model drug for hydrophobic drugs because of its low solubility in water (0.25 µg/mL) and fluorescence for tracking.[236–239] C6 was used in this study as a hydrophobic model drug for the poorly water-soluble anti-HIV drugs especially non-nucleoside reverse transcriptase inhibitors such as efavirenz and etravirine because of their similarities in solubility (2.81 and 0.36 µg/mL at 25 °C), molecular weight, and chemical structure (having amines and hydrophobic ring structures). The C6-encapsulated NP (C6-NP) was prepared by a

solvent-casting method.[209,241] The hydrophobic model drug C6 was entrapped in the hydrophobic core of the NP by physicochemical interaction with the conjugated phenethylamine. Briefly, specific mass ratios of C6 and the PASP-PEG-Ph (**Table 7-2**) were dissolved in organic solvent dichloromethane to break the self-assembled structure of PASP-PEG-Ph NPs and mix them with C6. After the solvent had been evaporated, the dried thin film of C6 and PASP-PEG-Ph was dispersed by adding distilled water. The solution was put through a vortexing process and gently sonicated as mentioned in the experimental section. During the vortexing and sonication process, C6 was encapsulated in the core of PASP-PEG-Ph NPs and C6 encapsulated self-assembled NPs were formed.

Table 7-2. Loading content and hydrodynamic diameter of model drug C6 loaded nanoparticles (C6-NPs, $n = 3$).

	NP (mg/mL)	C6 (mg/mL)	C6 loading content (wt%)	C6 loading efficiency (%)	Size of C6 loaded NP (nm)	Zeta-potential of C6 loaded NP (mV)
C6-NP 5	1	0.05	4.6 ± 0.3	93 ± 6	323 ± 10	-22.4 ± 0.1
C6-NP 10	1	0.10	6.4 ± 0.3	64 ± 3	328 ± 30	-30 ± 4
C6-NP 20	1	0.20	7.8 ± 0.6	39 ± 3	353 ± 32	-34 ± 4
C6-NP 30	1	0.30	6 ± 2	18 ± 5	348 ± 29	-29 ± 3

C6 was loaded in the NP at the highest loading efficiency 93 ± 6% when the feed ratio of the C6 and PASP-PEG-Ph was 1: 0.05 (**Table 7-2**). At the concentration of 1 mg/mL, all C6 loaded NPs (C6NP 5-30, **Table 7-2**), at full liberation, could give a payload concentration much higher than the therapeutic concentration of efavirenz (1-4 µg/mL),[242] and therapeutic trough concentration of etravirine (0.55 µg/mL).[243] Among all the studied formulations, C6-NP 20 showed the highest C6 loading content (7.8 ± 0.6 wt%). Average particle size was increased

from 186 ± 3 nm to 338 ± 8 nm (average size of all C6-NPs: C6-NP 5-30) after loading the C6 because of the physicochemical influence of loaded C6. C6-NP 10 was chosen for further C6 release and *in vitro* cellular studies because it gave the most balanced loading content (6.4 ± 0.3%) and loading efficiency (64 ± 3%).
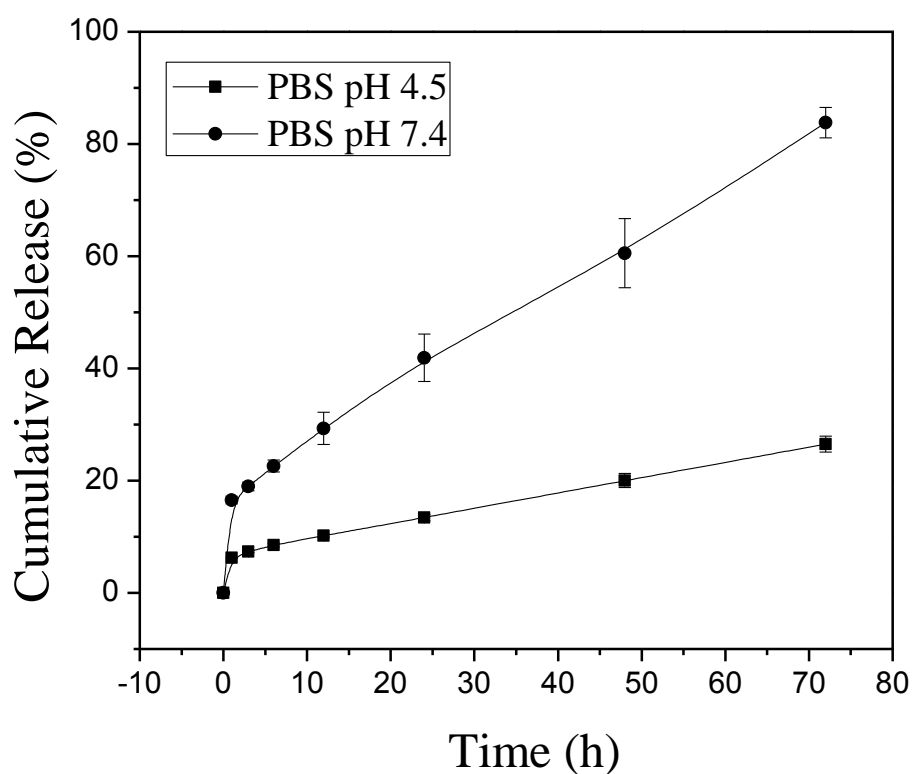
Figure 7-6. *In vitro* model drug release profile of the C6 encapsulated PASP-PEG-Ph NP in PBS at pH 7.4 (A) and pH 4.5 (B) using C6-NP 10 (*n* = 3).

C6-NP 10 was used for the *in vitro* drug release study. The model drug release profile was obtained by the membrane method (**Figure 7-6**).[244] C6-NP 10 was resuspended in PBS (at

pH 7.4 and 4.5) and added into a dialysis tubing. A non-ionic solubilizer and emulsifying agent, Kolliphor® HS 15, was used in the external medium (2 wt% of Kolliphor® HS 15 in PBS, pH 7.4, and 4.5). The released C6 diffused from the inside to the outside of the tubing and became dissolved in the release medium. The C6 release profile demonstrated sustained release of C6 from C6-NP 10. The results showed a burst release of C6 ($16.0 \pm 0.6\%$) within 3 h because of the relatively big difference of concentration between the inside and the outside of the membrane. However, after the burst release, the release of C6 was close to zero-order release and gradually released up to $83 \pm 3\%$ and $26 \pm 1\%$ of the entrapped drug at pH 7.4 and pH 4.5 over 72 h, respectively. At pH 7.4, C6-NP 10 released 3 times as much C6 ($83 \pm 3\%$) in comparison to release at pH 4.5 ($26 \pm 1\%$) because the hydrophobic interaction between the loaded drug and the amphiphilic nanocarrier became weaker at pH higher than the pKa of PASP (3.9).

7.4.4. *In vitro* cytotoxicity study

The MTS assay was adopted for the *in vitro* cell cytotoxicity study of the NP. Since vaginal drug delivery is the intended use of the newly developed nanocarriers, we chose VK2/E6E7 human vaginal epithelial cells for the evaluation of the biocompatibility of those nanocarriers. Sup-T1 cells were also chosen because they are the potential target for drug delivery. Various concentrations of empty NPs were applied to VK2/E6E7 and Sup-T1 cells. The viability of the VK2/E6E7 and Sup-T1 was evaluated after 24 h of the NP treatment in the enzymatic degradation time of poly(amino acid) to evaluate the cytotoxicity of the NPs including the effect of degradation products of the PASP-based copolymer. At all concentrations studied, the NP showed no cytotoxicity toward the Sup-T1 cell line and the NP showed very low cytotoxicity toward the VK2/E6E7 human vaginal epithelial cell as compared to positive control

(**Figure 7-7**). The results demonstrated that the NP is suitable for the proposed use as an intravaginal drug delivery carrier.
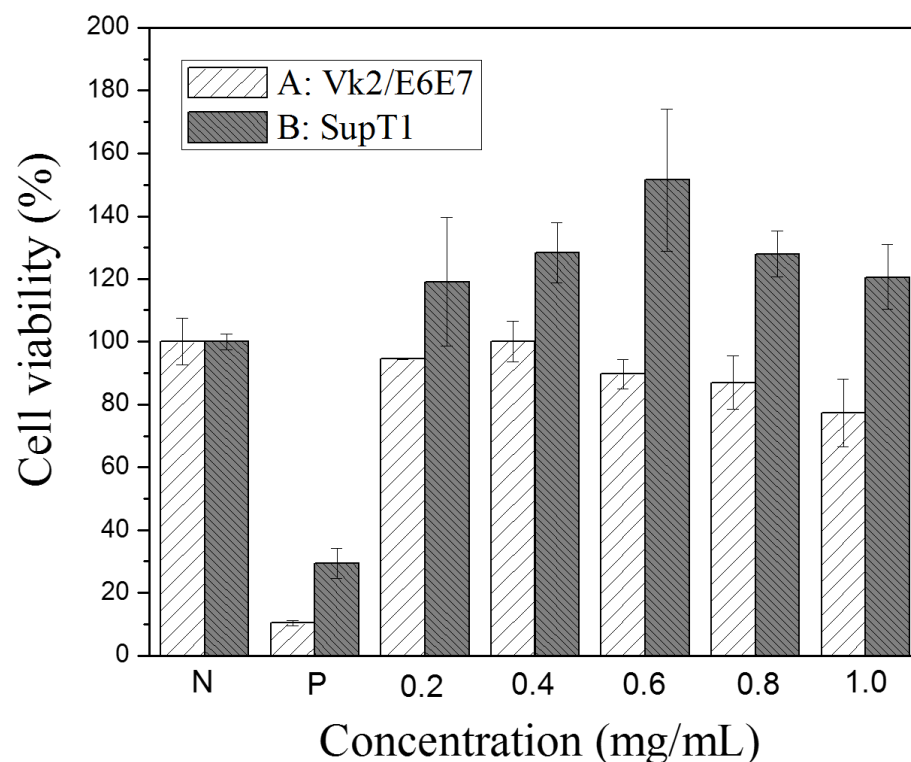
Figure 7-7. *In vitro* cell cytotoxicity of the PASP-PEG-Ph NPs toward Human vaginal epithelial cell VK2/E6E7 (A) and Human T-cell line Sup-T1 (B) ($n = 3$).

7.4.5 *In vitro* cellular uptake study

Anti-HIV drugs such as non-nucleoside reverse transcriptase inhibitors (efavirenz and etravirine) are considered the first exemplary drugs to be loaded into the newly developed nanocarriers for intravaginal delivery in our future studies. Non-nucleoside reverse transcriptase

inhibitors act inside of human T cells to block HIV transmission. It is therefore desirable to test whether C6-NPs can be internalized by T cells to potentially facilitate the therapeutic effect of the intended payloads. *In vitro* cellular uptake of the C6-NP 10 was examined using Sup-T1 cells (**Figure 7-8**).
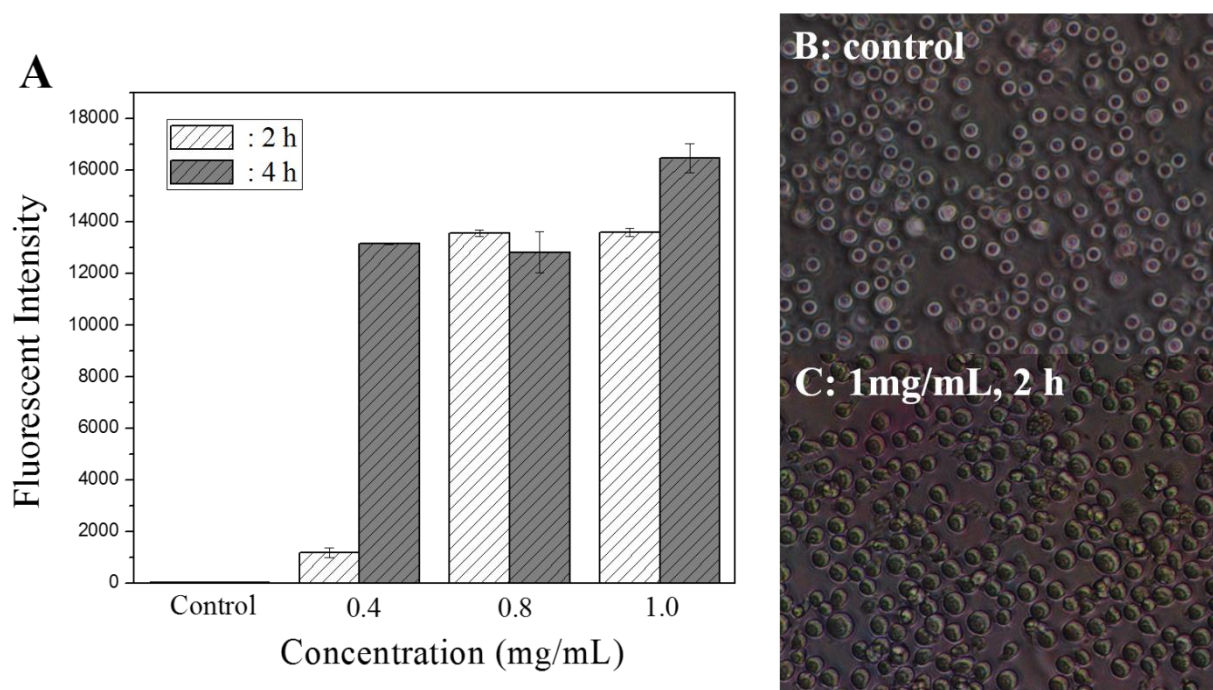
Figure 7-8. Cellular uptake of the C6-NP 10 by Sup-T1. (A) Fluorescent Intensity of C6-NP 10 uptake by Sup-T1, (B) Fluorescent microspore image of control at 2 h, (C) Fluorescent microspore image of 1mg/mL at 2 h. (after 2 h and 4 h treatment of different concentration of C6-NP 10, the images at magnification of 20 ×, $n = 3$.

The intracellular localization of C6 was investigated using flow cytometry and fluorescence microscopy. As can be seen from **Figure 7-8, A**, endocytosis of C6-NP 10 by Sup-T1 cells occurred after 2 h at the concentrations of 0.8 mg/mL and 1 mg/mL of C6-NP 10. At the

concentration of 0.4 mg/mL, C6-NP 10 became internalized by Sup-T1 cells after 4 hours. The fluorescence image (**Figure 7-8, B** and **C**) clearly showed intense green color inside the cells, indicating successful uptake of C6-NP 10 by Sup-T1 cells. Potentially, anti-HIV drugs such as efavirenz and etravirine can be delivered effectively inside Sup-T1 cells by the PASP-PEG-Ph NPs. To further increase the selectivity of the drug delivery, a target specific antibody could be conjugated on the surface of the NP using the carboxylic acid group.

7.5 Conclusions

The new amphiphilic PEGylated PASP graft copolymer was prepared as a nanocarrier for intravaginal delivery of poorly water-soluble drugs. The prepared nanoparticle showed an average particle size of 186 ± 3 nm (blank, in distilled water) and a successful model drug encapsulation efficiency of up to 93 ± 6% (323 ± 10 nm). The NPs maintained self-assembled nanostructure in VFS at pH 4.5 for 312 h and the average particle size was still smaller than 500 nm. The loaded model drug C6 showed sustained release in the *in vitro* release study. The model drug release study showed the slower release of the drug at pH 4.5 and faster release at pH 7.4. This result indicates the nanocarrier will continuously release a small amount of drug at normal vaginal pH and release an increased amount of drug at elevated pH by the presence of seminal fluid. This may not be desirable regarding the on-demand release. We may avoid the release of drug at pH 4.5 by increasing hydrophobic segment (phenethylamine) ratio of the PASP-PEG-Ph copolymer. The NP showed no cytotoxicity up to 1.0 mg/mL toward the human T-cell line Sup-T1 and low cytotoxicity at 1.0 mg/mL toward the VK2/E6E7 human vaginal epithelial cell. Moreover, cellular uptake of the C6-loaded NP by Sup-T1 was observed within 2 h. Overall, the

prepared PEGylated PASP NP successfully demonstrated its potential use as a carrier for intravaginal delivery of poorly water-soluble anti-HIV drugs.

7.6 Funding

7.7 Disclosure statement

No potential conflict of interest was reported by the authors.

7.8 Contribution of Authors

Seungil Kim[a]: initiated and contributed to the scope of the manuscript; performed synthesis and characterization of amphiphilic PEGylated poly(aspartic acid) copolymer (PASP-PEG-Ph); performed preparation of Coumarin 6-loaded NP (C6-NP); performed evaluation of *in vitro* model drug release; wrote the manuscript.

Yannick Leandre Traore[b]: performed *in vitro* cytotoxicity studies; performed *in vitro* cellular uptake test; contributed writing manuscript.

Jae Sang Lee[c]: performed synthesis of polysuccinimide (PSI).

Ji-Heung Kim[c]: contributed writing manuscript.

Emmanuel A Ho[a,b,*]: contributed writing manuscript; critically reviewed the manuscript.

Song Liu[a,d,e,*]: initiated and contributed to the scope of the manuscript; contributed writing manuscript; critically reviewed and revised the manuscript.

[a] Biomedical Engineering, Faculty of Engineering, University of Manitoba, Winnipeg, Manitoba, Canada

[b] Laboratory for Drug Delivery and Biomaterials, School of Pharmacy, University of Waterloo, Kitchener, Ontario, Canada

[c] School of Chemical Engineering, Sungkyunkwan University, Suwon, South Korea

[d] Department of Biosystems Engineering, Faculty of Agricultural and Food Sciences, University of Manitoba, Winnipeg, Manitoba, Canada

[e] Department of Chemistry, Faculty of Science, University of Manitoba, Winnipeg, Manitoba, Canada

References

(1)   Michel Sidibe. *Global Report: UNAIDS Report on the Global AIDS Epidemic 2012*; **2012**.

(2)   *WHO | HIV/AIDS*; World Health Organization, **2016**.

(3)   Morris, G. C.; Lacey, C. J. Microbicides and HIV Prevention: Lessons from the Past, Looking to the Future. *Curr. Opin. Infect. Dis.* **2010**, *23* (1), 57–63.

(4)   Hardy, E.; Hebling, E. M.; Sousa, M. H.; Almeida, A. F.; Amaral, E. Delivery of Microbicides to the Vagina: Difficulties Reported with the Use of Three Devices, Adherence to Use and Preferences. *Contraception* **2007**, *76* (2), 126–131.

(5)   Kiser, P. F.; Johnson, T. J.; Clark, J. T. State of the Art in Intravaginal Ring Technology for Topical Prophylaxis of HIV Infection. *AIDS Rev.* **2012**, *14* (1), 62–77.

(6)   Malcolm, R. K.; Edwards, K. L.; Kiser, P.; Romano, J.; Smith, T. J. Advances in Microbicide Vaginal Rings. *Antiviral Res.* **2010**, *88*, 30–39.

(7)   Barnhart, K. T.; Timbers, K.; Pretorius, E. S.; Lin, K.; Shaunik, A. In Vivo Assessment of NuvaRing Placement. *Contraception* **2005**, *72* (3), 196–199.

(8)   Novák, a.; De La Loge, C.; Abetz, L.; Van Der Meulen, E. a. The Combined Contraceptive Vaginal Ring, NuvaRing®: An International Study of User Acceptability. *Contraception* **2003**, *67* (3), 187–194.

(9)   Zhang, C.; Zhao, K.; Hu, T.; Cui, X.; Brown, N.; Boland, T. Loading Dependent Swelling and Release Properties of Novel Biodegradable, Elastic and Environmental Stimuli-Sensitive Polyurethanes. *J. Control. Release* **2008**, *131*, 128–136.

(10)   Zhang, C.; Wen, X.; Vyavahare, N. R.; Boland, T. Synthesis and Characterization of

Biodegradable Elastomeric Polyurethane Scaffolds Fabricated by the Inkjet Technique. *Biomaterials* **2008**, *29* (28), 3781–3791.

(11)　E. Kontou, G. Spathis, M. Niaounakis, V. K. D. Physical and Chemical Network Effects in Polyurethane Elastomers. *Colloid Polym. Sci.* **1990**, *268* (7), 636–644.

(12)　Gogolewski, S. Selected Topics in Biomedical Polyurethanes. A Review. *Colloid Polym. Sci.* **1989**, *267*, 757–785.

(13)　Born, L.; Hespe, H.; Crone, J.; Wolf, K. H. The Physical Crosslinking of Polyurethane Elastomers Studied by X-Ray Investigation of Model Urethanes. *Colloid Polym. Sci.* **1982**, *828*, 819–828.

(14)　Hoffman, A. S. The Origins and Evolution Of "controlled" drug Delivery Systems. *J. Control. Release* **2008**, *132* (3), 153–163.

(15)　Singh, R.; Lillard, J. W. Nanoparticle-Based Targeted Drug Delivery. *Exp. Mol. Pathol.* **2009**, *86* (3), 215–223.

(16)　Whitehead, K. A; Langer, R.; Anderson, D. G. Knocking down Barriers: Advances in siRNA Delivery. *Nat. Rev. Drug Discov.* **2009**, *8*, 129–138.

(17)　Lai, S. K.; Wang, Y. Y.; Hanes, J. Mucus-Penetrating Nanoparticles for Drug and Gene Delivery to Mucosal Tissues. *Adv. Drug Deliv. Rev.* **2009**, *61* (2), 158–171.

(18)　Campolongo, M. J.; Luo, D. Drug Delivery: Old Polymer Learns New Tracts. *Nat. Mater.* **2009**, *8* (6), 447–448.

(19)　Clavel, F.; Hance, A. J. HIV Drug Resistance. *N. Engl. J. Med.* **2004**, *350*, 1023–1035.

(20)　Voinnet, O. RNA Silencing as a Plant Immune System against Viruses. *Trends Genet.*

2001, *17* (8), 449–459.

(21)   Yang, S.; Chen, Y.; Ahmadie, R.; Ho, E. A. Advancements in the Field of Intravaginal

siRNA Delivery. *J. Control. Release* **2013**, *167*, 29–39.

(22)   Gu, J.; Yang, S.; Ho, E. A. Biodegradable Film for the Targeted Delivery of siRNA-

Loaded Nanoparticles to Vaginal Immune Cells. *Mol. Pharm.* **2015**, *12* (8), 2889–2903.

(23)   Johal, H. S.; Garg, T.; Rath, G.; Goyal, A. K. Advanced Topical Drug Delivery System

for the Management of Vaginal Candidiasis. *Drug Deliv.* **2016**, *23* (2), 550–563.

(24)   Bouvet, J. P.; Grésenguet, G.; Bélec, L. Vaginal pH Neutralization by Semen as a

Cofactor of HIV Transmission. *Clin. Microbiol. Infect.* **1997**, *3* (1), 19–23.

(25)   Gottlieb, S. L.; Low, N.; Newman, L. M.; Bolan, G.; Kamb, M.; Broutet, N. Toward

Global Prevention of Sexually Transmitted Infections (STIs): The Need for STI Vaccines.

Vaccine **2014**, *32* (14), 1527–1535.

(26)   Mamo, T.; Moseman, E. A.; Kolishetti, N.; Salvador-Morales, C.; Shi, J.; Kuritzkes, D.

R.; Langer, R.; Andrian, U. von; Farokhzad, O. C. Emerging Nanotechnology Approaches

for HIV/AIDS Treatment and Prevention. *Nanomedicine* **2010**, *5* (2), 269–285.

(27)   Christopoulos, K. A.; Olender, S.; Jaiswal, J.; Geng, E.; Koester, K. A. Retained in HIV

Care But Not on Antiretroviral Treatment: A Qualitative Patient-Provider Dyadic Study.

PLoS Med. **2015**, *12* (8), 1–19.

(28)   Deeks, S. G.; Lewin, S. R.; Havlir, D. V. The End of AIDS: HIV Infection as a Chronic

Disease. *Lancet* **2013**, *382* (9903), 1525–1533.

(29)   Saxena, B. B.; Han, Y.; Fu, D.; Rathnam, P.; Singh, M.; Laurence, J.; Lerner, S. Sustained

Release of Microbicides by Newly Engineered Vaginal Rings. *AIDS* **2009**, *23*, 917–922.

(30) De Clercq, E. Anti-HIV Drugs: 25 Compounds Approved within 25 Years after the Discovery of HIV. *Int. J. Antimicrob. Agents* **2009**, *33* (4), 307–320.

(31) Sharma, P.; Garg, S. Pure Drug and Polymer Based Nanotechnologies for the Improved Solubility, Stability, Bioavailability and Targeting of Anti-HIV Drugs. *Adv. Drug Deliv. Rev.* **2010**, *62* (4–5), 491–502.

(32) Singh Malik, D.; Mital, N.; Kaur, G. Topical Drug Delivery Systems: A Patent Review. *Expert Opin. Ther. Pat.* **2016**, *26* (2), 213–228.

(33) Owen, D. H.; Katz, D. F. A Review of the Physical and Chemical Properties of Human Semen and the Formulation of a Semen Simulant. *J. Androl.* **2005**, *26(1)* (4), 459–469.

(34) Carias, A. M.; McCoombe, S.; McRaven, M.; Anderson, M.; Galloway, N.; Vandergrift, N.; Fought, A. J.; Lurain, J.; Duplantis, M.; Veazey, R. S.; Hope, T. J. Defining the Interaction of HIV-1 with the Mucosal Barriers of the Female Reproductive Tract. *J. Virol.* **2013**, *87* (21), 11388–11400.

(35) Hussain, A.; Ahsan, F. The Vagina as a Route for Systemic Drug Delivery. *J. Control. Release* **2005**, *103* (2), 301–313.

(36) Srikrishna, S.; Cardozo, L. The Vagina as a Route for Drug Delivery: A Review. *Int. Urogynecol. J.* **2013**, *24* (4), 537–543.

(37) Bendas, E. R.; Basalious, E. B. Rapidly Disintegrating Vagina Retentive Cream Suppositories of Progesterone: Development, Patient Satisfaction and in Vitro / in Vivo Studies. *Pharm. Dev. Technol.* **2016**, *21* (3), 288–295.

(38) Karim, Q. A.; Karim, S. S. A.; Frohlich, J. A.; Grobler, A. C.; Baxter, C.; Mansoor, L. E.; Kharsany, A. B. M.; Sibeko, S.; Mlisana, K. P.; Omar, Z.; Gengiah, T. N.; Maarschalk, S.;

Arulappan, N.; Mlotshwa, M.; Morris, L.; Taylor, D.; Trial, C. Effectiveness and Safety of Tenofovir Gel, an Antiretroviral Microbicide, for the Prevention of HIV Infection in Women. *Science.* **2010**, *329* (5996), 1168–1174.

(39)   Ho, E. A. Intravaginal Rings as a Novel Platform for Mucosal Vaccination. *J. Mol. Pharm. Org. Process Res.* **2013**, *1* (2), 1–2.

(40)   Johnson, T. J.; Gupta, K. M.; Fabian, J.; Albright, T. H.; Kiser, P. F. Segmented Polyurethane Intravaginal Rings for the Sustained Combined Delivery of Antiretroviral Agents Dapivirine and Tenofovir. *Eur. J. Pharm. Sci.* **2010**, *39*, 203–212.

(41)   Friend, D. R.; Doncel, G. F. Combining Prevention of HIV-1, Other Sexually Transmitted Infections and Unintended Pregnancies: Development of Dual-Protection Technologies. *Antiviral Res.* **2010**, *88*, 47–54.

(42)   Kaur, M.; Gupta, K. M.; Poursaid, A. E.; Karra, P.; Mahalingam, A.; Aliyar, H. A.; Kiser, P. F. Engineering a Degradable Polyurethane Intravaginal Ring for Sustained Delivery of Dapivirine. *Drug Deliv. Transl. Res.* **2011**, *1* (3), 223–237.

(43)   Kim, S.; Traore, Y. L.; Lee, J. S.; Kim, J.-H.; Ho, E. A.; Liu, S. Self-Assembled Nanoparticles Made from a New PEGylated Poly(aspartic Acid) Graft Copolymer for Intravaginal Delivery of Poorly Water-Soluble Drugs. *J. Biomater. Sci. Polym. Ed.* **2017**, *28* (17), 2082–2099.

(44)   Jiang, Y.; Cao, S.; Bright, D. K.; Bever, A. M.; Blakney, A. K.; Suydam, I. T.; Woodrow, K. A. Nanoparticle-Based ARV Drug Combinations for Synergistic Inhibition of Cell-Free and Cell-Cell HIV Transmission. *Mol. Pharm.* **2015**, *12* (12), 4363–4374.

(45)   Mahajan, S. D.; Aalinkeel, R.; Law, W. C.; Prasad, P. N.; Schwartz, S. A. Anti-HIV-1

Nanotherapeutics: Promises and Challenges for the Future. *Int. J. Nanomedicine* **2012**, *7*, 5301–5314.

(46)   Santerre, J. P.; Woodhouse, K.; Laroche, G.; Labow, R. S. Understanding the Biodegradation of Polyurethanes: From Classical Implants to Tissue Engineering Materials. *Biomaterials* **2005**, *26* (35), 7457–7470.

(47)   Tsui, Y. K.; Gogolewski, S. Microporous Biodegradable Polyurethane Membranes for Tissue Engineering. *J. Mater. Sci. Mater. Med.* **2009**, *20*, 1729–1741.

(48)   Guelcher, S. A. Biodegradable Polyurethanes: Synthesis and Applications in Regenerative Medicine. *Tissue Eng. Part B. Rev.* **2008**, *14* (1), 3–17.

(49)   Detta, N.; Errico, C.; Dinucci, D.; Puppi, D.; Clarke, D. A.; Reilly, G. C.; Chiellini, F. Novel Electrospun Polyurethane/gelatin Composite Meshes for Vascular Grafts. *J. Mater. Sci. Mater. Med.* **2010**, *21* (5), 1761–1769.

(50)   Hasan, A.; Memic, A.; Annabi, N.; Hossain, M.; Paul, A.; Dokmeci, M. R.; Dehghani, F.; Khademhosseini, A. Electrospun Scaffolds for Tissue Engineering of Vascular Grafts. *Acta Biomater.* **2014**, *10* (1), 11–25.

(51)   Dayananda, K.; He, C.; Lee, D. S. In Situ Gelling Aqueous Solutions of pH- and Temperature-Sensitive Poly(ester Amino Urethane)s. *Polymer (Guildf).* **2008**, *49*, 4620–4625.

(52)   Dayananda, K.; He, C.; Park, D. K.; Park, T. G.; Lee, D. S. pH- and Temperature-Sensitive Multiblock Copolymer Hydrogels Composed of Poly(ethylene Glycol) and Poly(amino Urethane). *Polymer (Guildf).* **2008**, *49* (23), 4968–4973.

(53)   Yu, S.; He, C.; Ding, J.; Zhuang, X.; Chen, X. pH and Reduction Dual Responsive

Polyurethane Triblock Copolymers for Efficient Intracellular Drug Delivery. *Soft Matter* **2013**, *9* (9), 2637–2645.

(54) Sivakumar, C.; Nasar, A. S. Poly(ε-Caprolactone)-Based Hyperbranched Polyurethanes Prepared via A2 + B3 Approach and Its Shape-Memory Behavior. *Eur. Polym. J.* **2009**, *45* (8), 2329–2337.

(55) Shumaker, J. A.; McClung, A. J. W.; Baur, J. W. Synthesis of High Temperature Polyaspartimide-Urea Based Shape Memory Polymers. *Polymer (Guildf).* **2012**, *53* (21), 4637–4642.

(56) Singhal, P.; Rodriguez, J. N.; Small, W.; Eagleston, S.; Van de Water, J.; Maitland, D. J.; Wilson, T. S. Ultra Low Density and Highly Crosslinked Biocompatible Shape Memory Polyurethane Foams. *J. Polym. Sci. Part B Polym. Phys.* **2012**, *50* (10), 724–737.

(57) Miyazu, K.; Kawahara, D.; Ohtake, H.; Watanabe, G.; Matsuda, T. Luminal Surface Design of Electrospun Small-Diameter Graft Aiming at in Situ Capture of Endothelial Progenitor Cell. *J. Biomed. Mater. Res. - Part B Appl. Biomater.* **2010**, *94* (1), 53–63.

(58) Zhou, H.; Xun, R.; Liu, Q.; Fan, H.; Liu, Y. Preparation of Thermal and pH Dually Sensitive Polyurethane Membranes and Their Properties. *J. Macromol. Sci. Part B* **2014**, *53*, 398–411.

(59) Zhao, C.; Nie, S.; Tang, M.; Sun, S. Polymeric pH-Sensitive membranes—A Review. *Prog. Polym. Sci.* **2011**, *36* (11), 1499–1520.

(60) Zhou, L.; Liang, D.; Li, J.; Fu, Q.; Gu, Q. The Degradation and Biocompatibility of pH-Sensitive Biodegradable Polyurethanes for Intracellular Multifunctional Antitumor Drug Delivery. *Biomaterials* **2012**, *33* (9), 2734–2745.

(61)   Lu, Y.; Aimetti, A. A.; Langer, R.; Gu, Z. Bioresponsive Materials. *Nat. Rev. Mater.*
        2016, *2* (1).

(62)   Addington, M.; Schodek, D. L. *Smart Materials and New Technologies : For the*
        Architecture and Design Professions, 1st ed.; Architectural, 2005.

(63)   Wang, F.; Li, Z.; Lannutti, J. L.; Wagner, W. R.; Guan, J. Synthesis, Characterization and
        Surface Modification of Low Moduli Poly(ether Carbonate Urethane)ureas for Soft Tissue
        Engineering. *Acta Biomater.* **2009**, *5* (8), 2901–2912.

(64)   Stankus, J.; Hossainy, S. F. A.; Wan, J. Process of Making a Tubular Implantable Medical
        Device. US7824601, 2010.

(65)   Gu, L.; Wang, X.; Chen, X.; Zhao, X.; Wang, F. Thermal and pH Responsive High
        Molecular Weight Poly(urethane-Amine) with High Urethane Content. *J. Polym. Sci. Part*
        A Polym. Chem. **2011**, *49*, 5162–5168.

(66)   Wandera, D.; Wickramasinghe, S. R.; Husson, S. M. Stimuli-Responsive Membranes. *J.*
        Memb. Sci. **2010**, *357*, 6–35.

(67)   Wu, W.; Zhu, Q.; Qing, F.; Han, C. C. Water Repellency on a Fluorine-Containing
        Polyurethane Surface: Toward Understanding the Surface Self-Cleaning Effect. *Langmuir*
        2009, *25* (1), 17–20.

(68)   Zheng, J.; Song, W.; Huang, H.; Chen, H. Protein Adsorption and Cell Adhesion on
        polyurethane/Pluronic® Surface with Lotus Leaf-like Topography. *Colloids Surfaces B*
        Biointerfaces **2010**, *77* (2), 234–239.

(69)   Zdrahala, R. J.; Zdrahala, I. J. Biomedical Application of Polyurethanes: A Review of Past
        Promises, Present Realities, and a Vibrant Future. *J. Biomater. Appl.* **1999**, *14*, 67–90.

(70)   Huang, W. M.; Yang, B.; Zhao, Y.; Ding, Z. Thermo-Moisture Responsive Polyurethane Shape-Memory Polymer and Composites: A Review. *J. Mater. Chem.* **2010**, *20* (17), 3367.

(71)   Sun, L.; Huang, W. M.; Ding, Z.; Zhao, Y.; Wang, C. C.; Purnawali, H.; Tang, C. Stimulus-Responsive Shape Memory Materials: A Review. *Mater. Des.* **2012**, *33*, 577–640.

(72)   Kim, S. Y.; Lee, T. H.; Park, Y. Il; Nam, J. H.; Noh, S. M.; Cheong, I. W.; Kim, J. C. Influence of Material Properties on Scratch-Healing Performance of Polyacrylate- Graft - Polyurethane Network That Undergo Thermally Reversible Crosslinking. *Polymer (Guildf).* **2017**, *128*, 135–146.

(73)   Aguilar, L. E.; GhavamiNejad, A.; Park, C. H.; Kim, C. S. On-Demand Drug Release and Hyperthermia Therapy Applications of Thermoresponsive Poly-(NIPAAm-Co-HMAAm)/polyurethane Core-Shell Nanofiber Mat on Non-Vascular Nitinol Stents. *Nanomedicine Nanotechnology, Biol. Med.* **2017**, *13* (2), 527–538.

(74)   Serrano, M. C.; Carbajal, L.; Ameer, G. A. Novel Biodegradable Shape-Memory Elastomers with Drug-Releasing Capabilities. *Adv. Mater.* **2011**, *23* (19), 2211–2215.

(75)   Zhao, X.; Dong, R.; Guo, B.; Ma, P. X. Dopamine-Incorporated Dual Bioactive Electroactive Shape Memory Polyurethane Elastomers with Physiological Shape Recovery Temperature, High Stretchability, and Enhanced C2C12 Myogenic Differentiation. *ACS Appl. Mater. Interfaces* **2017**, *9* (35), 29595–29611.

(76)   Theron, J. P.; Knoetze, J. H.; Sanderson, R. D.; Hunter, R.; Mequanint, K.; Franz, T.; Zilla, P.; Bezuidenhout, D. Modification, Crosslinking and Reactive Electrospinning of a

Thermoplastic Medical Polyurethane for Vascular Graft Applications. *Acta Biomater.* **2010**, *6* (7), 2434–2447.

(77) Sinh, L. H.; Harri, K.; Marjo, L.; Minna, M.; Luong, N. D.; Jürgen, W.; Torsten, W.; Matthias, S.; Jukka, S. Novel Photo-Curable Polyurethane Resin for Stereolithography. *RSC Adv.* **2016**, *6* (56), 50706–50709.

(78) Wang, L.; Yang, X.; Chen, H.; Gong, T.; Li, W.; Yang, G.; Zhou, S. Design of Triple-Shape Memory Polyurethane with Photo-Cross-Linking of Cinnamon Groups. *ACS Appl. Mater. Interfaces* **2013**, *5* (21), 10520–10528.

(79) Yang, J.; Wen, H.; Zhuo, H.; Chen, S.; Ban, J. A New Type of Photo-Thermo Staged-Responsive Shape-Memory Polyurethanes Network. *Polymers (Basel).* **2017**, *9* (7), 287.

(80) Xu, H.; Ning, H.; Chen, Y.; Fan, H.; Shi, B. Sulfanilamide-Conjugated Polyurethane Coating with Enzymatically-Switchable Antimicrobial Capability for Leather Finishing. *Prog. Org. Coatings* **2013**, *76* (5), 924–934.

(81) Bezuidenhout, D.; Davies, N.; Black, M.; Schmidt, C.; Oosthuysen, A.; Zilla, P. Covalent Surface Heparinization Potentiates Porous Polyurethane Scaffold Vascularization. *J. Biomater. Appl.* **2010**, *24* (5), 401–418.

(82) Dadsetan, M.; Jones, J. A.; Hiltner, A.; Anderson, J. M. Surface Chemistry Mediates Adhesive Structure, Cytoskeletal Organization, and Fusion of Macrophages. *J. Biomed. Mater. Res. - Part A* **2004**, *71*, 439–448.

(83) Matheson, L. A.; Labow, R. S.; Santerre, J. P. Biodegradation of Polycarbonate-Based Polyurethanes by the Human Monocyte-Derived Macrophage and U937 Cell Systems. *J. Biomed. Mater. Res.* **2002**, *61* (4), 505–513.

(84) Labow, R. S.; Meek, E.; Matheson, L. a; Santerre, J. P. Human Macrophage-Mediated Biodegradation of Polyurethanes: Assessment of Candidate Enzyme Activities. *Biomaterials* **2002**, *23* (19), 3969–3975.

(85) Tang, Y. W.; Labow, R. S.; Santerre, J. P. Enzyme-Induced Biodegradation of Polycarbonate-Polyurethanes: Dependence on Hard-Segment Chemistry. *J. Biomed. Mater. Res.* **2001**, *57* (4), 597–611.

(86) Chandy, T.; Van Hee, J.; Nettekoven, W.; Johnson, J. Long-Term in Vitro Stability Assessment of Polycarbonate Urethane Micro Catheters: Resistance to Oxidation and Stress Cracking. *J. Biomed. Mater. Res. B. Appl. Biomater.* **2009**, *89* (2), 314–324.

(87) Xie, X.; Tan, H.; Li, J.; Zhong, Y. Synthesis and Characterization of Fluorocarbon Chain End-Capped Poly(carbonate Urethane)s as Biomaterials: Anovel Bilayered Surface Structure. *J. Biomed. Mater. Res. A* **2008**, *84A* (1), 30–43.

(88) Andriani, Y.; Morrow, I. C.; Taran, E.; Edwards, G. A.; Schiller, T. L.; Osman, A. F.; Martin, D. J. In Vitro Biostability of Poly(dimethyl Siloxane/hexamethylene Oxide)-Based Polyurethane/layered Silicate Nanocomposites. *Acta Biomater.* **2013**, *9* (9), 8308–8317.

(89) Styan, K. E.; Martin, D. J.; Simmons, A.; Poole-Warren, L. A. In Vivo Biostability of Polyurethane-Organosilicate Nanocomposites. *Acta Biomater.* **2012**, *8* (6), 2243–2253.

(90) Jewrajka, S. K.; Yilgor, E.; Yilgor, I.; Kennedy, J. P. Polyisobutylene-Based Segmented Polyureas. I. Synthesis of Hydrolytically and Oxidatively Stable Polyureas. *J. Polym. Sci. Part a-Polymer Chem.* **2009**, *47* (11), 38–48.

(91) Erdodi, G.; Kang, J.; Kennedy, J. P. Polyisobutylene-Based Polyurethanes. VI.

Unprecedented Combination of Mechanical Properties and Oxidative/Hydrolytic Stability by H-Bond Acceptor Chain Extenders. *J. Polym. Sci. Part A-Polymer Chem.* **2009**, *47* (11), 2361–2371.

(92)   Kang, J.; Erdodi, G.; Brendel, C. M.; Ely, D.; Kennedy, J. P. Polyisobutylene-Based Polyurethanes. V. Oxidative-Hydrolytic Stability and Biocompatibility. *J. Polym. Sci. Part A Polym. Chem.* **2010**, *48* (10), 2194–2203.

(93)   Erdodi, G.; Kang, J.; Kennedy, J. P.; Yilgor, E.; Yilgor, I. Polyisobutylene-Based Polyurethanes. III. Polyurethanes Containing PIB/PTMO Soft Co-Segments. *J. Polym. Sci. Part A-Polymer Chem.* **2009**, *20*, 5278–5290.

(94)   Jewrajka, S. K.; Kang, J.; Erdodi, G.; Kennedy, J. P.; Yilgor, E.; Yilgor, I. Polyisobutylene-Based Polyurethanes. II. Polyureas Containing Mixed PIB/PTMO Soft Segments. *J. Polym. Sci. Part A-Polymer Chem.* **2009**, *47* (11), 2787–2797.

(95)   Kang, J.; Erdodi, G.; Kennedy, J. P.; Yilgor, E.; Yilgor, I. PIB-Based Polyurethanes. IV. The Morphology of Polyurethanes Containing Soft Co-Segments. *J. Polym. Sci. Part A-Polymer Chem.* **2009**, *47* (22), 6180–6190.

(96)   Ojha, U.; Kulkarni, P.; Faust, R. Syntheses and Characterization of Novel Biostable Polyisobutylene Based Thermoplastic Polyurethanes. *Polymer (Guildf).* **2009**, *50* (15), 3448–3457.

(97)   Cozzens, D.; Ojha, U.; Kulkarni, P.; Faust, R.; Desai, S. Long Term in Vitro Biostability of Segmented Polyisobutylene-Based Thermoplastic Polyurethanes. *J. Biomed. Mater. Res. - Part A* **2010**, *95*, 774–782.

(98)   Cozzens, D.; Luk, A.; Ojha, U.; Ruths, M.; Faust, R. Surface Characterization and Protein

Interactions of Segmented Polyisobutylene-Based Thermoplastic Polyurethanes. *Langmuir* **2011**, *27* (23), 14160–14168.

(99)   Cozzens, D.; Wei, X.; Faust, R. Electrospinning of Biostable Polyisobutylene-Based Thermoplastic Polyurethanes. *J. Polym. Sci. Part B Polym. Phys.* **2013**, *51*, 452–459.

(100) Rosenberg, Z. F.; Devlin, B. Future Strategies in Microbicide Development. *Best Pract. Res. Clin. Obstet. Gynaecol.* **2012**, *26* (4), 503–513.

(101) Friend, D. R. Intravaginal Rings: Controlled Release Systems for Contraception and Prevention of Transmission of Sexually Transmitted Infections. *Drug Deliv. Transl. Res.* **2011**, *1* (3), 185–193.

(102) Kuo, S.; Kuzma, P. Long Term Drug Delivery Devices with Polyurethane Based Polymers and Their Manufacture. US7842303, 2010.

(103) Kim, S.; Chen, Y.; Ho, E. A.; Liu, S. Reversibly pH-Responsive Polyurethane Membranes for On-Demand Intravaginal Drug Delivery. *Acta Biomater.* **2017**, *47*, 100–112.

(104) Owen, D. H.; Katz, D. F. A Vaginal Fluid Simulant. *Contraception* **1999**, *59* (2), 91–95.

(105) Huang, C.; Soenen, S. J.; van Gulck, E.; Vanham, G.; Rejman, J.; Van Calenbergh, S.; Vervaet, C.; Coenye, T.; Verstraelen, H.; Temmerman, M.; Demeester, J.; De Smedt, S. C. Electrospun Cellulose Acetate Phthalate Fibers for Semen Induced Anti-HIV Vaginal Drug Delivery. *Biomaterials* **2012**, *33* (3), 962–969.

(106) Clark, M. R.; Johnson, T. J.; McCabe, R. T.; Elgendy, H.; Friend, D. R.; Kiser, P. F. A Hot-Melt Extruded Intravaginal Ring for the Sustained Delivery of the Antiretroviral Microbicide UC781. *J. Pharm. Sci.* **2012**, *101* (2), 576–587.

(107) Clark, J. T.; Johnson, T. J.; Clark, M. R.; Nebeker, J. S.; Friend, D. R.; Kiser, P. F.

Quantitative Evaluation of a Hydrophilic Matrix Intravaginal Ring for the Sustained Delivery of Tenofovir. *J. Control. Release* **2012**, *163* (2), 240–248.

(108) Mesquita, P. M. M.; Rastogi, R.; Segarra, T. J.; Teller, R. S.; Torres, N. M.; Huber, A. M.; Kiser, P. F.; Herold, B. C. Intravaginal Ring Delivery of Tenofovir Disoproxil Fumarate for Prevention of HIV and Herpes Simplex Virus Infection. *J. Antimicrob. Chemother.* **2012**, *67*, 1730–1738.

(109) Smith, J. M.; Rastogi, R.; Teller, R. S.; Herold, B. C.; Kiser, P. F. Intravaginal Ring Eluting Tenofovir Disoproxil Fumarate Completely Protects Macaques from Multiple Vaginal Simian-HIV Challenges. *Proc. Natl. Acad. Sci. U. S. A.* **2013**, *110* (40), 16145–16150.

(110) Johnson, T. J.; Srinivasan, P.; Albright, T. H.; Watson-Buckheit, K.; Rabe, L.; Martin, A.; Pau, C. P.; Hendry, R. M.; Otten, R.; McNicholl, J.; Buckheit, R.; Smith, J.; Kiser, P. F. Safe and Sustained Vaginal Delivery of Pyrimidinedione HIV-1 Inhibitors from Polyurethane Intravaginal Rings. *Antimicrob. Agents Chemother.* **2012**, *56* (3), 1291–1299.

(111) Johnson, T. J.; Clark, M. R.; Albright, T. H.; Nebeker, J. S.; Tuitupou, A. L.; Clark, J. T.; Fabian, J.; McCabe, R. T.; Chandra, N.; Doncel, G. F.; Friend, D. R.; Kiser, P. F. A 90-Day Tenofovir Reservoir Intravaginal Ring for Mucosal HIV Prophylaxis. *Antimicrob. Agents Chemother.* **2012**, *56* (12), 6272–6283.

(112) Clark, J. T.; Clark, M. R.; Shelke, N. B.; Johnson, T. J.; Smith, E. M.; Andreasen, A. K.; Nebeker, J. S.; Fabian, J.; Friend, D. R.; Kiser, P. F. Engineering a Segmented Dual-Reservoir Polyurethane Intravaginal Ring for Simultaneous Prevention of HIV

Transmission and Unwanted Pregnancy. *PLoS One* **2014**, *9* (3), 1–14.

(113) Chen, Y.; Traore, Y. L.; Li, A.; Fowke, K. R.; Ho, E. A. Development of Polyether Urethane Intravaginal Rings for the Sustained Delivery of Hydroxychloroquine. *Drug Des. Devel. Ther.* **2014**, *8*, 1801–1815.

(114) Traore, Y. L.; Chen, Y.; Bernier, A.-M.; Ho, E. A. Evaluating the Impact of Hydroxychloroquine-Loaded Polyurethane Intravaginal Rings on Lactobacilli. *Antimicrob. Agents Chemother.* **2015**, *59* (12), 7680–7686.

(115) Lalatsa, A.; Schätzlein, A. G.; Mazza, M.; Le, T. B. H.; Uchegbu, I. F. Amphiphilic Poly(l-Amino Acids) - New Materials for Drug Delivery. *J. Control. Release* **2012**, *161* (2), 523–536.

(116) Xu, H.; Yao, Q.; Cai, C.; Gou, J.; Zhang, Y.; Zhong, H.; Tang, X. Amphiphilic Poly(amino Acid) Based Micelles Applied to Drug Delivery: The in Vitro and in Vivo Challenges and the Corresponding Potential Strategies. *J. Control. Release* **2015**, *199*, 84–97.

(117) Akagi, T.; Higashi, M.; Kaneko, T.; Kida, T.; Akashi, M. Hydrolytic and Enzymatic Degradation of Nanoparticles Based on Amphiphilic Poly(γ-Glutamic Acid)-Graft-L-Phenylalanine Copolymers. *Biomacromolecules* **2006**, *7* (1), 297–303.

(118) Wang, X.; Uto, T.; Akagi, T.; Akashi, M. Poly(γ-Glutamic Acid) Nanoparticles as an Efficient Antigen Delivery and Adjuvant System: Potential for an AIDS Vaccine. *J. Med. Virol.* **2008**, *80*, 11–19.

(119) Akagi, T.; Kaneko, T.; Kida, T.; Akashi, M. Preparation and Characterization of Biodegradable Nanoparticles Based on Poly(γ-Glutamic Acid) with L-Phenylalanine as a

Protein Carrier. *J. Control. Release* **2005**, *108* (2–3), 226–236.

(120) Kim, S.; Son, C. M.; Jeon, Y. S.; Kim, J. H. Characterizations of Novel Poly(aspartic Acid) Derivatives Conjugated with γ-Amino Butyric Acid (GABA) as the Bioactive Molecule. *Bull. Korean Chem. Soc.* **2009**, *30* (12), 3025–3030.

(121) Kim, J. H.; Son, C. M.; Jeon, Y. S.; Choe, W. S. Synthesis and Characterization of Poly(aspartic Acid) Derivatives Conjugated with Various Amino Acids. *J. Polym. Res.* **2011**, *18* (5), 881–890.

(122) Kim, S. Il; Min, S. K.; Kim, J. H. Synthesis and Characterization of Novel Amino Acid-Conjugated Poly(aspartic Acid) Derivatives. *Bull. Korean Chem. Soc.* **2008**, *29* (10), 1887–1892.

(123) Nakato, T.; Tomida, M.; Suwa, M.; Morishima, Y.; Kusuno, A.; Kakuchi, T. Preparation and Characterization of Dodecylamine-Modified Poly(aspartic Acid) as a Biodegradable Water-Soluble Polymeric Material. *Polym. Bull.* **2000**, *44*, 385–391.

(124) Kang, H. S.; Shin, M.-S.; Kim, J.-D.; Yang, J.-W. Self-Aggregates of Poly(aspartic Acid) Grafted with Long Alkyl Chains. *Polym. Bull.* **2000**, *45*, 39–43.

(125) Kang, H. S.; Yang, S. R.; Kim, J. D.; Han, S. H.; Chang, I. S. Effects of Grafted Alkyl Groups on Aggregation Behavior of Amphiphilic Poly(aspartic Acid). *Langmuir* **2001**, *17* (8), 7501–7506.

(126) Jiang, T. Y.; Wang, Z. Y.; Tang, L. X.; Mo, F. K.; Chen, C. Polymer Micellar Aggregates of Novel Amphiphilic Biodegradable Graft Copolymer Composed of Poly(aspartic Acid) Derivatives: Preparation, Characterization, and Effect of pH on Aggregation. *J. Appl. Polym. Sci.* **2006**, *99*, 2702–2709.

(127) Jiang, T. Y.; Wang, Z. Y.; Chen, C.; Mo, F. K.; Xu, Y. L.; Tang, L. X.; Liang, J. J. Poly(aspartic-Acid) Derivatives as Polymeric Micelle Drug Delivery Systems. *J. Appl. Polym. Sci.* **2006**, *101*, 2871–2878.

(128) Jeong, J. H.; Kang, H. S.; Yang, S. R.; Kim, J. D. Polymer Micelle-like Aggregates of Novel Amphiphilic Biodegradable Poly(asparagine) Grafted with Poly(caprolactone). *Polymer (Guildf).* **2002**, *44* (3), 583–591.

(129) Rastogi, R.; Teller, R. S.; Mesquita, P. M. M.; Herold, B. C.; Kiser, P. F. Osmotic Pump Tablets for Delivery of Antiretrovirals to the Vaginal Mucosa. *Antiviral Res.* **2013**, *100* (1), 255–258.

(130) Tevi-Benissan, C.; Belec, L.; Levy, M.; Schneider-Fauveau, V.; Si Mohamed, A.; Hallouin, M. C.; Matta, M.; Gresenguet, G. In Vivo Semen-Associated pH Neutralization of Cervicovaginal Secretions. *Clin Diagn Lab Immunol* **1997**, *4* (3), 367–374.

(131) Haugen, T. B.; Grotmol, T. pH of Human Semen. *Int. J. Androl.* **1998**, *21* (2), 105–108.

(132) Zhou, J.; Chen, L.; Li, J.; Li, H.; Hong, Z.; Xie, M.; Chen, S.; Yao, B.; Drevet, J. R. The Semen pH Affects Sperm Motility and Capacitation. *PLoS One* **2015**, *10* (7), 1–15.

(133) Eungprabhanth, V. Finding of the Spermatozoa in the Vagina Related to Elapsed Time of Coitus. *Zeitschrift für Rechtsmedizin* **1974**, *74* (4), 301–304.

(134) Rohan, L. C.; Sassi, A. B. Vaginal Drug Delivery Systems for HIV Prevention. *AAPS J.* **2009**, *11* (1), 78–87.

(135) Hladik, F.; Hope, T. J. HIV Infection of the Genital Mucosa in Women. *Curr. HIV/AIDS Rep.* **2009**, *6* (1), 20–28.

(136) Foss, A. M.; Hossain, M.; Vickerman, P. T.; Watts, C. H. A Systematic Review of

Published Evidence on Intervention Impact on Condom Use in Sub-Saharan Africa and Asia. *Sex Transm Infect* **2007**, *83* (7), 510–516.

(137) Guelcher, S. A.; Gallagher, K. M.; Didier, J. E.; Klinedinst, D. B.; Doctor, J. S.; Goldstein, A. S.; Wilkes, G. L.; Beckman, E. J.; Hollinger, J. O. Synthesis of Biocompatible Segmented Polyurethanes from Aliphatic Diisocyanates and Diurea Diol Chain Extenders. *Acta Biomater.* **2005**, *1* (4), 471–484.

(138) Zhou, L.; Yu, L.; Ding, M.; Li, J.; Tan, H.; Wang, Z.; Fu, Q. Synthesis and Characterization of pH-Sensitive Biodegradable Polyurethane for Potential Drug Delivery Applications. *Macromolecules* **2011**, *44* (4), 857–864.

(139) Wang, A.; Gao, H.; Sun, Y.; Wang, Y.; Fan, Y.; Ma, J. Temperature- and pH-Responsive Nanoparticles of Biocompatible Polyurethanes for Doxorubicin Delivery. *Int. J. Pharm.* **2013**, *441*, 30–39.

(140) Chuasuwan, D. B.; Binjesoh, V.; Polli, J.E.; Zhang, H.; Amidon, G.L.; Junginger, H.E.; Midha, K.K.; Shah, V.P.; Stavchansky, S. Biowaiver Monographs for Immediate Release Solid Oral Dosage Forms: Diclofenac Sodium and Diclofenac Potassium. *J. Pharm. Sci.* **2009**, *98* (4), 1206–1219.

(141) Hiemenz, P.; Lodge, T. *Polymer Chemistry*, Second Edi.; CRC Press, 2007.

(142) Beachell, H. C.; Peterson, J. C. Dilute Solution Properties of Polyurethane. 1. Linear Polymers. *J. Polym. Sci. Part A-1* **1969**, *42* (7), 2021–2029.

(143) Kim, S.; Lim, J. I.; Jung, Y.; Mun, C. H.; Kim, J. H.; Kim, S. H. Preparation of Enhanced Hydrophobic Poly(l-Lactide-Co-ε-Caprolactone) Films Surface and Its Blood Compatibility. *Appl. Surf. Sci.* **2013**, *276*, 586–591.

(144) Jeon, O.; Lee, S.; Kim, S. H.; Lee, Y. M.; Kim, Y. H. Synthesis and Characterization of Poly (L-Lactide) - Poly (Ɛ-Caprolactone) Multiblock Copolymers. *Macromolecules* **2003**, *36*, 5585–5592.

(145) Giammona, G.; Pitarresi, G.; Craparo, E. F.; Cavallaro, G.; Buscemi, S. New Biodegradable Hydrogels Based on a Photo-Cross-Linkable Polyaspartamide and Poly(ethylene Glycol) Derivatives. Release Studies of an Anticancer Drug. *Colloid Polym. Sci.* **2001**, *279*, 771–783.

(146) Heda, A. A.; Gadade, D. D.; Kathiriya, J. M.; Puranik, P. K. HPLC Method Development and Validation for Simultaneous Analysis of Diclofenac Sodium and Rabeprazole Sodium. *E-Journal Chem.* **2010**, *7*, 386–391.

(147) Costin, G.-E.; Raabe, H. A.; Priston, R.; Evans, E.; Curren, R. D. Vaginal Irritation Models: The Current Status of Available Alternative and in Vitro Tests. *Altern. Lab. Anim.* **2011**, *39* (4), 317–337.

(148) Shintani, H. Formation and Elution of Toxic Compounds from Sterilized Medical Products: Methylenedianiline Formation in Polyurethane. *J. Biomater. Appl.* **1995**, *10* (1), 23–58.

(149) Szycher, M. Biostability of Polyurethane Elastomers: A Critical Review. *J. Biomater. Appl.* **1988**, *3* (2), 297–402.

(150) Pretsch, T.; Jakob, I.; Müller, W. Hydrolytic Degradation and Functional Stability of a Segmented Shape Memory Poly(ester Urethane). *Polym. Degrad. Stab.* **2009**, *94* (1), 61–73.

(151) Yang, H. Y.; Zhang, X. M.; Duan, L. J.; Zhang, M. Y.; Gao, G. H.; Zhang, H. X.

Synthesis and Characterization of Fluorescent PEG-Polyurethane with Free Carboxyl Groups. *J. Polym. Res.* **2012**, *19*, 1–7.

(152) Yang, L.; Heatley, F.; Blease, T. G.; Thompson, R. I. G. A Study of the Mechanism of the Oxidative Thermal Degradation of Poly(ethylene Oxide) and Poly(propylene Oxide) Using 1H- and 13C-NMR. *Eur. Polym. J.* **1996**, *32* (5), 535–547.

(153) Wu, J.; Ge, Q.; Mather, P. T. PEG-POSS Multiblock Polyurethanes: Synthesis, Characterization, and Hydrogel Formation. *Macromolecules* **2010**, *43*, 7637–7649.

(154) Chen, Y.; Liu, Y.; Fan, H.; Li, H.; Shi, B.; Zhou, H.; Peng, B. The Polyurethane Membranes with Temperature Sensitivity for Water Vapor Permeation. *J. Memb. Sci.* **2007**, *287* (2), 192–197.

(155) Kim, S. H.; Misner, M. J.; Xu, T.; Kimura, M.; Russell, T. P. Highly Oriented and Ordered Arrays from Block Copolymers via Solvent Evaporation. *Adv. Mater.* **2004**, *16* (3), 226–231.

(156) Nowicka-Sans, B.; Protack, T.; Lin, Z.; Li, Z.; Zhang, S.; Sun, Y.; Samanta, H.; Terry, B.; Liu, Z.; Chen, Y.; Sin, N.; Sit, S.-Y.; Swidorski, J. J.; Chen, J.; Venables, B. L.; Healy, M.; Meanwell, N. A.; Cockett, M.; Hanumegowda, U.; Regueiro-Ren, A.; Krystal, M.; Dicker, I. B. BMS-955176: Identification and Characterization of a Second-Generation HIV-1 Maturation Inhibitor with Improved Potency, Anti-Viral Spectrum and Gag Polymorphic Coverage. *Antimicrob. Agents Chemother.* **2016**, *60*, 3956–3969.

(157) Qian, K.; Bori, I. D.; Chen, C. H.; Huang, L.; Lee, K. H. Anti-AIDS Agents 90. Novel C-28 Modified Bevirimat Analogues as Potent HIV Maturation Inhibitors. *J. Med. Chem.* **2012**, *55* (18), 8128–8136.

(158) Timilsina, U.; Ghimire, D.; Timalsina, B.; Nitz, T. J.; Wild, C. T.; Freed, E. O.; Gaur, R. Identification of Potent Maturation Inhibitors against HIV-1 Clade C. *Sci. Rep.* **2016**, *6*, 1–6.

(159) Wang, D.; Lu, W.; Li, F. Pharmacological Intervention of HIV-1 Maturation. *Acta Pharm. Sin. B* **2015**, *5* (6), 493–499.

(160) Wen, Z.; Stern, S. T.; Martin, D. E.; Lee, K.-H.; Smith, P. C. Structural Characterization of Anti-HIV Drug Candidate PA-457 [3- O- (3, 3-Dimethylsuccinyl) -Betulinic Acid] and Its Acyl Glucuronides in Rat Bile and Evaluation of in Vitro Stability in Human and Animal Liver Microsomes and Plasm. *Drug Metab. Dispos.* **2006**, *34* (9), 1436–1442.

(161) Wakao, N.; Smith, J. Diffusion in Catalyst Pellets. *Chem. Engny Sci.* **1962**, *17*, 825–834.

(162) McGinty, K. M.; Brittain, W. J. Hydrophilic Surface Modification of Poly(vinyl Chloride) Film and Tubing Using Physisorbed Free Radical Grafting Technique. *Polymer (Guildf).* **2008**, *49*, 4350–4357.

(163) Fichorova, R. N. Interleukin (IL)-1, IL-6, and IL-8 Predict Mucosal Toxicity of Vaginal Microbicidal Contraceptives. *Biol. Reprod.* **2004**, *71* (3), 761–769.

(164) Haase, A. T. Targeting Early Infection to Prevent HIV-1 Mucosal Transmission. *Nature* **2010**, *464* (7286), 217–223.

(165) Wu, S. Y.; Chang, H. I.; Burgess, M.; McMillan, N. A. J. Vaginal Delivery of siRNA Using a Novel PEGylated Lipoplex-Entrapped Alginate Scaffold System. *J. Control. Release* **2011**, *155* (3), 418–426.

(166) Gupta, S. K.; Nutan. Clinical Use of Vaginal or Rectally Applied Microbicides in Patients Suffering from HIV/AIDS. *HIV/AIDS - Res. Palliat. Care* **2013**, *5*, 295–307.

(167) Murray, J. M.; Kelleher, A. D.; Cooper, D. A. Timing of the Components of the HIV Life Cycle in Productively Infected CD4+ T Cells in a Population of HIV-Infected Individuals. *J. Virol.* **2011**, *85* (20), 10798–10805.

(168) Cooper, G. M. *The Cell: A Molecular Approach*, 2nd ed.; Sinauer Associates, **2000**.

(169) Kalepu, S.; Nekkanti, V. Insoluble Drug Delivery Strategies: Review of Recent Advances and Business Prospects. *Acta Pharm. Sin. B* **2015**, *5* (5), 442–453.

(170) Mallipeddi, R.; Rohan, L. C. Progress in Antiretroviral Drug Delivery Using Nanotechnology. *Int. J. Nanomedicine* **2010**, *5* (1), 533–547.

(171) Steinbach, J. M.; Weller, C. E.; Booth, C. J.; Saltzman, W. M. Polymer Nanoparticles Encapsulating siRNA for Treatment of HSV-2 Genital Infection. *J. Control. Release* **2012**, *162* (1), 102–110.

(172) Reynolds, A.; Leake, D.; Boese, Q.; Scaringe, S.; Marshall, W. S.; Khvorova, A. Rational siRNA Design for RNA Interference. *Nat. Biotechnol.* **2004**, *22* (3), 326–330.

(173) Hester, J. F.; Olugebefola, S. C.; Mayes, A. M. Preparation of pH-Responsive Polymer Membranes by Self-Organization. *J. Memb. Sci.* **2002**, *208* (1–2), 375–388.

(174) Zhang, K.; Wu, X. Y. Temperature and pH-Responsive Polymeric Composite Membranes for Controlled Delivery of Proteins and Peptides. *Biomaterials* **2004**, *25* (22), 5281–5291.

(175) Jin, X.; Hsieh, Y. Lo. PH-Responsive Swelling Behavior of Poly(vinyl Alcohol)/poly(acrylic Acid) Bi-Component Fibrous Hydrogel Membranes. *Polymer (Guildf).* **2005**, *46* (14), 5149–5160.

(176) Qu, J. B.; Chu, L. Y.; Yang, M.; Xie, R.; Hu, L.; Chen, W. M. A pH-Responsive Gating Membrane System with Pumping Effects for Improved Controlled Release. *Adv. Funct.*

Mater. **2006**, *16* (14), 1865–1872.

(177) Nunes, S. P.; Behzad, A. R.; Hooghan, B.; Sougrat, R.; Karunakaran, M.; Pradeep, N.; Vainio, U.; Peinemann, K. V. Switchable pH-Responsive Polymeric Membranes Prepared via Block Copolymer Micelle Assembly. *ACS Nano* **2011**, *5* (5), 3516–3522.

(178) Abràmoff, M. D.; Magalhães, P. J.; Ram, S. J. Image Processing with imageJ. *Biophotonics Int.* **2004**, *11* (7), 36–41.

(179) Gopal, R.; Kaur, S.; Ma, Z.; Chan, C.; Ramakrishna, S.; Matsuura, T. Electrospun Nanofibrous Filtration Membrane. *J. Memb. Sci.* **2006**, *281*, 581–586.

(180) Bergmeister, H.; Schreiber, C.; Grasl, C.; Walter, I.; Plasenzotti, R.; Stoiber, M.; Bernhard, D.; Schima, H. Healing Characteristics of Electrospun Polyurethane Grafts with Various Porosities. *Acta Biomater.* **2013**, *9* (4), 6032–6040.

(181) Gopal, R.; Kaur, S.; Feng, C. Y.; Chan, C.; Ramakrishna, S.; Tabe, S.; Matsuura, T. Electrospun Nanofibrous Polysulfone Membranes as Pre-Filters: Particulate Removal. *J. Memb. Sci.* **2007**, *289* (1–2), 210–219.

(182) Szymczyk, A.; Dirir, Y. I.; Picot, M.; Nicolas, I.; Barrière, F. Advanced Electrokinetic Characterization of Composite Porous Membranes. *J. Memb. Sci.* **2013**, *429*, 44–51.

(183) Liao, Y.; Farrell, T. P.; Guillen, G. R.; Li, M.; Temple, J. A. T.; Li, X.-G.; Hoek, E. M. V.; Kaner, R. B. Highly Dispersible Polypyrrole Nanospheres for Advanced Nanocomposite Ultrafiltration Membranes. *Mater. Horiz.* **2014**, *1* (1), 58–64.

(184) Coday, B. D.; Luxbacher, T.; Childress, A. E.; Almaraz, N.; Xu, P.; Cath, T. Y. Indirect Determination of Zeta Potential at High Ionic Strength: Specific Application to Semipermeable Polymeric Membranes. *J. Memb. Sci.* **2015**, *478*, 58–64.

(185) Gross, B. C.; Erkal, J. L.; Lockwood, S. Y.; Chen, C.; Spence, D. M. Evaluation of 3D Printing and Its Potential Impact on Biotechnology and the Chemical Sciences. *Anal. Chem.* **2014**, *86* (7), 3240–3253.

(186) Cha, D.; Kim, K. W.; Chu, G. H.; Kim, H. Y.; Lee, K. H.; Bhattarai, N. Mechanical Behaviors and Characterization of Electrospun Polysulfone/polyurethane Blend Nonwovens. *Macromol. Res.* **2006**, *14* (3), 331–337.

(187) Kidoaki, S.; Kwon, I. K.; Matsuda, T. Structural Features and Mechanical Properties of in Situ-Bonded Meshes of Segmented Polyurethane Electrospun from Mixed Solvents. *J. Biomed. Mater. Res. - Part B Appl. Biomater.* **2006**, *76* (1), 219–229.

(188) Woodrow, K. A.; Cu, Y.; Booth, C. J.; Saucier-Sawyer, J. K.; Wood, M. J.; Mark Saltzman, W. Intravaginal Gene Silencing Using Biodegradable Polymer Nanoparticles Densely Loaded with Small-Interfering RNA. *Nat. Mater.* **2009**, *8* (6), 526–533.

(189) Yang, S.; Chen, Y.; Kaien, G.; Davies, N. M.; Ho, E. a. Novel Intravaginal Nanomedicine for the Targeted Delivery of Saquinavir to CD+ Immune Cells. *Int. J. Nanomedicine* **2013**, *8*, 2847–2858.

(190) Lai, S. K.; O'Hanlon, D. E.; Cone, R.; Hanes, J. Rapid Transport of Large Polymeric Nanoparticles in Fresh Undiluted Human Mucus. *Proc. Natl. Acad. Sci. U. S. A.* **2007**, *104*, 1482–1487.

(191) Lunov, O.; Syrovets, T.; Loos, C.; Beil, J.; Delacher, M.; Tron, K.; Nienhaus, G. U.; Musyanovych, A.; Mailänder, V.; Landfester, K.; Simmet, T. Differential Uptake of Functionalized Polystyrene Nanoparticles by Human Macrophages and a Monocytic Cell Line. *ACS Nano* **2011**, *5* (3), 1657–1669.

(192) Liu, Y.; Li, W.; Lao, F.; Liu, Y.; Wang, L.; Bai, R.; Zhao, Y.; Chen, C. Intracellular Dynamics of Cationic and Anionic Polystyrene Nanoparticles without Direct Interaction with Mitotic Spindle and Chromosomes. *Biomaterials* **2011**, *32* (32), 8291–8303.

(193) Frick, S. U.; Bacher, N.; Baier, G.; Mailänder, V.; Landfester, K.; Steinbrink, K. Functionalized Polystyrene Nanoparticles Trigger Human Dendritic Cell Maturation Resulting in Enhanced CD4+ T Cell Activation. *Macromol. Biosci.* **2012**, *12* (12), 1637–1647.

(194) dos Santos, T.; Varela, J.; Lynch, I.; Salvati, A.; Dawson, K. A. Effects of Transport Inhibitors on the Cellular Uptake of Carboxylated Polystyrene Nanoparticles in Different Cell Lines. *PLoS One* **2011**, *6* (9).

(195) Kumar, S.; Dory, Y. L.; Lepage, M.; Zhao, Y. Surface-Grafted Stimuli-Responsive Block Copolymer Brushes for the Thermo-, Photo- and pH-Sensitive Release of Dye Molecules. *Macromolecules* **2011**, *44* (18), 7385–7393.

(196) Ndesendo, V. M. K.; Pillay, V.; Choonara, Y. E.; Buchmann, E.; Bayever, D. N.; Meyer, L. C. R. A Review of Current Intravaginal Drug Delivery Approaches Employed for the Prophylaxis of HIV/AIDS and Prevention of Sexually Transmitted Infections. *AAPS PharmSciTech* **2008**, *9* (2), 505–520.

(197) Gorna, K.; Gogolewski, S. The Effect of Gamma Radiation on Molecular Stability and Mechanical Properties of Biodegradable Polyurethanes for Medical Applications. *Polym. Degrad. Stab.* **2003**, *79* (3), 465–474.

(198) Palliser, D.; Chowdhury, D.; Wang, Q.-Y.; Lee, S. J.; Bronson, R. T.; Knipe, D. M.; Lieberman, J. An siRNA-Based Microbicide Protects Mice from Lethal Herpes Simplex

Virus 2 Infection. *Nature* **2006**, *439* (January), 89–94.

(199) Kim, P. S.; Read, S. W. Nanotechnology and HIV: Potential Applications for Treatment and Prevention. *Wiley Interdiscip. Rev. Nanomedicine Nanobiotechnology* **2010**, *2* (6), 693–702.

(200) Parboosing, R.; Maguire, G. E. M.; Govender, P.; Kruger, H. G. Nanotechnology and the Treatment of HIV Infection. *Viruses* **2012**, *4* (4), 488–520.

(201) Mccormick-thomson, L. A.; Duncan, R. Poly(amino Acid) Copolymers as a Potential Soluble Drug Delivery System. 1. Pinocytic Uptake and Lysosomal Degradation Measured In Vitro. *Bioact. Compat. Polym. Biomed. Appl.* **1989**, *4* (July), 242–251.

(202) Craparo, E. F.; Giammona, G.; Cavallaro, G. Pegylated Polyaspartamide-Polylactide-Based Nanoparticles Penetrating Cystic Fibrosis Artificial Mucus. *Biomacromolecules* **2016**, *17* (3), 767–777.

(203) Fu, H.; Gao, H.; Wu, G.; Wang, Y.; Fan, Y.; Ma, J. Preparation and Tunable Temperature Sensitivity of Biodegradable Polyurethane Nanoassemblies from Diisocyanate and Poly(ethylene Glycol). *Soft Matter* **2011**, *7* (7), 3546.

(204) Sun, X.; Gao, H.; Wu, G.; Wang, Y.; Fan, Y.; Ma, J. Biodegradable and Temperature-Responsive Polyurethanes for Adriamycin Delivery. *Int. J. Pharm.* **2011**, *412* (1–2), 52–58.

(205) Cheng, X.; Jin, Y.; Sun, T.; Qi, R.; Li, H.; Fan, W. An Injectable, Dual pH and Oxidation-Responsive Supramolecular Hydrogel for Controlled Dual Drug Delivery. *Colloids Surfaces B Biointerfaces* **2016**, *141*, 44–52.

(206) Nakashima, T.; Yamada, Y.; Yoshizawa, H. Synthesis of Monodisperse Polystyrene

Microspheres by Dispersion Polymerization Using Sodium Polyaspartate. *Colloid Polym. Sci.* **2007**, *285*, 1487–1493.

(207) Park, H. D.; Kim, J. H.; Kim, S. H.; Kim, Y. H. Preparation and Properties of Poly(aspartic Acid)-Based Hydrogel. *Polym.* **1999**, *23* (2), 247–254.

(208) An, J. H.; Huynh, N. T.; Jeon, Y. S.; Kim, J. H. Surface Modification Using Bio-Inspired Adhesive Polymers Based on Polyaspartamide Derivatives. *Polym. Int.* **2011**, *60* (11), 1581–1586.

(209) Moon, J. R.; Jeon, Y. S.; Zrinyi, M.; Kim, J. H. pH-Responsive PEGylated Nanoparticles Based on Amphiphilic Polyaspartamide: Preparation, Physicochemical Characterization and in Vitro Evaluation. *Polym. Int.* **2013**, *62* (8), 1218–1224.

(210) Sze, A.; Erickson, D.; Ren, L.; Li, D. Zeta-Potential Measurement Using the Smoluchowski Equation and the Slope of the Current-Time Relationship in Electroosmotic Flow. *J. Colloid Interface Sci.* **2003**, *261* (2), 402–410.

(211) Craparo, E. F.; Licciardi, M.; Giammona, G.; De Leo, G.; Cavallaro, G. Hepatocyte-Targeted Fluorescent Nanoparticles Based on a Polyaspartamide for Potential Theranostic Applications. *Polym. (United Kingdom)* **2015**, *70*, 257–270.

(212) Promega Corporation. Calculating Nucleic Acid Samples or Protein Concentration Using GloMax-Multi Microplate Instrument https://www.promega.ca/resources/pubhub/applications-notes/calculating-nucleic-acid-or-protein-concentration-using-the-glomax-multi-plus-microplate-instrument/ (accessed Oct 16, 2017).

(213) Chen, W.; Chen, H.; Hu, J.; Yang, W.; Wang, C. Synthesis and Characterization of

Polyion Complex Micelles between Poly(ethylene Glycol)-Grafted Poly(aspartic Acid) and Cetyltrimethyl Ammonium Bromide. *Colloids Surfaces A Physicochem. Eng. Asp.* **2006**, *278*, 60–66.

(214) Craparo, E. F.; Cavallaro, G.; Bondi, M. L.; Giammona, G. PEGylated Nanoparticles Based on a Polyaspartamide. Preparation, Physico-Chemical Characterization, and Intracellular Uptake. *Biomacromolecules* **2006**, *7* (11), 3083–3092.

(215) Kohno, M.; Sasao, S.; Murahashi, S.-I. Synthesis of Phenetyhlamines by Hydrogenation of B-Nitrostyrenes. *Bulletin of the Chemical Society of Japan*. 1990, pp 1252–1254.

(216) López, C.; Valade, A. G.; Combourieu, B.; Mielgo, I.; Bouchon, B.; Lema, J. M. Mechanism of Enzymatic Degradation of the Azo Dye Orange II Determined by Ex situ1H Nuclear Magnetic Resonance and Electrospray Ionization-Ion Trap Mass Spectrometry. *Anal. Biochem.* **2004**, *335* (1), 135–149.

(217) Alli, A.; Hazer, B.; Menceloğlu, Y.; Süzer, Ş. Synthesis, Characterization and Surface Properties of Amphiphilic Polystyrene-B-Polypropylene Glycol Block Copolymers. *Eur. Polym. J.* **2006**, *42*, 740–750.

(218) Birtalan, E.; Rudat, B.; Kölmel, D. K.; Fritz, D.; Vollrath, S. B. L.; Schepers, U.; Bräse, S. Investigating Rhodamine B-Labeled Peptoids: Scopes and Limitations of Its Applications. *Biopolymers* **2011**, *96* (5), 694–701.

(219) Feng, J.; Gao, L.; Wen, R.; Deng, Y.; Wu, X.; Deng, S. Fluorescent Polyaspartic Acid with an Enhanced Inhibition Performance against Calcium Phosphate. *Desalination* **2014**, *345*, 72–76.

(220) Molina-Guijarro, J. M.; Pérez, J.; Muñoz-Dorado, J.; Guillén, F.; Moya, R.; Herńndez, M.;

Arias, M. E. Detoxification of Azo Dyes by a Novel pH-Versatile, Salt-Resistant Laccase from Streptomyces Ipomoea. *Int. Microbiol.* **2009**, *12* (1), 13–21.

(221) Wang, L. F.; Ji, Q.; Glass, T. E.; Ward, T. C.; McGrath, J. E.; Muggli, M.; Burns, G.; Sorathia, U. Synthesis and Characterization of Organosiloxane Modified Segmented Polyether Polyurethanes. *Polymer (Guildf).* **2000**, *41*, 5083–5093.

(222) Amalvy, O. R. P. J. I. FTIR, 1H-NMR Spectra, and Thermal Characterization of Water-based Polyurethane/acrylic Hybrids. *J. Appl. Polym. Sci.* **2008**, *107* (2), 1207–1214.

(223) Pérez-Limiñana, M. A.; Arán-Aís, F.; Torró-Palau, A. M.; Orgilés-Barceló, A. C.; Martín-Martínez, J. M. Characterization of Waterborne Polyurethane Adhesives Containing Different Amounts of Ionic Groups. *Int. J. Adhes. Adhes.* **2005**, *25* (6), 507–517.

(224) Higgins, J. A.; Hoffman, S.; Dworkin, S. L. Rethinking Gender, Heterosexual Men, and Women's Vulnerability to HIV/AIDS. *Am. J. Public Health* **2010**, *100* (3), 435–445.

(225) Mashat, A.; Deng, L.; Altawashi, A.; Sougrat, R.; Wang, G.; Khashab, N. M. Zippered Release from Polymer-Gated Carbon Nanotubes. *J. Mater. Chem.* **2012**, *22* (23), 11503.

(226) Pistone, A.; Iannazzo, D.; Ansari, S.; Milone, C.; Salamò, M.; Galvagno, S.; Cirmi, S.; Navarra, M. Tunable Doxorubicin Release from Polymer-Gated Multiwalled Carbon Nanotubes. *Int. J. Pharm.* **2016**, *515*, 30–36.

(227) Iannazzo, D.; Piperno, A.; Ferlazzo, A.; Pistone, A.; Milone, C.; Lanza, M.; Cimino, F.; Speciale, A.; Trombetta, D.; Saija, A.; Galvagno, S. Functionalization of Multi-Walled Carbon Nanotubes with Coumarin Derivatives and Their Biological Evaluation. *Org. Biomol. Chem.* **2012**, *10* (5), 1025.

(228) Mishra, B.; Patel, B. B.; Tiwari, S. Colloidal Nanocarriers: A Review on Formulation

Technology, Types and Applications toward Targeted Drug Delivery. *Nanomedicine Nanotechnology, Biol. Med.* **2010**, *6* (1), 9–24.

(229) Iannazzo, D.; Pistone, A.; Galvagno, S.; Ferro, S.; De Luca, L.; Monforte, A. M.; Da Ros, T.; Hadad, C.; Prato, M.; Pannecouque, C. Synthesis and Anti-HIV Activity of Carboxylated and Drug-Conjugated Multi-Walled Carbon Nanotubes. *Carbon N. Y.* **2015**, *82* (C), 548–561.

(230) He, C.; Hu, Y.; Yin, L.; Tang, C.; Yin, C. Effects of Particle Size and Surface Charge on Cellular Uptake and Biodistribution of Polymeric Nanoparticles. *Biomaterials* **2010**, *31* (13), 3657–3666.

(231) Liu, R.; Li, D.; He, B.; Wang, G.; Gu, Z. Anti-Tumor Drug Delivery of pH-Sensitive Poly(ethylene Glycol)-poly(L- Histidine-)-poly(L-Lactide) Nanoparticles. *J. Control. Release* **2011**, *152* (1), 49–56.

(232) Gao, G. H.; Li, Y.; Lee, D. S. Environmental pH-Sensitive Polymeric Micelles for Cancer Diagnosis and Targeted Therapy. *J. Control. Release* **2013**, *169* (3), 180–184.

(233) Lee, S. J.; Min, K. H.; Heo, J. S.; Lee, S. C. Ketal Cross-Linked Poly(ethylene Glycol)-Poly(amino Acid)s Copolymer Micelles for Efficient Intracellular Delivery of Doxorubicin. *Biomacromolecules* **2011**, *12* (4), 1224–1233.

(234) Akagi, T.; Wang, X.; Uto, T.; Baba, M.; Akashi, M. Protein Direct Delivery to Dendritic Cells Using Nanoparticles Based on Amphiphilic Poly(amino Acid) Derivatives. *Biomaterials* **2007**, *28* (23), 3427–3436.

(235) Matsusaki, M.; Hiwatari, K.; Higashi, M.; Kaneko, T.; Akashi, M. Stably-Dispersed and Surface-Functional Bionanoparticles Prepared by Self-Assembling Amphipathic Polymers

of Hydrophilic Poly(γ-Glutamic Acid) Bearing Hydrophobic Amino Acids. *Chem. Lett.* **2004**, *33* (4), 398–399.

(236) Miao, X.; Li, Y.; Wyman, I.; Lee, S. M. Y.; Macartney, D. H.; Zheng, Y.; Wang, R. Enhanced in Vitro and in Vivo Uptake of a Hydrophobic Model Drug Coumarin-6 in the Presence of cucurbit[7]uril. *Med. Chem. Commun.* **2015**, *6* (7), 1370–1374.

(237) Dailey, L. A.; Schmehl, T.; Gessler, T.; Wittmar, M.; Grimminger, F.; Seeger, W.; Kissel, T. Nebulization of Biodegradable Nanoparticles: Impact of Nebulizer Technology and Nanoparticle Characteristics on Aerosol Features. *J. Control. Release* **2003**, *86* (1), 131–144.

(238) Eley, J. G.; Tirumalasetty, P. P. Release Characteristics of Polymethacrylate Nanospheres Containing Coumarin-6. *J. Microencapsul.* **2003**, *20* (5), 653–659.

(239) Zhao, Z.; Wang, Y.; Han, J.; Wang, K.; Yang, D.; Yang, Y.; Du, Q.; Song, Y.; Yin, X. Self-Assembled Micelles of Amphiphilic poly(L-Phenylalanine)-B-poly(L-Serine) Polypeptides for Tumor-Targeted Delivery. *Int. J. Nanomedicine* **2014**, *9* (1), 5849–5862.

(240) Beck-Broichsitter, M.; Thieme, M.; Greiner, A.; Kissel, T. Novel "Nano in Nano" Composites for Sustained Drug Delivery: Biodegradable Nanoparticles Encapsulated into Nanofiber Non-Wovens. *Macromol. Biosci.* **2010**, *10* (12), 1527–1535.

(241) Ko, J.; Park, K.; Lee, D. S.; Kwon, I. C. Tumoral Acidic Extracellular pH Targeting of pH-Responsive MPEG-Poly(β-Amino Ester) Block Copolymer Micelles for Cancer Therapy. *J. Control. Release* **2007**, *123* (2), 109–115.

(242) Maartens, G.; Meintjes, G. Lower-Dose Efavirenz: What Is Needed before Implementation? *Lancet Infect. Dis.* **2015**, *15* (7), 749–751.

(243) Schöller-Gyüre, M.; Kakuda, T. N.; Raoof, A.; De Smedt, G.; Hoetelmans, R. M. W. Clinical Pharmacokinetics and Pharmacodynamics of Etravirine. *Clin. Pharmacokinet.* **2009**, *48* (9), 561–574.

(244) Souza, S. D. A Review of In Vitro Drug Release Test Methods for Nano-Sized Dosage Forms. *Adv. Pharm.* **2014**, *2014*, 1–12.